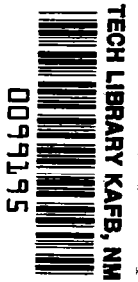


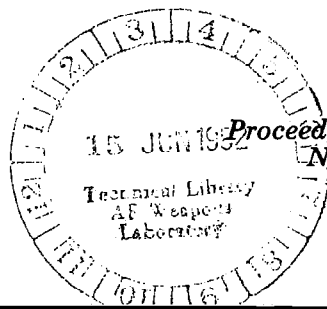
NASA
CP
2225
c. 1

NASA Conference Publication 2225

Wind-Tunnel/Flight Correlation - 1981



LOAN COPY: RETURN TO
AFWL TECHNICAL LIBRARY
WRIGHT PATT. AFB, OH.



*Proceedings of a miniworkshop held at
NASA Langley Research Center
Hampton, Virginia
November 19-20, 1981*

NASA



NASA Conference Publication 2225

Wind-Tunnel/Flight Correlation - 1981

Edited by
L. Wayne McKinney
Langley Research Center
Hampton, Virginia

Donald D. Baals
Consultant to Langley Research Center


Proceedings of a miniworkshop held at
NASA Langley Research Center
Hampton, Virginia
November 19-20, 1981

NASA

National Aeronautics
and Space Administration

**Scientific and Technical
Information Branch**

1982



The use of trade names in this publication does not constitute endorsement, either expressed or implied, by the National Aeronautics and Space Administration.

PREFACE

This Miniworkshop on Wind-Tunnel/Flight Correlation was an outgrowth of the December 1980 Workshop on High Reynolds Number Research held at the Langley Research Center where a broad spectrum of research programs and technology applicable to the National Transonic Facility (NTF), including wind-tunnel/flight correlation, was considered. The members of the panel on wind-tunnel/flight correlation from the 1980 workshop served as the nucleus for this workshop, supplemented by other invited specialists. A list of attendees is included in this report.

The purpose of this workshop was to review both past and present activities in the area of wind-tunnel/flight comparison and attempt to obtain a consensus of opinion on several key issues. The following basic issues were addressed:

- o Problems with past correlations
- o Requirements for a good correlation program
- o Key measurement areas for correlation
- o Suitability of existing flight data
- o Desirability of using new or advanced aircraft
- o Should a new flight program be initiated as a base for wind-tunnel correlation?

This report documents the material presented.

The workshop was conducted by Donald D. Baals under contract to the Langley Research Center. The active support of the potential users of NTF in attending the workshop and their comments and recommendations made this workshop a success.

L. Wayne McKinney

Donald D. Baals



CONTENTS

PREFACE iii

INTRODUCTORY SESSION

1. STATUS OF THE NATIONAL TRANSONIC FACILITY 1
Robert L. Swain

2. REVIEW OF THE 1980 WIND-TUNNEL/FLIGHT CORRELATION PANEL 23
Theodore G. Ayers

PAST VEHICLES

3. WIND-TUNNEL/FLIGHT-DRAG CORRELATION 33
John H. Paterson

4. TUNNEL-TO-TUNNEL CORRELATION 47
Frank W. Steinle, Jr.

5. WIND-TUNNEL/FLIGHT CORRELATION PROGRAM ON THE XB-70-1 65
John B. Peterson, Jr.

6. PROBLEMS IN CORRELATION CAUSED BY PROPULSION SYSTEMS 93
Ronald H. Smith

EXISTING DATA BASE

7. TACT/F-111 WIND-TUNNEL/FLIGHT CORRELATION
(Paper not available for publication)
Lowell C. Keel

8. F-15 WIND-TUNNEL/FLIGHT CORRELATIONS 109
Larry G. Niedling

9. B-1 RESULTS
(Paper not available for publication)
Richard D. Child

10. AERODYNAMIC COMPARISONS OF STS-1 SPACE SHUTTLE ENTRY VEHICLE 117
James C. Young

11. AERODYNAMIC COMPARISONS OF SPACE SHUTTLE ASCENT: STS-1 FLIGHT
VERSUS WIND-TUNNEL PREDICTIONS 133
Rodney O. Wallace

FUTURE VEHICLES

12. OPPORTUNITIES FOR WIND-TUNNEL/FLIGHT CORRELATION WITH NEW BOEING
AIRPLANES 141
Adelbert L. Nagel

13.	F-16E PROGRAM OVERVIEW AND WIND TUNNEL/FLIGHT CORRELATION	159
	A. P. Madsen	
14.	SPACE-VEHICLE CORRELATION OF GROUND AND FLIGHT EXPERIMENTS	173
	William I. Scallion	
15.	X-29A FORWARD-SWEPT-WING DEMONSTRATOR AIRPLANE	177
	Douglas R. Frei	
16.	X-29A FOR NTF WIND-TUNNEL/FLIGHT CORRELATIONS	191
	Gianky DaForno	

COMPUTATIONAL FLUID DYNAMICS (CFD)

17.	APPLICATIONS OF COMPUTATIONAL FLUID DYNAMICS (CFD) IN TRANSONIC WIND-TUNNEL/FLIGHT-TEST CORRELATION	199
	Earl M. Murman	
18.	SOME IDEAS AND OPPORTUNITIES CONCERNING THREE-DIMENSIONAL WIND-TUNNEL WALL CORRECTIONS	217
	Paul E. Rubbert	
	LIST OF ATTENDEES	231

STATUS OF THE NATIONAL TRANSONIC FACILITY

Robert L. Swain
NASA Langley Research Center
Hampton, Virginia

Miniworkshop on Wind-Tunnel/Flight Correlation
November 19-20, 1981

SUMMARY STATUS (NOV. 1981) OF THE NATIONAL TRANSONIC FACILITY

Construction of the National Transonic Facility (NTF), an advanced high Reynolds number (120×10^6 at $M = 1$) capability wind tunnel utilizing cryogenic nitrogen as the fluid medium, remains on schedule for operational readiness in late CY 1982. A summary of the construction status of major tunnel systems/subsystems is presented below in outline form:

- o Pressure Shell: Complete; hydrotested to 195 psi in August 1980.
- o Major Internals (e.g., nacelles, turning vanes, shroud/flow liner, etc.): Complete except for installation of selected fairings and seals.
- o Test Section: Complete.
- o Fan Region Internals (inlet/exit vanes, fan blades): Metal-parts installation complete; fan blades (plastic composite) are complete and will be installed by January 1982.
- o Tunnel Drive System: Complete.
- o Heat Exchanger: Complete.
- o Thermal Insulation: Approximately 75-percent complete; estimated May 1982 completion date. Installation more complex and time consuming than originally estimated.
- o LN₂ Storage/Transfer System: Complete; being modified by addition of small flow rate pump for tunnel cooldown; estimated January 1982 readiness.
- o Tunnel Vent/Acoustic Muffler System: Complete.
- o Internal/External Wiring/Piping: Completion delayed approximately 2 months due to lag in insulation installation; estimate complete February 1982.
- o Process Controls/Data Acquisition: Control-room components installed; awaiting completion of tunnel wiring for initiation of system functional testing (February 1982).
- o Site/Building: All major items complete; painting to be completed in January 1982. User model buildup rooms/offices will be complete in January 1982.

The following figures illustrate the near-completion of the construction of the NTF. Systems-level functional checkout will begin in January 1982, culminating in a no-flow air-pressure test of the tunnel in June 1982. Integrated air operations (fan-driven air) will immediately follow for a period of about 2 months. In mid-August 1982, cryogenic nitrogen will be introduced into the tunnel circuit for the first time; 2 months of integrated cryo operations are planned. A facility Operational Readiness Review (ORR) will be held in the late October or November time frame to review all test results and to determine readiness of the NTF for commencement of research operations.

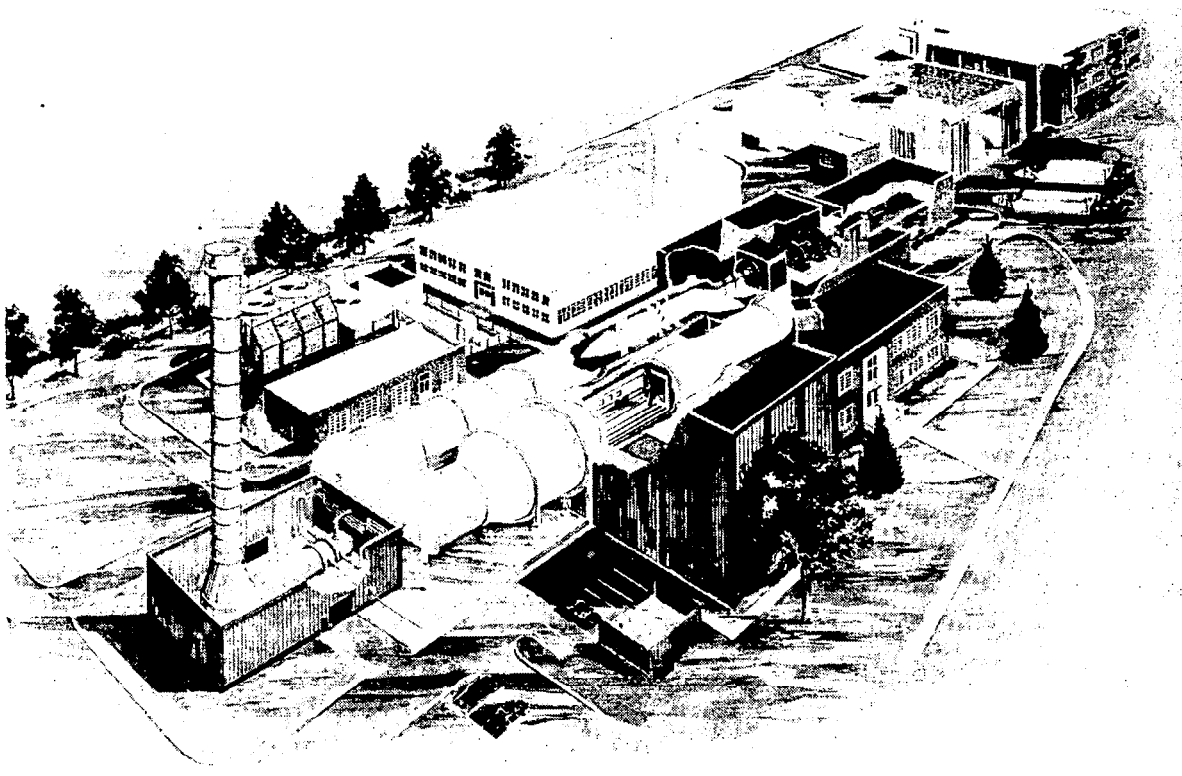


Figure 1.- Artist's rendition of the National Transonic Facility.

OBJECTIVE: TO DESIGN, CONSTRUCT, AND BRING TO AN OPERATIONAL STATUS
 A NATIONAL WIND-TUNNEL FACILITY UTILIZING A CRYOGENIC TEST
 MEDIUM CAPABLE OF SIMULATING FULL-SCALE AERODYNAMIC PARAMETERS
 ON TEST MODELS IN THE SUBSONIC-TRANSONIC SPEED RANGE.

DESCRIPTION:

TEST SECTION SIZE	8.2 FT SQUARE
DESIGN PRESSURE	130 PSI
DESIGN MACH NUMBER	0.2 - 1.2
STREAM FLUID	NITROGEN
BASIC DRIVE POWER	130,000 HP
PRODUCTIVITY/EFFICIENCY	8000 POLARS/YEARS
REYNOLDS NUMBER	120×10^6 ($M = 1.0$)

PROGRAMMATIC:

4-YEAR CoF PROJECT (FY 77 - 80); NOT TO EXCEED \$85M

Figure 2.- Introduction and background.

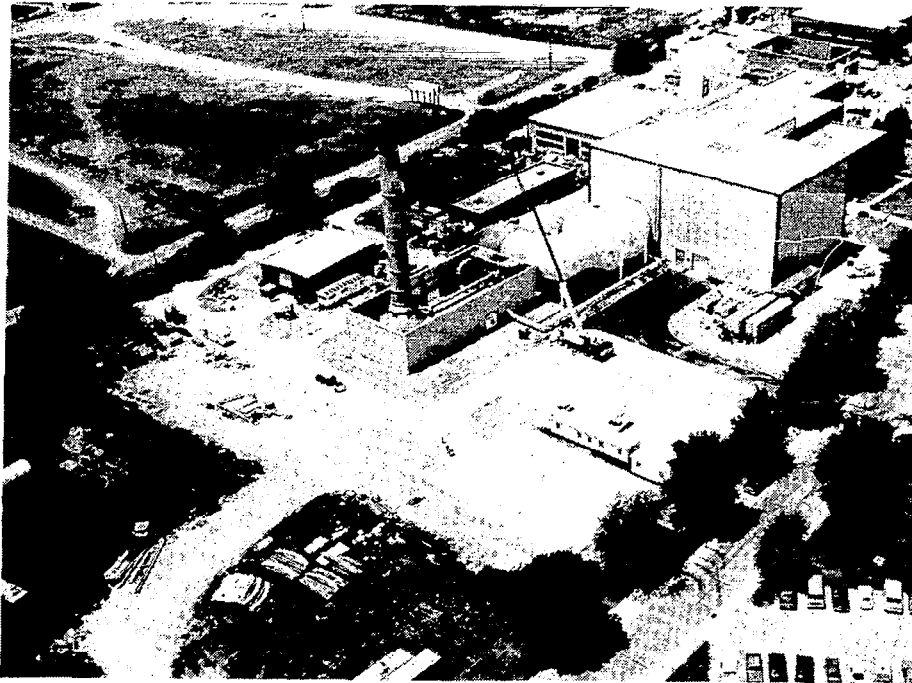


Figure 3.- Aerial photograph of NTF progress.

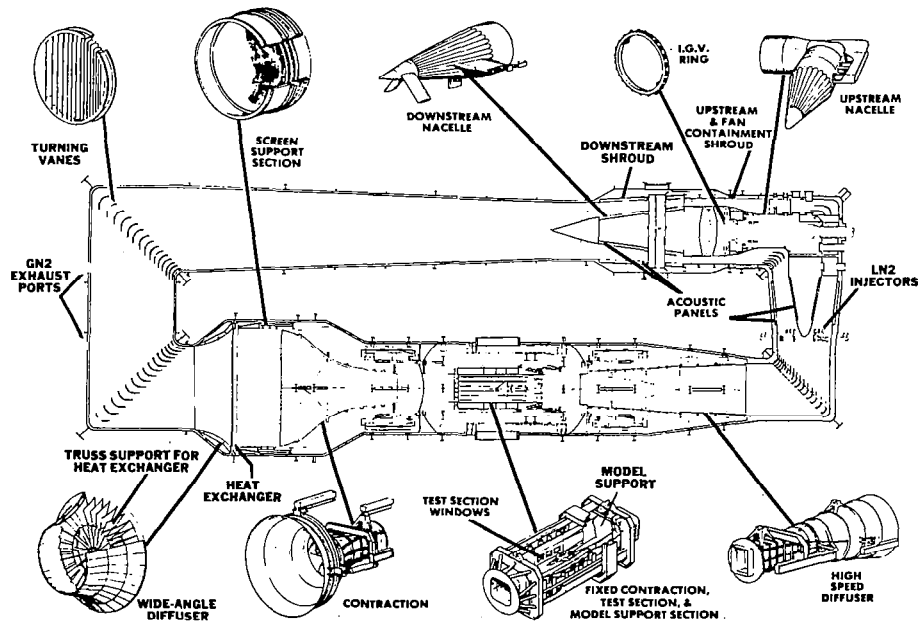


Figure 4.- Circuit plan view.

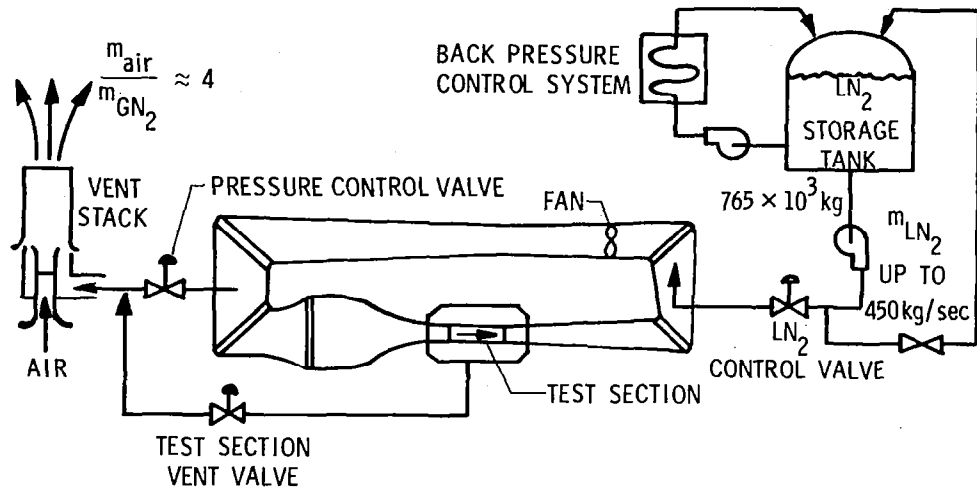


Figure 5.- Schematic diagram of nitrogen supply and vent system.

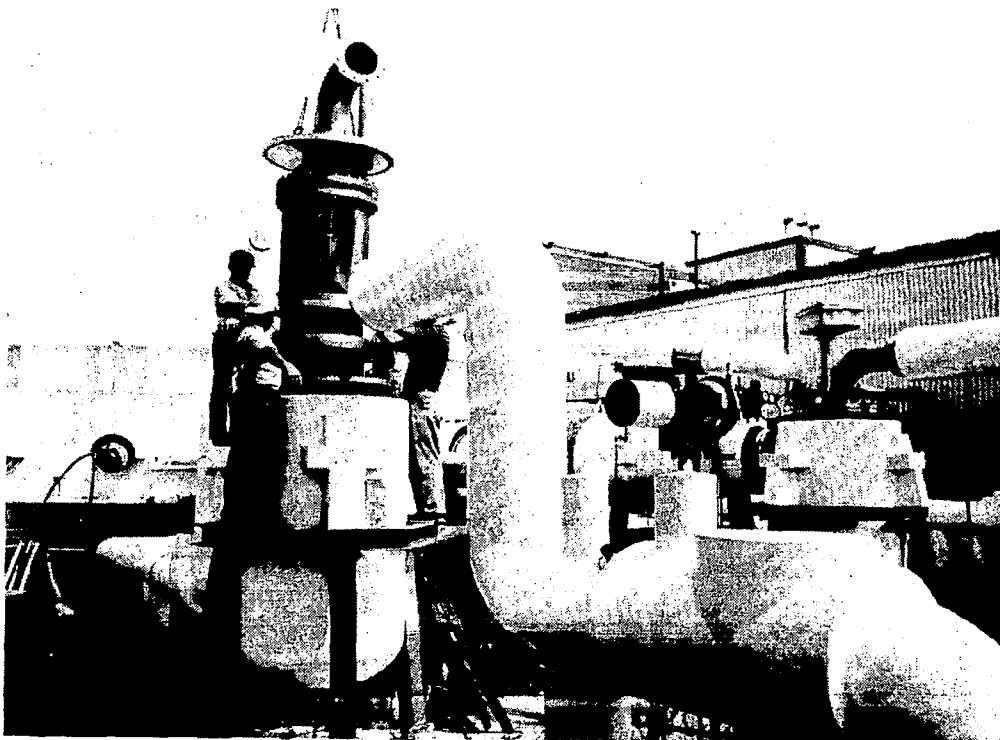


Figure 6.- LN₂ storage tank and piping.

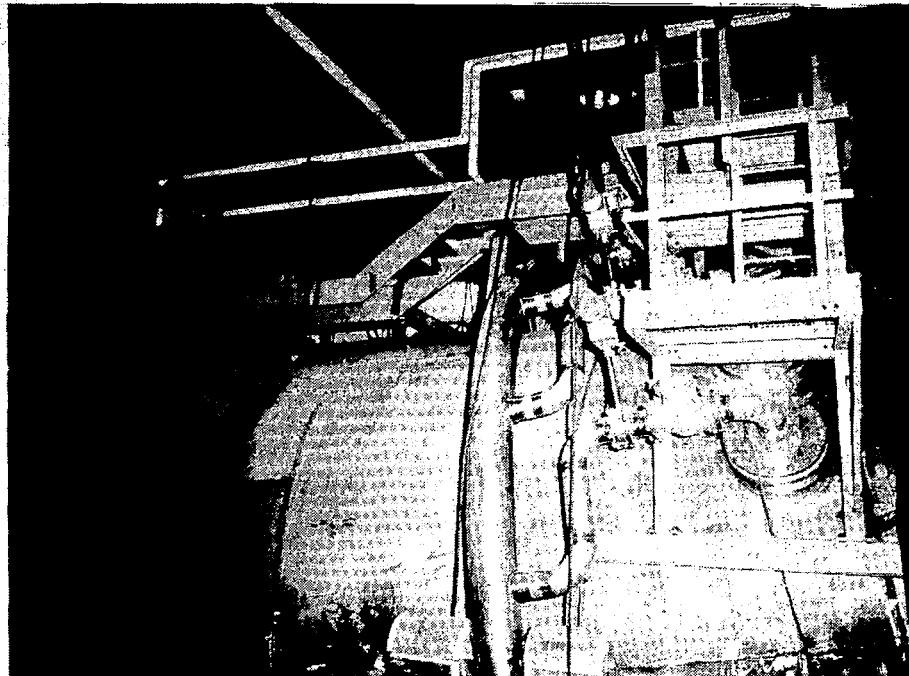


Figure 7.- LN₂ piping at injection station.

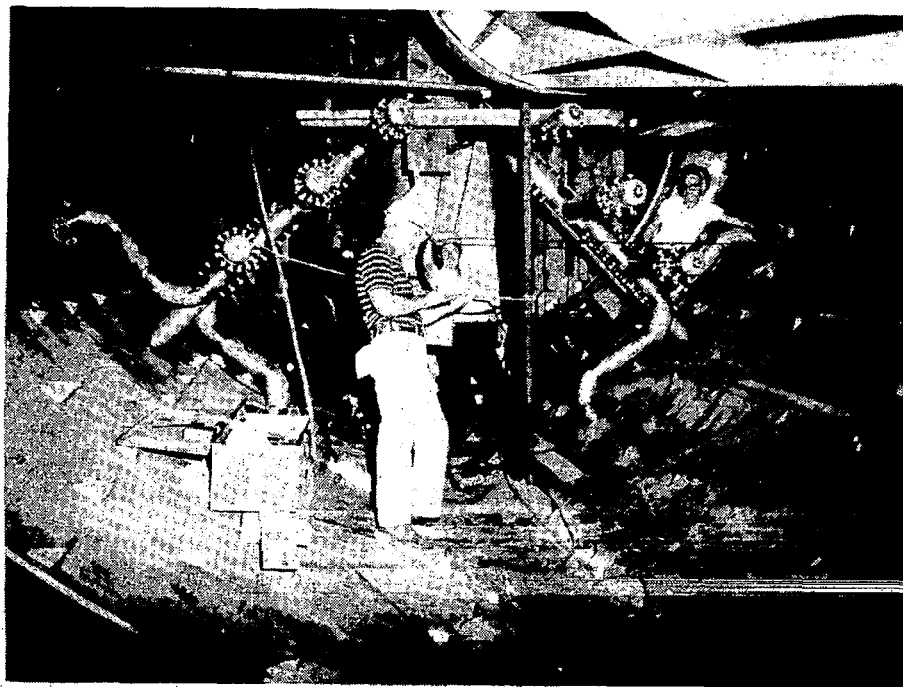


Figure 8.- LN₂ injector nozzles.

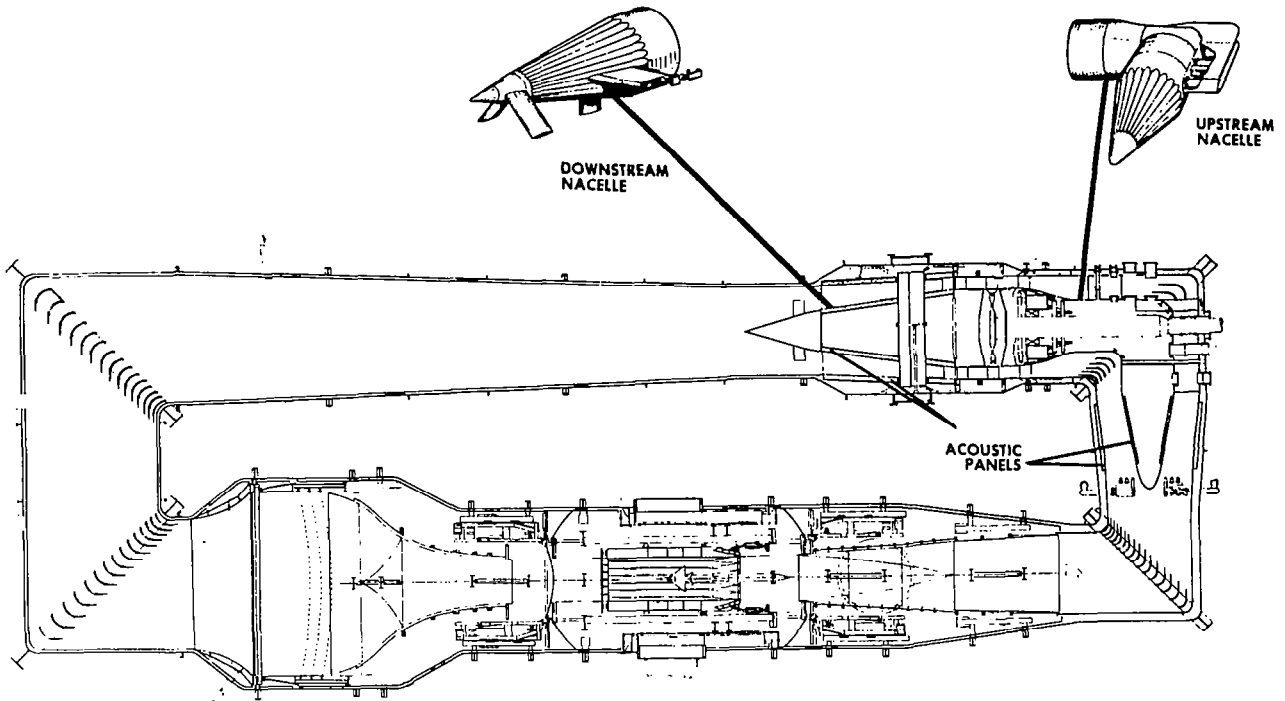


Figure 9.- Internal acoustic treatment installation.

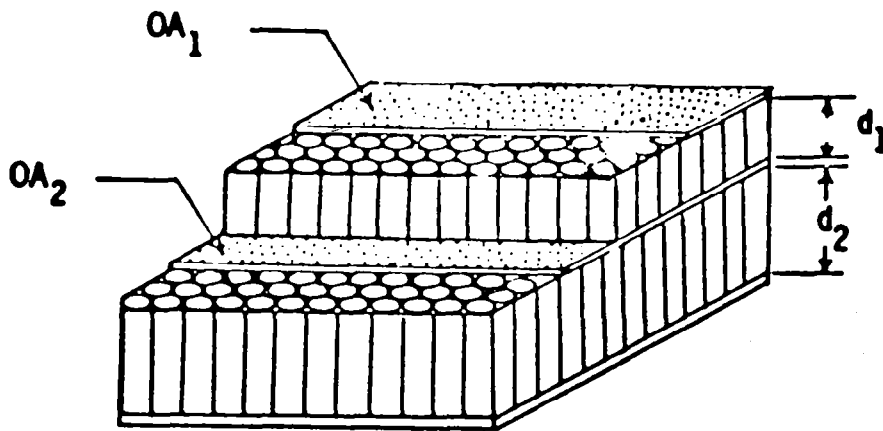


Figure 10.- Concept of fan-duct dual-resonator acoustic treatment.

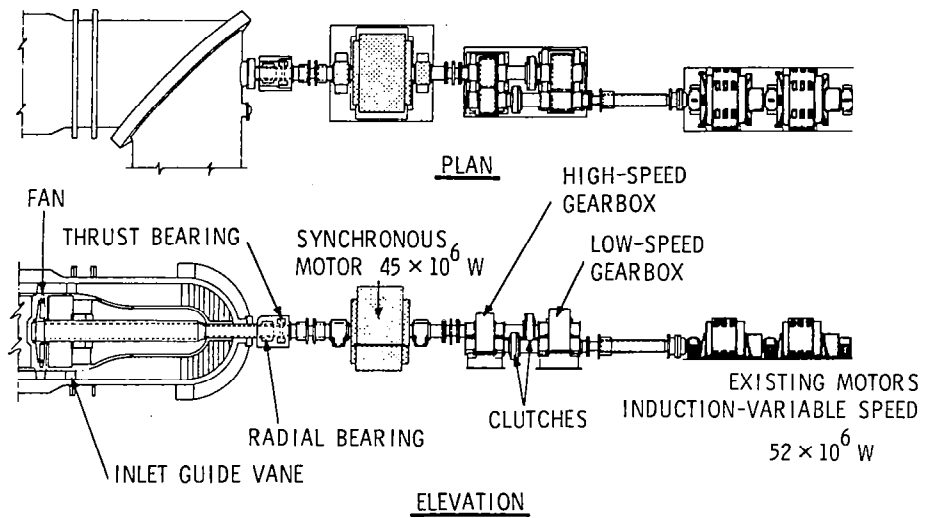


Figure 11.- Schematic diagram of drive system.

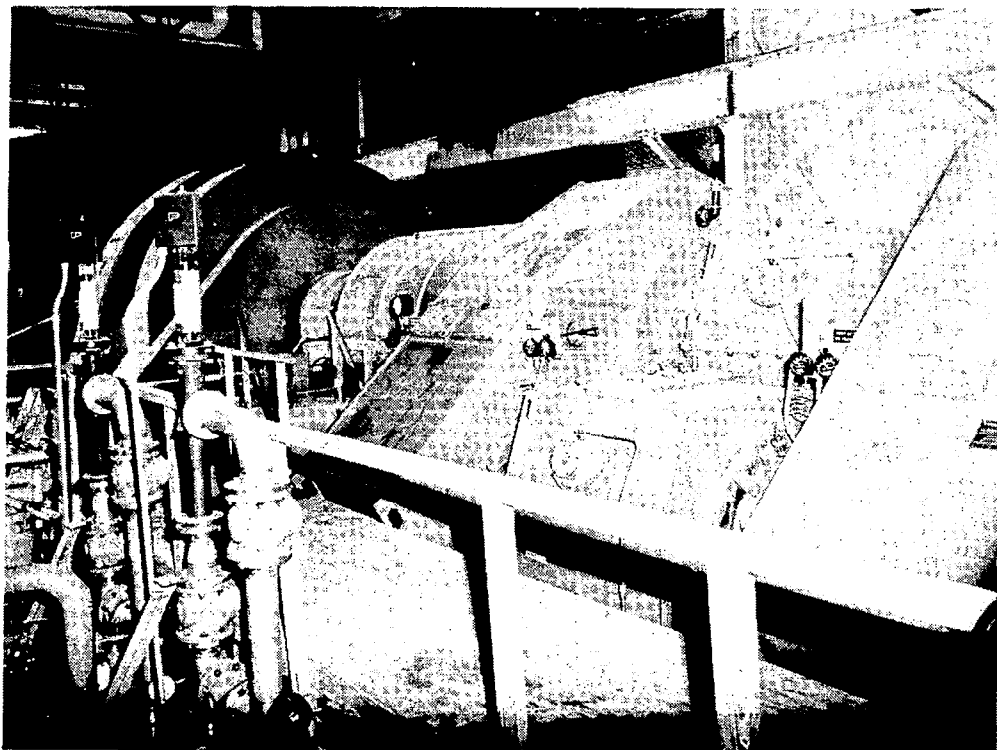


Figure 12.- Synchronous motor drive with gear boxes.

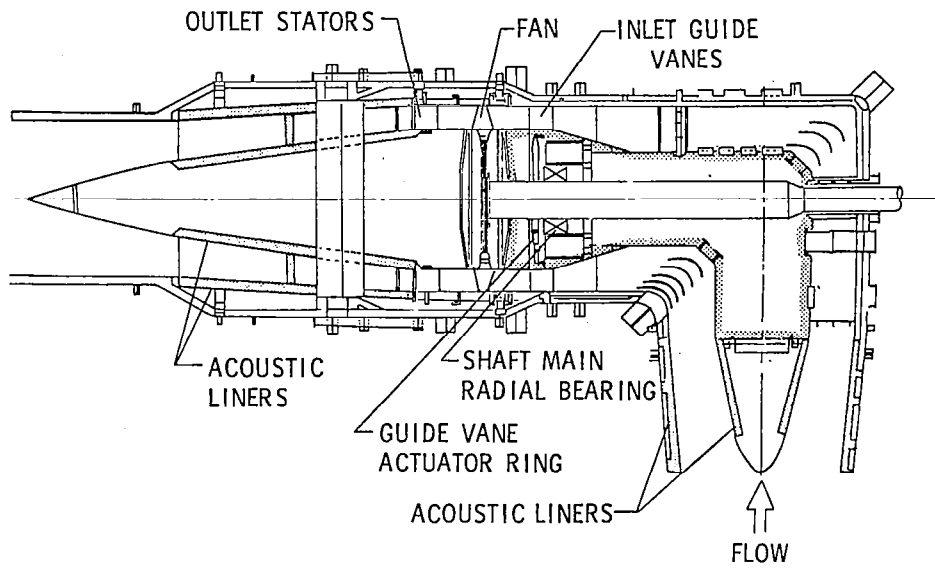


Figure 13.- Fan-section assembly.

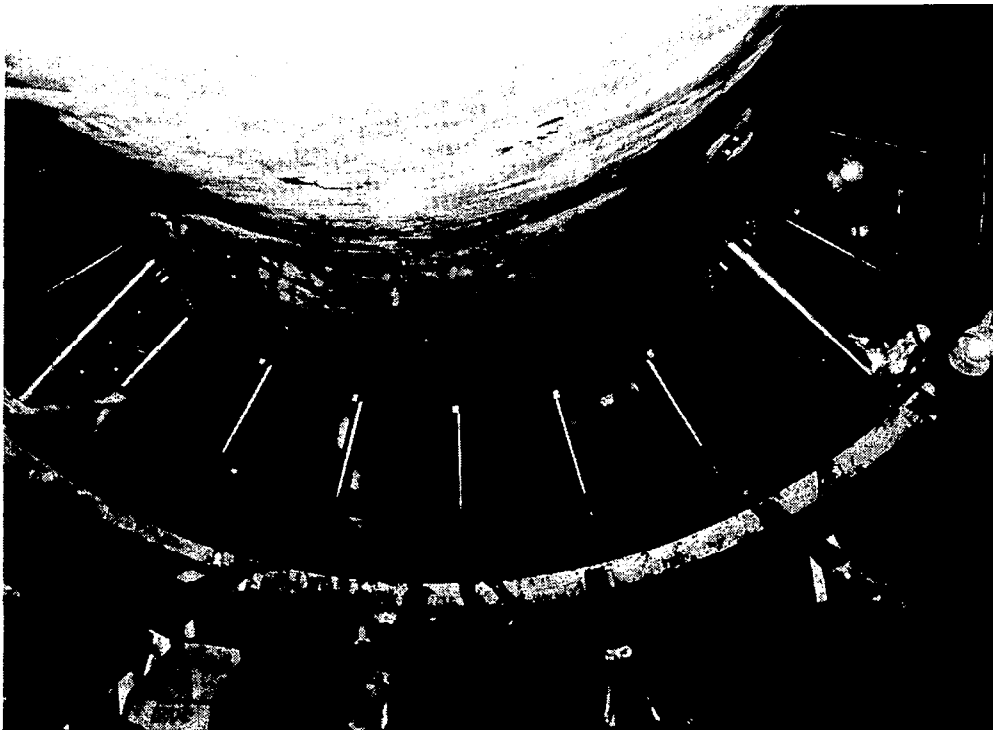


Figure 14.- Inlet guide vanes.

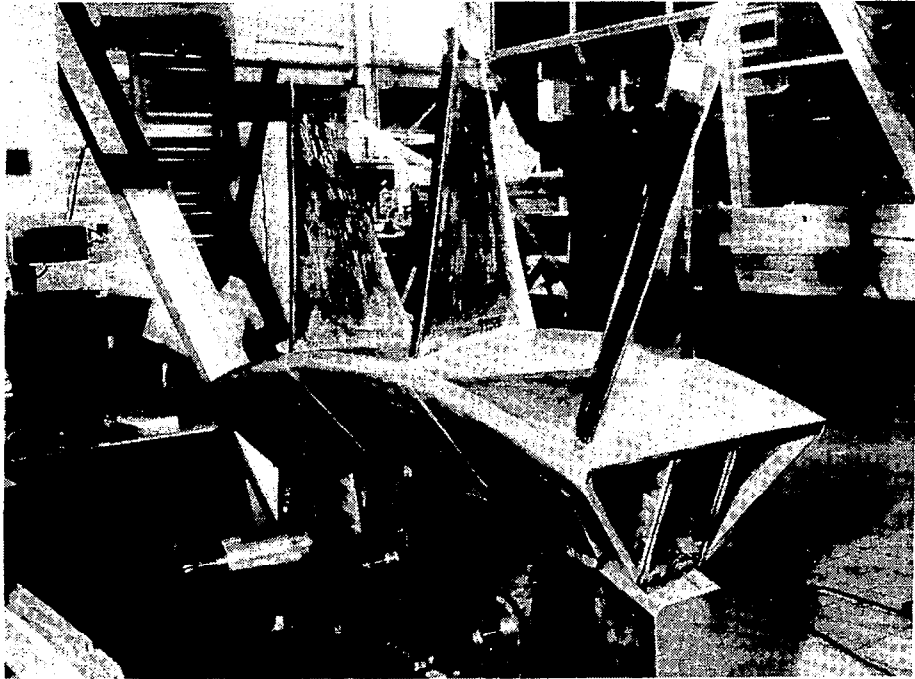


Figure 15.- Sector of fan blades.

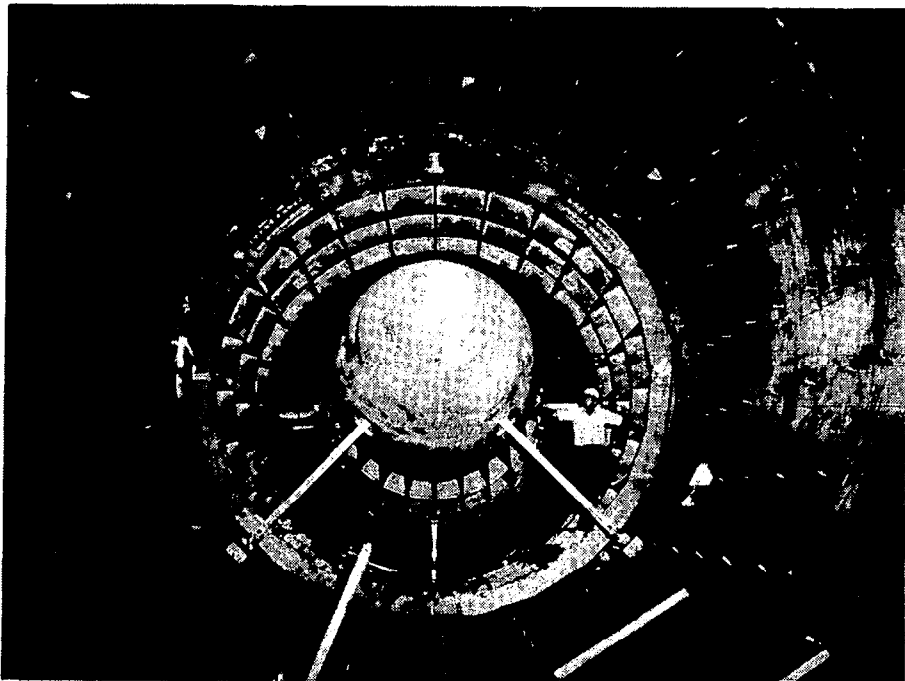


Figure 16.- Fan nacelle with recesses for acoustic liners.

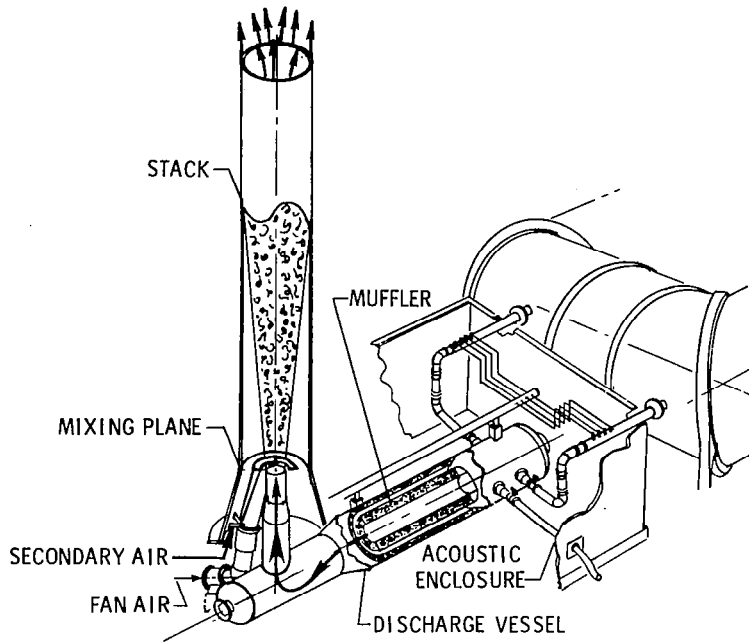


Figure 17.- Fan-ejector system.

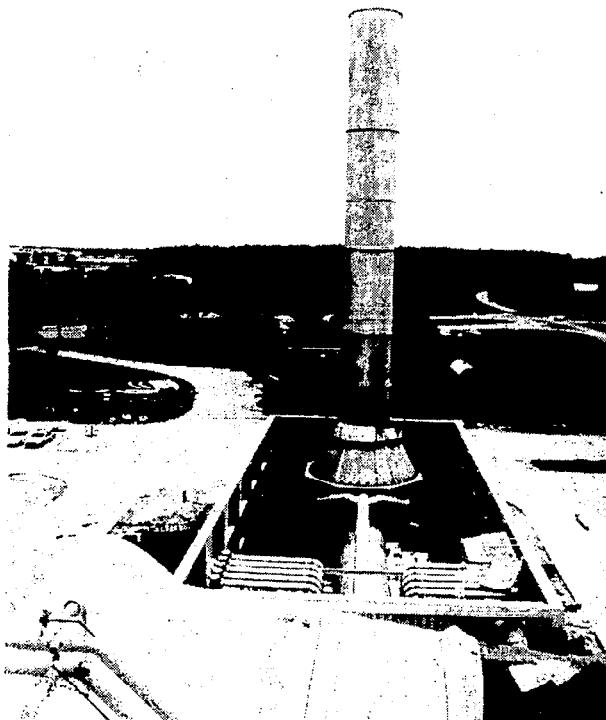


Figure 18.- Nitrogen vent stack.

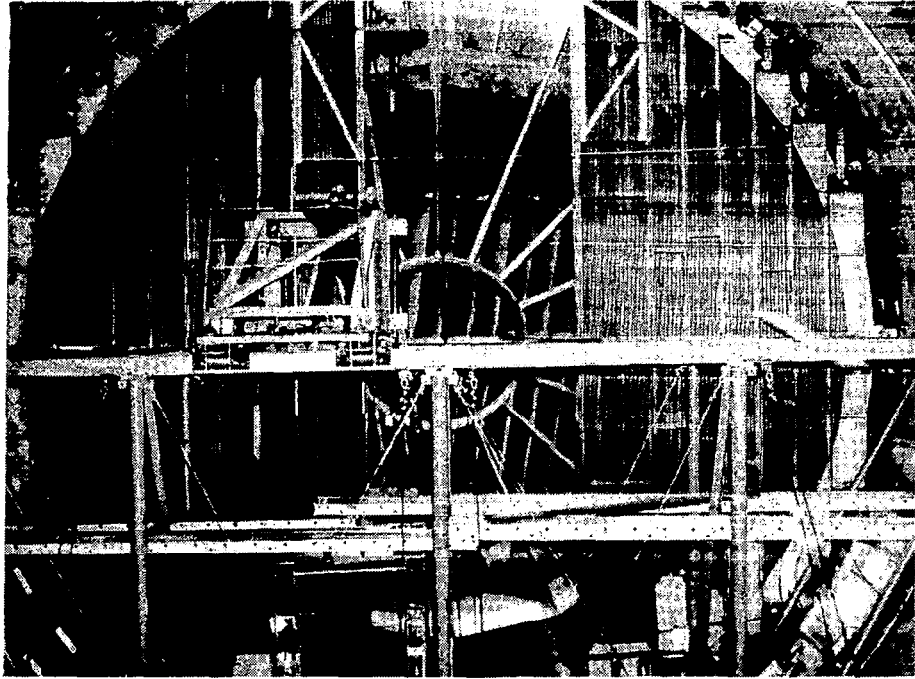


Figure 19.- Cooling-coil installation.

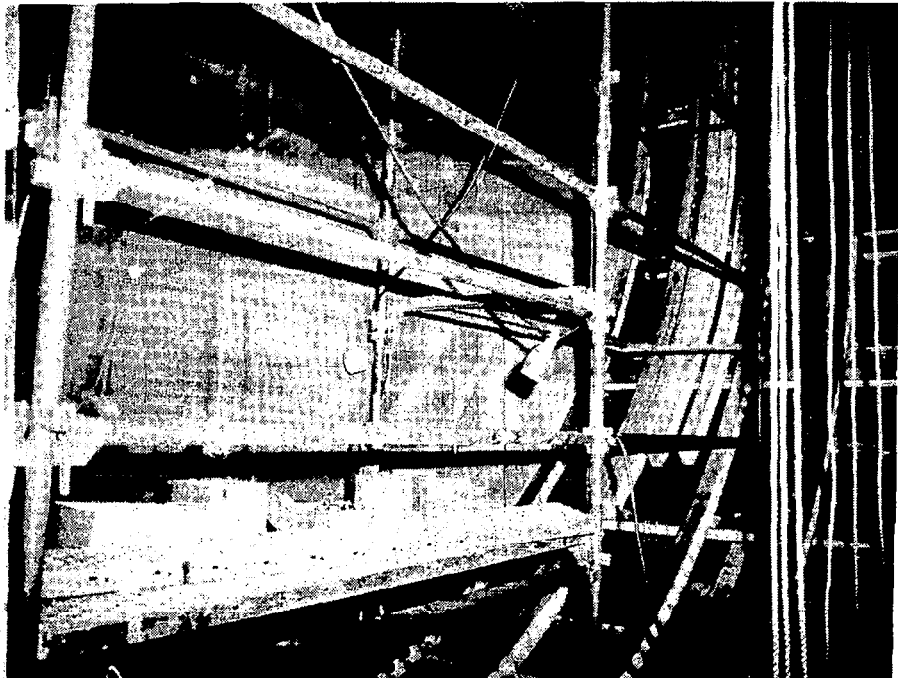


Figure 20.- Screen installation.

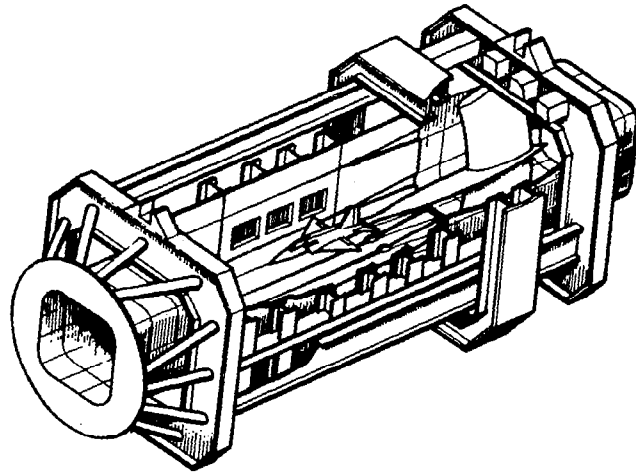


Figure 21.- Fixed contraction, test section, and model support section.



Figure 22.- Slotted-wall test section.

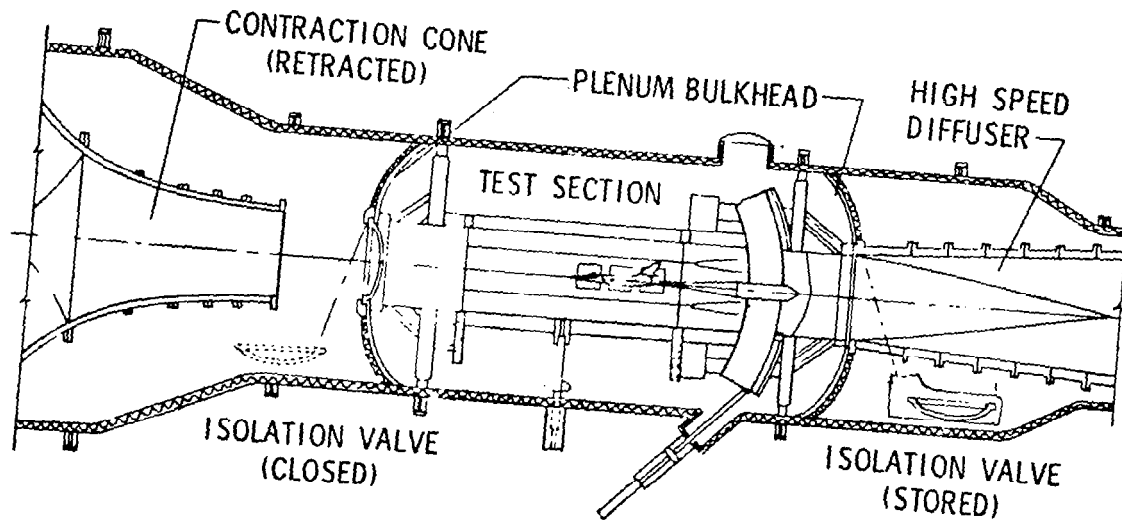


Figure 23.- Plenum isolation system.

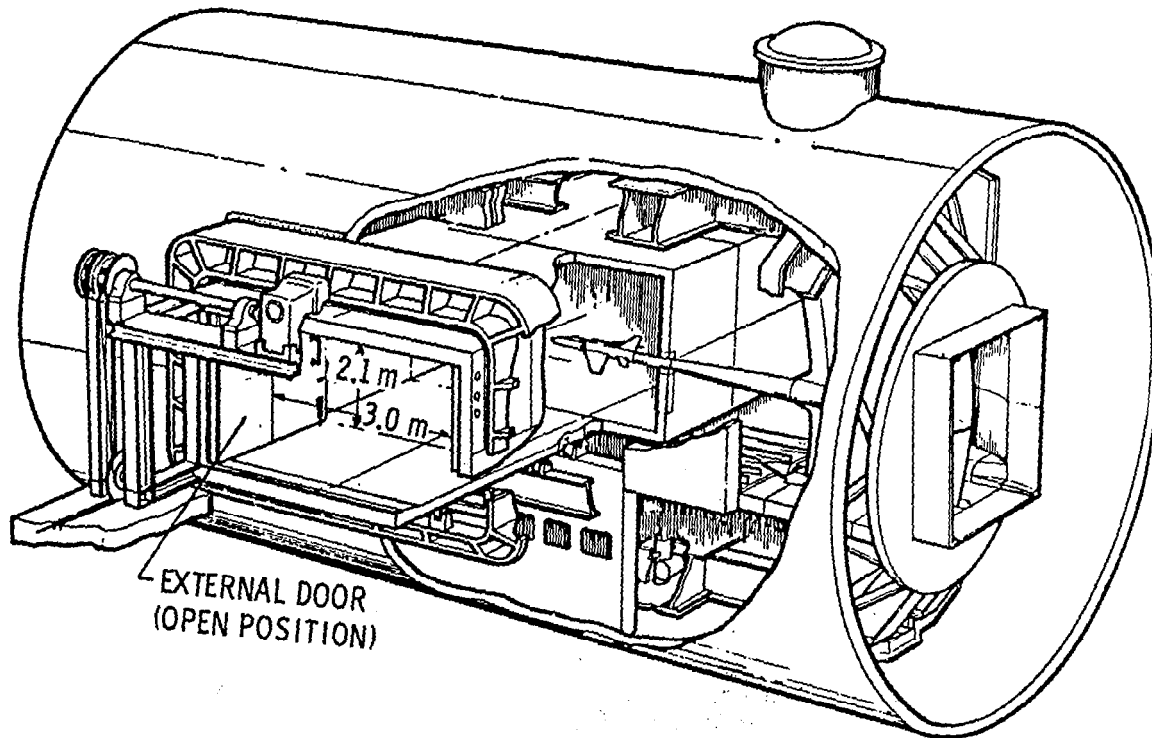


Figure 24.- Model access system.

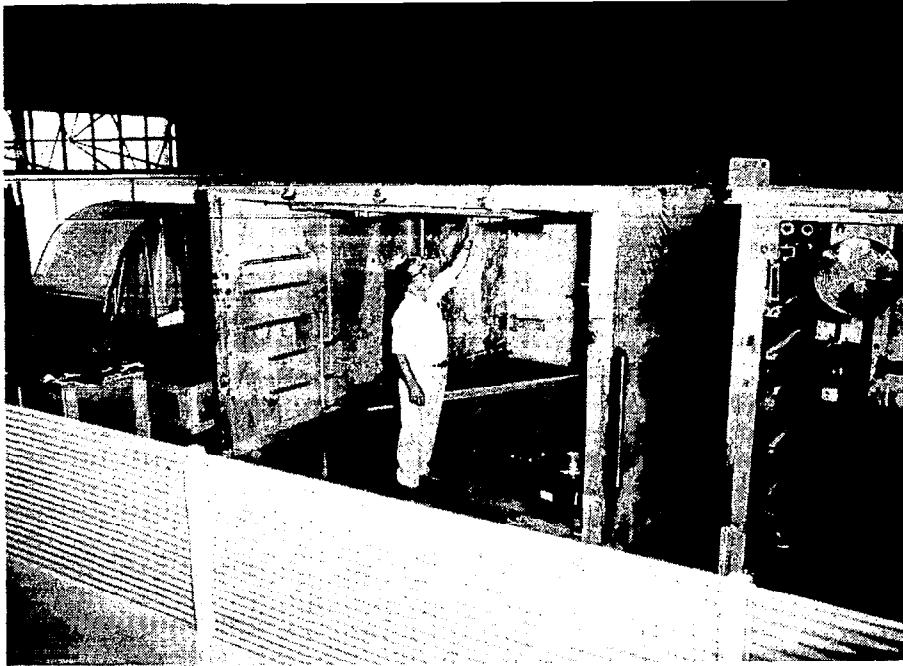


Figure 25.- Partially completed model access housing.

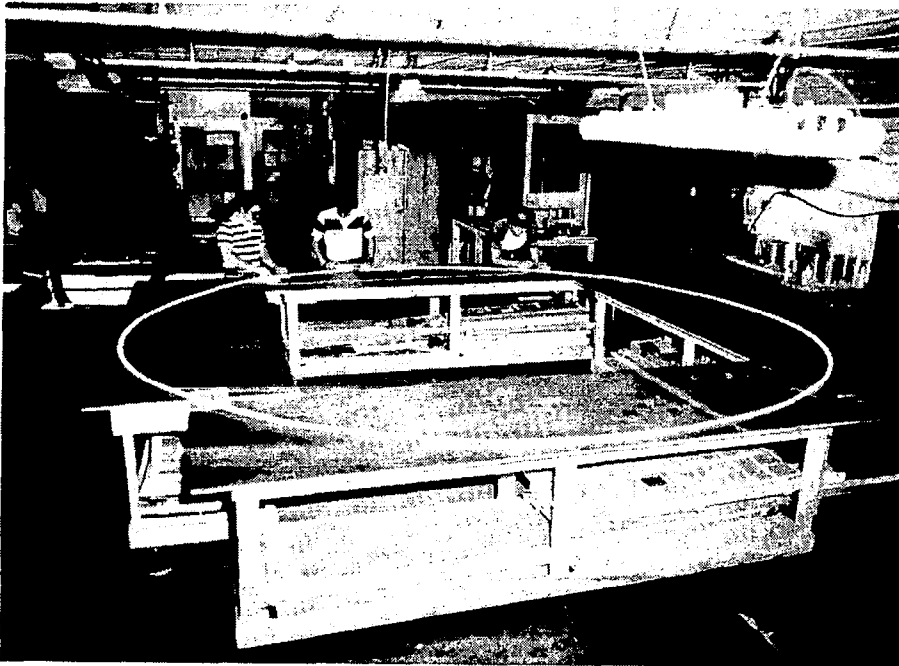


Figure 26.- Teflon cryogenic seal.



Figure 27.- Installation of internal insulation.

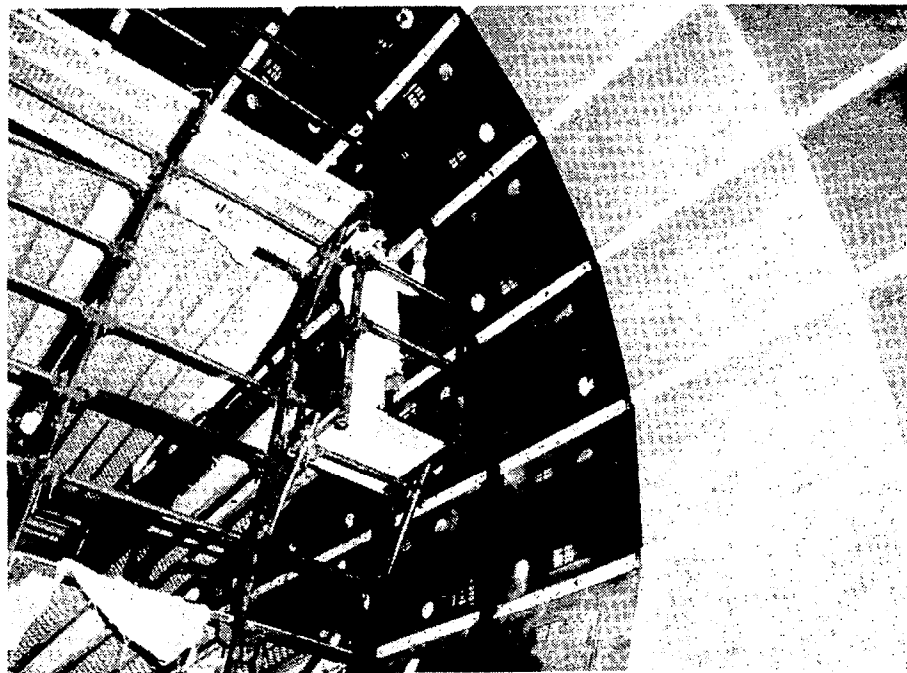


Figure 28.- Internal insulation with aluminum liner.

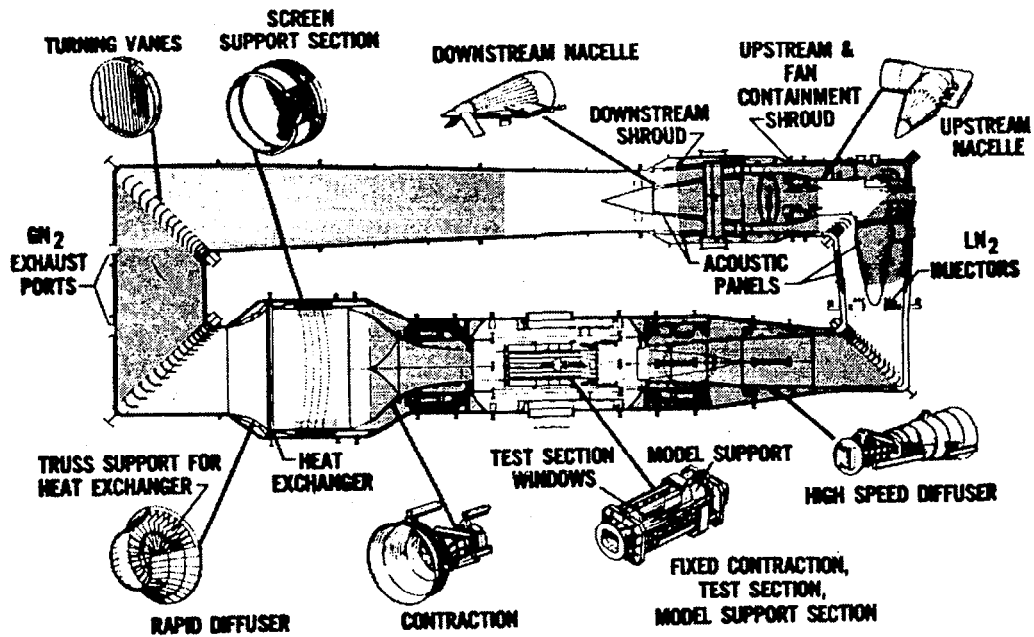


Figure 29.- Sketch of circuit plan view showing insulation progress.

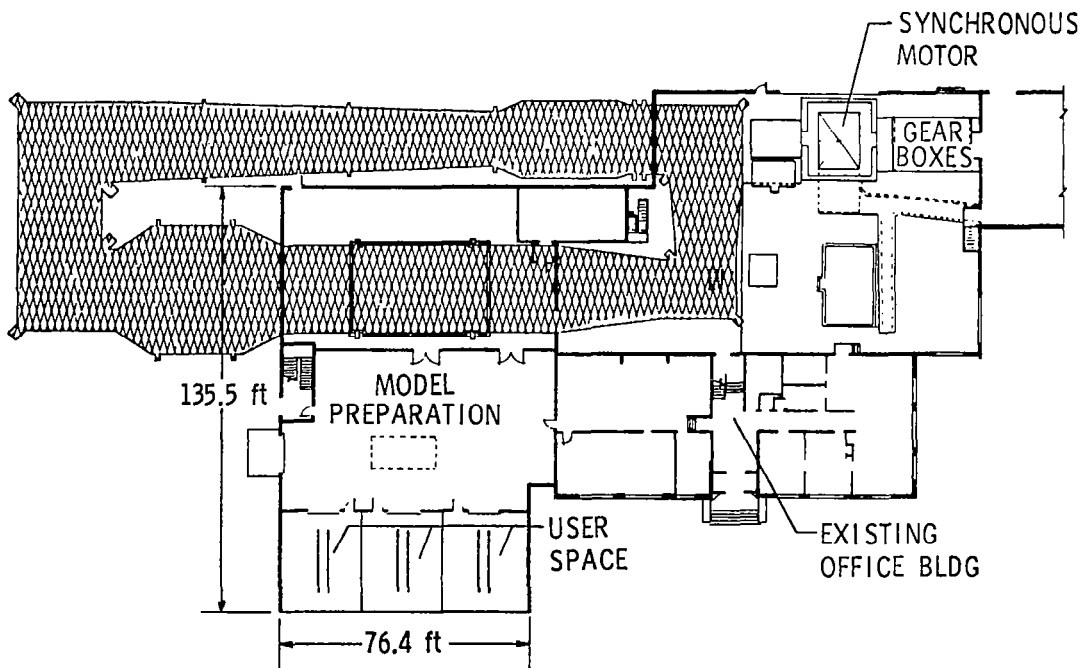


Figure 30.- Sketch showing first-floor plan of building addition.

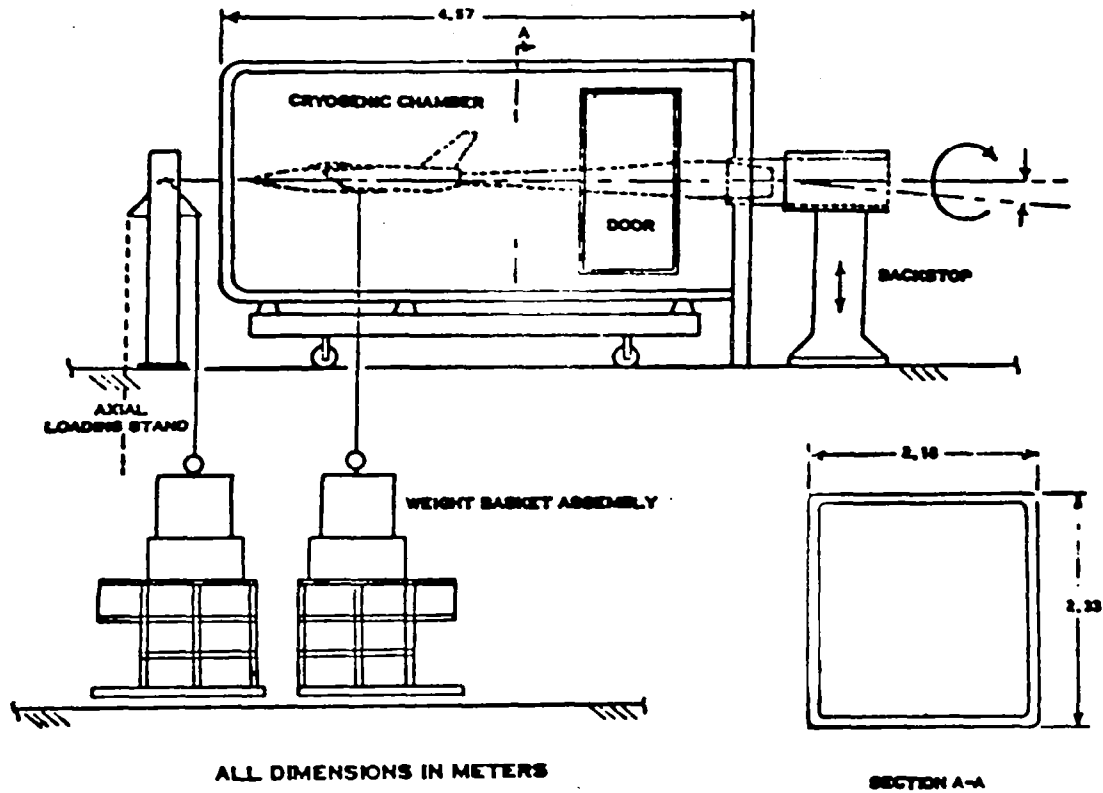


Figure 31.- Model checkout equipment.

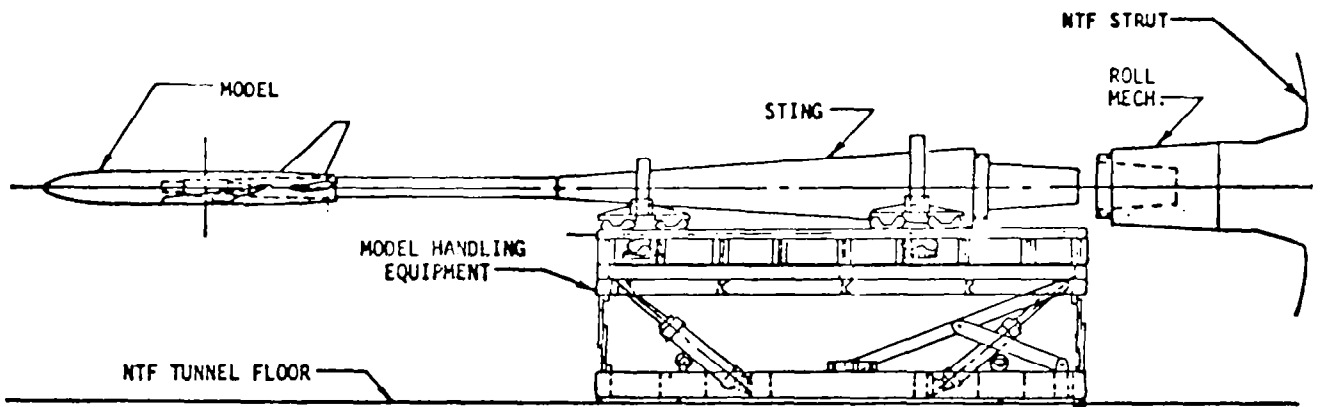


Figure 32.- Sketch of model handling cart for within-building transportation.

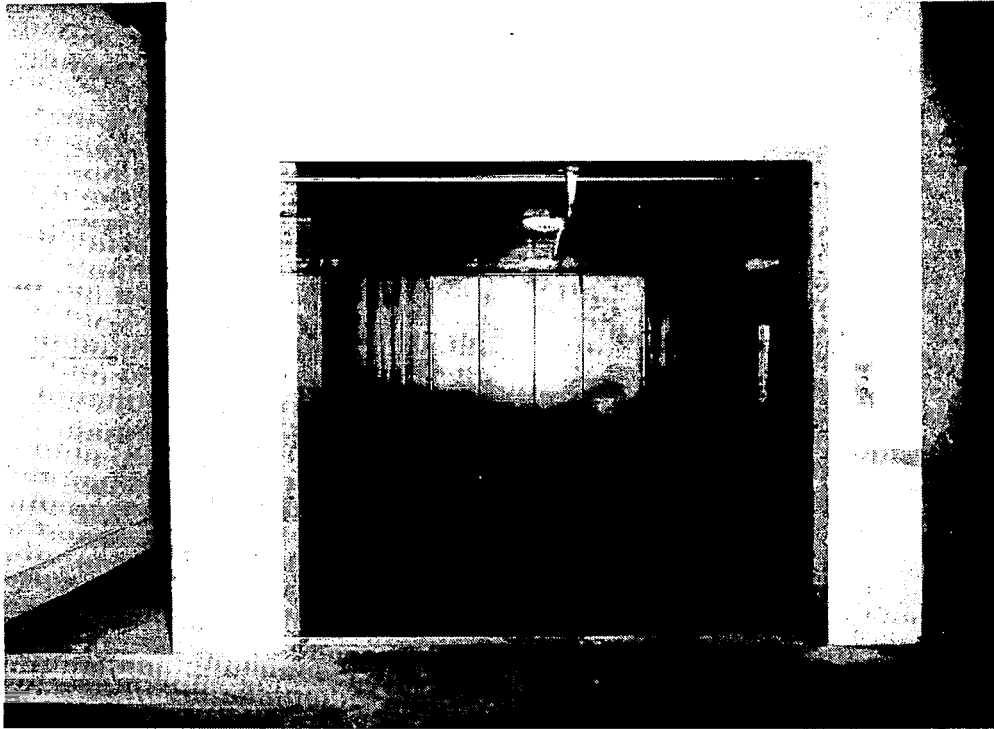


Figure 33.- Service elevator for model transport from build-up area to test section.

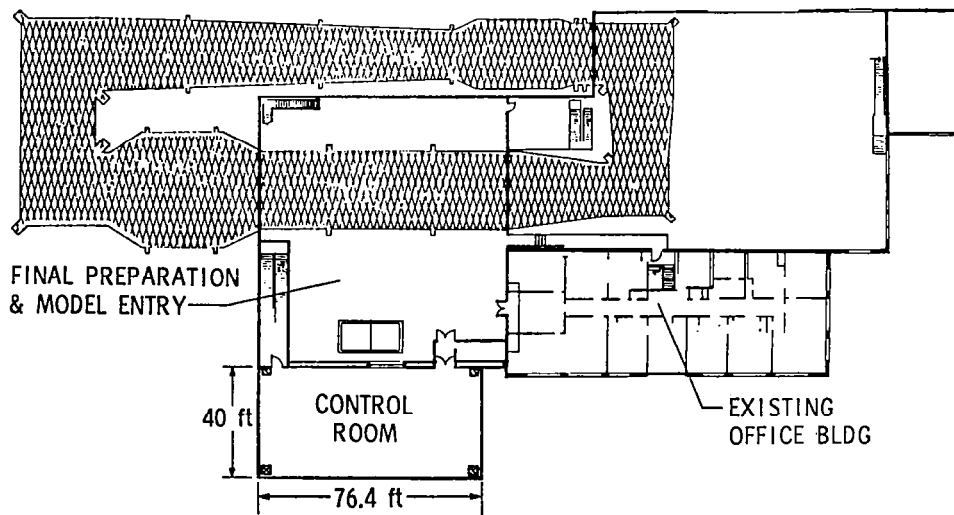


Figure 34.- Sketch showing second-floor plan of building addition.

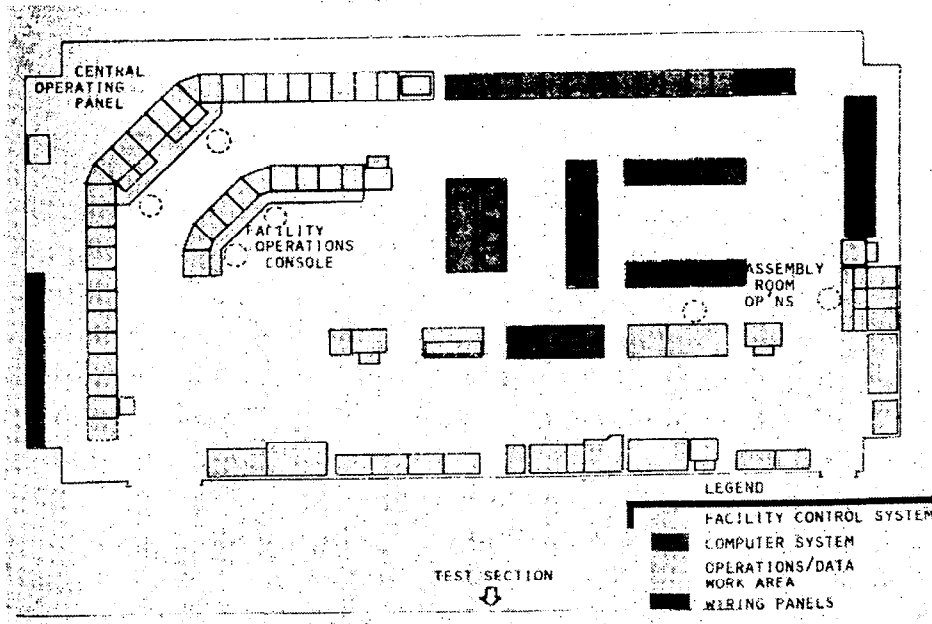


Figure 35.- NTF control-room layout.

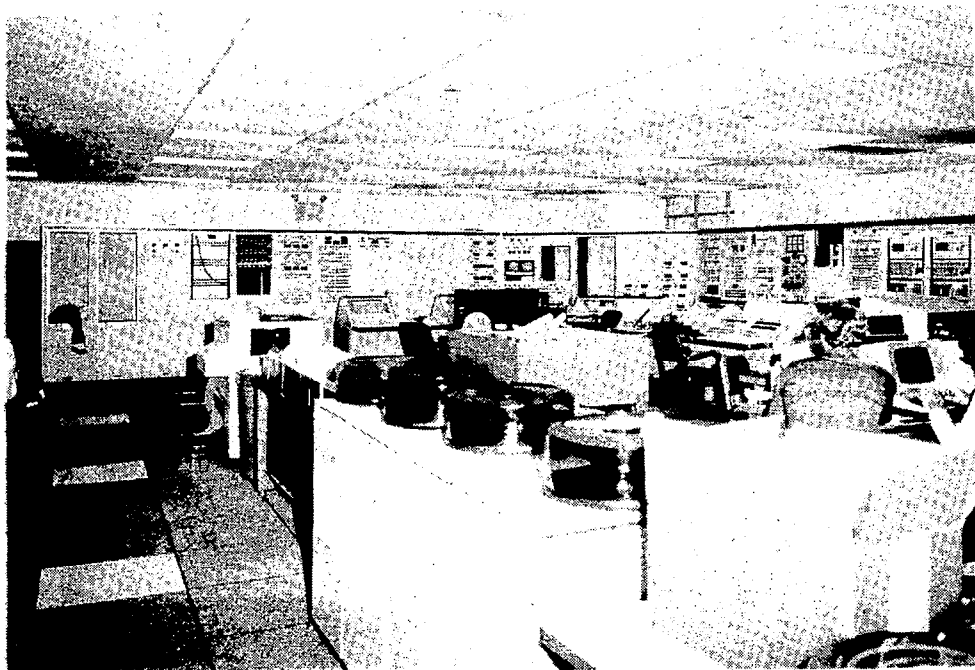


Figure 36.- Photograph of control room showing operation panels.



Figure 37.- Photograph of control room showing computer system.

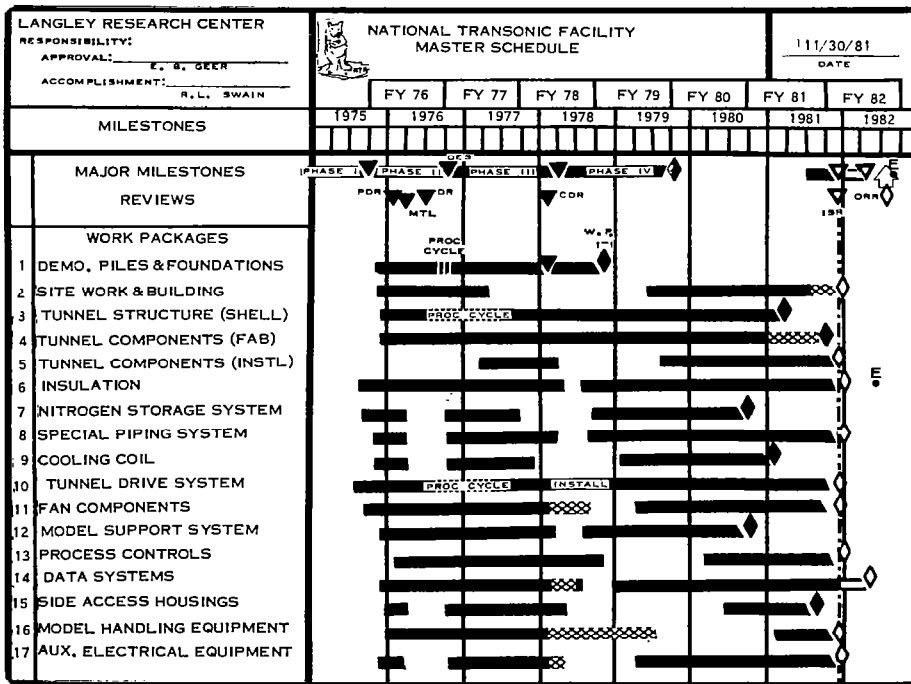


Figure 38.- Master schedule for the National Transonic Facility.

1

1

REVIEW OF THE 1980 WIND-TUNNEL/FLIGHT CORRELATION PANEL

Theodore G. Ayers
NASA Ames Research Center
Dryden Flight Research Facility

MINIWORKSHOP ON WIND-TUNNEL/FLIGHT CORRELATION

November 19-20, 1981

INTRODUCTION

In order to remain brief, I have elected to use only summary word charts to review the 1980 Wind-Tunnel/Flight Correlation Panel Report. The complete report of that panel is included in reference 1. As a preface to this review, I would like to show some information that I have extracted from a paper presented at the joint AIAA/SETP/SFTE/SAE/ITEA/IEEE First Flight Testing Conference in Las Vegas (1981). The information was presented by Ed Saltzman and is reported in reference 2. This paper is by no means comprehensive, however, it does point out some significant aspects of correlation. The information shown in figure 1 spans some 35 years of correlation history beginning with the P-51 and ending with the F-8 supercritical wing. The point to be made from this information is that although significant strides in aerodynamic performance have been made, the researchers continue to be faced with nearly identical discrepancies in predicted versus measured drag. In each of the cases cited, disappointing model to flight comparisons were observed. It is anticipated that the unique capabilities of the National Transonic Facility (NTF) will allow an accurate assessment of some of the effects which have heretofore plagued the researchers and aircraft designers.

DISCUSSION

The primary sources of discrepancies relating to figure 1 are summarized in figure 2. These include Reynolds number, wall interference, sting support, and aeroelasticity. The unique capability of the National Transonic Facility to vary Reynolds number and dynamic pressure independently should provide the researcher with a means of separating Reynolds number and aeroelastic effects, something which has not previously been possible. The National Transonic Facility will not eliminate wall interference or sting support effects. However, the NTF has provided a focus for wall interference research, and significant studies are being made to minimize these wall effects through contoured or "smart walls." Sting support effects will continue to be present and, in fact, could become a major source of error in data obtained in the NTF because of high model loads imposed during operation at high dynamic pressures.

The original Workshop on High Reynolds Number Research held in 1976 did not include a panel dedicated to wind-tunnel/flight correlation. This area was addressed by the Configuration Aerodynamics Panel. A brief summary of that panel's recommendations relating to wind-tunnel/flight comparisons is shown in figure 3. The significant point of those recommendations was to avoid attempts at absolute drag measurements because of uncertainties in thrust measurement. Instead, comparisons should be made on the basis of pressure distribution and wake profile measurements. In essence, this implies comparisons of local aerodynamics or aircraft components. In order for such comparisons to be meaningful, the instrumentation for both wind tunnel and flight must be accurate. Therefore, any aircraft chosen to provide flight data for such comparisons must have a precisely calibrated air data system for determining Mach number, dynamic pressure, and free-stream pressure. Accurate instrumentation must also exist for precise angle of attack and sideslip measurements. Finally, measurements of the structural deformation of both the wind-tunnel model and the flight vehicle are mandatory for determining configuration geometry at the conditions for data comparisons.

The 1980 Workshop on High Reynolds Number Research included a Wind-Tunnel/Flight Correlation Panel. This panel consisted of members representing most of the

major airframe manufacturers as well as the U. S. Government (fig. 4). The membership brought to the workshop a broad insight and diverse views relative to the needs in the area of wind-tunnel/flight correlation for validating the National Transonic Facility. At the same time, however, it must be noted that this diversity precluded any consensus relative to the type of configuration to be selected for validating the NTF. More discussion of this subject will follow later in this presentation.

The Wind-Tunnel/Flight Correlation Panel discussed the validation of the National Transonic Facility (NTF) in the order shown in figure 5. The first three items relate to experimental studies which the panel believed to be of primary importance to the aerospace community in determining industry utilization of the NTF. The fourth item addresses an approach to validating the facility.

The panel was unanimous in its concern for providing a complete calibration of the facility prior to conducting any R & D tests (fig. 6). Aircraft operating costs and performance requirements associated with high development and energy costs as well as intense foreign competition are forcing designers to extract the utmost in efficiency from new and/or derivative aircraft. These requirements are manifested in complex systems to provide relaxed static stability and active controls, both flight and propulsion, which continue to push aircraft designs near the limit. As a result, stability and control characteristics are becoming just as important as drag. This means that one must predict with reasonable certainty the stability levels and control requirements for future aircraft. Therefore, the NTF calibration should include a complete mapping of the test section including total- and static-pressure measurements in the longitudinal, lateral, and vertical planes. In addition, dynamic measurements should be made to define the frequency and spectra for turbulence definition and scaling and acoustic environment.

The influence of cryogenic operation on these measurements as well as flow angularities need to be established. Early consideration should be given to conducting tests with the existing 10-degree cone hardware. This hardware has been used to obtain transition Reynolds number data from some 23 wind tunnels throughout the United States and Europe. In addition, flight tests were conducted with the identical hardware to establish the free-air data base for assessing wind-tunnel turbulence effects.

As was the case with the Fluid Dynamics Panel, the Wind-Tunnel/Flight Correlation Panel identified the desirability of providing a longitudinal heat-transfer measurement capability in the cone experiment for NTF. While the 10-degree cone experiment is important in the tunnel calibration, it is equally important to establish unit Reynolds number and heat-transfer effects on the transition location for lifting surfaces. For this reason a two-dimensional airfoil experiment should be considered as part of the NTF calibration.

The major portion of the panel deliberations focused on those areas which were viewed as Reynolds number dependent and therefore required wind-tunnel/flight correlation for validating the NTF. These areas were separated into seven categories (fig. 7). It should be pointed out that because of the makeup of the panel membership it was not possible to arrive at a consensus on the configuration to be used in validating the NTF. Rather it was the opinion of members that configurations representing both attached and vortex flow fighters and military and commercial transports be selected for tests in the NTF. Obviously that would require a large resource investment. Therefore a decision will have to be made by NASA and

the aerospace community as to which configurations will suffice for validation tests.

Wing Cruise Drag and Drag Rise

It was the consensus of the panel that both wind-tunnel and flight data are required to provide detailed pressure distributions, accurate definition of shock wave location, and boundary-layer and wake surveys for determining airfoil section characteristics.

Wing Separation and Stall

These discussions focused on leading-edge and shock-induced separation for both thick and thin wings. The $C_{L_{max}}$ dependence (with and without flaps) on Reynolds number is a major concern in control and Mach buffet.

Afterbody and Base Drag

The prediction of full-scale aircraft drag has historically been hampered by the inability to adequately extrapolate afterbody and base effects. This has been true for fighter aircraft and to a lesser extent for transport aircraft including both commercial and military logistic vehicles. Although model support system interference effects can be a major contributor to afterbody and base drag measurements, the predominant effect is believed to be that of Reynolds number simulation. Model data obtained at flight Reynolds numbers are required to provide for correlation with flight results for airplanes having afterbody and base configurations sensitive to Reynolds number.

Propulsion Effects

Classical fighter aircraft configurations generally have aft fuselage-mounted engines. In these instances, as much as 40 percent of the total vehicle drag can be associated with afterbody effects, including boattail, base, and propulsion-system drag. The advent of high bypass ratio turbofan engines has resulted in large engine-to-wing size ratios which result in large propulsion-system integration effects. It was recognized by the panel that initial configuration testing in the NTF will not address propulsion-system integration effects. However, it was strongly recommended that early planning be initiated to provide the capability for propulsion testing in the NTF. The need for wind tunnel and flight data correlation was recognized by all panel members.

Vortex Flows

The panel identified forebody vortex shedding, vortex bursting, and structural loads as areas susceptible to Reynolds number effects. In view of the complexity and uncertainty of vortex flow interference and nonlinear aerodynamic effects, and the probability that many future aircraft will employ some version of the vortex

lift concept, it is important to provide wind-tunnel/flight correlation for validating the full-scale simulation capability of such flows in the NTF.

Cavity Flows

It is an extremely difficult and many times impossible task to predict the unsteady aerodynamics associated with cavity flows such as landing gear wells and open bomb-bay areas of full-scale aircraft. The loads associated with landing gear wells can have significant structural implications. In the case of bomb-bay cavities, the unsteady flow not only has structural implications, but is also a major factor affecting weapons separation. The NTF will provide a capability for obtaining data at or near flight Reynolds numbers and full-scale validation is strongly recommended.

Excrescences

The continuing need for a data base from which to predict excrescence drag was recognized by the panel. While there may be instances where the NTF can and will be used to determine excrescence drag, it was agreed that such tests should generally be done in other facilities.

The recommendations of the 1980 Wind-Tunnel/Flight Correlation Panel were divided into five areas (fig. 8).

Open-Ended Flight/Wind-Tunnel Program

The experience gained from previous attempts at correlating wind-tunnel and flight data clearly suggests a need for retaining the ability to retest configurations, both in the wind tunnel and in flight. The implication of this is that both the wind-tunnel models and the full-scale airplane should be retained in their correlation configurations until the final analysis is complete and all questions have been satisfactorily addressed.

Fighter and Transport Aircraft Category Required

Because of the diversity of the organizations represented by the panel members, it was not possible to achieve consensus for one representative configuration for conducting a wind-tunnel/flight correlation to validate the NTF. Therefore, a recommendation was made to pursue wind-tunnel/flight correlation in both fighter and transport categories. The fighter category should include both attached-flow and separated-vortex-flow wing designs. The transport category should include configurations having low-wing arrangements with gentle afterbody slopes and high-wing arrangements with steep afterbodies. Finally, a configuration such as the Space Shuttle orbiter should be included, if possible, in the overall correlation.

Total Drag Correlation Not Advisable

The Configuration Aerodynamics Panel of the High Reynolds Number Research Workshop held at Langley Research Center in 1976 strongly recommended that attempts

at total drag correlation be discouraged. This position was generally supported by the 1980 Wind-Tunnel/Flight Correlation Panel. Developing an understanding of component effects is the area in which wind-tunnel/flight correlation can best be accomplished in the near future. Such an approach will also provide an acceptable validation of the full-scale simulation capability of the NTF.

Wind-Tunnel/Flight Correlation Team Essential

The question of how best to accomplish the required correlations for validating the NTF was discussed in considerable detail. The use of previously obtained data from configurations such as the C-5A, C-141, and Transonic Aircraft Technology (TACT) was pursued at length. An attitude of pessimism about the usefulness of these data generally prevailed among the panel members. The panel made three recommendations; (1) the initiation of new correlation efforts to be accomplished by establishing a dedicated team of government and aerospace community investigators, (2) defining an open-ended non-proprietary wind-tunnel/flight test program, and (3) establishing accountability to assure that the correlation and validation of the NTF are completed. The dedicated team of investigators should be encouraged and, if possible, required to interact in all aspects of the correlation effort.

Accountability

The subject was discussed because of a general belief that very little feedback had been provided from the 1976 High Reynolds Number Research Workshop. There was unanimous agreement among the panel members that some method of accountability should be established to insure that action is taken by NASA to consider and/or carry out the recommendations of all panels. It was also recommended that the Wind-Tunnel/Flight Correlation Panel reconvene at an appropriate time (perhaps annually) to provide the necessary and desirable interaction with the NTF staff. The fact that this miniworkshop is taking place can be viewed as a positive reaction to our 1980 recommendation.

REFERENCES

1. Baals, Donald D., ed.: High Reynolds Number Research. NASA CP-2183, 1980.
2. Saltzman, Edwin J., and Ayers Theodore G.: A Review of Flight To Wind Tunnel Correlation. AIAA 81-2475, Nov. 1981.

Aircraft	Decade	Discrepancy	Apparent cause
P 51	Mid-1940's	Flight drag after pullout higher than for model	Different separation locations
X-5	Early 1950's	Drag difference at Mach 1, though the same at drag divergence Mach number	Chubby body, different separation locations
M-2/F-3	1960's	Base drag and boattail drag	Sting and different separation location
X-15	1960's	Base drag	Sting-affected base pressure
XB-70	Late 1960's	Model drag too low at Mach 1.18	
F-8 super-critical wing	Early 1970's	2nd-velocity peak larger and farther aft in flight	Tunnel wall effects

Figure 1.- Summary of wind-tunnel/flight discrepancies.

- REYNOLDS NUMBER EFFECTS
- WALL-INTERFERENCE EFFECTS
- STING-SUPPORT EFFECTS
- AEROELASTIC EFFECTS

Figure 2.- Primary sources of discrepancies.

NTF MODEL-TO-FLIGHT COMPARISONS

- AVOID ABSOLUTE DRAG COMPARISONS BECAUSE OF THRUST MEASURING UNCERTAINTIES
- BASE COMPARISONS ON
 - (A) PRESSURE DISTRIBUTION MEASUREMENTS
 - (B) SECTION DRAG FROM WAKE PROFILE MEASUREMENTS
- THE AIRCRAFT CHOSEN FOR THIS TASK MUST HAVE
 - (A) A PRECISE, CALIBRATED, "AIR-DATA" SYSTEM FOR DEFINITION OF M, q, AND P
 - (B) PRECISE α AND β DATA
- STRUCTURAL DEFORMATION MEASUREMENTS ARE MANDATORY FOR BOTH MODEL AND AIRCRAFT

Figure 3.- Recommendations of 1976 Configuration Aerodynamics Panel.

CHAIRMAN
TECHNICAL SECRETARY

THEODORE G. AYERS
THOMAS C. KELLY
GWU/JIAFS

JOSEPH D. CADWELL	DOUGLAS AIRCRAFT COMPANY
JAMES F. CAMPBELL	NASA LARC
JAMES M. COOKSEY	VOUGHT CORPORATION
ROBERT O. DIETZ	SVERDRUP/ARO, INC.
E. DABNEY HOWE	NORTHROP CORPORATION
LOWELL C. KEEL	WRIGHT PATTERSON AFB
AL P. MADSEN	GENERAL DYNAMICS
JAMES G. MITCHELL	ARNOLD AIR FORCE STATION
A. L. NAGEL	THE BOEING COMPANY
ODIS C. PENDERGRAFT, JR.	NASA LARC
JOHN B. PETERSON	NASA LARC
WILLIAM I. SCALLION	NASA LARC

Figure 4.- Membership of 1980 Wind-Tunnel/Flight Correlation Panel.

- BASIC TUNNEL CALIBRATION
- ESTABLISH CONFIDENCE IN TUNNEL
- AREAS OF CONCENTRATION
- RECOMMENDATIONS

Figure 5.- 1980 Wind-Tunnel/Flight Correlation Panel discussion summary.

THOROUGH CALIBRATION OF TEST SECTION

- PRESSURE
- TURBULENCE
- ACOUSTICS
- FLOW ANGULARITIES

Figure 6.- Requirements for NTF calibration.

- WING CRUISE DRAG AND DRAG RISE
- WING SEPARATION AND STALL
- AFTERBODY AND BASE DRAG
- PROPULSION EFFECTS
- VORTEX FLOWS
- CAVITY FLOWS
- EXCRESCENCES

Figure 7.- Areas of concentration.

- OPEN-ENDED FLIGHT/WIND-TUNNEL PROGRAM
- FIGHTER AND TRANSPORT AIRCRAFT CATEGORY REQUIRED
- TOTAL DRAG CORRELATION NOT ADVISABLE
- WIND-TUNNEL/FLIGHT CORRELATION TEAM ESSENTIAL
- ACCOUNTABILITY

Figure 8.- Recommendations from 1980 Wind-Tunnel/Flight Correlation Panel for validating the NTF.

WIND-TUNNEL/FLIGHT-DRAG CORRELATION

John H. Paterson
Lockheed-Georgia Company
Marietta, Georgia

Miniworkshop on Wind-Tunnel/Flight Correlation
November 19-20, 1981

CORRELATION OF PREDICTED AND FLIGHT-TEST DRAG ON THE C-5A
AT A MACH NUMBER OF 0.7

Correlation of aerodynamic drag between predictions based on wind-tunnel data and flight measurements is subject to numerous sources of error, and rigorous efforts are required in wind-tunnel tests, prediction methods, and flight measurements to achieve acceptable results. The following figures illustrate results achieved on the C-5A and C-141A airplanes.

Figure 1 illustrates the correlation achieved between the predicted and flight-test drag on the C-5A at a Mach number of 0.7. Three prediction techniques are shown representing different methods of calculating profile drag. The first method uses flat-plate skin-friction coefficients corrected by form factors based on measured pressure distributions. The other two methods are based on subsonic viscous theory. The correlation is quite good, particularly at cruise lift coefficient where there is excellent agreement between the empirical prediction and the flight measurements.

SYMBOL

- FLT TEST DATA FOR $0.65 < M_{TEST} < 0.725$
- FLT TEST DATA FOR $0.6 < M_{TEST} < 0.762$
- FAIRED FLT TEST MEAN LINE
- - - FULL-SCALE ESTIMATE BASED ON WIND-TUNNEL DATA

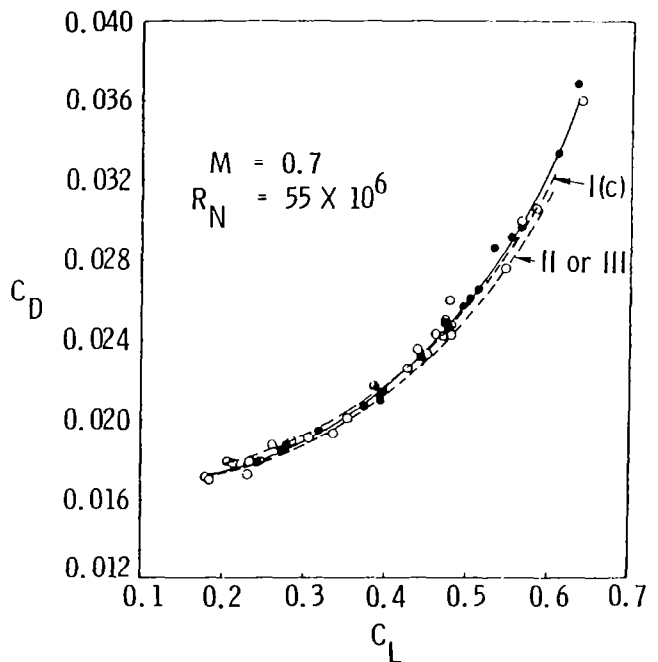


Figure 1

CORRELATION OF C-5A PREDICTED AND FLIGHT-TEST PROFILE DRAG

The correlation of airframe profile drag is shown in figure 2. Agreement of C_{DP} is within ± 1 percent for Method I(c) and ± 3 percent for Method II. There is a slight difference in the lift coefficients for a minimum profile drag of about 0.025. The variation of profile drag with lift coefficient is generally in close agreement over the C_L range from 0.2 to 0.45. The discrepancies at higher values of C_L must be viewed as accumulated errors in either flight-test data, where the high C_L range exhibits greater scatter, or in further unknown errors in the wind-tunnel data, such as support-interference inaccuracies, transition fixing, or tunnel flow and interference effects. The agreement in values of $C_{DP_{min}}$ and the lift-dependent profile drag is, nevertheless, considered quite good.

$$M = 0.7$$

$$R_N = 55 \times 10^6 / MAC$$

—○— FLIGHT-TEST DATA-EQUIVALENT RIGID C_{DP}

NORMALIZED TO $R_N = 55 \times 10^6 / MAC$ AND $M = 0.7$
 FOR DATA POINTS WHERE $0.65 < M_{TEST} < 0.725$

— — FULL-SCALE ESTIMATE BASED ON WIND-TUNNEL DATA

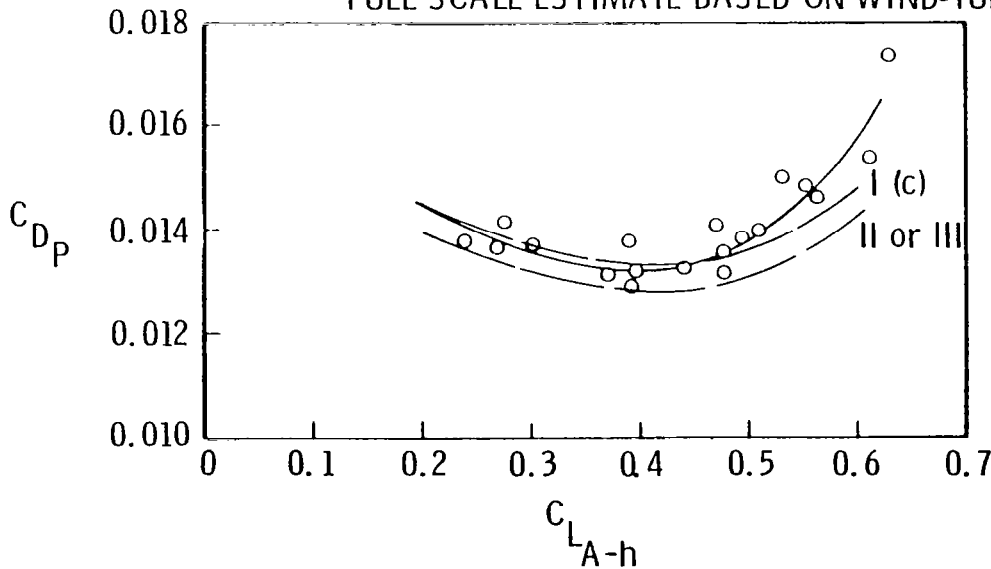


Figure 2

CORRELATION OF C-5 EQUIVALENT RIGID FLIGHT-TEST PROFILE DRAG
WITH THE RIGID ESTIMATE BASED ON WIND-TUNNEL DATA

The effect of Reynolds number on the rigid airplane minimum profile drag is shown in figure 3 compared to a prediction based on wind-tunnel data with extrapolation based on using Method I(c) to compute profile drag. Agreement is excellent. Use of subsonic viscous theory would result in a slightly larger scale correction, and agreement would not be as good. Statistical analyses of these data show that the scatter in the flight-test data averages $\Delta C_D = \pm 0.00045$ which represents only ± 3.5 percent of profile drag or about ± 2 percent of total cruise drag.

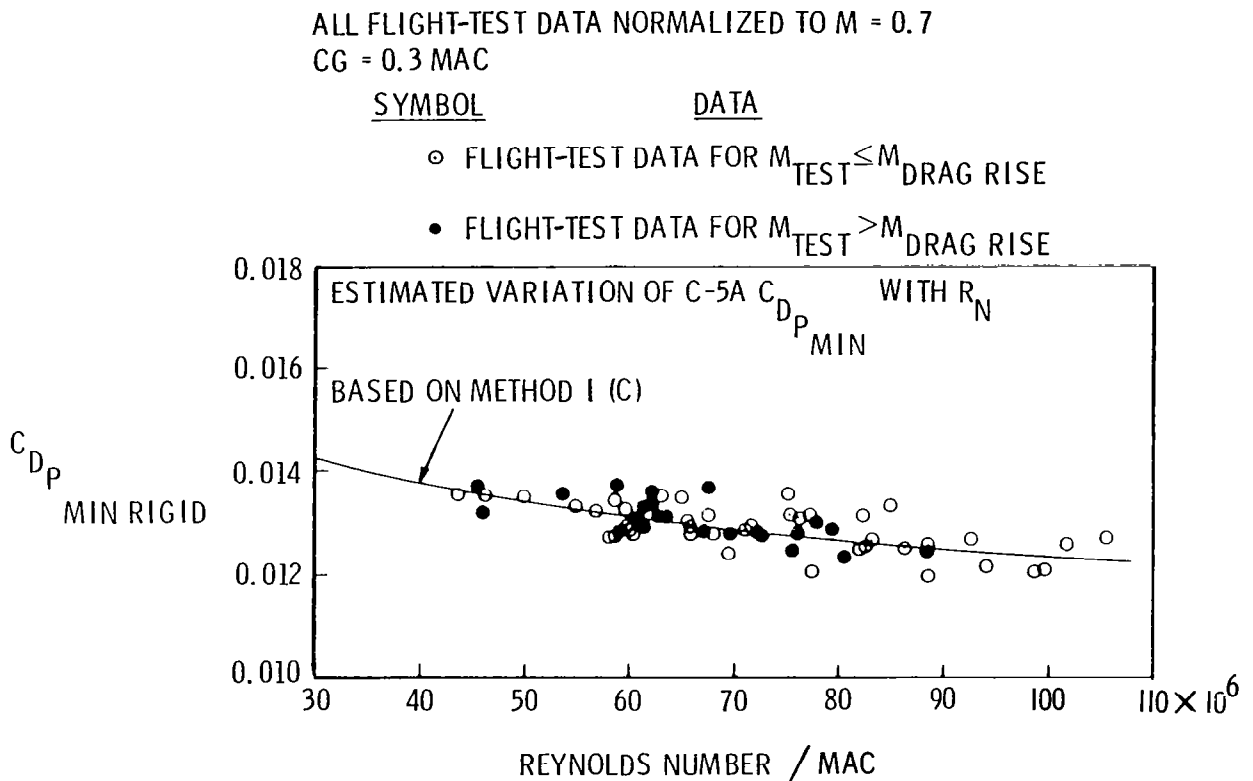


Figure 3

C-5A DRAG-RISE COMPARISON

Figure 4 compares the drag-rise characteristics of the C-5A from wind-tunnel data having fixed transition with flight-test data. Flight characteristics for both the flexible and rigid airplanes are shown, indicating a small difference in drag rise due to flexibility. The agreement in drag-rise Mach number defined as $dC_D/dM = 0.05$ is within a value of ΔM_D of 0.001; however, there is a significant difference in creep drag at Mach numbers below M_D . The favorable reduction in creep drag exhibited by the flight data is attributed in part to a favorable Reynolds number effect on the viscous form drag, because of the method of fixing transition in the wind tunnel, and in part to the complex problems of simulating high Reynolds number flows in mixed-flow conditions.

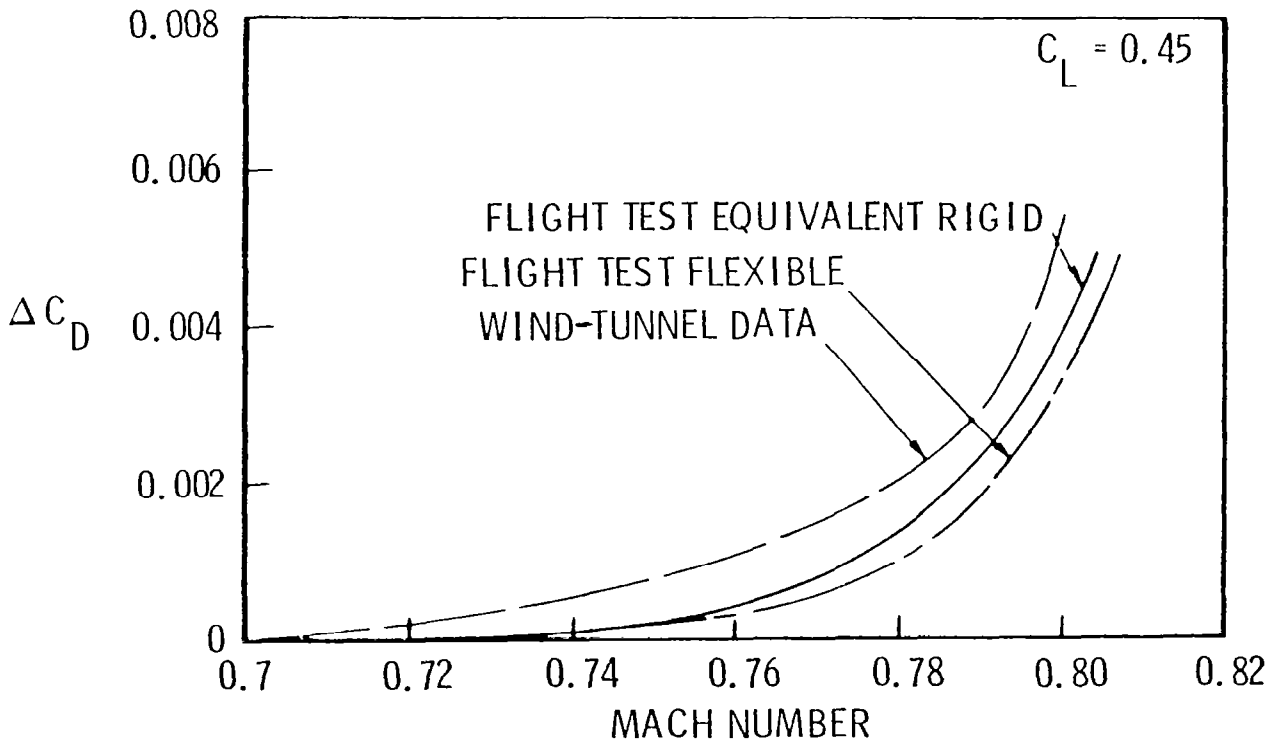


Figure 4

CORRELATION OF C-141 PREDICTED AND FLIGHT-TEST PROFILE DRAG

Another example of wind-tunnel/flight correlation of profile drag is shown in figure 5 for the C-141 airplane. Two sources of wind-tunnel data are presented: The Ames data were obtained before flight test, whereas Langley data were acquired after flight testing was completed. The Langley data show good agreement with the flight data over the C_L range from 0.1 to 0.5. At higher values of C_L the data diverge; disagreement at the higher values of C_L may be attributed to the transition-fixing technique used in the wind tunnel and to the paucity of flight data at high values of C_L . The obvious discrepancy between the Langley and Ames wind-tunnel data is primarily attributable to the method of fixing transition in the Ames test. A wind band of carborundum particles was used in this test, whereas a very narrow band of sparsely applied, Ballottini glass beads was used in the Langley test.

CLEAR SYMBOLS - RIGID FLIGHT-TEST DATA

- LANGLEY DATA CORRECTED TO FULL SCALE
- AMES 088 DATA CORRECTED TO FULL SCALE

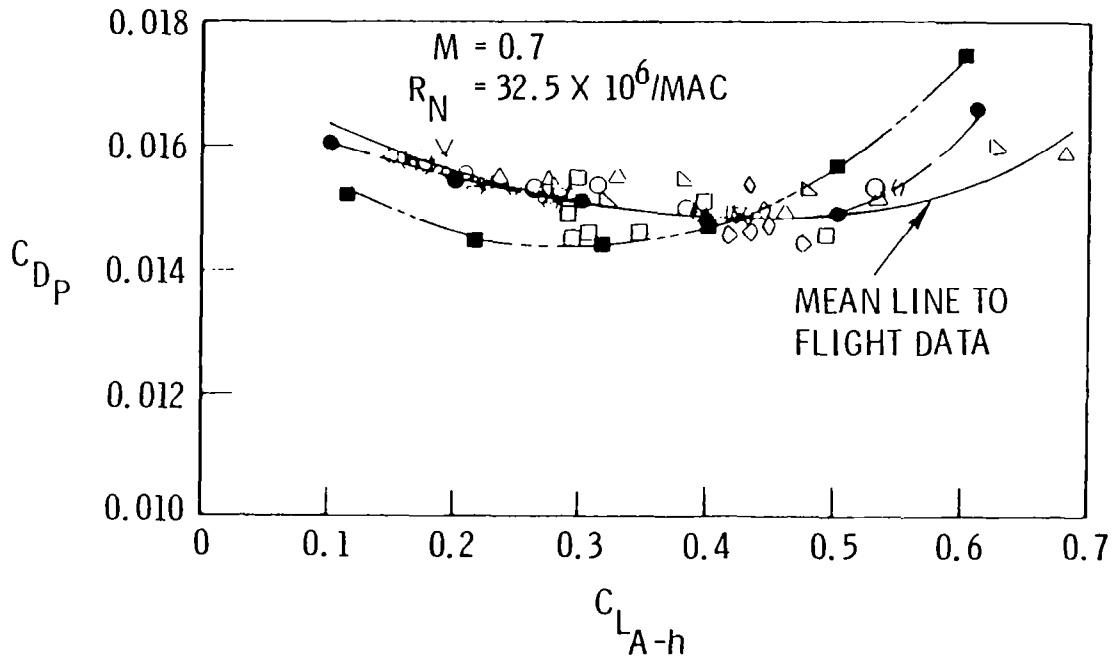


Figure 5

FLIGHT/WIND-TUNNEL CORRELATIONS FOR THE NTF

Scale effects on the occurrence, and the effects, of shock-induced separation have been studied extensively since the revelation on the C-141 that such scale effects can be profound. This work, sponsored by NASA Ames, has resulted in a method for extrapolating low Reynolds number wind-tunnel pressure-distribution data to full-scale flight conditions. When combined with appropriate aeroelastic estimations, this method will provide a proper prediction of flight-load distributions.

Figure 6 illustrates the magnitude of potential changes in upper surface load distribution as they were observed on the C-141. Separation aft of the shock at low Reynolds number results in a large change in shock location and, therefore, in large changes in lift and pitching moment.

Wing Chordwise Pressure Distribution

C-141
 $M = 0.82$
 $\eta = .389$
 $\alpha = 0^\circ$

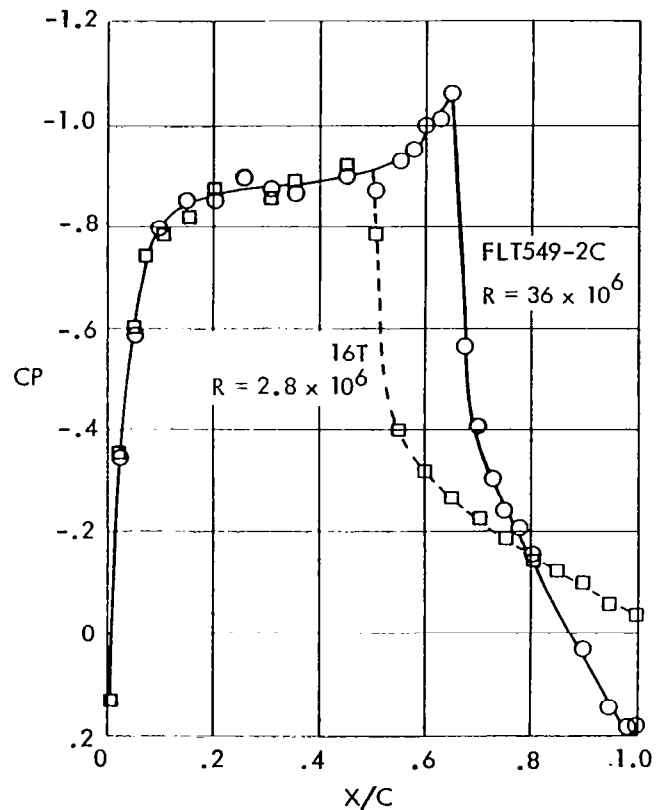


Figure 6

VARIATION WITH MACH NUMBER, α , AND A CORRELATION PARAMETER

In figure 7, the plot on the left shows the variation in trailing-edge pressure recovery as measured at a Reynolds number of 10.4 million. Not only does the pressure recovery vary considerably with both Mach number and angle of attack but this whole array changes with each change in Reynolds number.

The plot on the right shows the same data plotted against a correlation parameter which has been found to collapse these data into a single curve. Similar correlations for a number of different wings have demonstrated that data for each Reynolds number collapse into a similarly shaped curve and that the effect of Reynolds number change is simply to shift the location of that curve.

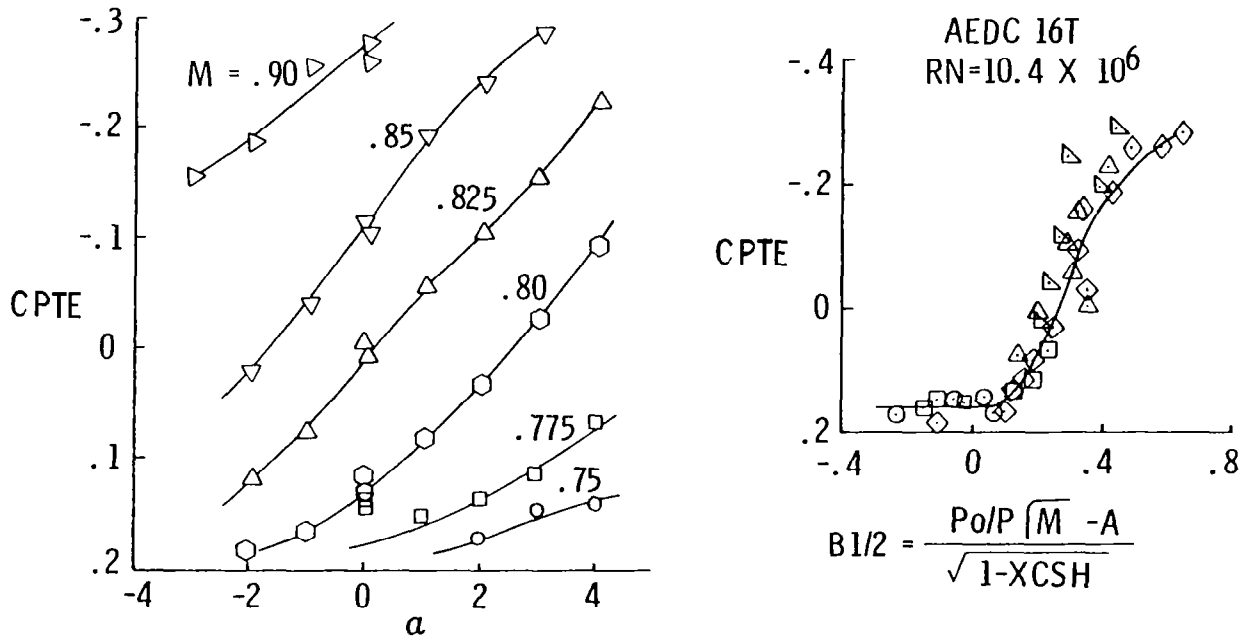


Figure 7

ILLUSTRATION OF SCALE EFFECTS

Figure 8 demonstrates the manner in which the correlated data vary with Reynolds number. Traces of constant angles of attack show that a wide variety of shapes of scale-effect curves can result from the peculiar shape of these plots.

The effect of changes in Reynolds number can be shown quantitatively by plotting values of the correlation parameter $B_l/2$ (such as those indicated by tics on this plot) against Reynolds number. Vertical shifts of the curves can be illustrated in a similar way by plotting values of the plateau level of pressure recovery against Reynolds number.

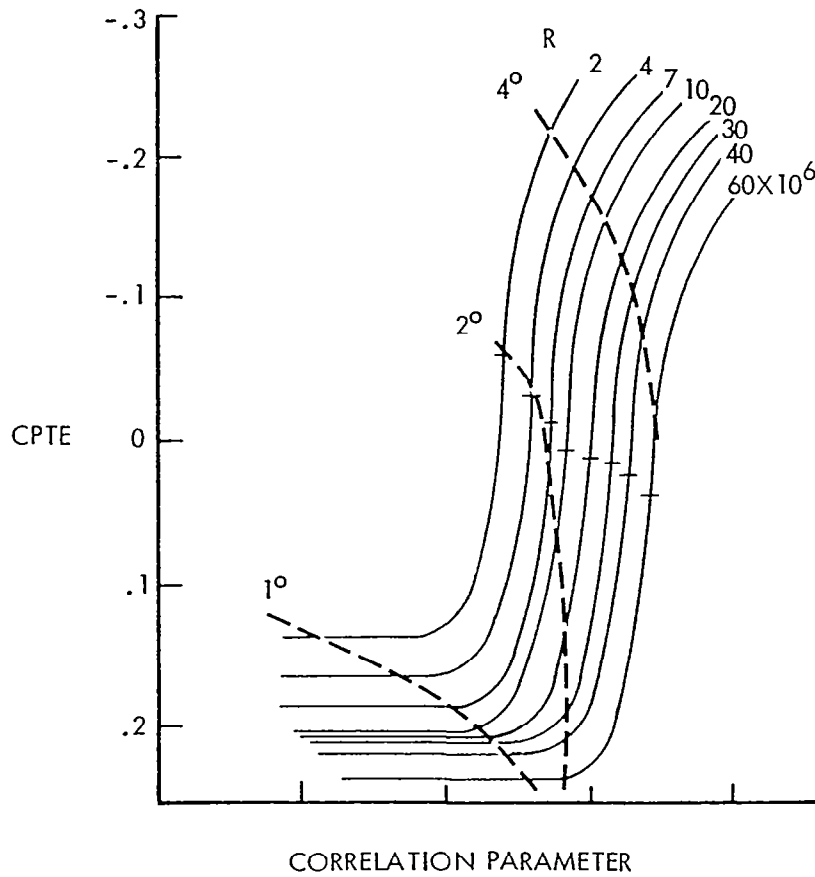


Figure 8

COMPOSITE SCALE EFFECT

Figure 9 shows this scale effect for a number of cases which have been analyzed to date. These data show that these changes, from a base value at a Reynolds number of 10 million, all fall rather nicely along a single straight line as a function of the logarithm of chord Reynolds number. This fact is the cornerstone of an extrapolation procedure which is outlined in a subsequent figure.

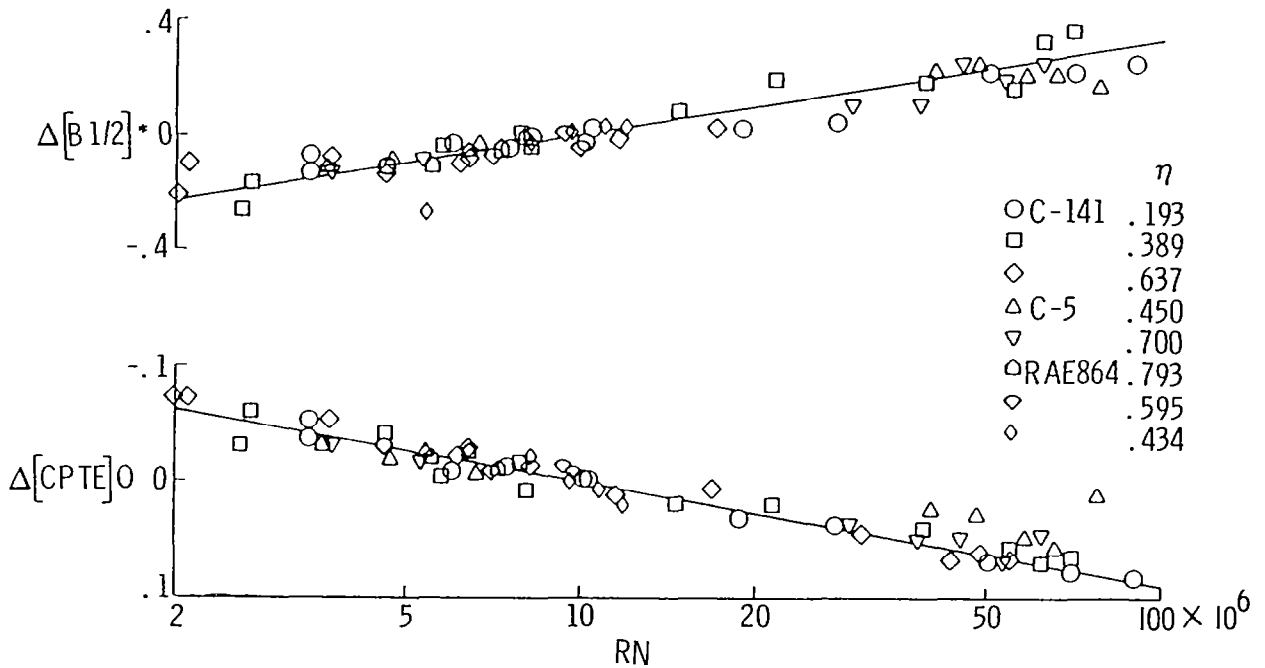


Figure 9

EXTRAPOLATION CONCEPT

The steps involved in extrapolating low Reynolds number data progress from right to left in figure 10. First is illustrated a typical chordwise pressure distribution as measured at low Reynolds number. (Circle symbols on this and other sketches indicate tunnel-measured data.) Next is shown the relationship between shock location and pressure recovery which has been shown to be unaffected by changes in Reynolds number. The correlation of trailing-edge pressure recovery, using the parameter $B_{1/2}$, can be established from the wind-tunnel data, and points on the scale-effect plots can be fixed at the wind-tunnel Reynolds numbers.

The extrapolation now goes back from left to right. By using the previously discussed straight-line scale effect, the key values of $B_{1/2}$ and $CTPEO$ can now be determined for the flight Reynolds number, and the correlation curve can be shifted as indicated by the second sketch. By knowing the trailing-edge pressure, shock location can be determined; and, finally, the complete chordwise pressure distribution is defined at the flight Reynolds number.

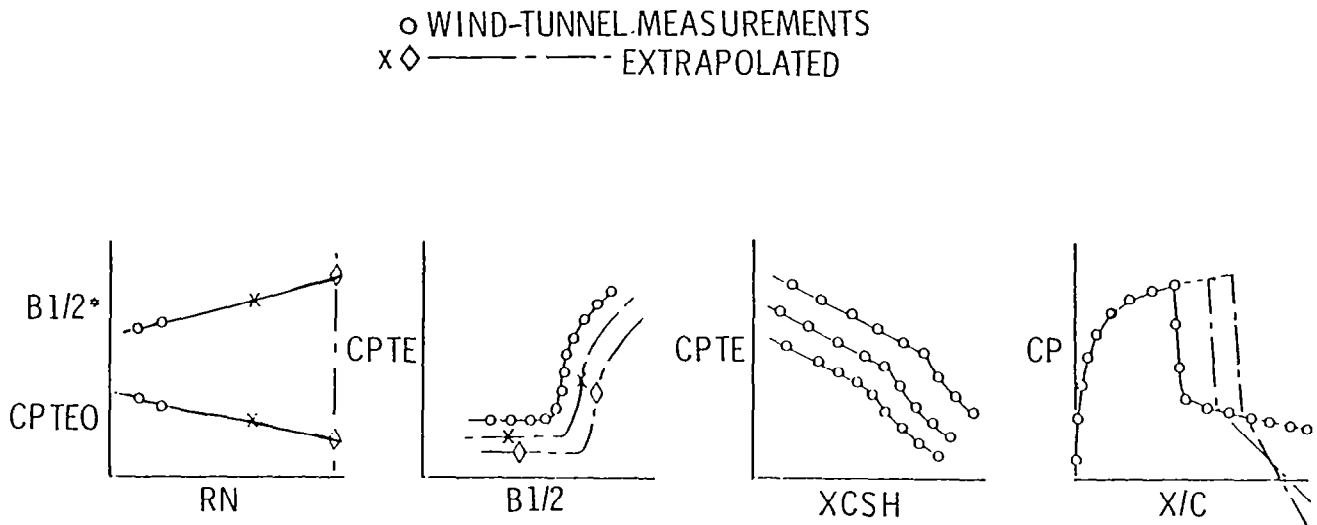


Figure 10

SCOPE OF CORRELATION

This correlation concept has been successfully applied to a wide range of wing designs, including extensive applications of supercritical design principles. (See fig. 11.) No case has been encountered where data on shock-induced separation has failed to collapse into a single curve. (For low-aspect-ratio, high-sweep cases, leading-edge separations may supersede the phenomena being considered.)

Cases for which both wind tunnel and flight data are available are rather scarce, and there is now a search for additional data to support the Reynolds number variation which has been shown.

Work now underway under a contract with NASA Ames has produced an analytical verification of the correlation concept and has led to new correlation parameters which include boundary-layer properties. These new parameters are now being evaluated. A cooperative NASA program has been initiated to test C-141 models in the Ludwig Tube at the Marshall Space Flight Center to provide additional data in the Reynolds number range from conventional wind tunnels to the flight range.

Data are also being made available by NASA from AFT1/F-111 wind tunnel and flight tests to enable this kind of analysis on a wing incorporating full implementation of supercritical design principles.

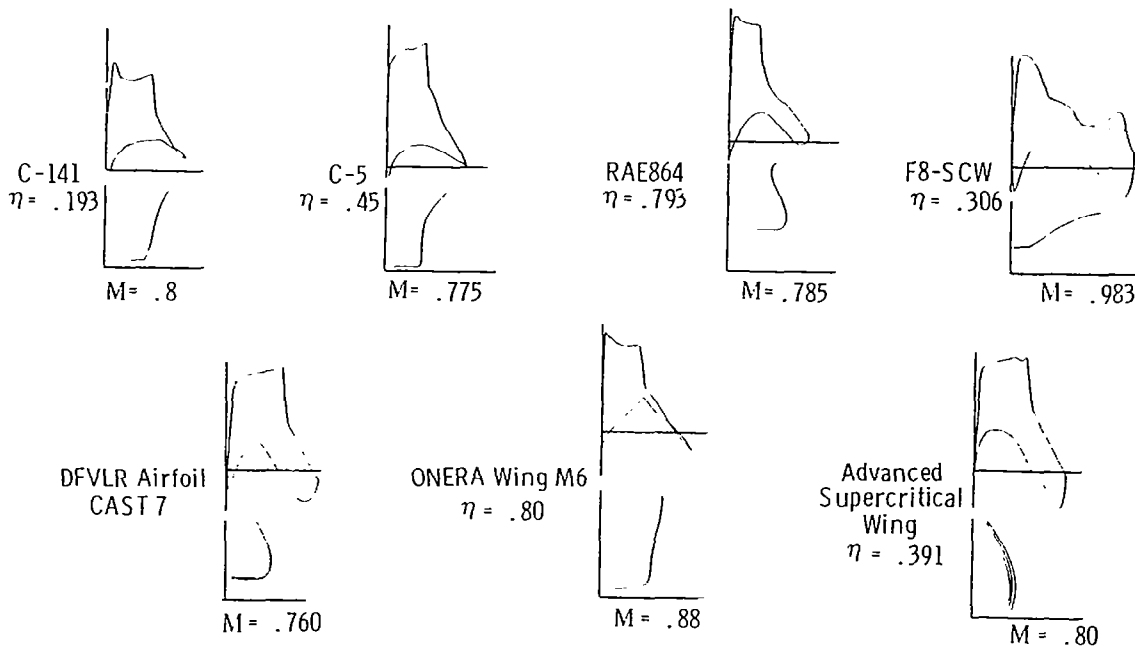


Figure 11

C-141 TRANSONIC SCALING STUDIES

The C-141 configuration has been used for a wide range of transonic scaling studies on both shock-induced separation and cruise drag. (See fig. 12.) The phenomena leading to scale effects are the same as on newer designs. It is an ideal candidate for studies in the NTF.

SHOCK-INDUCED SEPARATION

- NASA-AMES 11' TUNNEL
- NASA-LANGLEY 8' TUNNEL
- AEDC 16T
- CORRELATION AND EXTRAPOLATION STUDIES CR-3178
- FLIGHT TEST
- GELAC CFWT
- NASA-MARSHALL LUDWIEG TUBE

DRAG

- ANALYSIS OF FLIGHT-TEST DATA CR-1558
- DRAG PREDICTIONS, WIND-TUNNEL-DATA ANALYSIS
AND CORRELATION CR-2333
- WIND-TUNNEL TEST AND BASIC DATA CR-2334

Figure 12

BIBLIOGRAPHY

Cahill, J. F.; and Connor, P. C.: Correlation of Data Related to Shock-Induced Trailing-Edge Separation and Extrapolation to Flight Reynolds Number. NASA CR-3178, 1979.

MacWilkinson, D. G.; Blackerby, W. T.; and Paterson, J. H.: Correlation of Full-Scale Drag Predictions With Flight Measurements on the C-141A Aircraft - Phase II, Wind Tunnel Test, Analysis, and Prediction Techniques. Volume 1 - Drag Predictions, Wind Tunnel Data Analysis and Correlation. NASA CR-2333, 1974.

MacWilkinson, D. G.; Blackerby, W. T.; and Paterson, J. H.: Correlation of Full-Scale Drag Predictions With Flight Measurements on the C-141A Aircraft - Phase II, Wind Tunnel Test, Analysis, and Prediction Techniques. Volume 2 - Wind Tunnel Test and Basic Data. NASA CR-2334, 1974.

Paterson, J. H.; Blackerby, W. T.; Schwanebeck, J. C.; and Braddock, W. F.: An Analysis of Flight Test Data on the C-141A Aircraft. NASA CR-1558, 1970.

Paterson, J. H.; MacWilkinson, D. B.; and Blackerby, W. T.: A Survey of Drag Prediction Techniques Applicable to Subsonic and Transonic Aircraft Design. AGARD Conference on "Aerodynamic Drag," Izmir, Turkey, Apr. 1973. AGARD CPP-124 Paper #1.

TUNNEL-TO-TUNNEL CORRELATION

Frank W. Steinle, Jr.
NASA Ames Research Center

Miniworkshop on Wind-Tunnel/Flight Correlations - 1981
November 19-20, 1981

KEY FACTORS IN TUNNEL-TO-TUNNEL CORRELATION

Someone once said, "The difference between theory and practice is that in practice, you can't neglect anything." This is certainly true when correlating data derived from the "same" model tested at different times, much less in different facilities. The first reported correlation effort in the history of the National Advisory Committee for Aeronautics (NACA) is of an international series of tests involving an N.P.L. R.A.F. 15 airfoil model. The report of the U.S. data which were obtained at the Bureau of Standards, the Langley Memorial Aeronautical Laboratory, Massachusetts Institute of Technology, and McCook Field is presented in reference 1. The conclusions presented in this report regarding correlation are still valid today. In attempting not to neglect anything (as indicated in this early report), one can make up a broad list of factors that are the key to correlating results. An abbreviated list is given in figure 1.

KEY FACTORS

- MODEL FIDELITY
- SUPPORT SYSTEM
- INSTRUMENTATION
- DATA REDUCTION
- TEST TECHNIQUE
- FLOW QUALITY

Figure 1

SIGNIFICANT FLOW QUALITY ELEMENTS IN TUNNEL-TO-TUNNEL CORRELATION

A partial list of the more significant flow quality elements are given in figure 2. More recent tests involving a model of the C-5A airplane in the Calspan 8-Foot (formerly Cornell 8-Foot) (8-TWT), Ames 11- by 11-Foot (11-TWT) and AEDC 16T (16-T) Transonic Wind Tunnels are presented in references 2 and 3. Aside from the factors identified in reference 1, the more recent tests identified effects ascribed to the quality of flow in the tunnel. The presentation that follows will focus on those effects. Figures 3 through 13 are taken from reference 3.

FLOW QUALITY ELEMENTS

- FLOW CALIBRATION
- TUNNEL EMPTY GRADIENTS
- BLOCKAGE
- STREAM ANGLE
- LIFT INTERFERENCE
- TUNNEL DYNAMICS
- AERO-ACOUSTICS AND TURBULENCE

Figure 2

INCREMENTAL COMPARISON OF $\Delta\alpha$ AS FUNCTION OF C_N

Figure 3 is basic body axis data showing comparison of incremental angle of attack $\Delta\alpha$ against normal-force coefficient C_N for a wing-fuselage with fixed transition. In this figure, as well as figures 4 through 13 (unless indicated otherwise), incremental quantities are referenced to the average of the results from the three facilities. There is some suggestion of the classical lift interference type of effect. Reduction of the computed angle of attack in the Ames 11-TWT by the estimated value for this model of $-0.05^\circ/C_L$ would clearly improve the agreement at cruise level lift coefficients. The symbol R is Reynolds number per foot in millions and M is Mach number.

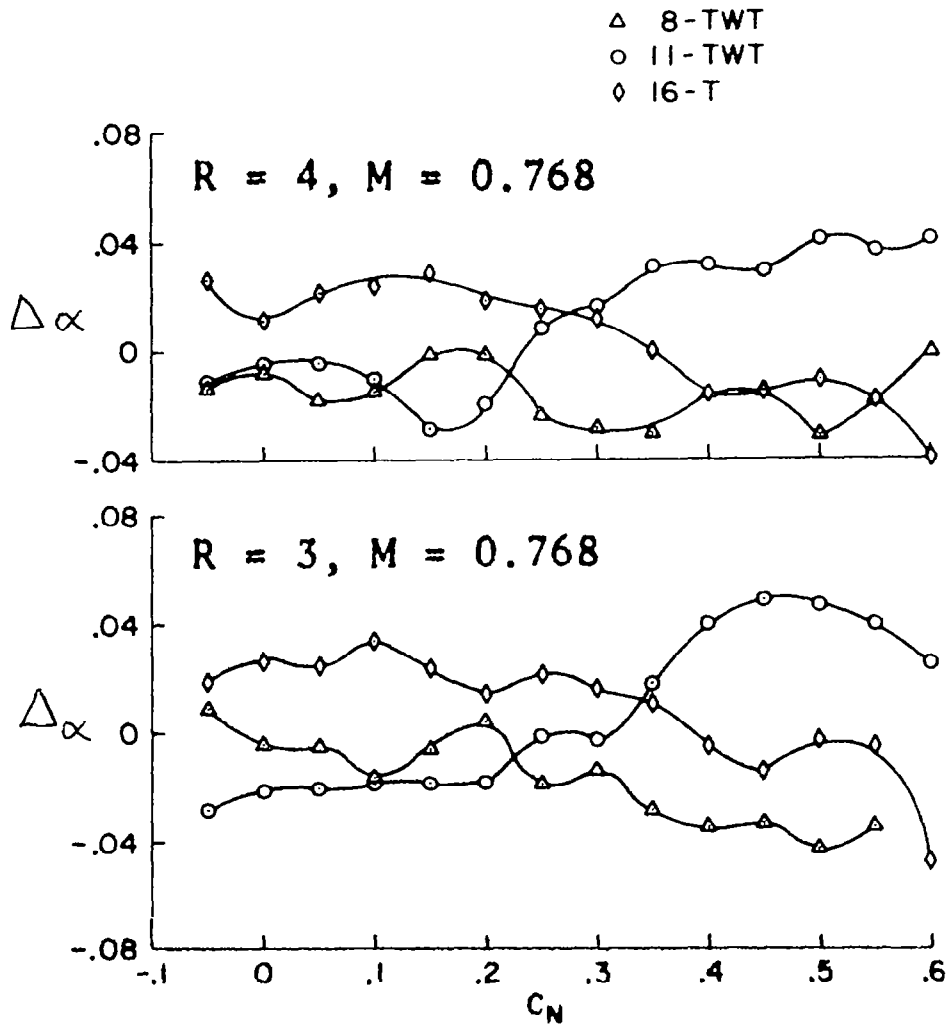


Figure 3

INCREMENTAL COMPARISON OF ΔC_A AS FUNCTION OF C_N

The basic body axis data of figure 4 shows a comparison of incremental axial-force coefficient (ΔC_A) against normal-force coefficient for wing-fuselage with fixed transition. Agreement at zero normal force is indicative of the ability to correct for stream angle through testing upright and inverted.

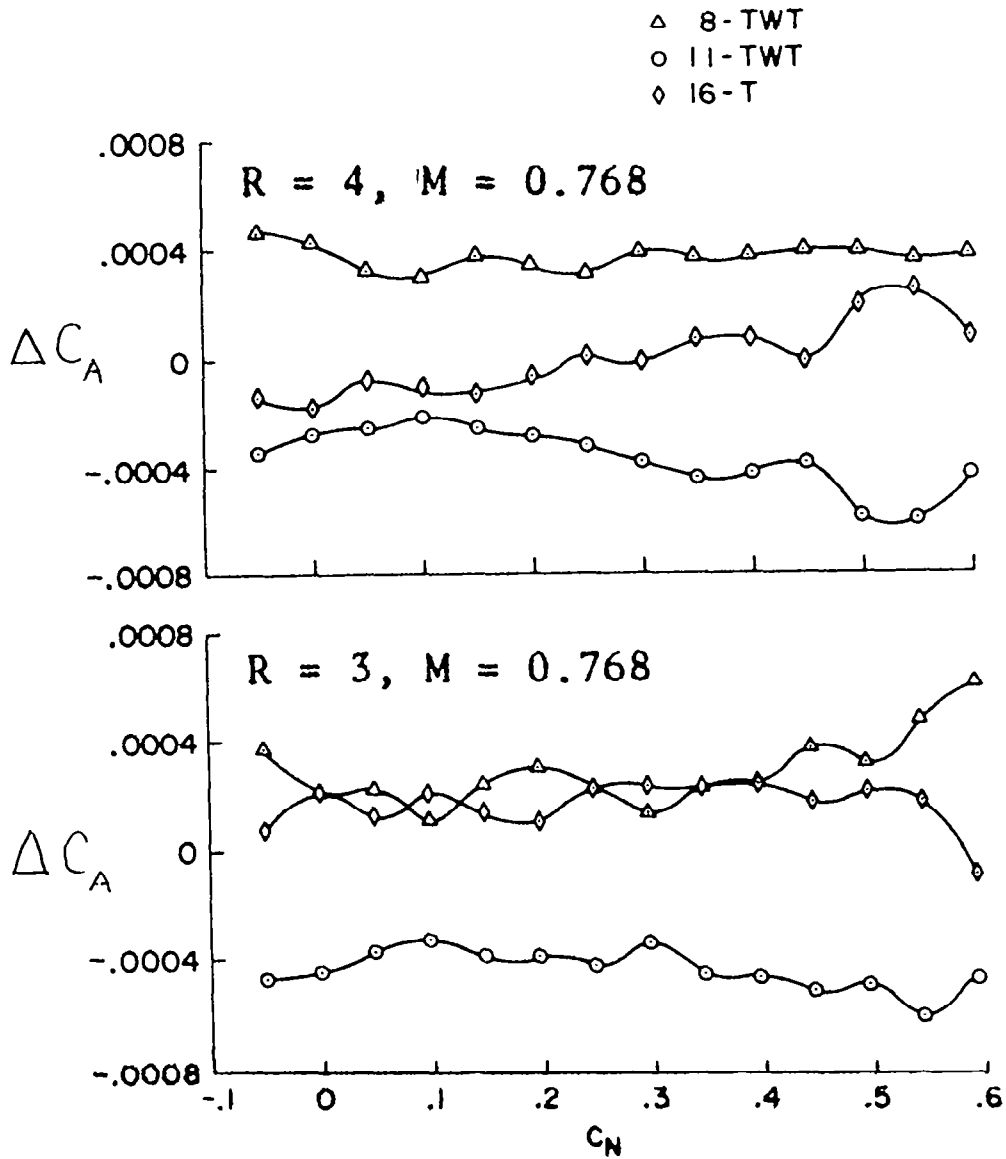


Figure 4

INCREMENTAL COMPARISON OF ΔC_{Ab} AS FUNCTION OF C_N

Figure 5 is a comparison of the incremental base cavity axial-force coefficient ΔC_{Ab} against C_N for the three tests. These test were for a wing-fuselage with fixed transition at $M = 0.768$ and $R = 4$. As will be shown in succeeding figures, this is indicative of differing blockage/buoyancy effects.

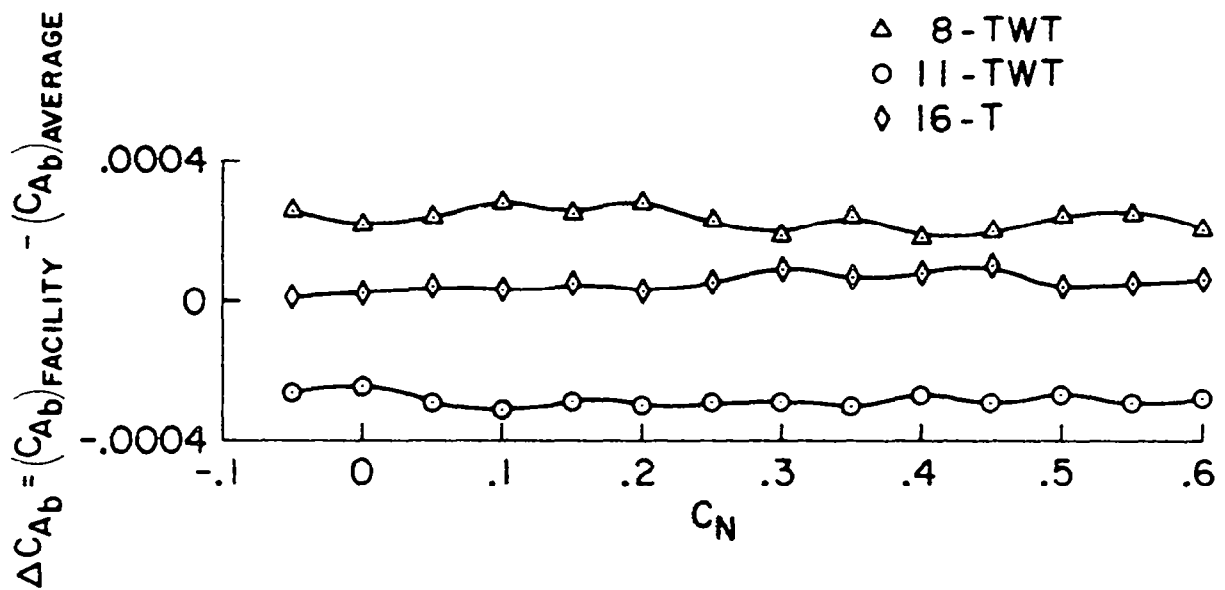
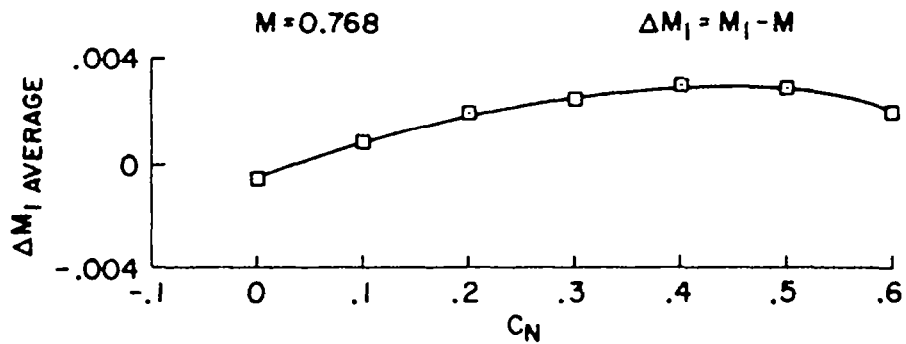


Figure 5

CHARACTERISTIC VARIATIONS OF REFERENCE MODEL ORIFICE FOR
RELATIVE BLOCKAGE DETERMINATION

Figure 6 is a comparison of computed local Mach number from a reference model orifice which was located on top of the fuselage, just aft of the cockpit region. The tests are for a wing-fuselage with fixed transition at $R = 4$. The top plot of figure 6 shows the orifice to be a good static-pressure source; the bottom plot shows that the combination of tunnel calibration and any residual blockage correction to Mach number is in excellent agreement. Since blockage corrections were not applied, they are shown to be negligible.



NOTE: DATA POINTS SHOWN ARE THE AVERAGE VALUES
FOR THE THREE FACILITIES

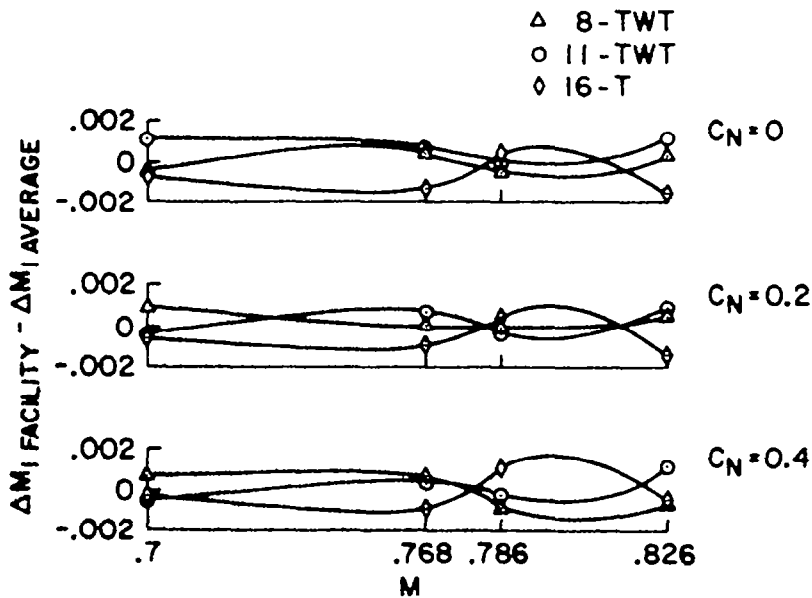


Figure 6

REPRESENTATIVE AM DISTRIBUTIONS USED FOR RELATIVE BUOYANCY CORRECTIONS

Figure 7 is an incremental comparison relative to 16-T test results of local Mach number from fuselage orifices for tests of a wing-fuselage with fixed transition at $M = 0.768$ and $R = 4$. The runout value at the end of the fuselage is derived from the base cavity pressure differences depicted in figure 5. Clearly, these gradients at zero normal force produce a buoyancy-type effect on drag. The symbol x is the distance from the nose and L is the model length.

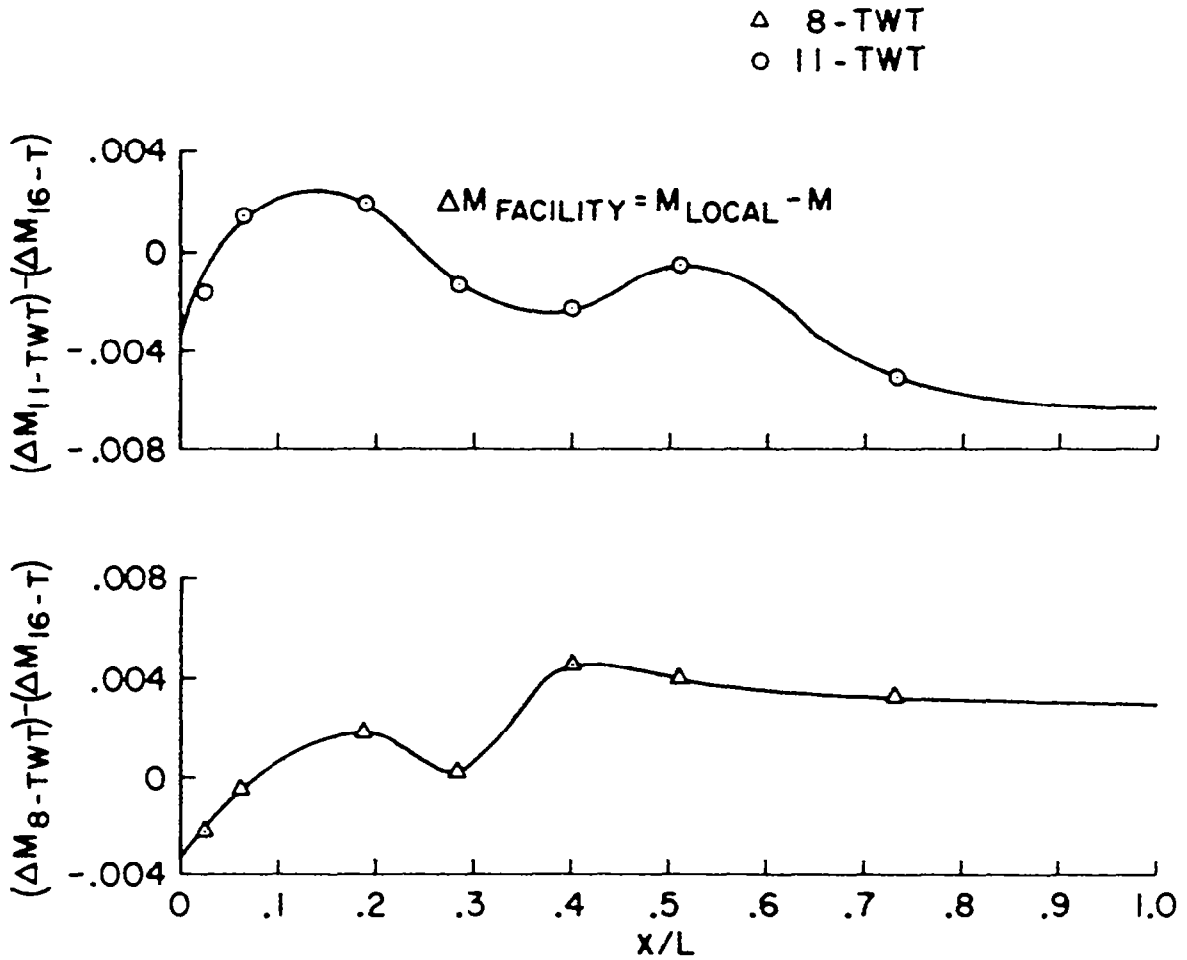


Figure 7

RELATIVE BUOYANCY CORRECTIONS TO C_A AND C_D

Figure 8 is a presentation of the resulting buoyancy correction as a function of normal-force coefficient for a wing-fuselage at $M = 0.768$. The levels are more than significant. The effect seems to be associated with tunnel dynamics, that is, a change in the basic effective area distribution of the tunnel due to the model flow field interacting with the tunnel-wall boundary layer, coupled with wall cross-flow effects. For compliant wall tests in an adaptive sense, accounting for the change in displacement thickness is now known to be required. The symbol C_D is drag coefficient.

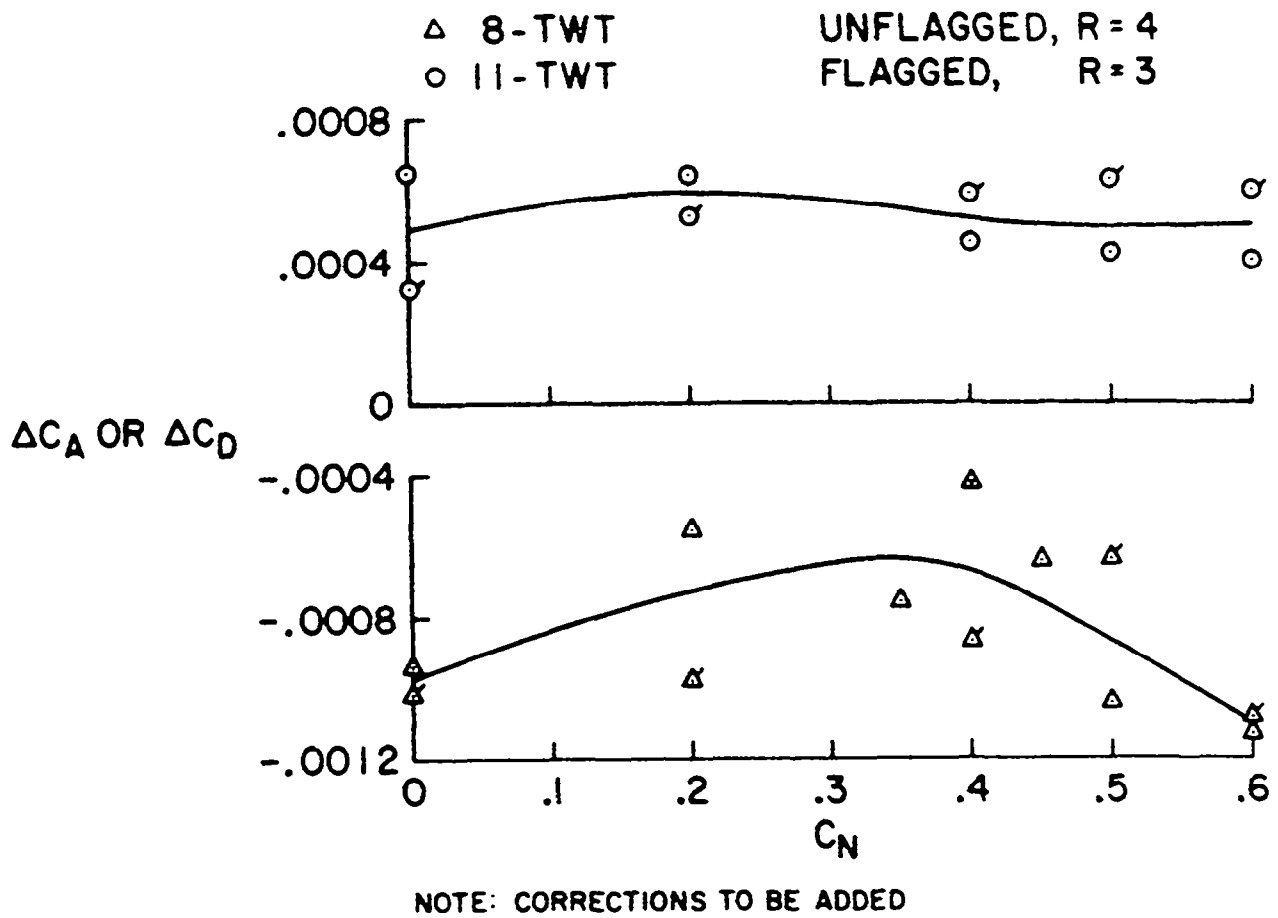


Figure 8

BOUNDARY-LAYER TRANSITION LENGTH

Figure 9 shows results from the now well-known AEDC 10° cone which has been tested in flight. In general, transition Reynolds number in the Calspan 8-TWT is significantly lower than in the Ames 11-TWT and AEDC 16-T. Differences in transition are attributed to aero-acoustic and turbulence effects.

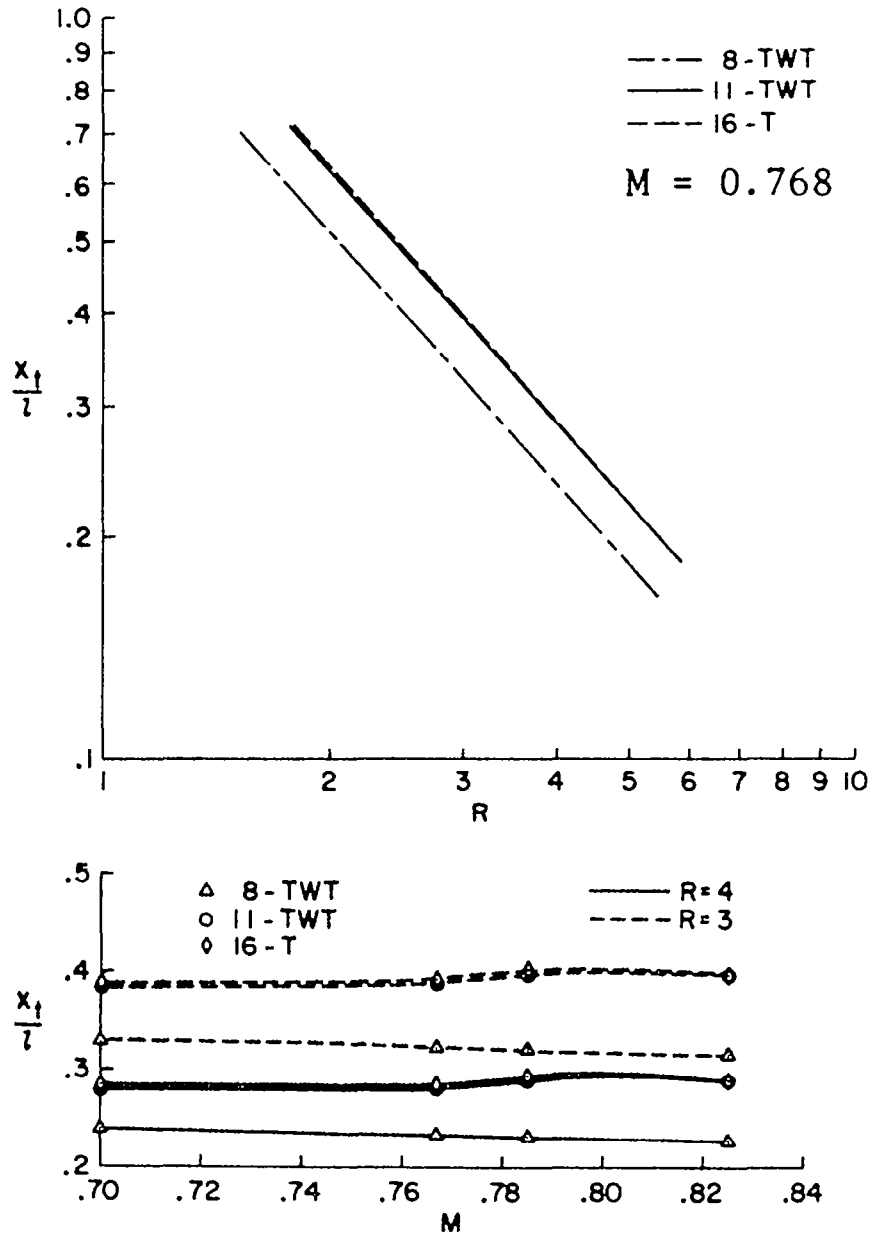


Figure 9

VARIATION OF $\alpha_{C_N=0}$ WITH R

Figure 10 is a comparison of angle of attack at zero normal force $\alpha_{C_N=0}$ of a wing-fuselage at $M = 0.768$ for both fixed and free transition as a function of Reynolds number. Fixed transition is relatively insensitive to Reynolds number. There are considerable Reynolds number effects shown in the free-transition data. Adjusting the Calspan data on the supposition that a "transonic turbulence factor" as defined by the cone transition Reynolds number was valid is shown to give significantly improved agreement. This rather large variation is a strong indicator of the delicate nature of transition-free data. It is imperative to maintain the condition of the leading edges in any such tests. Otherwise, correlation with any confidence may be impossible.

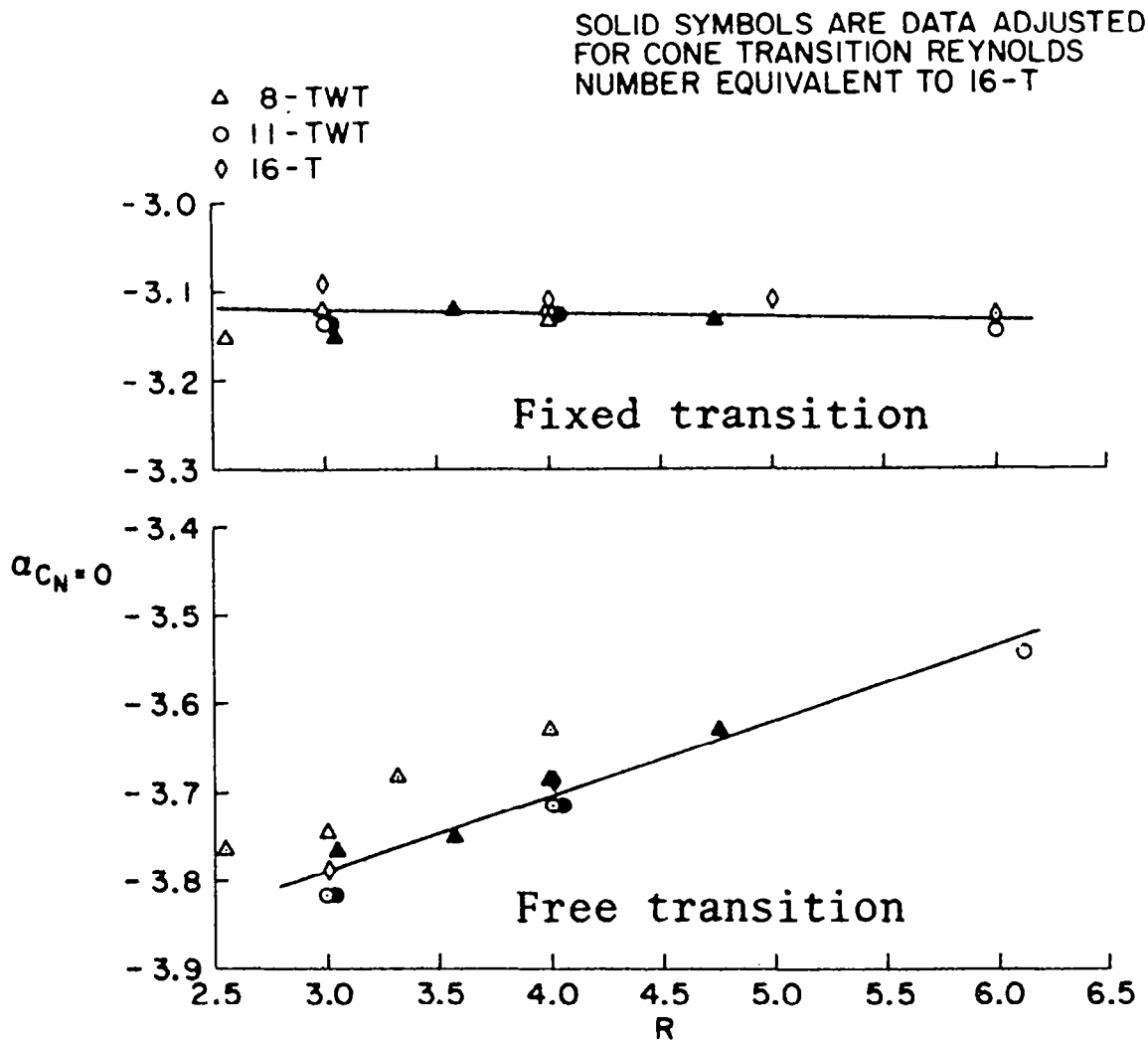


Figure 10

INCREMENTAL VARIATION OF C_A WITH R

Figure 11 is a comparison of axial-force coefficient as a function of Reynolds number for various normal-force coefficients in the AEDC 16-T of a wing-fuselage with fixed transition at $M = 0.768$. These results are used in adjusting the data for the assumed "transonic turbulence factor."

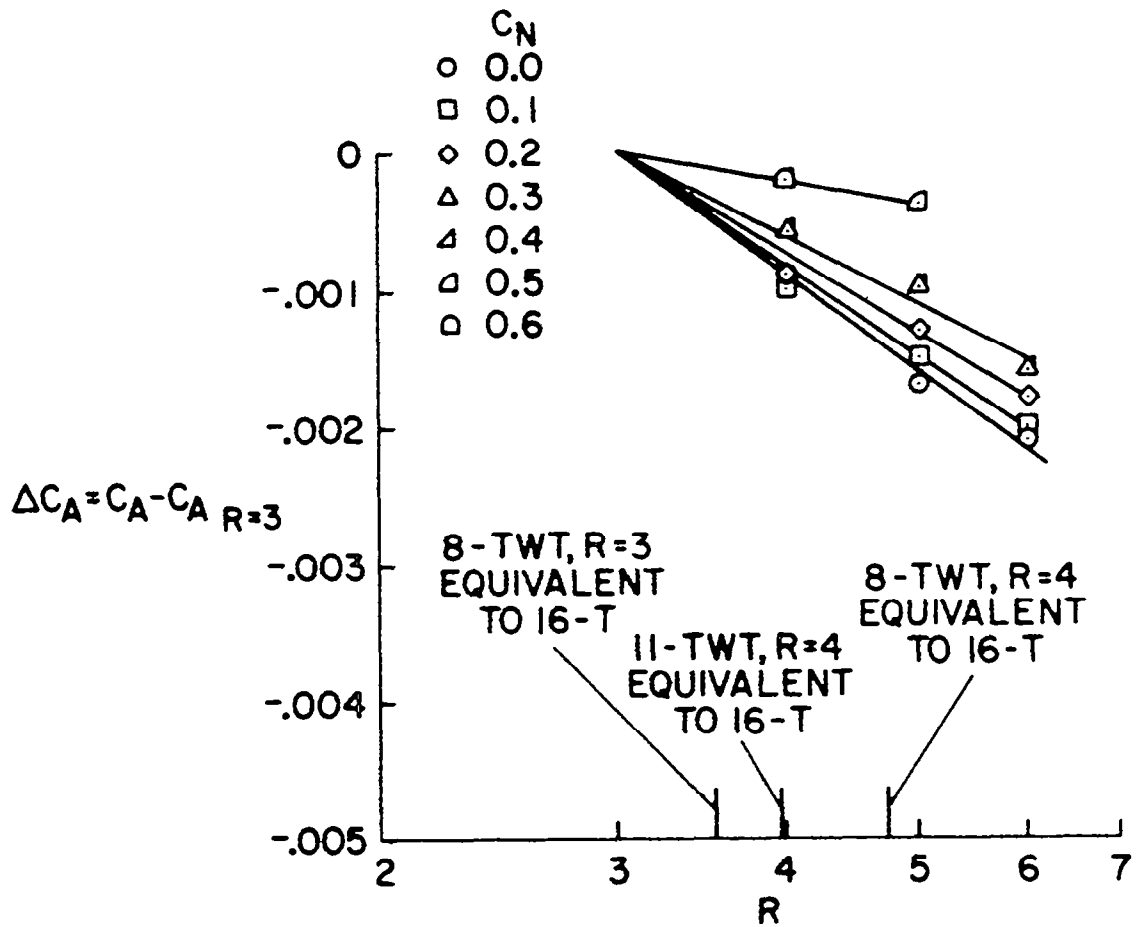


Figure 11

CORRECTIONS TO C_A FOR BUOYANCY AND R

Figure 12 is a composite of the corrections to axial force due to the buoyancy induced by tunnel dynamics and the Reynolds number correction from figure 11 for a wing-fuselage with fixed transition at $M = 0.768$.

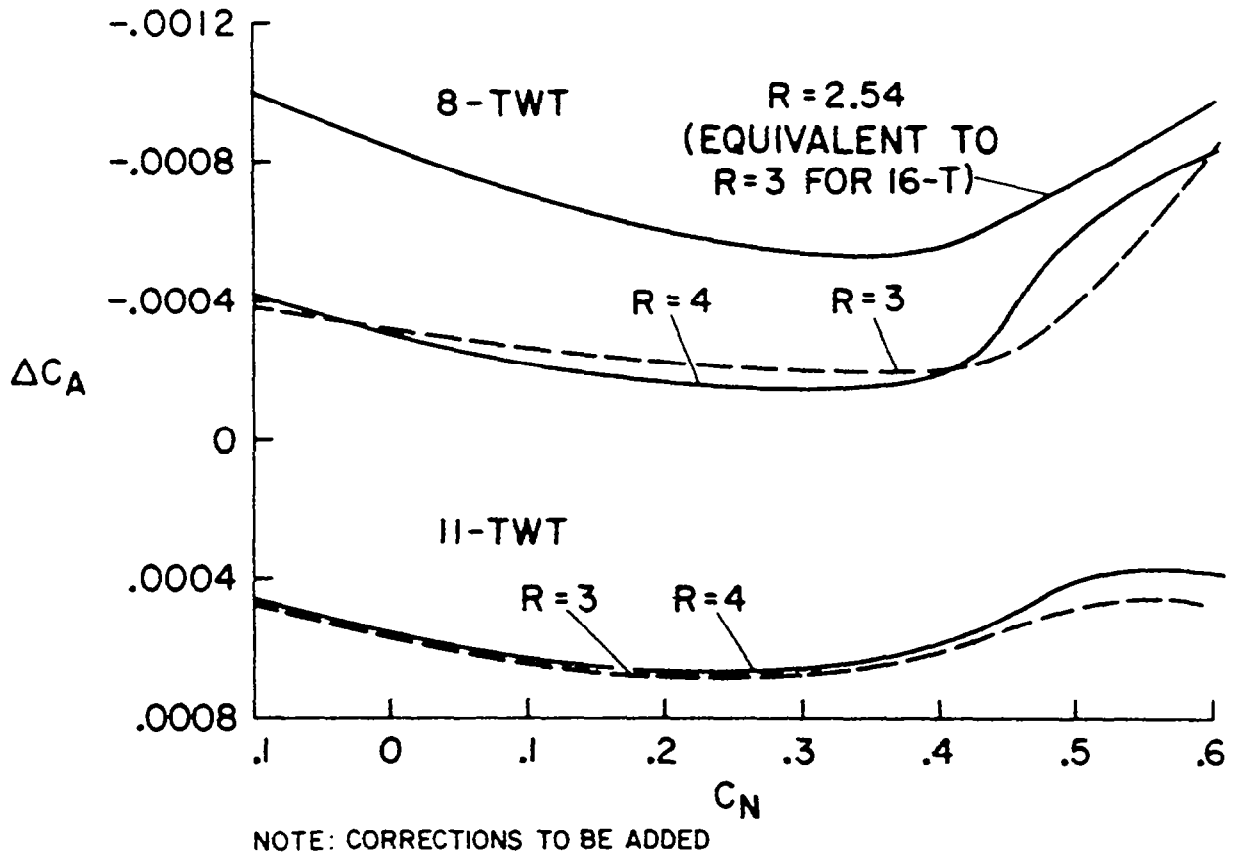


Figure 12

COMPARISONS OF ΔC_A CORRECTED FOR RELATIVE BUOYANCY AND EFFECTIVE R

Figure 13 is a comparison of the adjusted axial-force coefficient as a function of normal-force coefficient for a wing-fuselage with fixed transition at $M = 0.768$. Comparing with figure 4, it is seen that the spread in axial-force coefficient has been reduced from $C_A = 0.0008$ or more down to 0.0004 or less. If generalization from this series of tests is valid, then the above corrections should be developed and applied routinely.

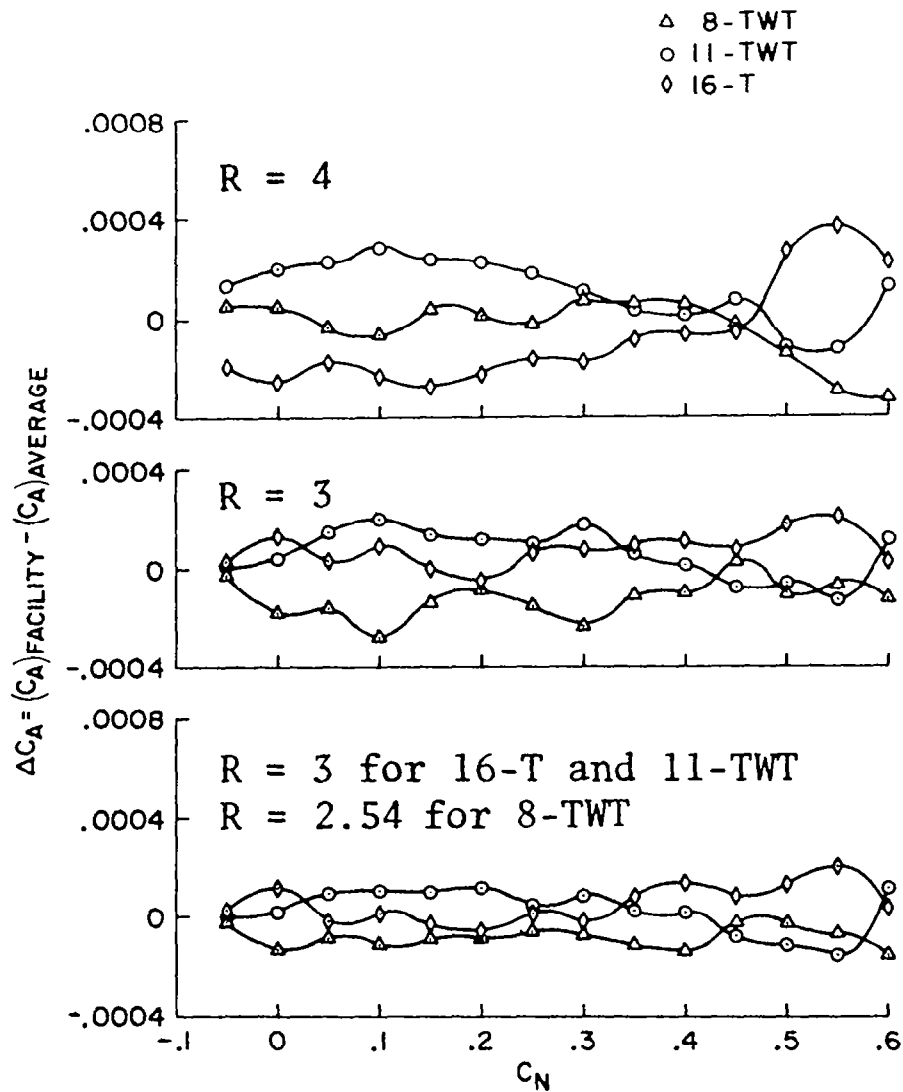


Figure 13

EFFECT OF NOISE ON BOUNDARY-LAYER TRANSITION

Figure 14 is a comparison of AEDC 10° cone data at Mach 0.8 from several wind tunnels as well as flight. The large difference in transition Reynolds number Re_T gives pause to wonder at the significance to correlating between tunnels as well as extrapolating to flight. Flight data are from reference 4; data from AEDC, Ames, and Langley wind tunnels are from reference 5; and the RAE data are from reference 6.

The curve for $Re_T = 3.7 \times 10^6 \left[\frac{\sqrt{\bar{p}_i^2}}{q_\infty} \right]^{-.25} \times 100$ is from reference 7.

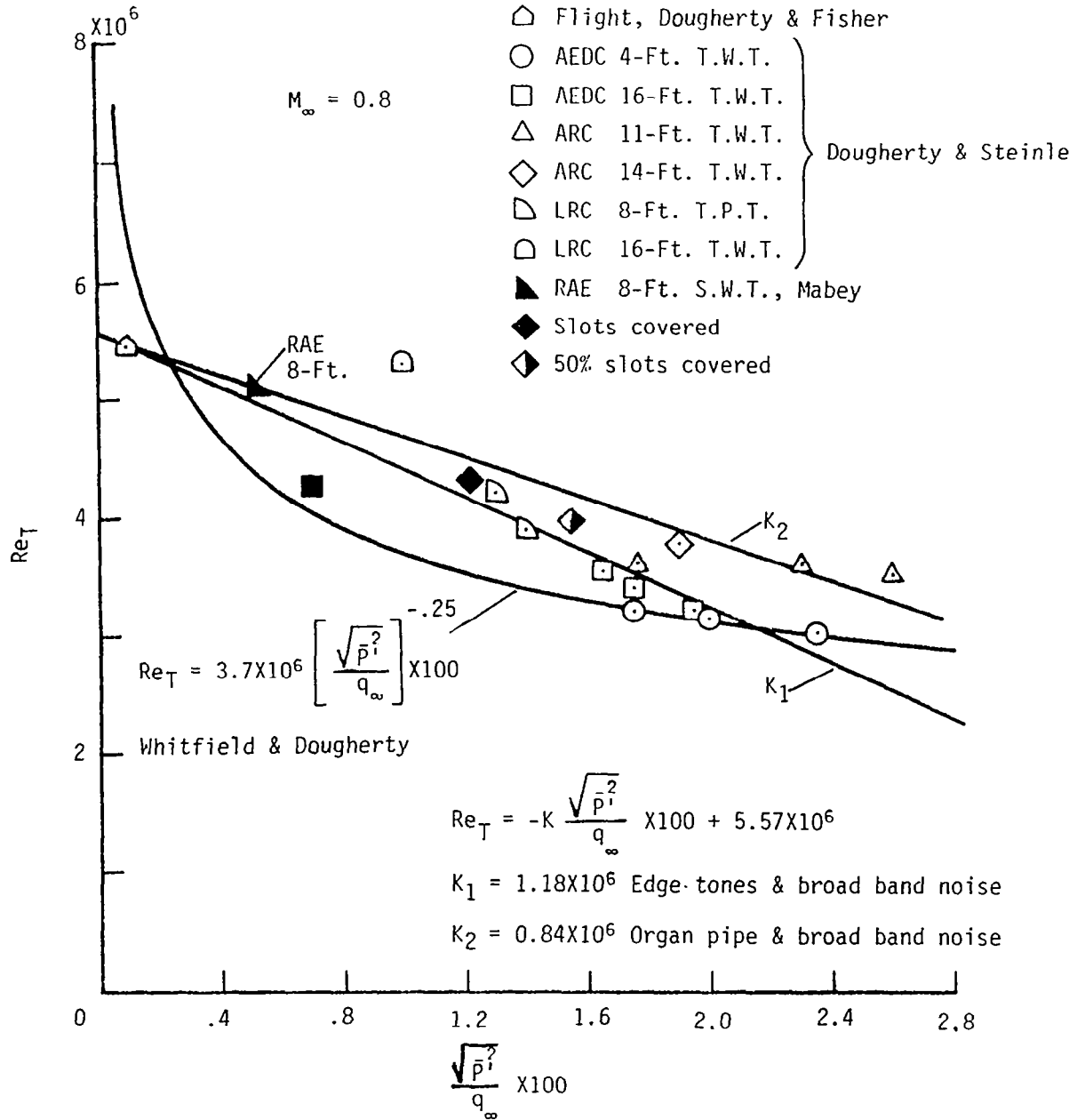


Figure 14

OBSERVATIONS

Aside from what was known in 1929, the impact of the quality of the flow field is of most significance. The technical community at large is now well in tune with wall interference and great hope is being placed on adaptive walls for the ultimate solution. Adaptive walls will automatically account for the blockage buoyancy caused by the tunnel-model-wall dynamic interaction. However, adaptive walls will not be for everybody in the near future (if ever), and the buoyancy effect is there to a significant degree. Transonic turbulence factor (or by some other name) is of increasing interest. There is a growing body of evidence to indicate that the effect is both there and of significance.

RECOMMENDATIONS

(1) Each facility should undertake to define the tunnel induced buoyancy due to dynamic effect. A venture of this sort, involving several models as well as considerable computational effort, could best be accomplished through a cooperative effort.

(2) Interested parties should join in a coordinated effort to define the effect of the aero-acoustic and turbulence environment ("transonic turbulence factor") on the data. NASA Ames is planning to initiate such an effort soon.

REFERENCES

1. Diehl, Walter S.: Joint Report on Standardization Tests on N.P.L. R.A.F. 15 Airfoil Model. NACA Rep. 309, 1929.
2. Treon, Stuart L.; Steinle, Frank W.; Hofstetter, William R.; and Hagerman, John R.: Data Correlation From Investigations of a High-Subsonic Speed Transport Aircraft Model in Three Major Transonic Wind Tunnels. AIAA Paper No. 69-794, July 1969.
3. Treon, Stuart L.; Steinle, Frank W.; Hagerman, John R.; Black, John A.; and Buffington, Robert J.: Further Correlation of Data From Investigations of a High-Subsonic-Speed Transport Aircraft Model in Three Major Transonic Wind Tunnels. AIAA Paper No. 71-291, Mar. 1971.
4. Dougherty, N. S., Jr.; and Fisher, D. F.: Boundary-Layer Transition on a 10-Deg Cone: Wind Tunnel/Flight Correlation. AIAA-80-0154, Jan. 1980.
5. Dougherty, N. S., Jr.; and Steinle, Frank W., Jr.: Transition Reynolds Number Comparisons in Several Major Transonic Tunnels. AIAA Paper No. 74-627, July 1974.
6. Pope, Alan; and Harper, John J.: Low-Speed Wind Tunnel Testing. John Wiley & Sons, Inc., c.1966.
7. Whitfield, Jack D.; and Dougherty, N. Sam, Jr.: A Survey of Transition Research at AEDC. Laminar-Turbulent Transition, AGARD-CPP-224, 1977, pp. 25-1-25-20.

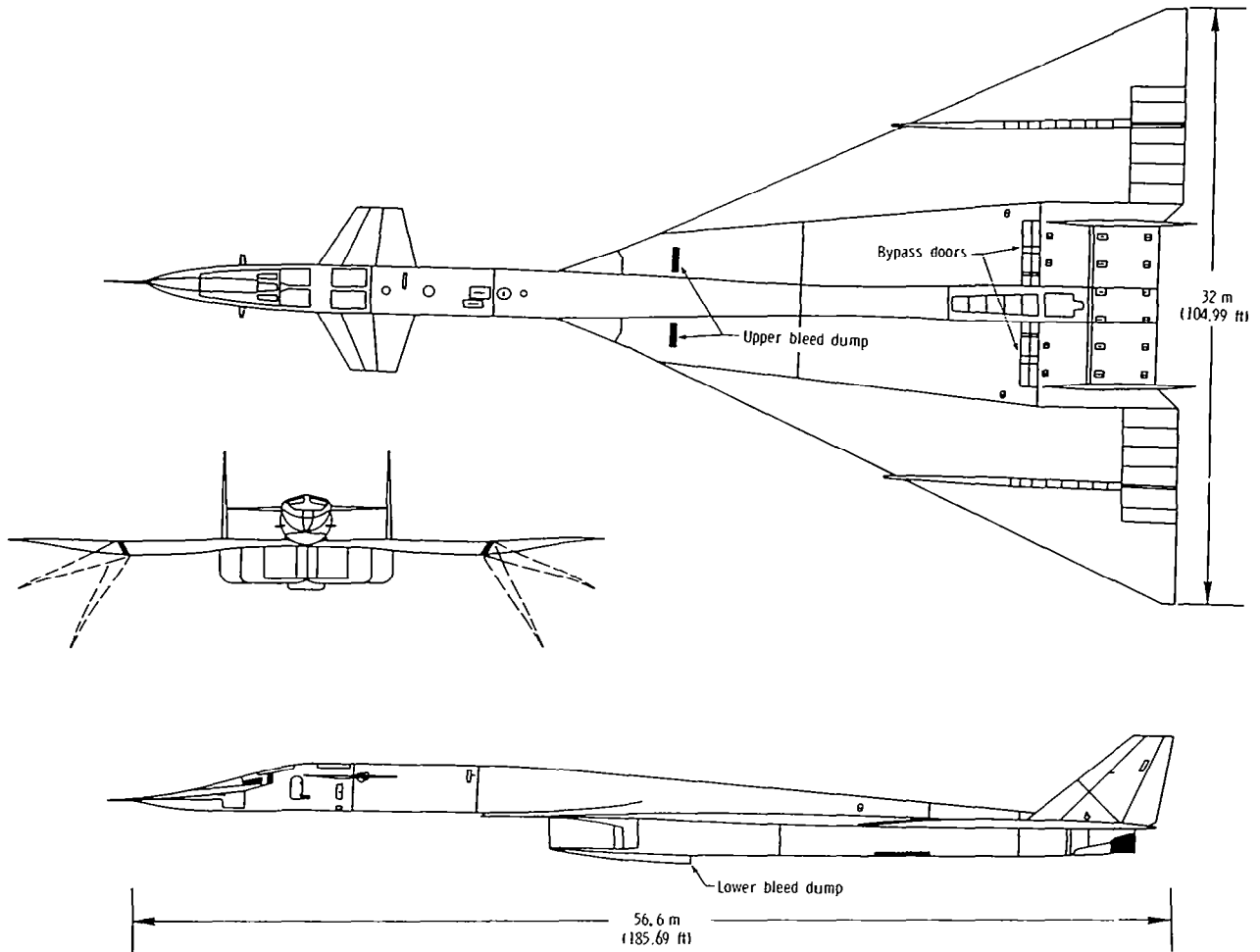
WIND-TUNNEL/FLIGHT CORRELATION PROGRAM ON XB-70-1

John B. Peterson, Jr.
NASA Langley Research Center
Hampton, Virginia

MINIWORKSHOP ON WIND-TUNNEL/FLIGHT CORRELATION - 1981
November 19-20, 1981

XB-70-1 AIRPLANE

The XB-70-1 was a large supersonic cruise bomber designed to cruise at Mach 3.0 at an altitude of 21 340 meters (70 000 ft). It was powered by six YJ93-GE-3 after-burning turbojet engines and weighed 226 800 kg (500 000 lb) at take-off. The airplane had folding wing tips to improve directional stability and reduce wave drag and canards and elevons which acted together to control longitudinal attitude.



XB-70 WIND-TUNNEL/FLIGHT CORRELATION PROGRAM

The XB-70-1 was selected for a wind-tunnel/flight correlation program as representative of a large, flexible, supersonic airplane similar to a supersonic transport. The program was conducted by three NASA centers: Dryden Flight Research Center, Ames Research Center, and Langley Research Center. The results have been published in four NASA reports from all three centers. (see refs. 1 to 4.)

- SELECTED AS REPRESENTATIVE OF A LARGE, FLEXIBLE, SUPERSONIC AIRPLANE

- FLIGHT TESTS AT DRYDEN FLIGHT RESEARCH CENTER (ARNAIZ, NASA TM X-3532)

- WIND-TUNNEL TESTS AT AMES RESEARCH CENTER (0.03-SCALE MODEL BUILT TO 1-g SHAPE, DAUGHERTY, NASA TP-1514)

- EXTRAPOLATION TO FULL SCALE BY LANGLEY RESEARCH CENTER (PETERSON, MANN, SORRELLS, SAWYER, AND FULLER, NASA TP-1515)

- COMPARISON REPORT BY ALL THREE CENTERS (ARNAIZ, PETERSON, AND DAUGHERTY, NASA TP-1516)

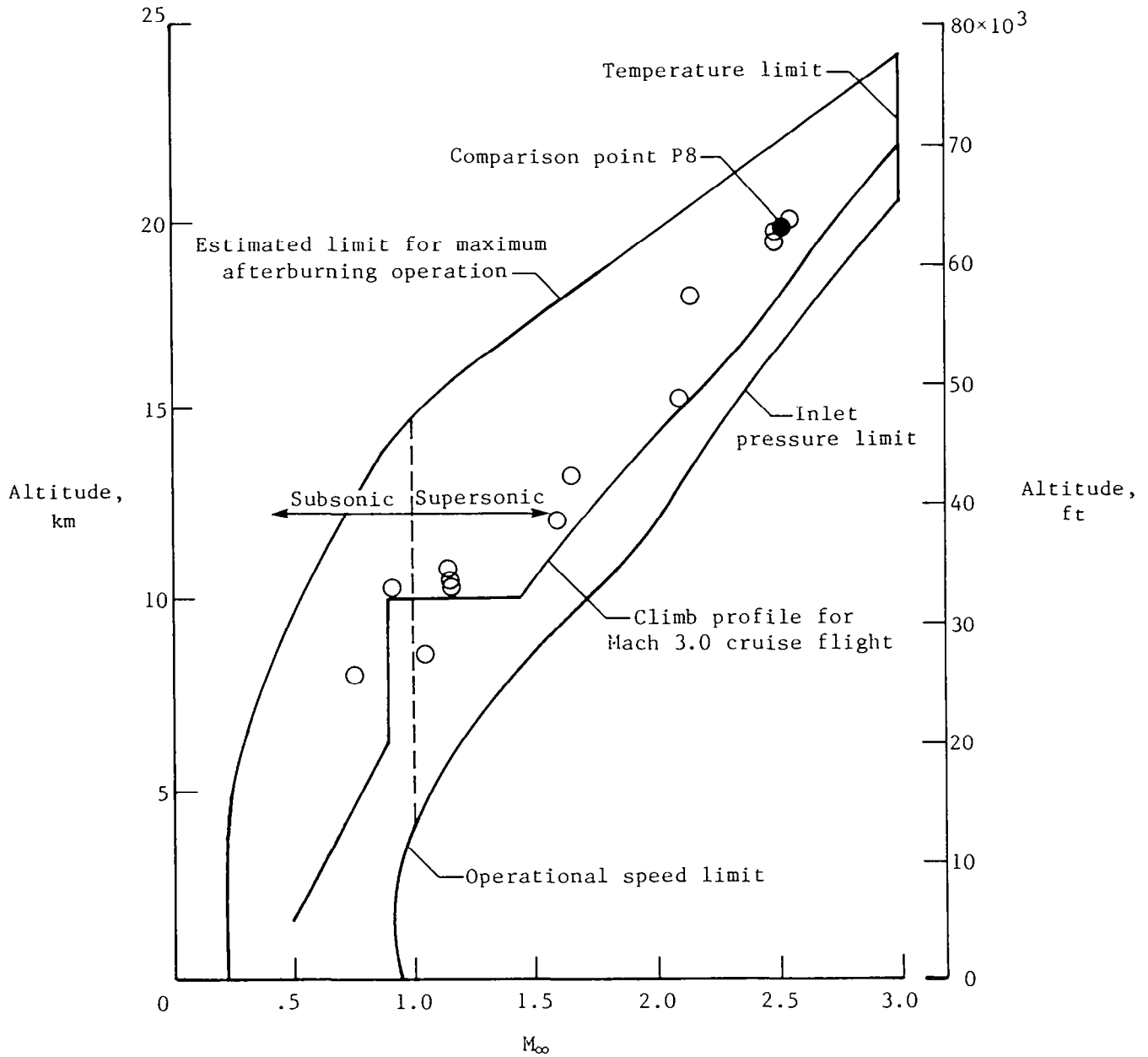
TEST POINTS SELECTED FOR XB-70 WIND-TUNNEL/FLIGHT CORRELATION

Fourteen flight test points at Mach numbers from 0.76 to 2.56 were selected for comparison with wind-tunnel data. Points P1 through P10 were taken in 1-g equilibrium flight, points P3L and P8L were taken in low-g flight, and points P3H and P8H were taken in high-g flight. Extensive calibrations were made of the XB-70-1 engine performance in order to accurately determine the engine thrust during the flight tests. Additional information on the calibration of the engines can be found in references 5 and 6.

Point	Mach No.	Altitude, Meters	α , deg	C_L
P1	0.76	7 842	4.4	0.166
P2	0.93	9 988	5.7	.230
P3	1.18	10 278	3.2	.107
P4	1.61	11 756	3.1	.082
P5	1.67	12 807	2.9	.085
P6	2.10	14 813	2.9	.077
P7	2.15	17 563	4.3	.106
P8	2.53	19 187	4.7	.098
P9	2.50	18 784	4.6	.098
P10	1.06	8 272	3.9	.122
P3L	1.15	10 400	2.2	.073
P3H	1.17	10 046	4.4	.153
P8L	2.51	19 205	3.7	.080
P8H	2.56	19 224	6.7	.141

OPERATIONAL FLIGHT ENVELOPE OF XB-70

This figure shows a plot of the 14 selected flight test points on the operational flight envelope of the XB-70. Additional information on the flight tests can be found in reference 1.



XB-70 WIND-TUNNEL TESTS

The wind-tunnel tests were conducted on a specially built model in the Ames Unitary Plan Wind Tunnel at Mach numbers of 0.60, 0.75, 0.80, 0.95, 1.20, 1.40, 1.60, 2.10, and 2.53. The model was built in the 1-g shape for a Mach number of 2.53 at 19 187 meters (flight test point P8). The wind-tunnel tests were very careful and complete. All standard corrections were made to the wind-tunnel data including measurements of the internal drag of the inlet air. Tests were made to determine the effects of control deflections, wing tip deflection, and variations in inlet mass flow (additive drag). Additional information on the wind-tunnel tests can be found in reference 2.

- 0.03 SCALE XB-70-I
 - ONE-g SHAPE AT $M = 2.53$

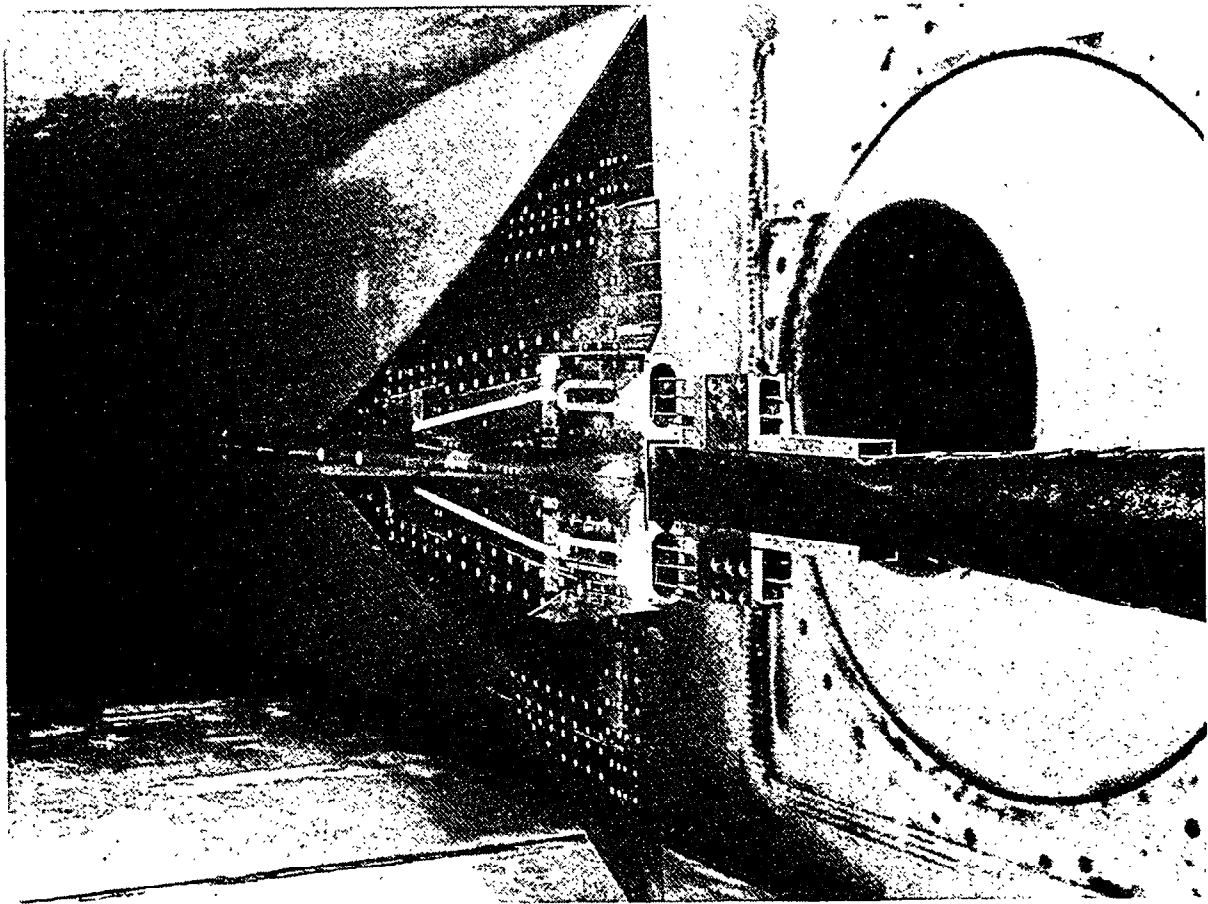
- AMES UNITARY PLAN WIND TUNNEL
 - $M = 0.60$ to 2.53
 - $R_c = 9.4 \times 10^6$

- WIND-TUNNEL DATA FOR THE EFFECTS OF
 - α and β
 - ELEVON AND CANARD DEFLECTION
 - RUDDER DEFLECTION
 - WING TIP DEFLECTION
 - BYPASS DOOR POSITION
 - INLET MASS-FLOW RATIO

- WIND-TUNNEL DATA CORRECTED FOR
 - STREAM ANGLE
 - MODEL/BALANCE ALIGNMENT
 - STING DEFLECTION
 - INTERNAL DRAG
 - BUOYANCY
 - BASE PRESSURE DRAG

XB-70-1 WIND-TUNNEL MODEL IN AMES UNITARY PLAN WIND TUNNEL

A photograph is presented of the 0.03-scale XB-70-1 wind-tunnel model in the 9- by 7-foot supersonic test section of the Ames Unitary Plan Wind Tunnel showing the total-pressure rake used to measure the exit momentum of the internal air flow during the tests. Also to be noted are the segmented elevons used on the XB-70-1 and duplicated on the wind-tunnel model.



ITEMS USED IN WIND-TUNNEL/FLIGHT EXTRAPOLATION

The items used in the extrapolation to full scale are shown in the table. The aircraft flexibility effects were determined by calculation of the differences in lift, drag, and moment of the wind-tunnel shape and the flight shape. The roughness and protuberance drags were determined by measurement of the actual roughnesses on the XB-70-1 airplane at the Air Force Museum, Dayton, Ohio, and calculation of the drag of the roughnesses and known protuberances on the airplane. The measured base drag in flight was used in order to reduce uncertainties in the wind-tunnel/flight comparison due to this component. Additional information on the extrapolation can be found in reference 3.

SPILLAGE DRAG INCREMENT

WIND-TUNNEL MODEL TRIP DRAG

AFTERBODY CLOSURE DRAG INCREMENT

REYNOLDS NUMBER EFFECT ON C_F

AIRPLANE FLEXIBILITY EFFECTS

INLET BLEED AIR DRAG

BYPASS DOOR AND BYPASS AIR DRAG

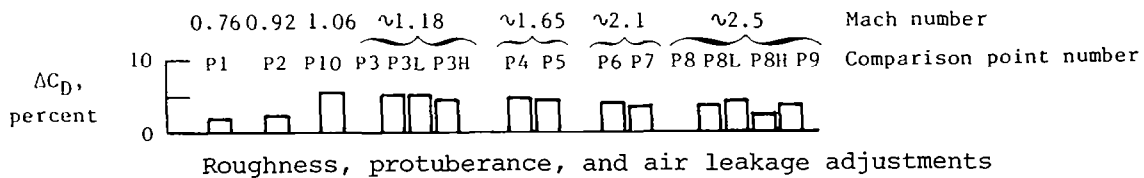
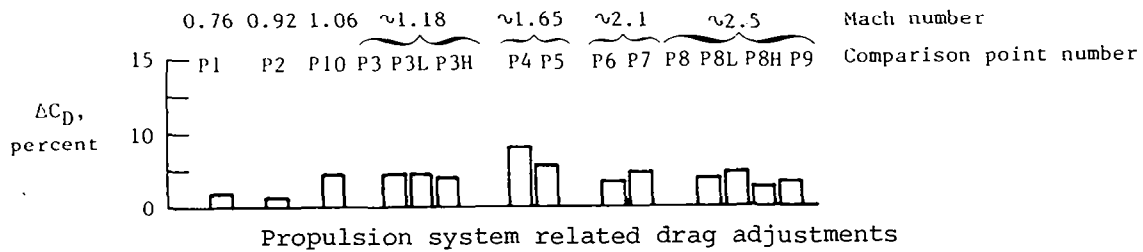
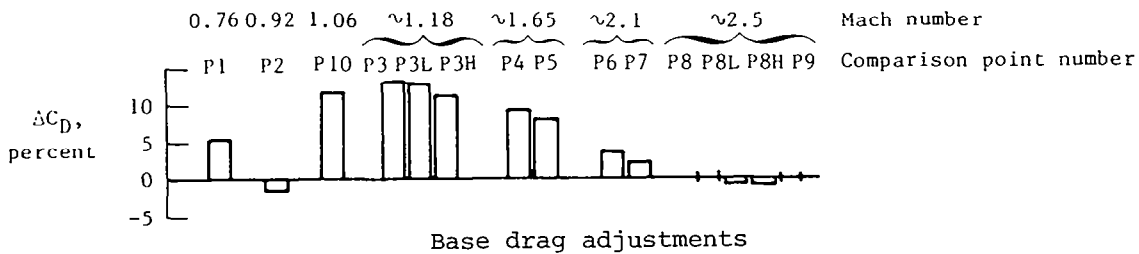
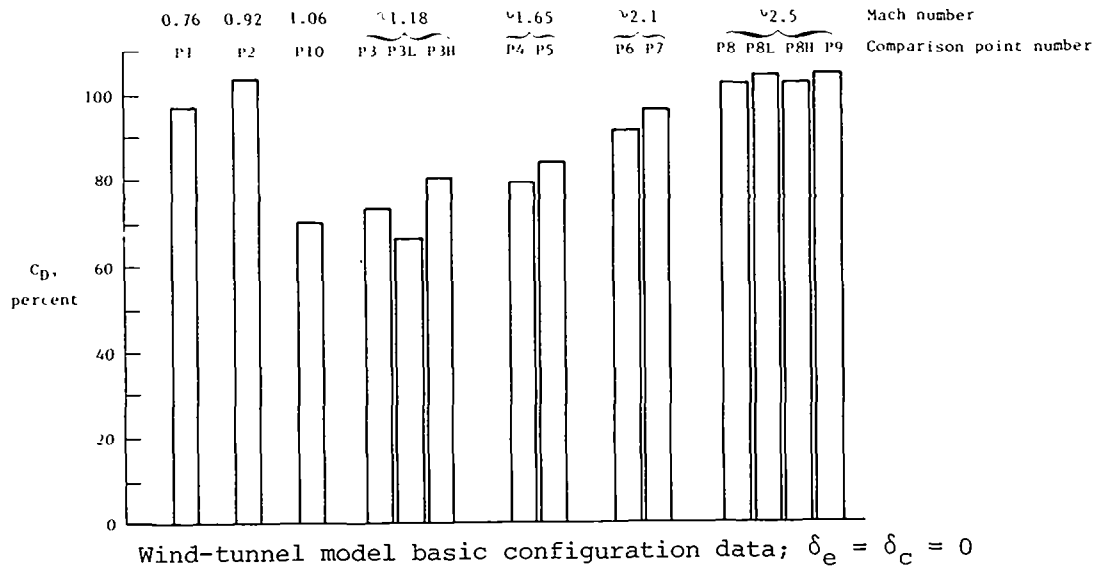
ROUGHNESS AND PROTUBERANCE DRAG

LEAKAGE DRAG

BASE DRAG (MEASURED IN FLIGHT)

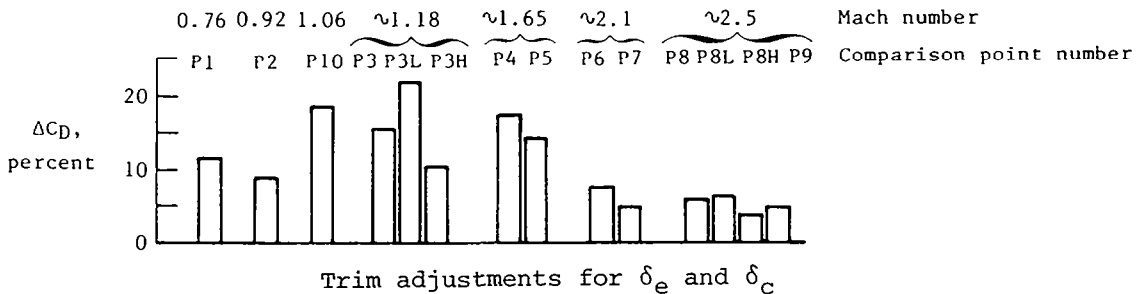
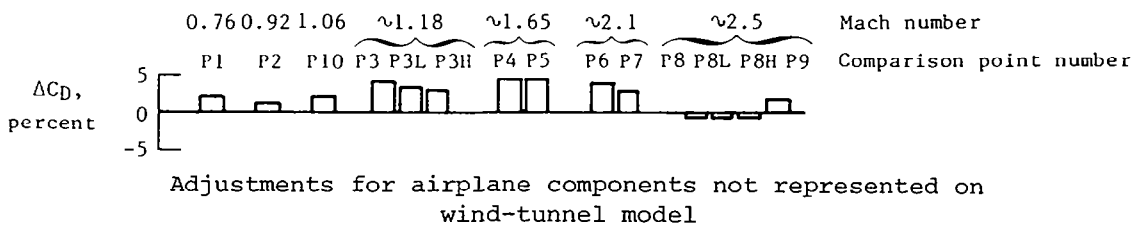
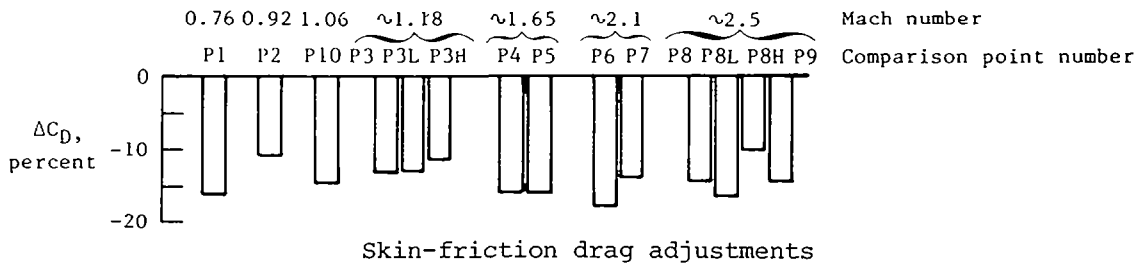
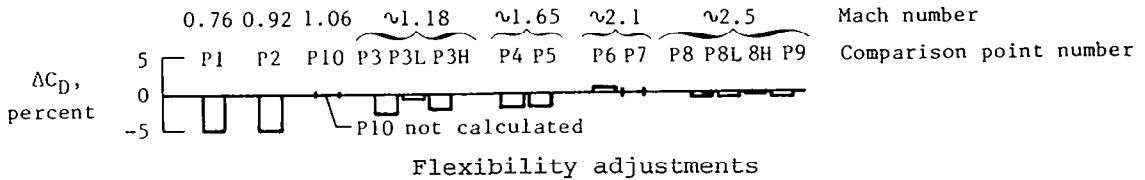
EXTRAPOLATION INCREMENTS FOR XB-70-1

The extrapolation increments for each of the 14 selected flight test points are shown, as a percentage of the final predicted drag, for the basic wind-tunnel data, the base drag increment, the propulsion-system drag increments such as spillage drag, and the roughness, protuberance, and air-leakage drag increments.



EXTRAPOLATION INCREMENTS FOR XB-70-1 - Continued

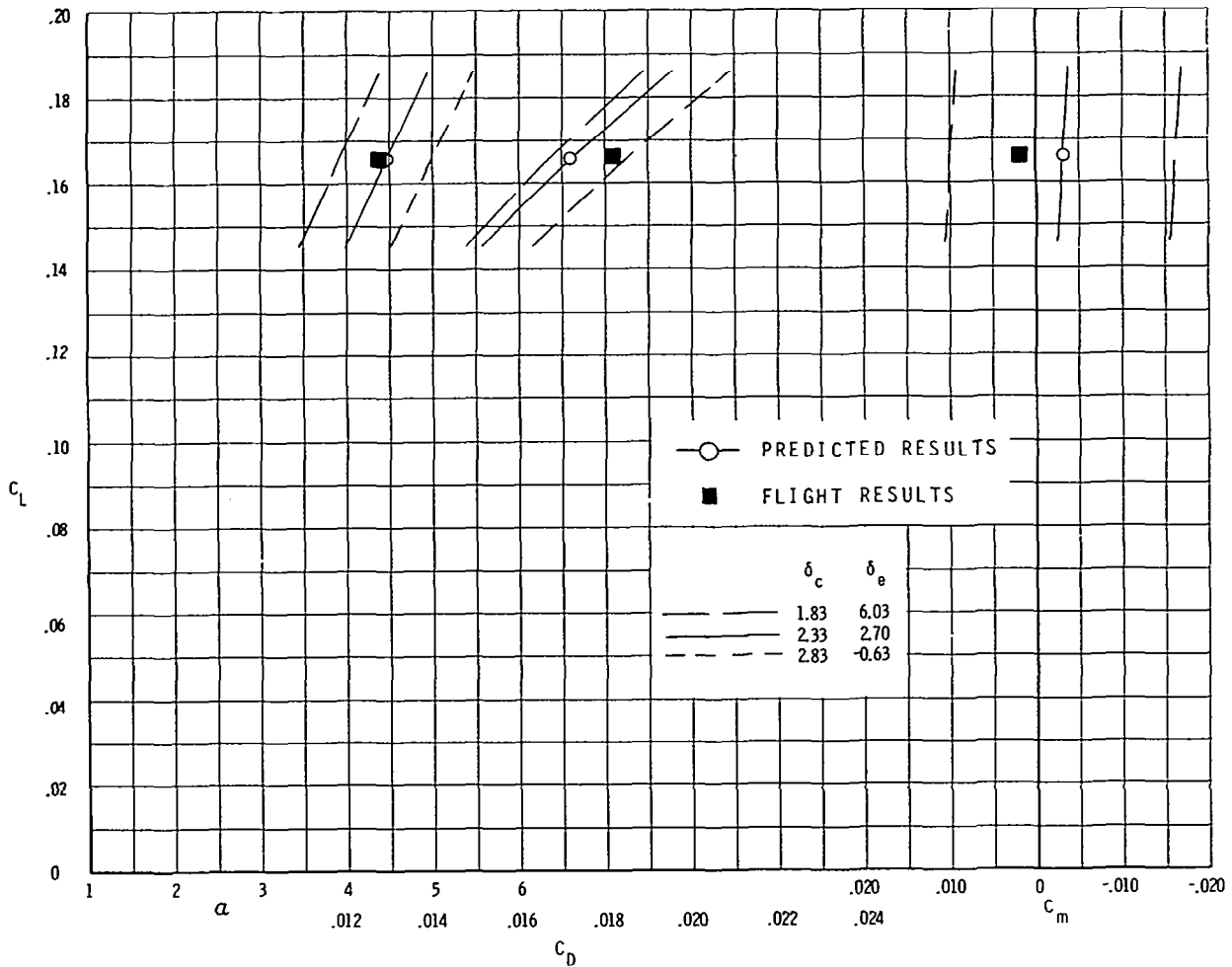
The extrapolation increments, as a percentage of the final predicted drag, are shown for the effects of flexibility, the skin-friction drag adjustment due to Reynolds number change, drag of airplane items not represented on the wind-tunnel model such as afterbody closure and bypass doors, the trim drag due to canard and elevon deflections.



COMPARISON BETWEEN PREDICTED AND FLIGHT-MEASURED RESULTS FOR P1

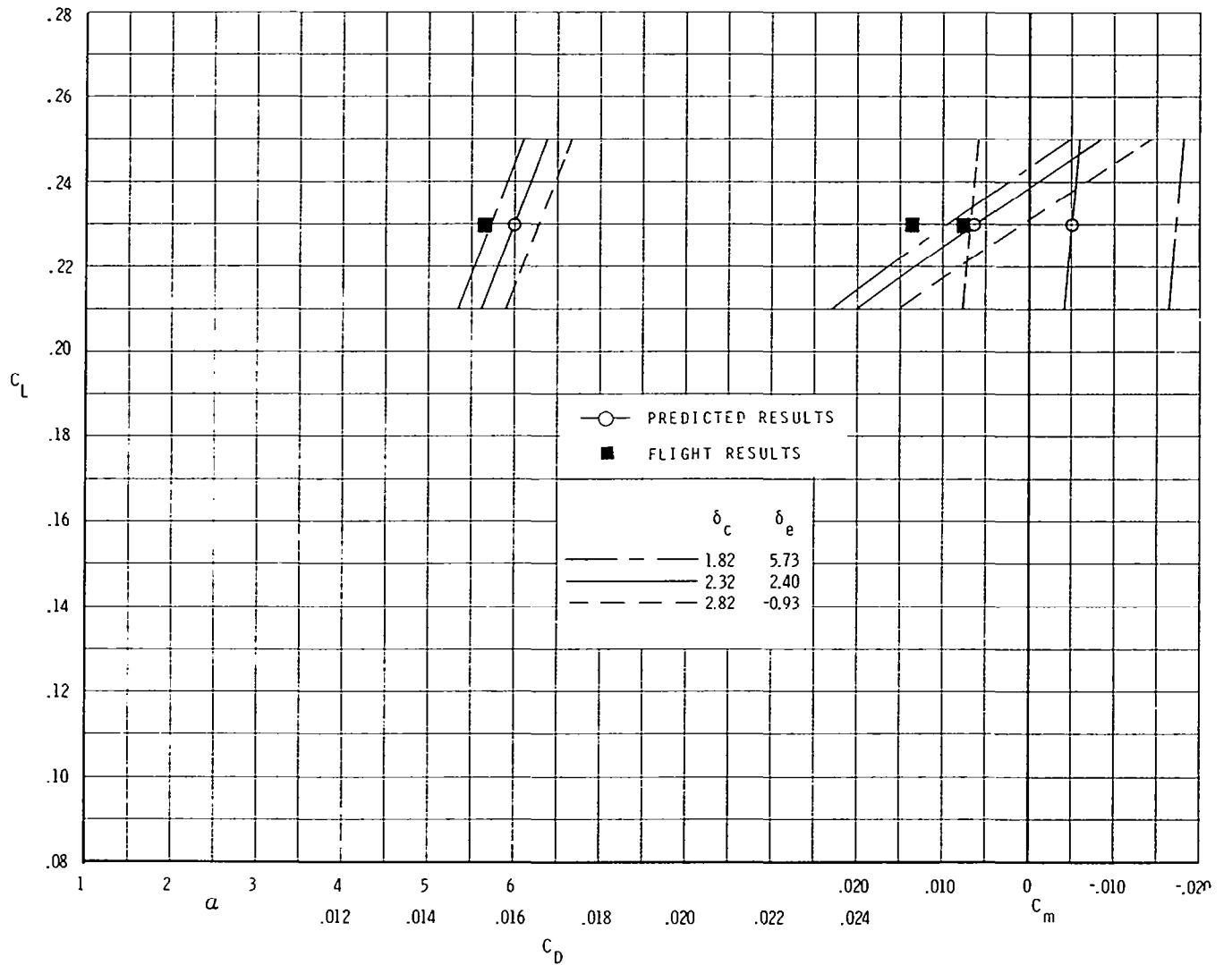
A comparison between the predicted (curves) and flight-measured (solid square) results is shown for point P1 at $M = 0.76$. The prediction based on the flight-measured deflection is shown as a solid curve and predictions based on canard deflections $\pm 0.5^\circ$ from the measured deflection are shown as dashed lines.

Assuming that the weight and C_L of the XB-70 were known accurately, it is apparent that the predicted and flight-measured angles of attack agree well, the predicted drag is less than the flight-measured drag, and the predicted pitching moment was different from the flight-measured pitching moment at the flight-measured control deflections. However, if the control deflections are changed to match the pitching moments, then the drag values would agree more closely but the angle of attack would show less agreement.



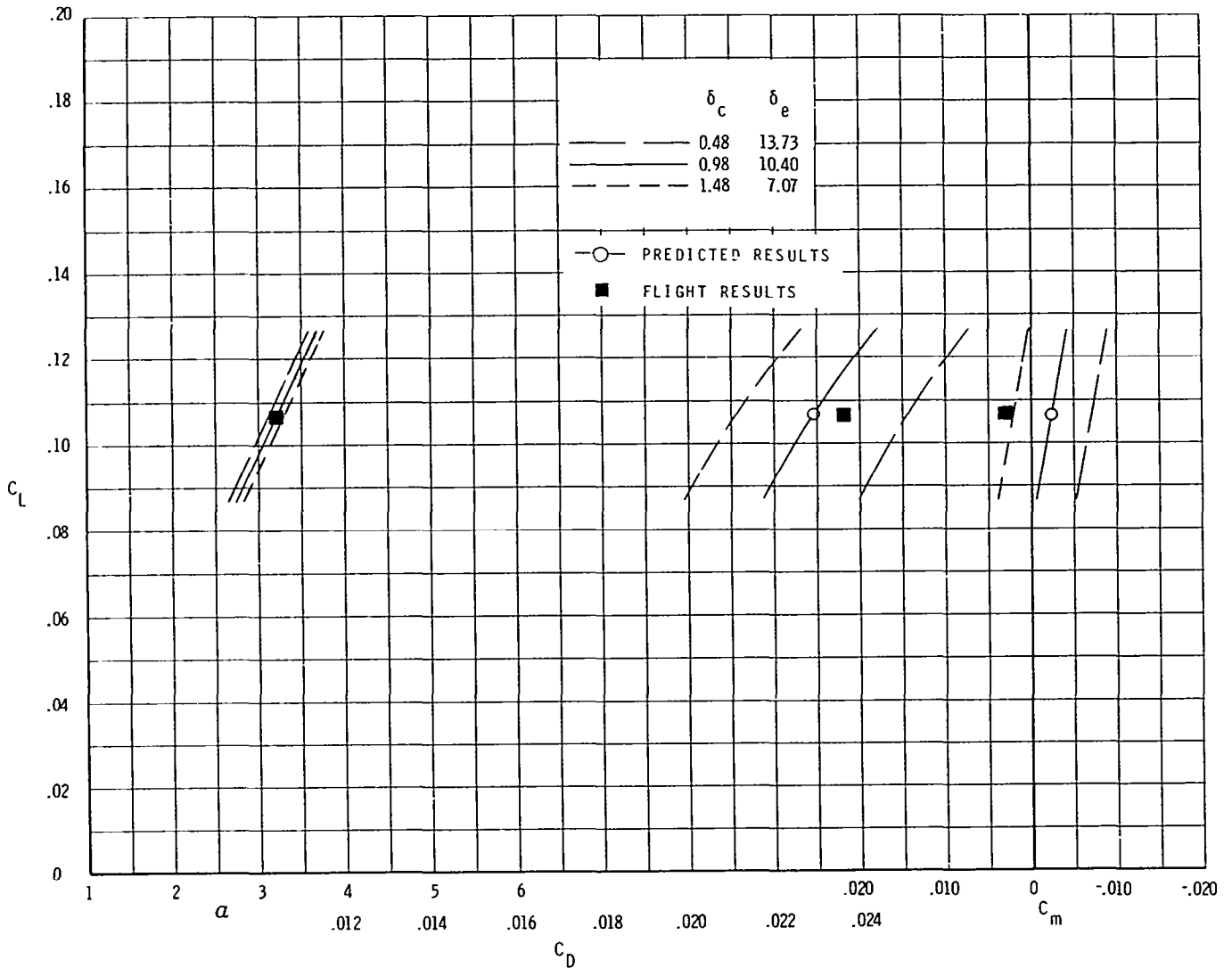
COMPARISON BETWEEN PREDICTED AND FLIGHT-MEASURED RESULTS FOR P2

A comparison between the predicted (curves) and flight-measured (solid square) results is shown for point P2 at $M = 0.93$. The prediction based on the flight-measured deflection is shown as a solid curve and predictions based on canard deflections $\pm 0.5^\circ$ from the measured deflection are shown as dashed lines. The predicted drag (0.0267) is considerably above the measured flight drag (0.0253).



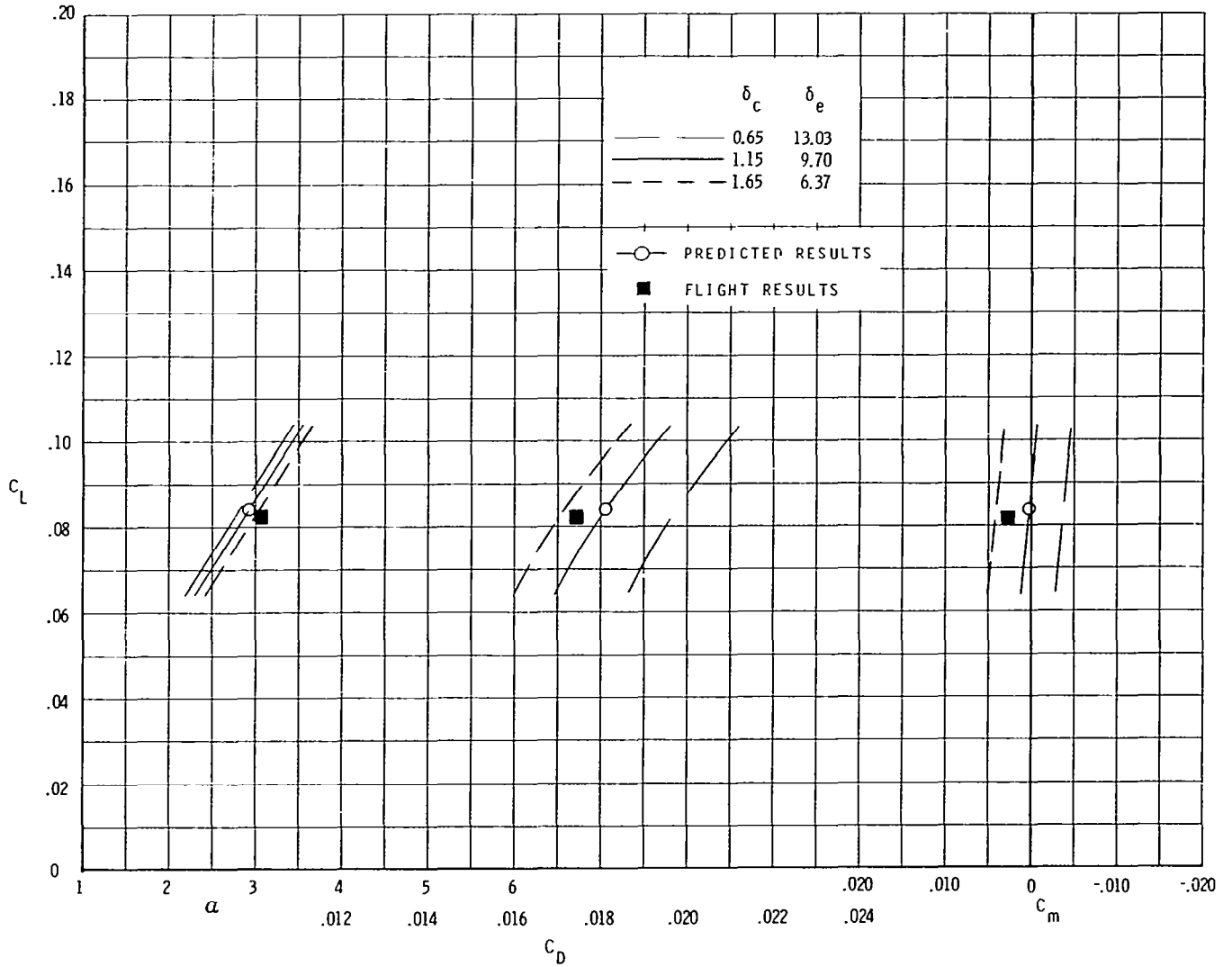
COMPARISON BETWEEN PREDICTED AND FLIGHT-MEASURED RESULTS FOR P3

A comparison between the predicted (curves) and flight-measured (solid square) results is shown for point P3 at $M = 1.18$. The prediction based on the flight-measured deflection is shown as a solid curve and predictions based on canard deflections $\pm 0.5^\circ$ from the measured deflection are shown as dashed lines. The predicted and flight-measured drag values agree fairly well, but the pitching-moment coefficients predicted from the wind-tunnel data using the flight-measured control deflection do not agree well.



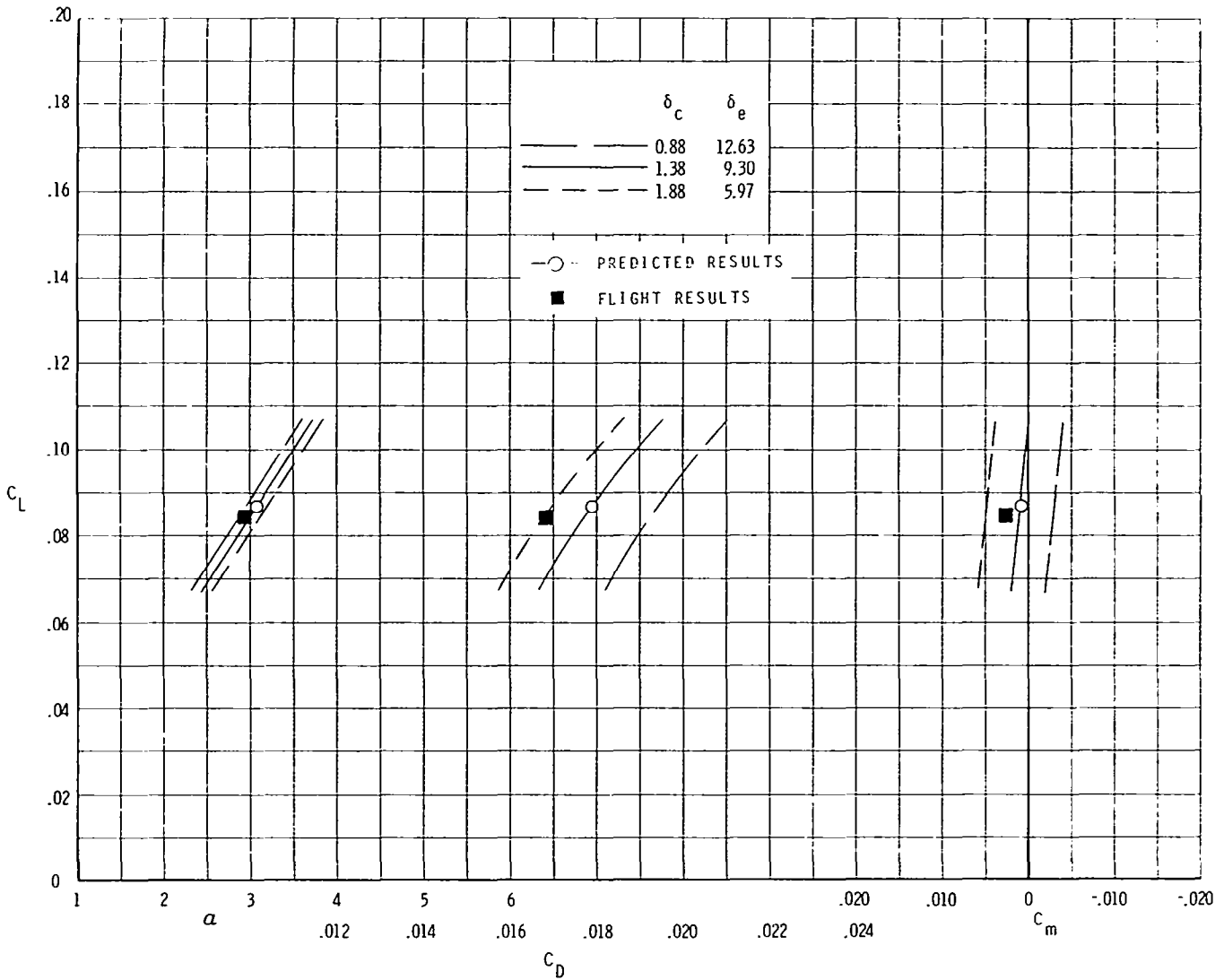
COMPARISON BETWEEN PREDICTED AND FLIGHT-MEASURED RESULTS FOR P4

A comparison between the predicted (curves) and flight-measured (solid square) results is shown for point P4 at $M = 1.60$. The prediction based on the flight-measured deflection is shown as a solid curve and predictions based on canard deflections $\pm 0.5^\circ$ from the measured deflection are shown as dashed lines. The predicted and flight-measured values of angle of attack, C_D , and C_m agree fairly well.



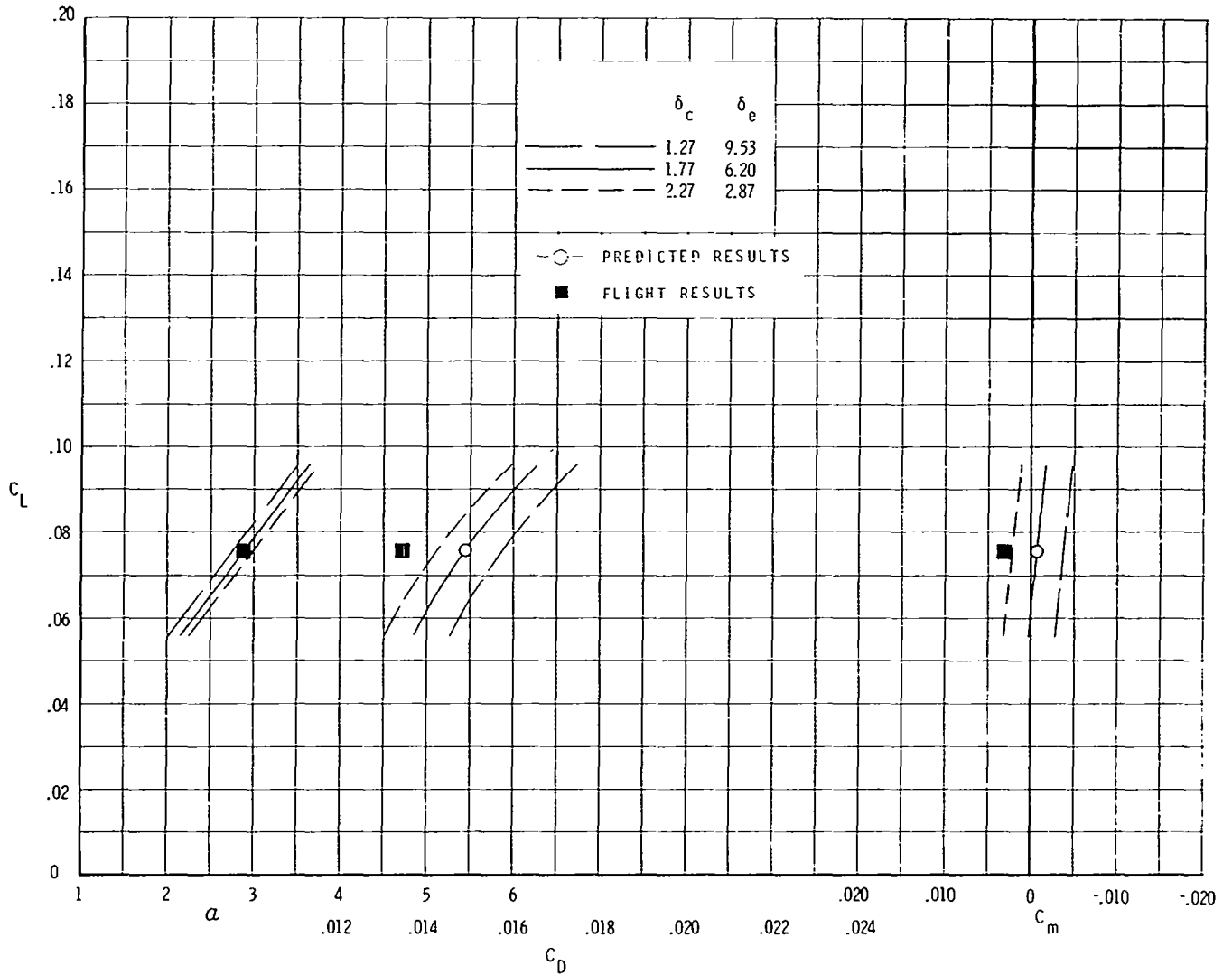
COMPARISON BETWEEN PREDICTED AND FLIGHT-MEASURED RESULTS FOR P5

A comparison between the predicted (curves) and flight-measured (solid square) results is shown for point P5 at $M = 1.67$. The prediction based on the flight-measured deflection is shown as a solid curve and predictions based on canard deflections $\pm 0.5^\circ$ from the measured deflection are shown as dashed lines. The predicted drag coefficient is somewhat higher than the flight-measured drag coefficient.



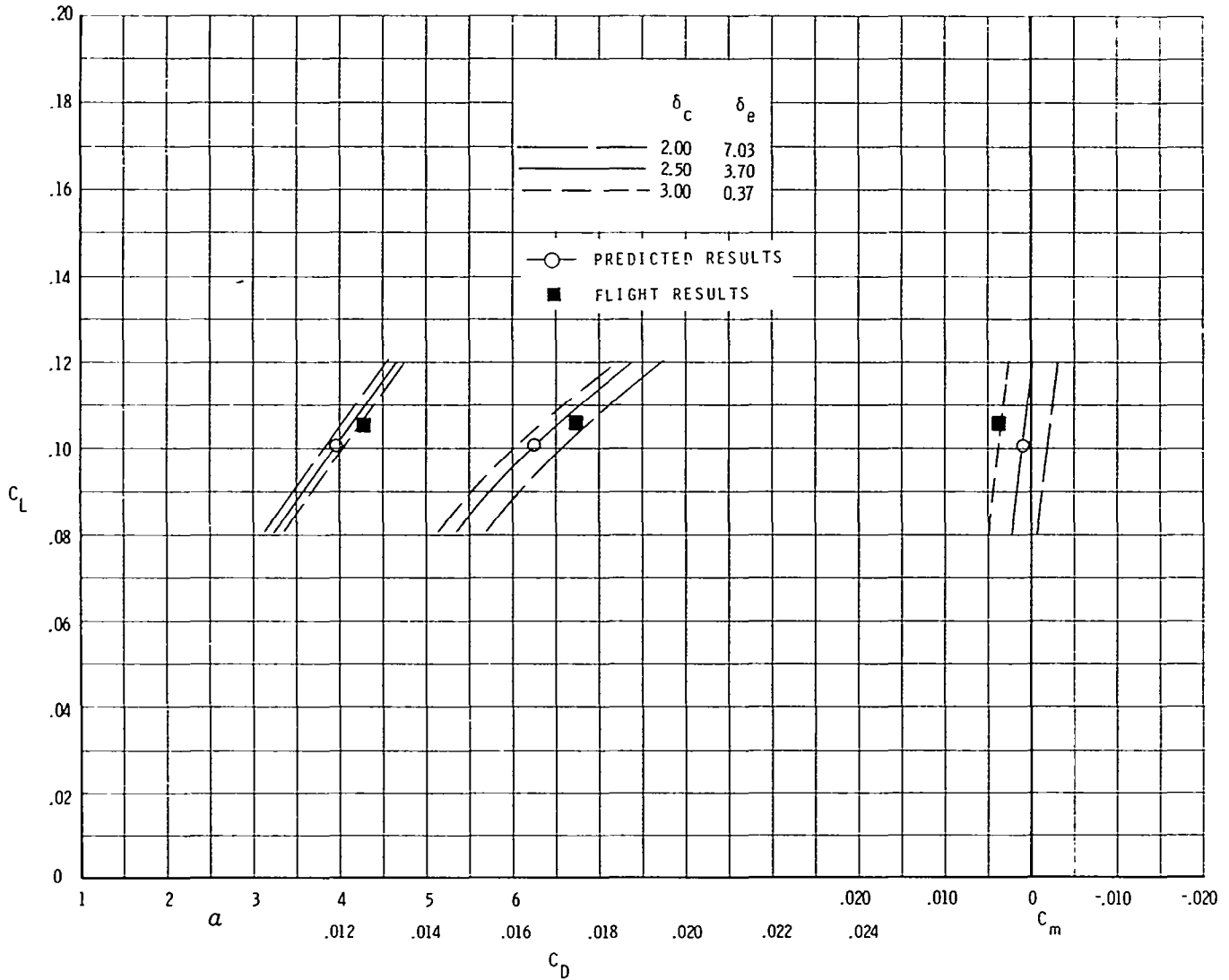
COMPARISON BETWEEN PREDICTED AND FLIGHT-MEASURED RESULTS FOR P6

A comparison between the predicted (curves) and flight-measured (solid square) results is shown for point P6 at $M = 2.10$. The prediction based on the flight-measured deflection is shown as a solid curve and predictions based on canard deflections $\pm 0.5^\circ$ from the measured deflection are shown as dashed lines. The predicted drag is higher than the flight-measured drag; however, if the control deflection is changed from the flight-measured deflection to match C_m , the drag values would agree fairly well.



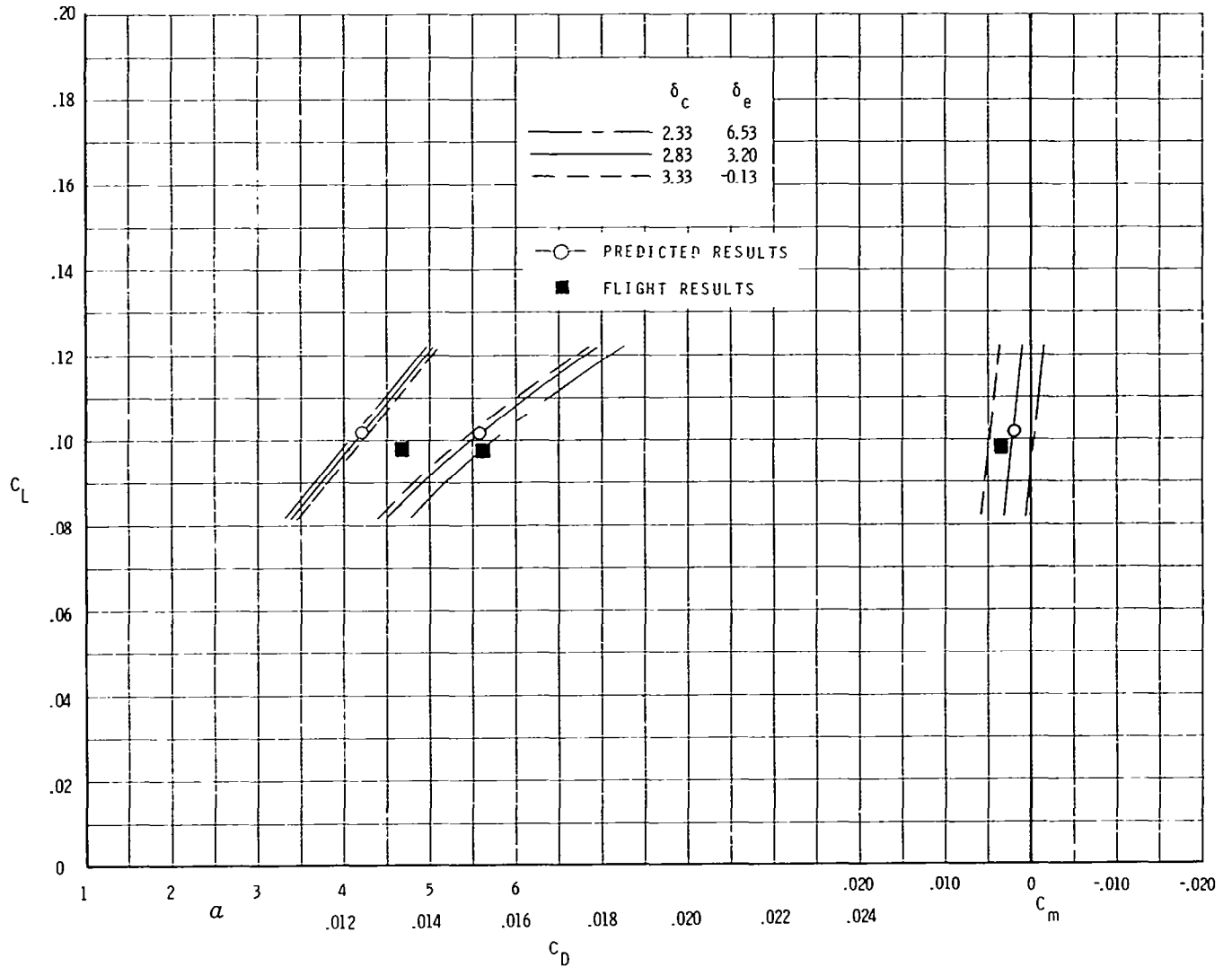
COMPARISON BETWEEN PREDICTED AND FLIGHT-MEASURED RESULTS FOR P7

A comparison between the predicted (curves) and flight-measured (solid square) results is shown for point P7 at $M = 2.15$. The prediction based on the flight-measured deflection is shown as a solid curve and predictions based on canard deflections $\pm 0.5^\circ$ from the measured deflection are shown as dashed lines. The values of angle of attack and C_D agree fairly well.



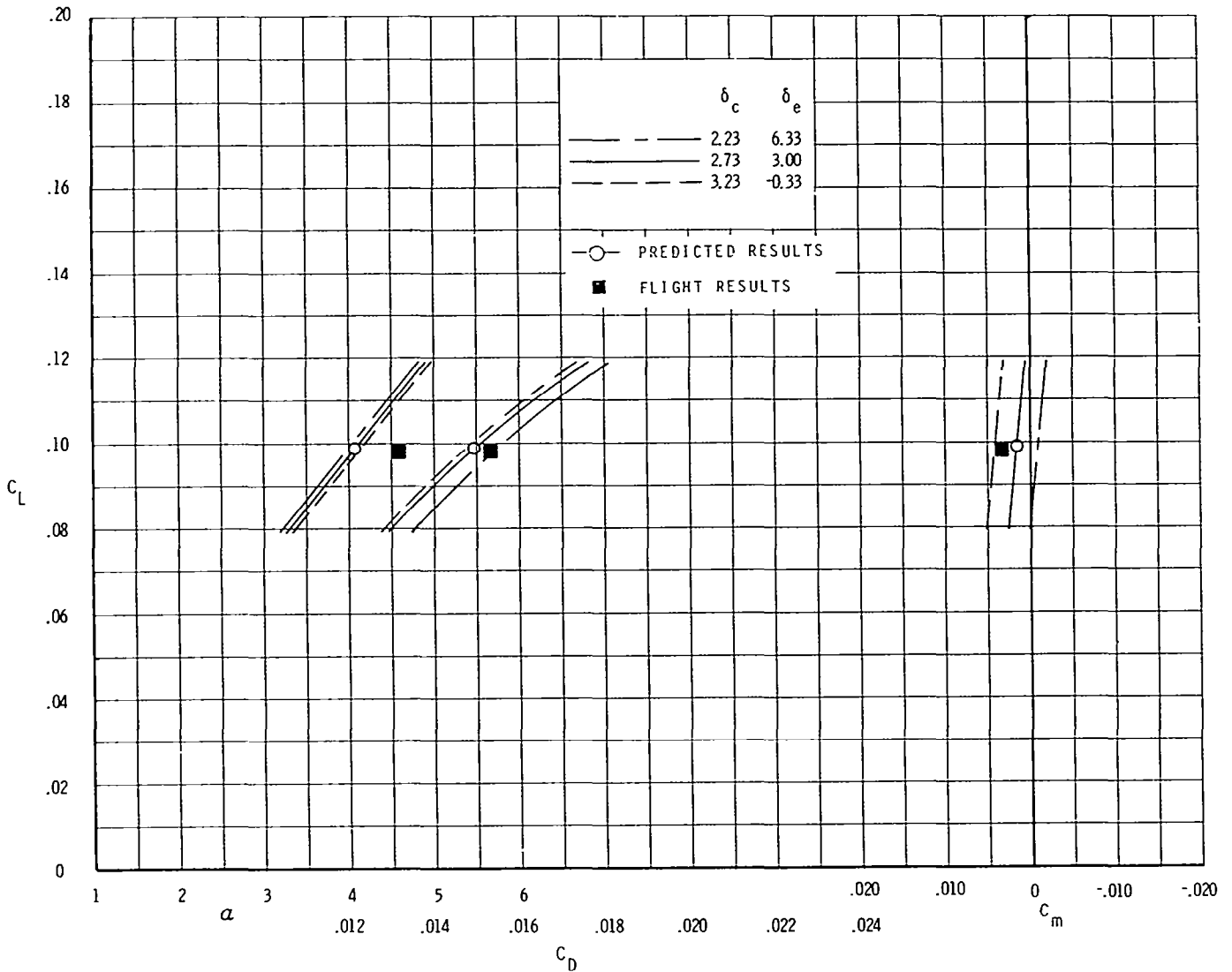
COMPARISON BETWEEN PREDICTED AND FLIGHT-MEASURED RESULTS FOR P8

A comparison between the predicted (curves) and flight-measured (solid square) results is shown for point P8 at $M = 2.53$. The prediction based on the flight-measured deflection is shown as a solid curve and predictions based on canard deflections $\pm 0.5^\circ$ from the measured deflection are shown as dashed lines. The drag coefficients and pitching-moment coefficients agree fairly well, but the difference in angle of attack is about 0.5° which is considerably above the expected accuracy in measuring the angle of attack in flight ($\pm 0.3^\circ$) or in the wind tunnel ($\pm 0.1^\circ$).



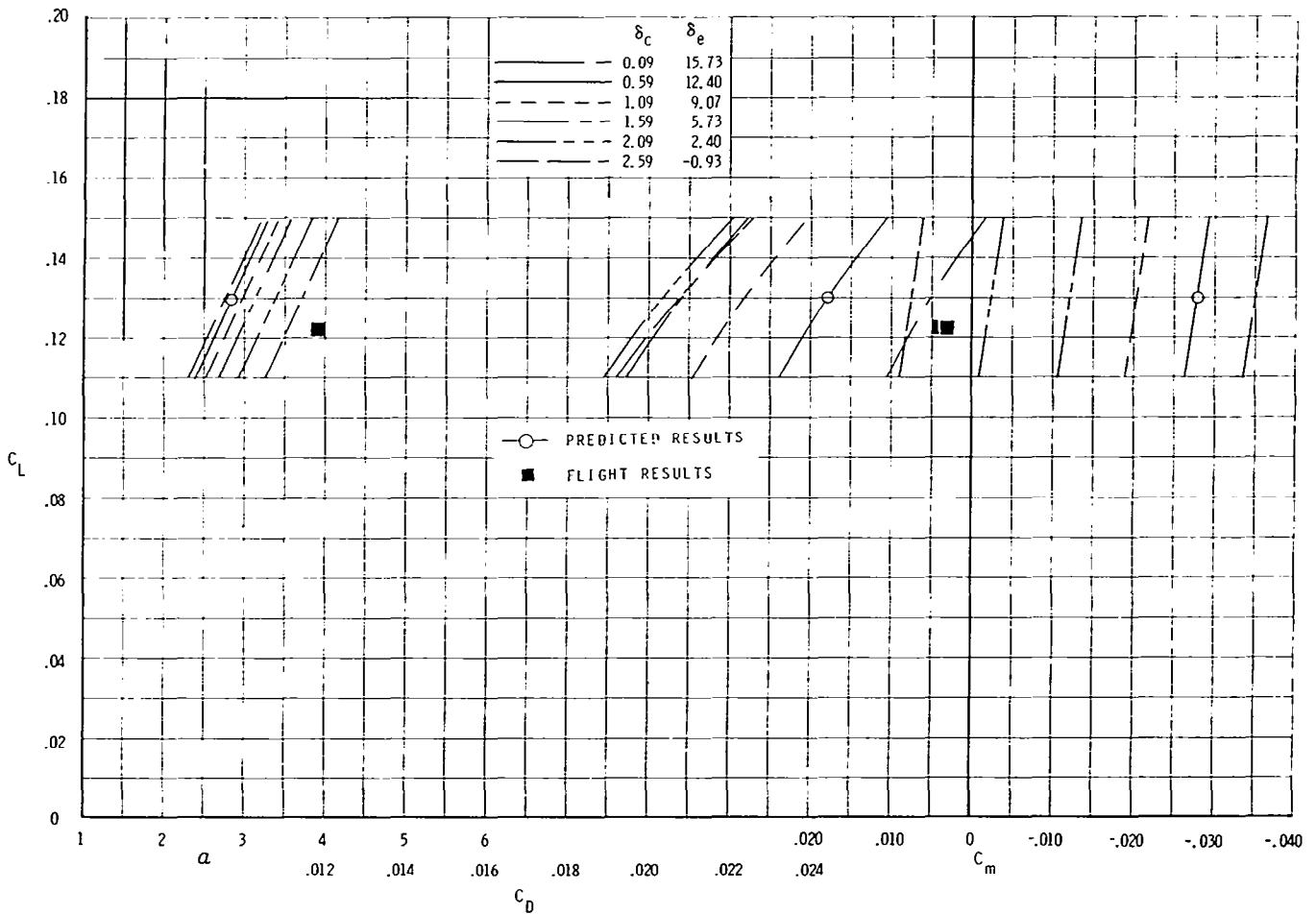
COMPARISON BETWEEN PREDICTED AND FLIGHT-MEASURED RESULTS FOR P9

A comparison between the predicted (curves) and flight-measured (solid square) results is shown for point P9 at $M = 2.50$. The prediction based on the flight-measured deflection is shown as a solid curve and predictions based on canard deflections $\pm 0.5^\circ$ from the measured deflection are shown as dashed lines. The values of C_D and C_m agree fairly well, but the difference in angle of attack (about 0.6°) is higher than expected.



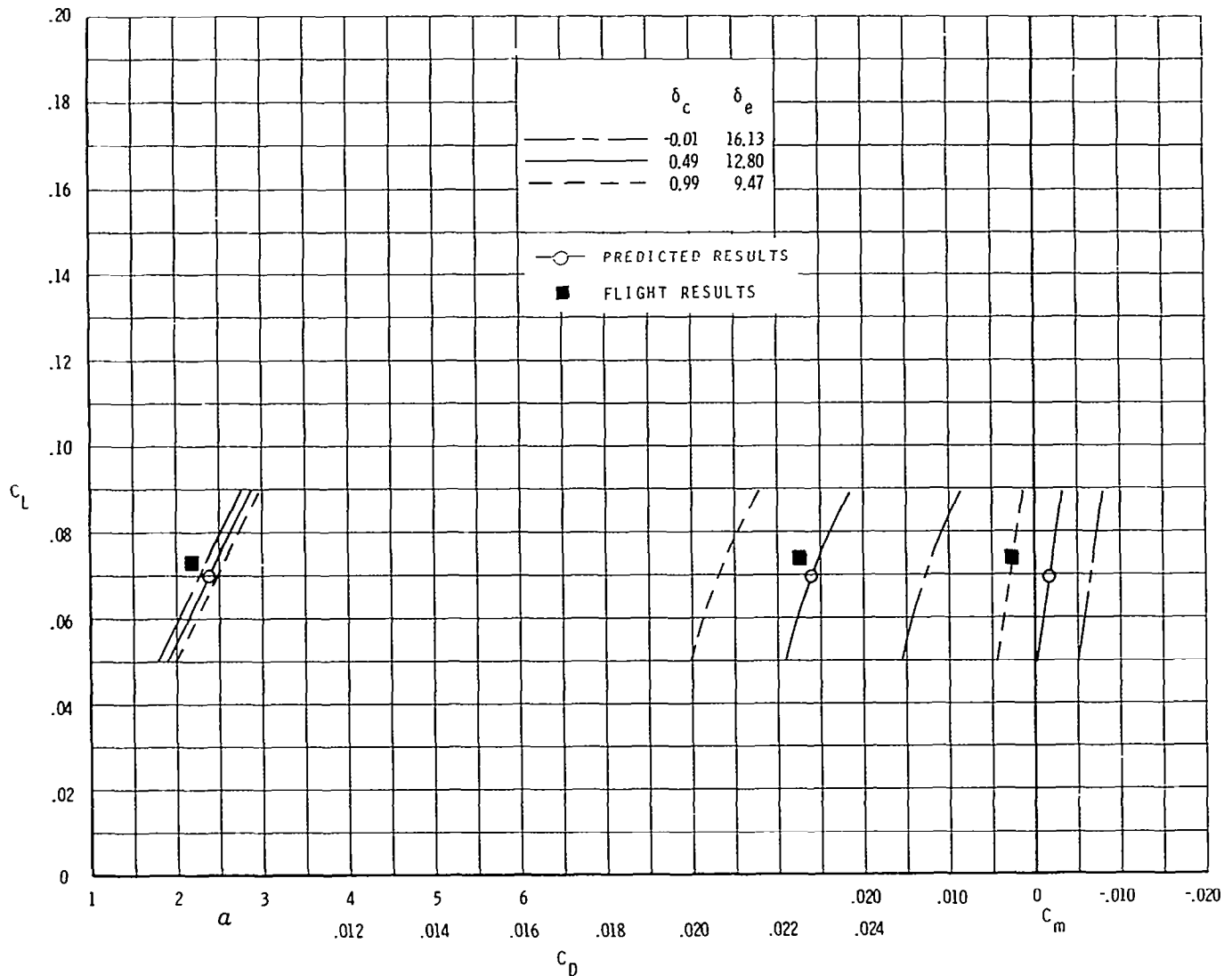
COMPARISON BETWEEN PREDICTED AND FLIGHT-MEASURED RESULTS FOR P10

A comparison between the predicted (curves) and flight-measured (solid square) results is shown for point P10 at $M = 1.06$. The prediction based on the flight-measured deflection is shown as a solid curve and predictions based on canard deflections several degrees different from the measured deflection are shown as dashed lines. This point was the most difficult point to predict since wind-tunnel data could not be obtained at $M = 1.06$ and data at Mach numbers below 0.95 and above 1.2 had to be interpolated to obtain data at $M = 1.06$. It is apparent that there are large differences in the angle of attack, C_D , and C_m (or control deflection necessary to trim the airplane).



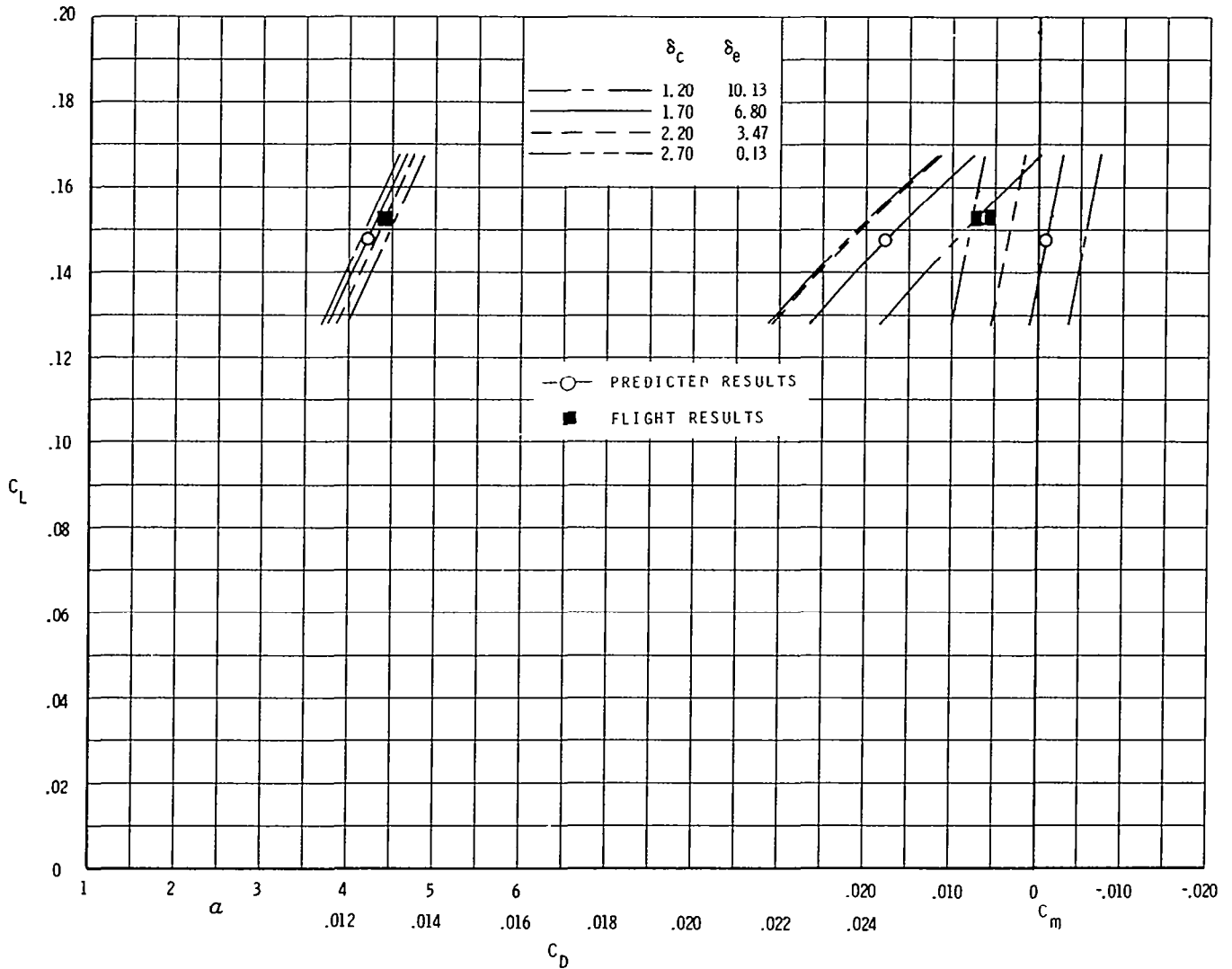
COMPARISON BETWEEN PREDICTED AND FLIGHT-MEASURED RESULTS FOR P3L

A comparison between the predicted (curves) and flight-measured (solid square) results is shown for point P3L at $M = 1.15$. The prediction based on the flight-measured deflection is shown as a solid curve and predictions based on canard deflections $\pm 0.5^\circ$ from the measured deflection are shown as dashed lines. The values of C_D agree fairly well, but if the control deflections required to trim the airplane were used, then the predicted C_D would be less than the flight C_D .



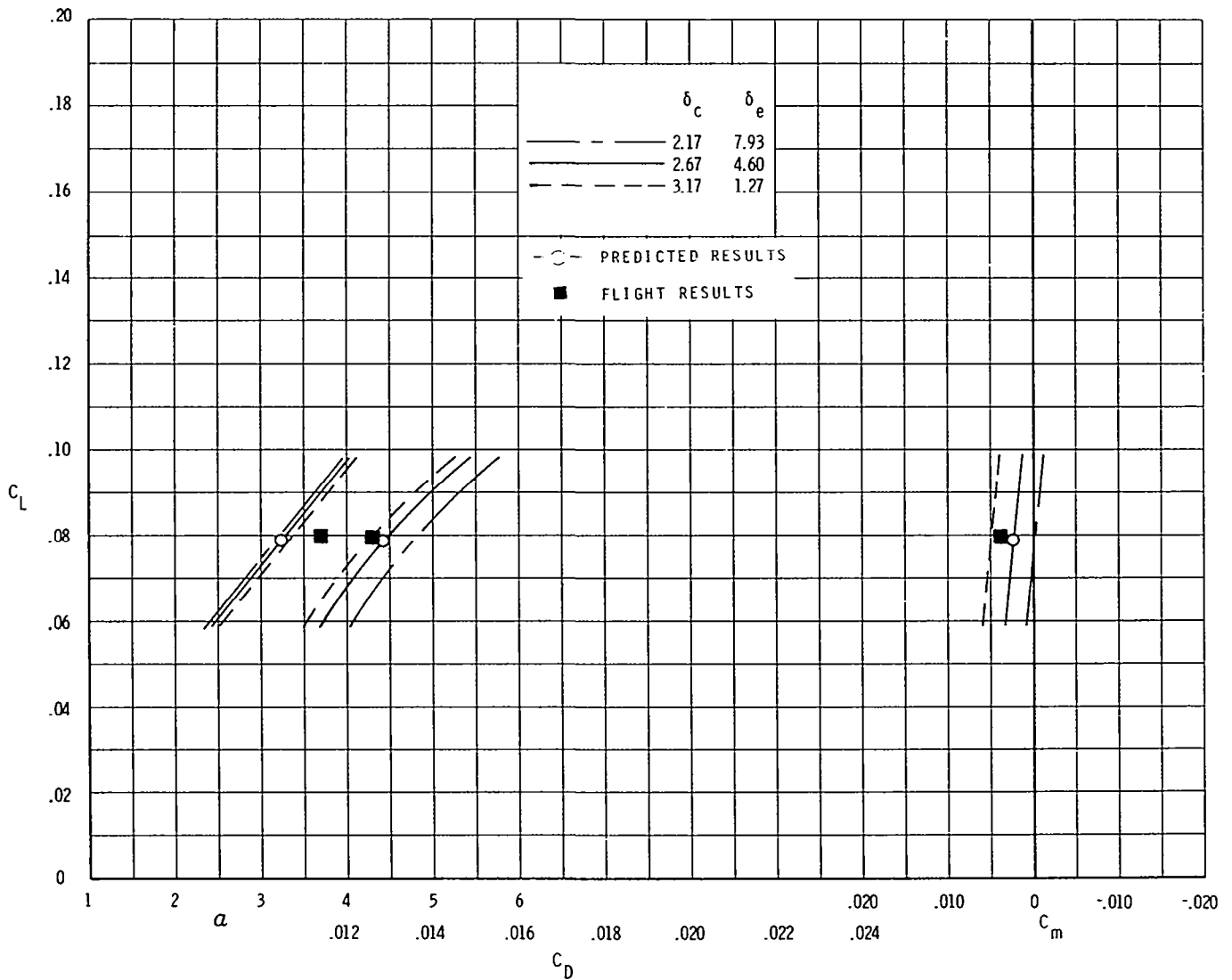
COMPARISON BETWEEN PREDICTED AND FLIGHT-MEASURED RESULTS FOR P3H

A comparison between the predicted (curves) and flight-measured (solid square) results is shown for point P3H at $M = 1.17$. The prediction based on the flight-measured deflection is shown as a solid curve and predictions based on canard deflections of -0.5° , 0.5° , and 1.0° from the measured deflection are shown as dashed lines. The predicted C_D (0.0251) is below the flight-measured C_D (0.0266) and the predicted C_m (-0.0015) is less than the flight-measured C_m (0.0061).



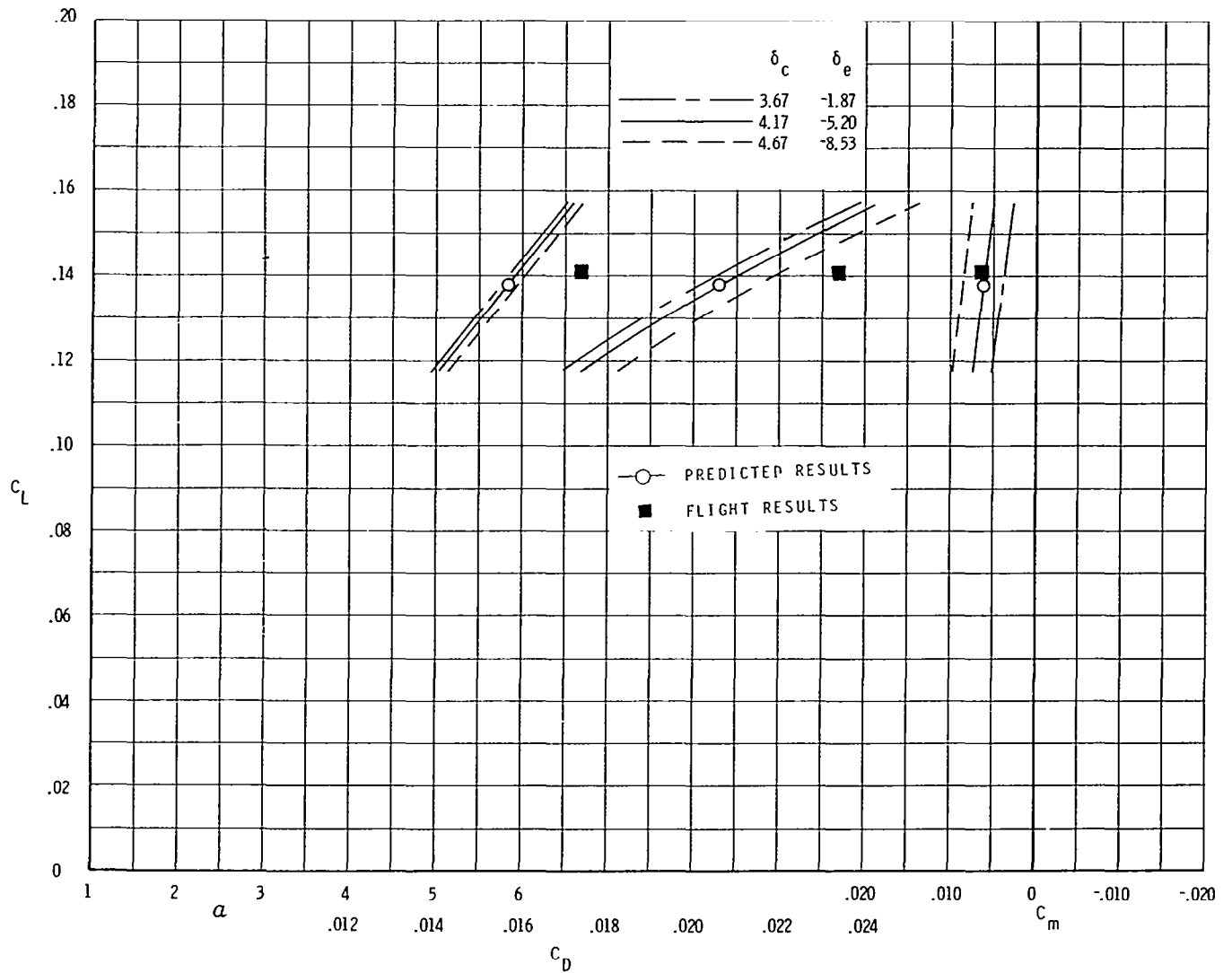
COMPARISON BETWEEN PREDICTED AND FLIGHT-MEASURED RESULTS FOR P8L

A comparison between the predicted (curves) and flight-measured (solid square) results is shown for point P8L at $M = 2.51$. The prediction based on the flight-measured deflection is shown as a solid curve and predictions based on canard deflections $\pm 0.5^\circ$ from the measured deflection are shown as dashed lines. The predicted and flight-measured values of C_D and C_m agree well, but the predicted angle of attack is about 0.4° less than the flight-measured angle of attack.



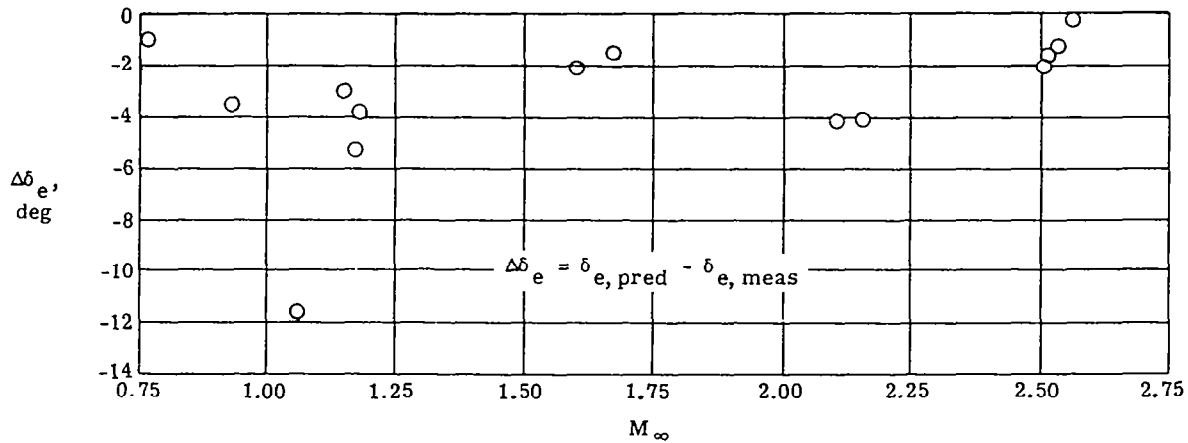
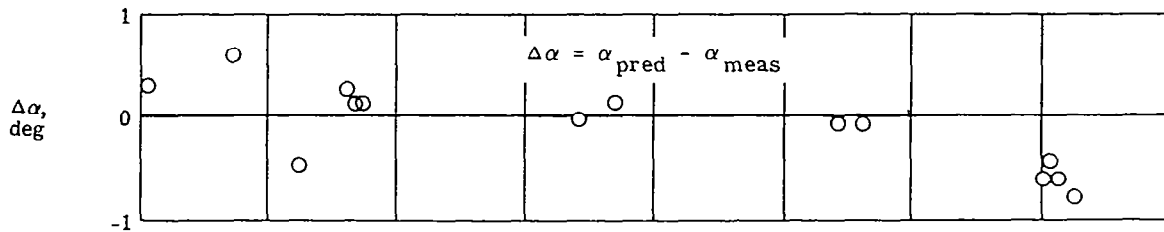
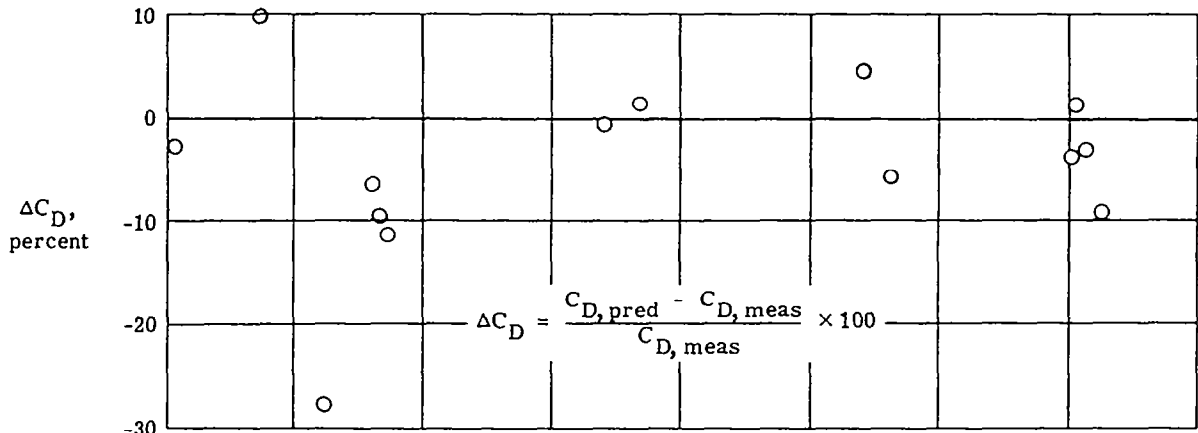
COMPARISON BETWEEN PREDICTED AND FLIGHT-MEASURED RESULTS FOR P8H

A comparison between the predicted (curves) and flight-measured (solid square) results is shown for point P8H at $M = 2.56$. The prediction based on the flight-measured deflection is shown as a solid curve and predictions based on canard deflections $\pm 0.5^\circ$ from the measured deflection are shown as dashed lines. The predicted C_D is considerably less than the flight-measured C_D and the predicted angle of attack is about 0.7° less than the flight-measured angle of attack.



SUMMARY OF DIFFERENCE BETWEEN PREDICTED AND FLIGHT-MEASURED
DRAG COEFFICIENT, ANGLE OF ATTACK, AND ELEVON DEFLECTION

The differences are shown between the predicted values for the airplane trimmed about the flight center of gravity and the flight-measured values at the same lift and moment coefficients. The drag coefficients generally agreed within 10 percent except for the point at $M = 1.06$ where the difference was 27 percent. The angles of attack generally showed good agreement except at Mach 2.5 where the flight-measured angle of attack was about 0.5° higher than that predicted. The elevon deflections required to trim the airplane about the flight center of gravity were generally 2° to 4° higher in flight than predicted except at $M = 1.06$ where the difference was almost 12° .



RESULTS OF XB-70 WIND-TUNNEL/FLIGHT CORRELATION

The main results found from the XB-70 wind-tunnel/flight correlation program are as follows:

1. The angle of attack for a given lift coefficient was about 0.5° higher in flight than predicted at Mach numbers near 2.5. These differences are higher than would be expected from errors in the wind-tunnel and flight instrumentation. An examination of possible sources of error, such as fuselage and nose-boom bending, upwash around the nose boom, and aerodynamic-vane floating angle, did not indicate any sources that are believed large enough to account for these discrepancies.
2. Large differences were found for the drag and pitching-moment coefficients at $M = 1.06$, probably because no wind-tunnel data could be obtained at $M = 1.06$ and data at Mach numbers of 0.75, 0.8, 0.95, 1.20, and 1.40 had to be interpolated to obtain data at $M = 1.06$.
3. The elevon deflection necessary to trim the XB-70 was about 2° to 4° higher in flight than predicted at all Mach numbers (except $M = 1.06$ where the difference was about 12°). This difference is equivalent to about 0.002 to 0.004 in C_m or about 2 to 4 percent mean aerodynamic chord change in the center of gravity. A possible reason for the differences in pitching moments is a different aeroelastic distortion of the airframe from the calculated values. Measurements of the distortions in flight to compare with the calculated values would be very desirable.
4. The stability augmentation system caused the controls to be varying about $\pm 1^\circ$ during the time of the flight data points. In order to determine the effects of small deflections of the control surfaces (such as 1° rudder deflection), it is more accurate to interpolate measurements made at large deflections (i.e., 0° , 5° , and 10°).

REFERENCES

1. Arnaiz, Henry H.: Flight-Measured Lift and Drag Characteristics of a Large, Flexible, High Supersonic Cruise Airplane. NASA TM X-3532, 1977.
2. Daugherty, James C.: Wind-Tunnel/Flight Correlation Study of Aerodynamic Characteristics of a Large Flexible Supersonic Cruise Airplane (XB-70-1). I - Wind-Tunnel Tests of a 0.03-Scale Model at Mach Numbers From 0.6 to 2.53. NASA TP-1514, 1979.
3. Peterson, John B., Jr.; Mann, Michael J.; Sorrells, Russell B., III; Sawyer, Wallace C.; and Fuller, Dennis E.: Wind-Tunnel/Flight Correlation Study of Aerodynamic Characteristics of a Large Flexible Supersonic Cruise Airplane (XB-70-1). II - Extrapolation of Wind-Tunnel Data to Full-Scale Conditions. NASA TP-1515, 1980.
4. Arnaiz, Henry H.; Peterson, John B., Jr.; and Daugherty, James C.: Wind-Tunnel/Flight Correlation Study of Aerodynamic Characteristics of a Large Flexible Supersonic Cruise Airplane (XB-70-1). III - A Comparison Between Characteristics Predicted From Wind-Tunnel Measurements and Those Measured in Flight. NASA TP-1516, 1980.
5. Arnaiz, Henry H.; and Schweikhard, William G.: Validation of the Gas Generator Method of Calculating Jet-Engine Thrust and Evaluation of XB-70-1 Airplane Engine Performance at Ground Static Conditions. NASA TN D-7028, 1970.
6. Arnaiz, Henry H.: Techniques for Determining Propulsion System Forces for Accurate High Speed Vehicle Drag Measurements in Flight. AIAA Paper No. 75-964, Aug. 1975.

PROBLEMS IN CORRELATION CAUSED BY PROPULSION SYSTEMS

Ronald H. Smith
NASA Langley Research Center

Miniworkshop on Wind Tunnel/Flight Correlation
November 19-20, 1981

ABSTRACT

Transonic drag has been poorly predicted in the past, particularly for multi-engined military supersonic aircraft. The attempts to explain the discrepancies and anomalies in predictability of propulsive drag effects suggest strongly that careful systematic well-coordinated tunnel and flight measurements are required also, to assure better resolution in aerodynamic drag measurements. This paper reviews correlation efforts and selected results since the mid-1960's which attempted to explain propulsion-related anomalies. Drawing on reference 1 which suggests improvements to aircraft prediction methods, a process is summarized to reduce the typical error sources to decrease the errors inherent in the transonic aircraft development process.

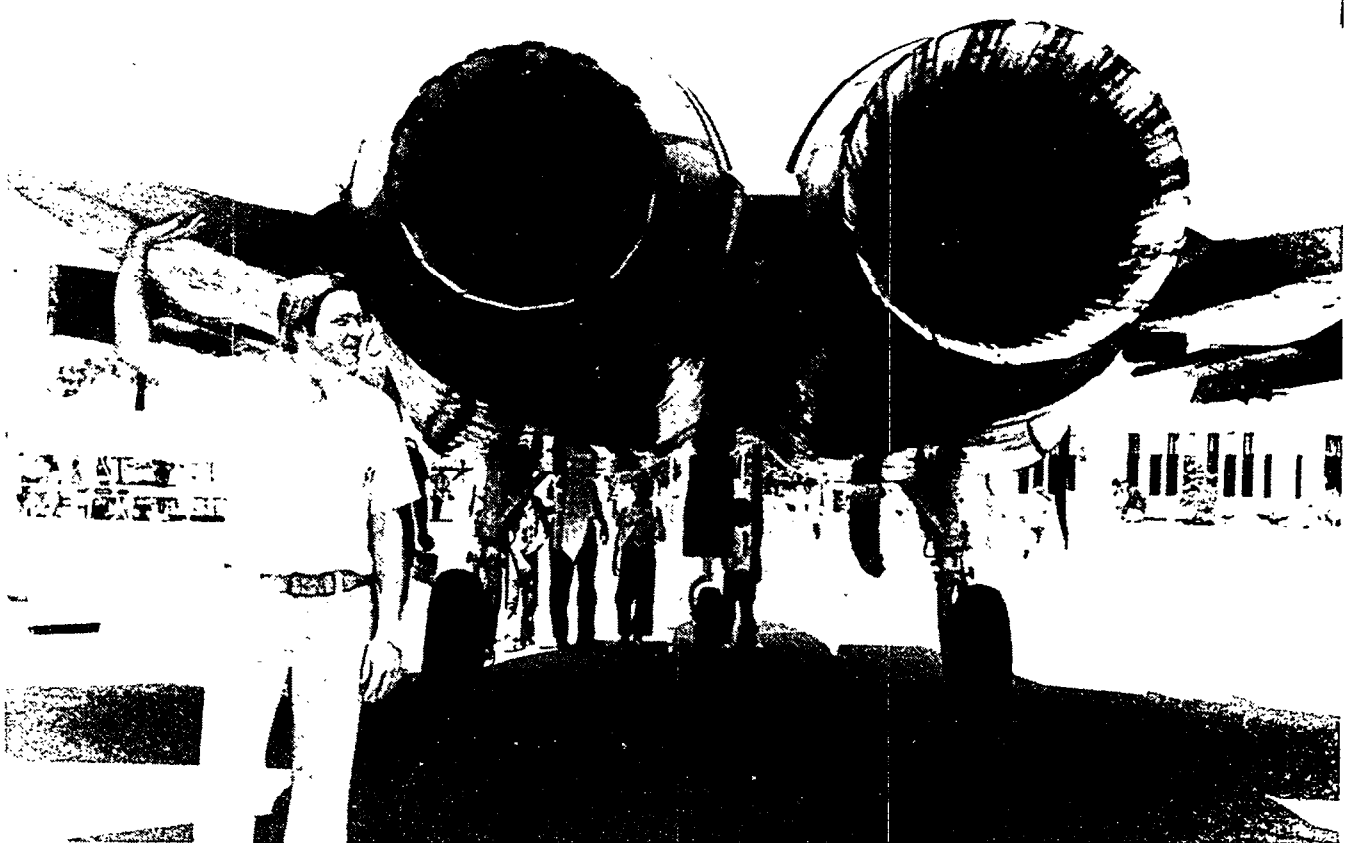
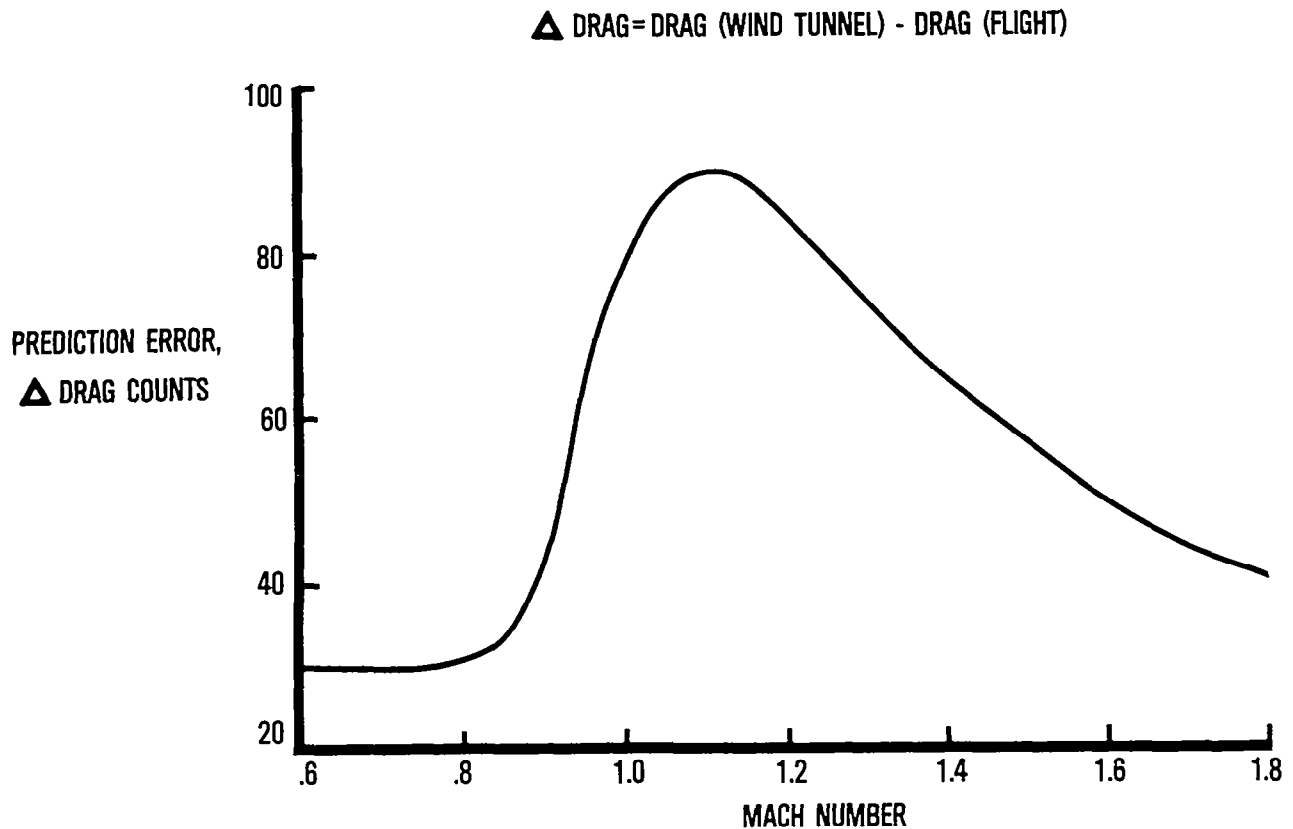


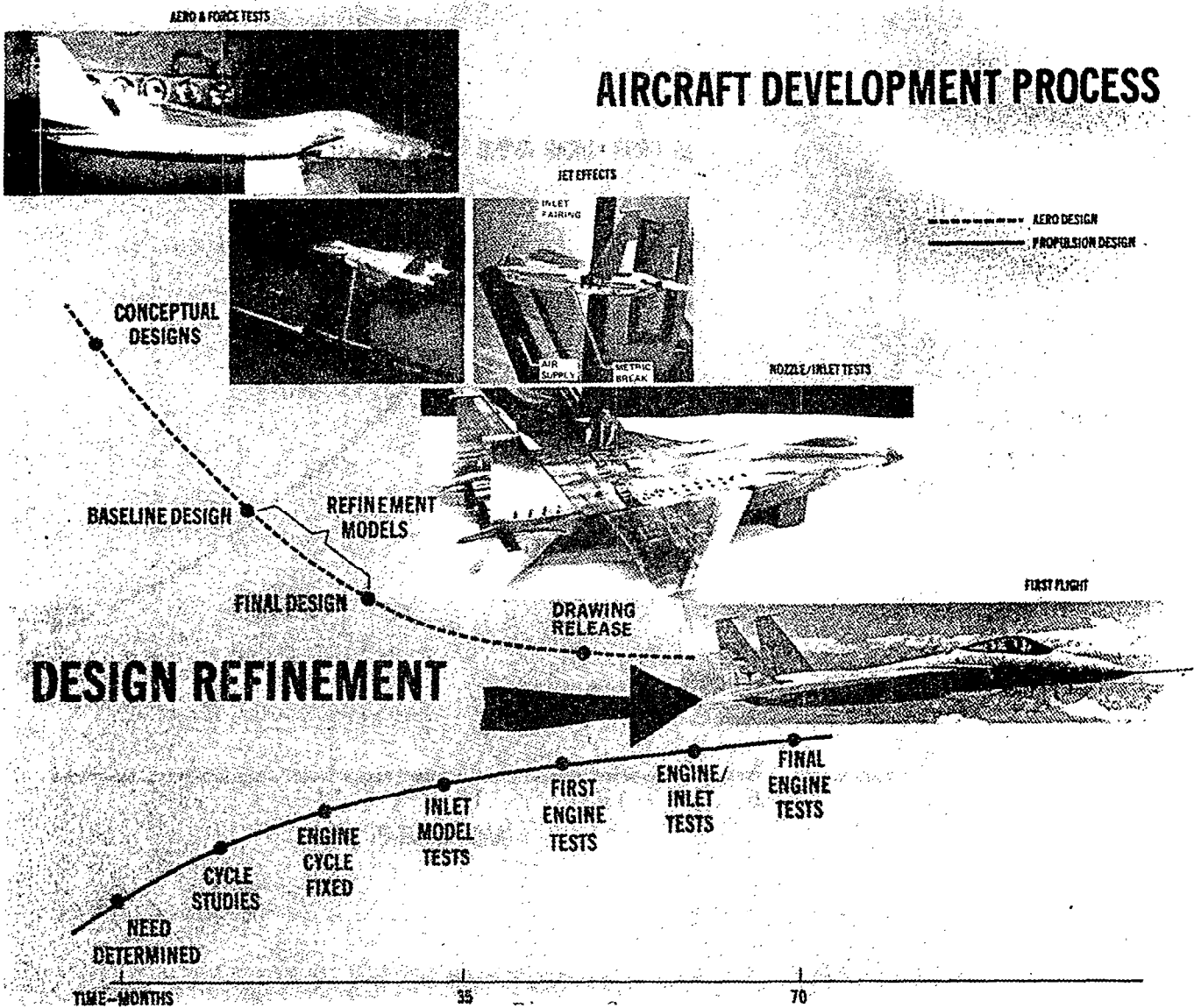
ILLUSTRATION OF THE MAGNITUDE OF THE PROPULSION INTEGRATION PROBLEM

- The error in prediction of installed drag for a late 1950's fighter, even with extreme care in tunnel and flight tests, was greater than 80 drag counts near a Mach number of 1.2.
- Many attempts to explain the causes have been made since the early 1960's.
- In most cases, the reasons are not resolved but are left explained by possible Reynolds number effects, configuration differences, or poor testing procedures.



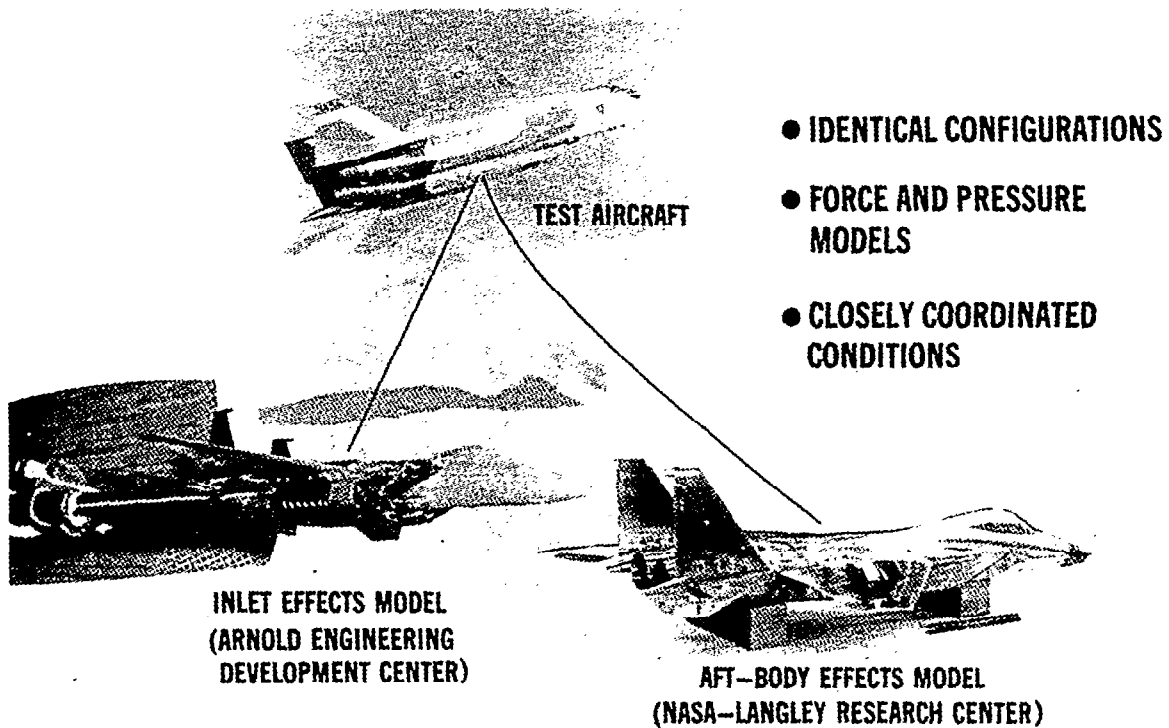
COMPARISON OF AERODYNAMIC CONFIGURATION AND PROPULSION DEVELOPMENT SCHEDULES

- Inequities in time of development of the engine installation and aerodynamic configuration could explain why a consistent set of data are not available to resolve drag prediction differences.
- The realities of rushed development schedules have prevented a thorough analysis of significant propulsion effects.
- A NASA program in 1975 was developed to retrace causes of propulsion drag in a systematic manner after the aircraft development.



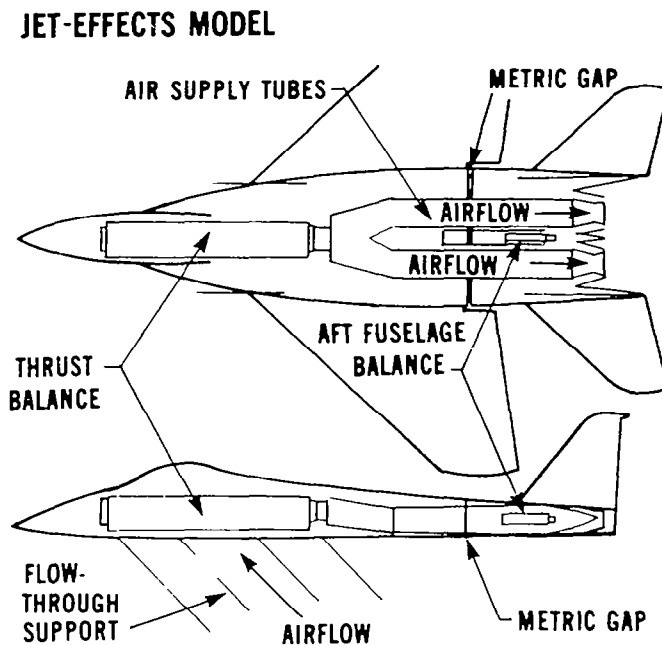
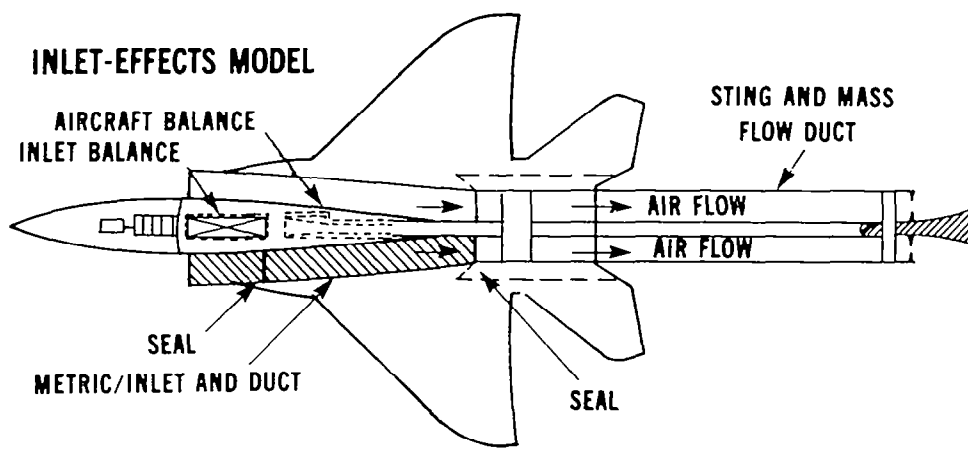
MODELS AND AIRCRAFT USED IN THE NASA F-15 PROPULSION EFFECTS PROGRAM

- Models used in developing the F-15 were modified.
- Precise configuration modifications were made to match the test aircraft.
- Both force and pressure distributions were measured on the aft-body (Langley) and inlet-effects (AEDC) models.
- Flight and wind-tunnel test conditions were precisely matched.



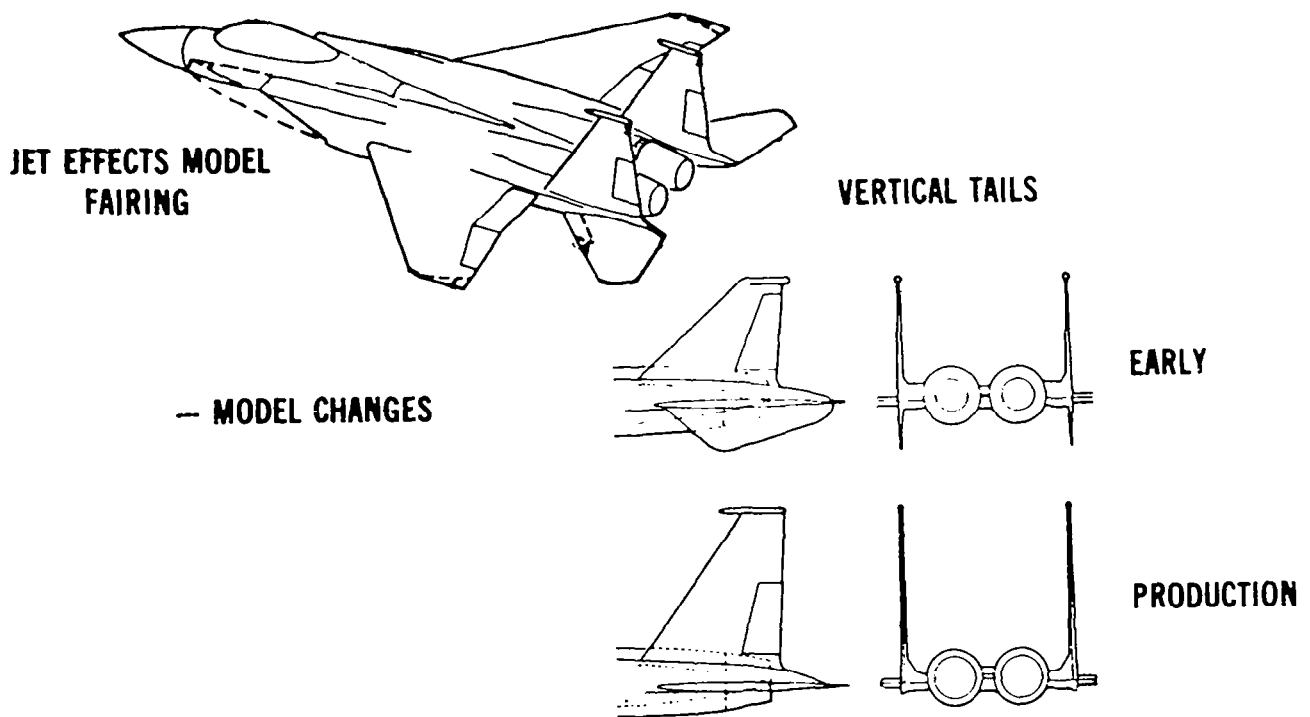
DETAILS OF THE INLET- AND JET-EFFECTS MODELS

- Both models simulated airflow as in the aircraft.
- Independent measurements of inlet and aft-body forces were made.
- Pressure distributions on external surfaces were measured on both models to compare with similar flight measurements.



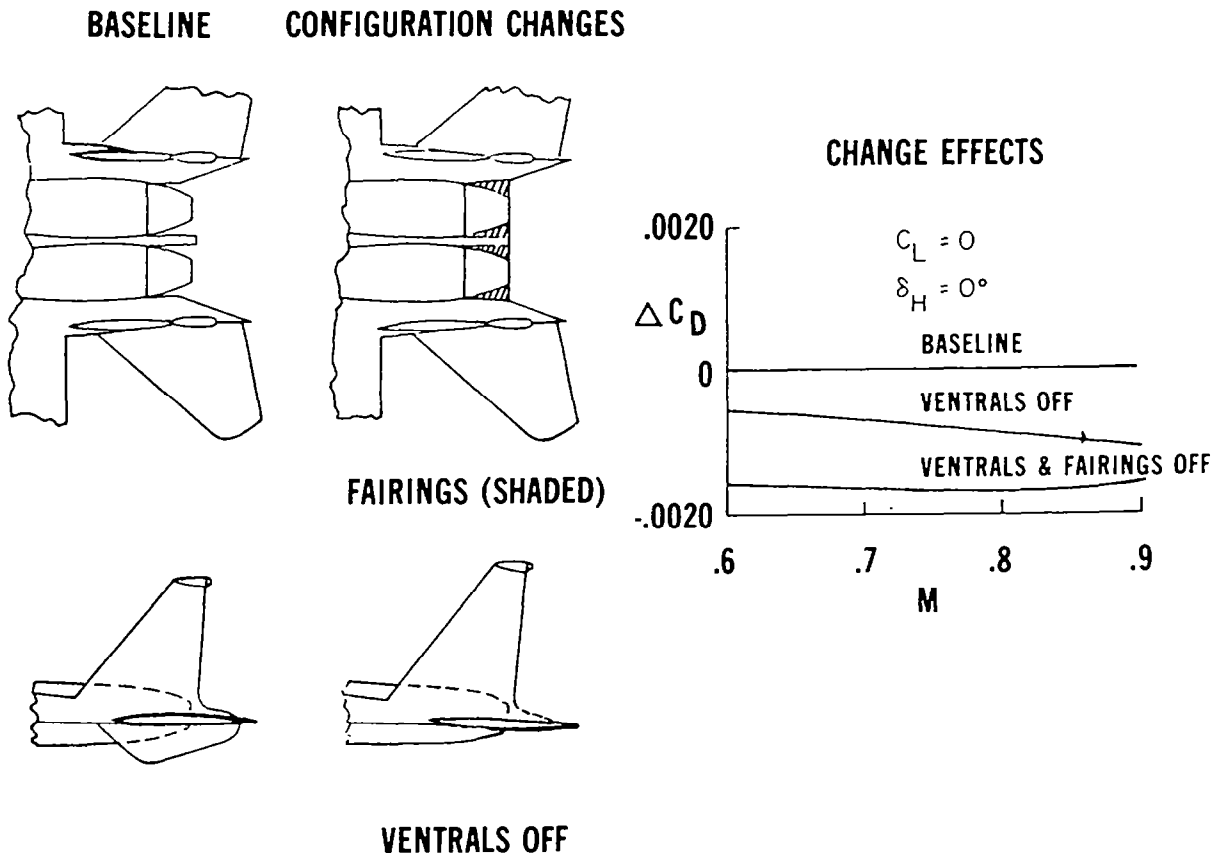
EXAMPLE CONFIGURATION CHANGES FROM EARLY DEVELOPMENT UNTIL PRODUCTION

- Changes in low ventral, wing tip, and vertical tails were made to the aircraft.
- Fairings on the jet-effects model were different from the real aircraft.
- The inlet-effects model was precise in the inlet region but was distorted by the stings in the nozzle region.
- The NASA program precisely modeled the aircraft in wind-tunnel tests.



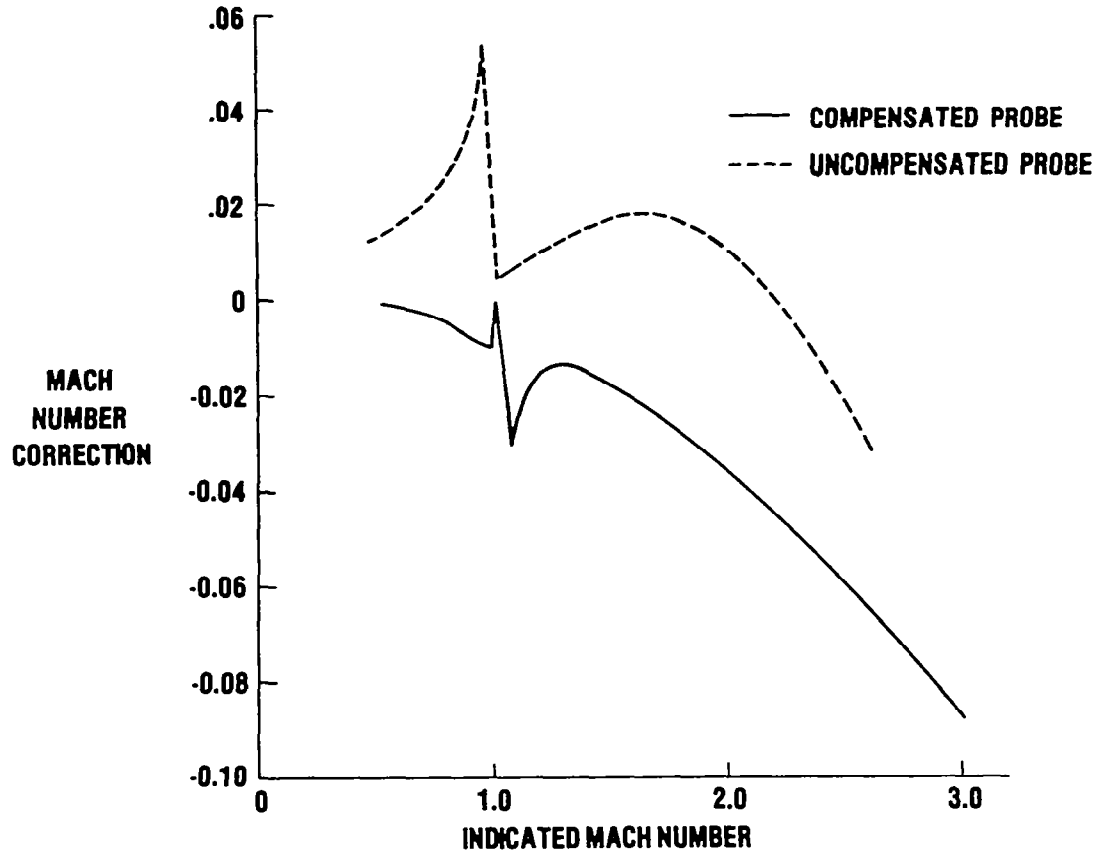
TYPICAL DRAG INCREMENTS FOR SMALL CONFIGURATION MODIFICATIONS

- Drag differences of about 10 counts at a Mach number of 0.8 could be attributed to not considering lower ventral effects.
- An internozzle fairing was also considered which might have reduced the drag by another 5 counts.
- Such seemingly minor changes are sometimes not considered in tunnel/flight comparisons and are collectively significant.



CORRECTIONS TYPICAL FOR AIRSPEED PROBES

- Precision of flight data is often questioned when compared to model data.
- The airspeed parameters strongly influence such flight comparisons.
- Corrections in Mach number indicated are shown for a typical installation.
- As much as 0.04 error in Mach number could occur at a Mach number of 2.0 if an uncompensated probe is used.



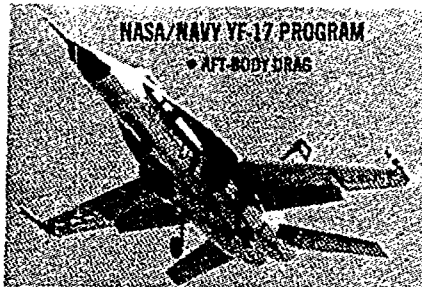
AIRCRAFT USED IN THE JOINT NASA/NAVY/AIR FORCE CORRELATIONS

- In addition to the F-15, the YF-17, B-1, and YF-12 supplied similar flight-to-wind-tunnel research correlations.
- Emphasis was on inlet, nozzle, and engine effects.
- Fundamental flow models were also flown. The 10° cone on the F-15 and the circular cylinder on the YF-12 are examples.



NASA F-15 PROGRAM

- AFT-BODY EFFECTS
- INLET EFFECTS
- 10° CONE EVALUATION
- INLET/ENGINE COMPATIBILITY



NASA/NAVY YF-17 PROGRAM
● AFT-BODY DRAG



NASA YF-12

- BOUNDARY LAYER PREDICTIONS
- FLOWFIELD STUDIES
- INLET PERFORMANCE

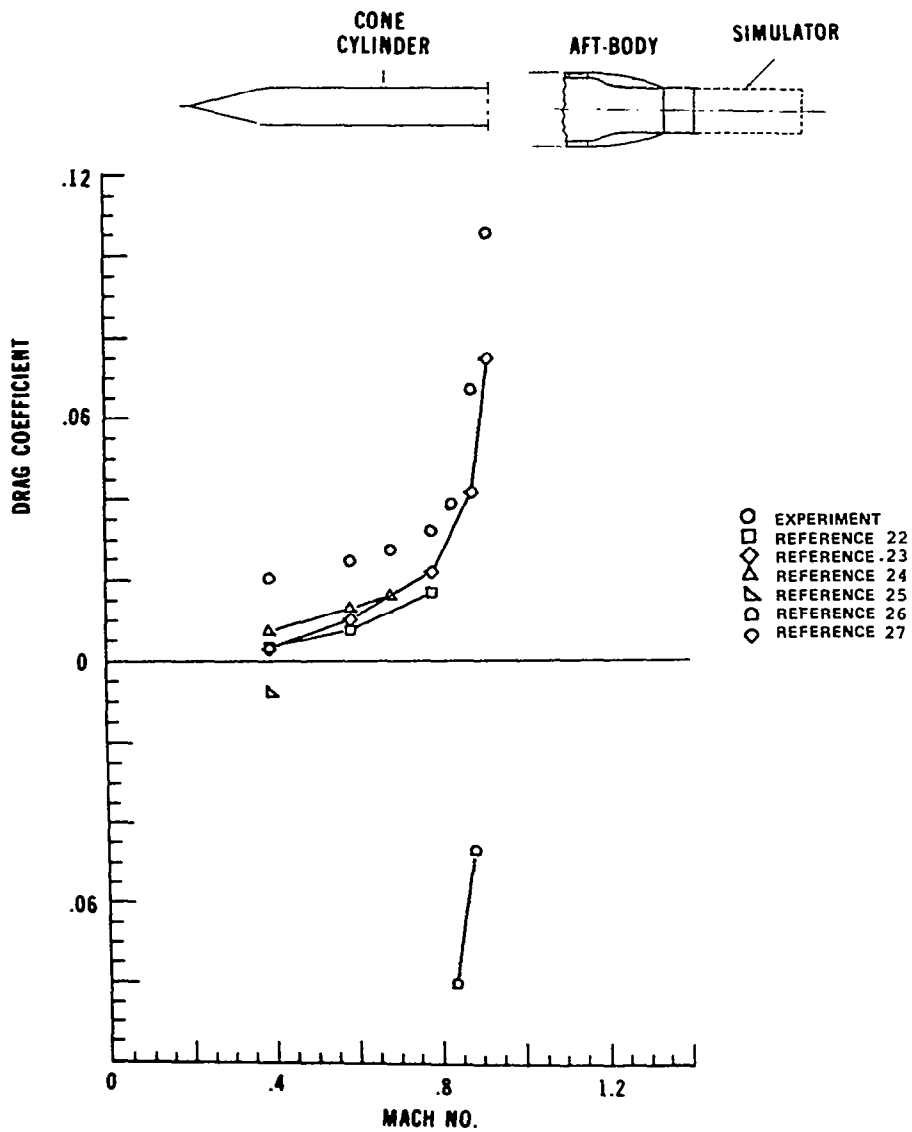


AIR FORCE/NASA B-1 PROGRAM

- RACELLE DRAG
- INLET/ENGINE COMPATIBILITY

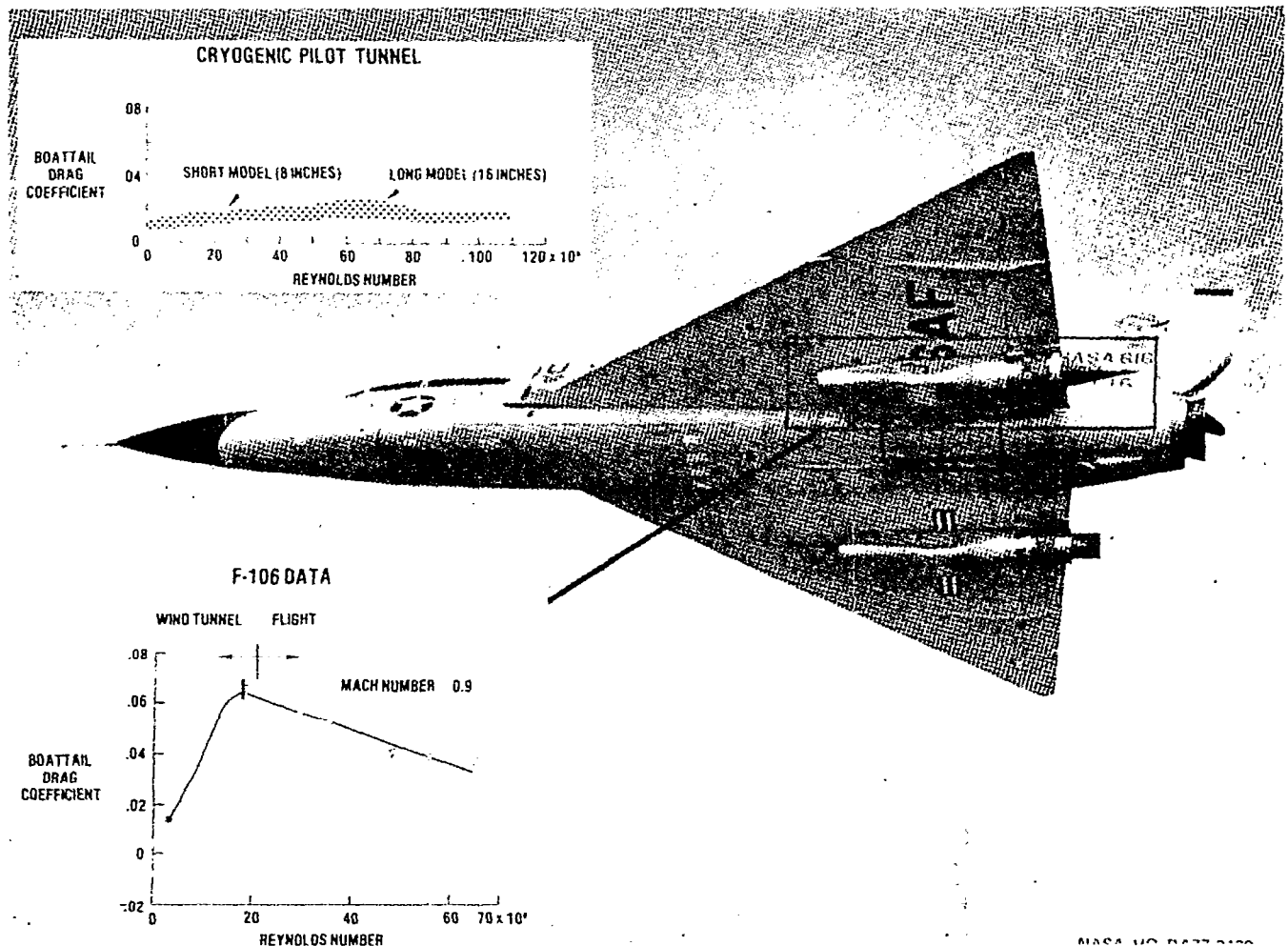
COMPARISON OF TEST DATA AND THEORY FOR A SIMPLE CONE, CYLINDER, AND AFT-BODY

- Langley Research Center tested a simple shape for theory comparisons.
- Most theoretical approaches were inadequate by large increments.
- More complex or realistic shapes would be expected to be more difficult to predict.



REYNOLDS NUMBER EFFECTS FOR AN F-106 NACELLE AND MODELS IN THE NTF
CRYOGENIC PILOT TUNNEL¹

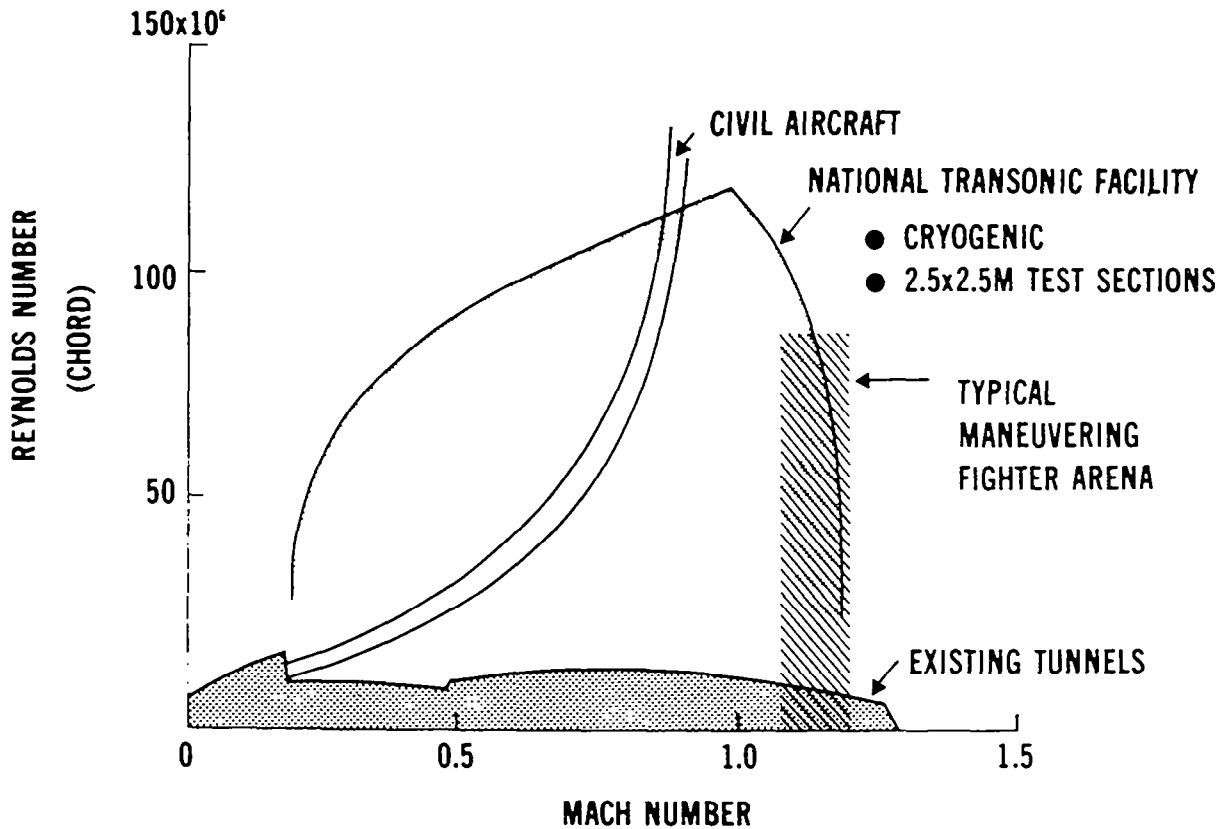
- Reynolds number effects on drag coefficients had been suspected from differences in predicted drag.
- Lewis Research Center compared drag effects in the wind tunnel and in flight on the F-106.
- The trend was reversed as Reynolds number increased (in flight).
- Recent data from the high Reynolds number Cryogenic Pilot Tunnel showed only small changes in drag for simple bodies.



¹This tunnel is now known as the Langley 0.3-Meter Transonic Cryogenic Tunnel (0.3 m TCT).

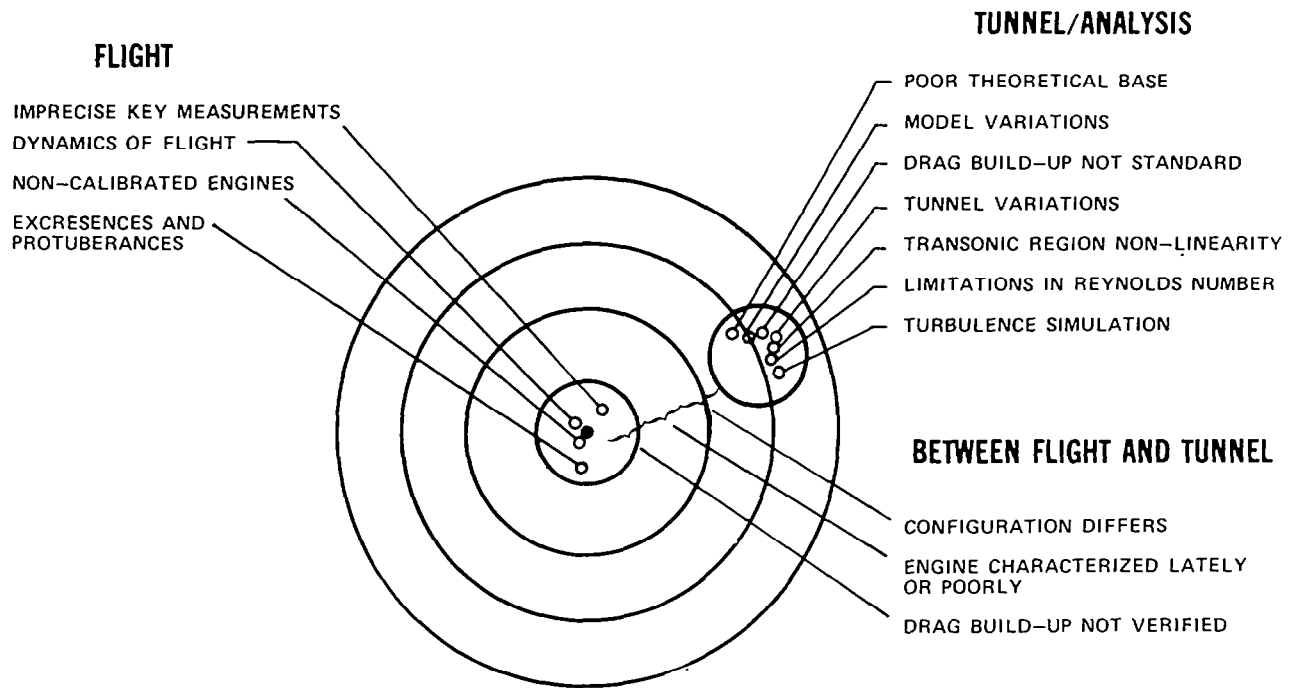
APPLICABILITY OF NTF CAPABILITY TO FUTURE FIGHTER PREDICTIONS

- The National Transonic Facility will have higher Reynolds number capability than any existing tunnels.
- Many of the questions on propulsion effects as influenced by increased flight Reynolds numbers could be answered by the NTF.
- Future fighters could be designed with more precise estimates of drag through better knowledge of Reynolds number influences.



SOURCES OF ERROR IN PROPULSION RELATED DRAG PREDICTIONS

- Sources of error can be found in the processes in tunnel and flight.
- Comparisons should account for changes to configuration and engine.
- The effects of changes should be verified better than current practice allows.
- Fourteen sources of potential prediction error are shown.



REFERENCE

1. Performance Prediction Methods. AGARD CP-242, May 1978. (Available from DTIC as AD A056 193.)

F-15 WIND-TUNNEL/FLIGHT CORRELATIONS

Larry G. Niedling
McDonnell Aircraft Company
St. Louis, Missouri

Miniworkshop on Wind-Tunnel/Flight Correlation
November 19-20, 1981

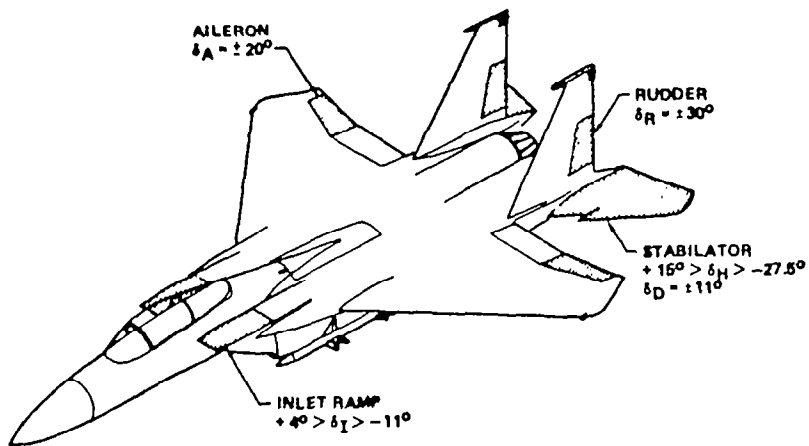
CORRELATION OF F-15 LONGITUDINAL CONTROL EFFECTIVENESS

The following figure presents the correlation of longitudinal control effectiveness at low angles of attack. The data are presented for the derivative $C_{m\delta_H}$ as a function of Mach number.

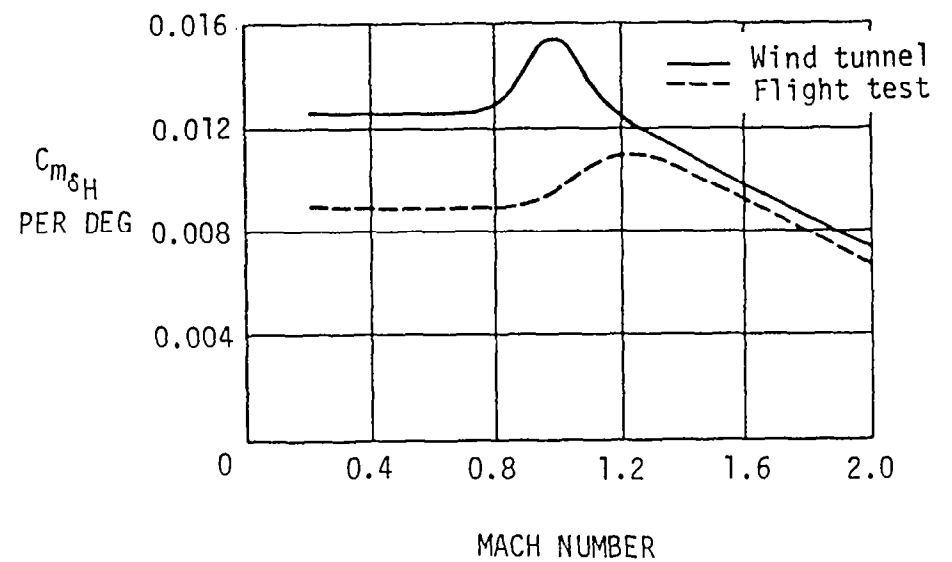
The difference shown at subsonic and transonic speeds may be surprising. The difference is too large to be attributable to data accuracy. As will be evident from the discussion that follows, the reduced flight control effectiveness has no significant impact on the system performance. As a matter of fact, only one area has been encountered where the lower stabilator control effectiveness could be discerned from a system-performance standpoint. At certain flight conditions (low bare-airframe damping), the longitudinal damping ratio with the CAS ON was slightly less than predicted. However, the reduction in artificial damping was not sufficient to warrant a control-system gain increase. It should also be noted that flight-loads tests conducted in the low-angle-of-attack range showed that the loss in effectiveness is not associated with a significant decrease in stabilator panel load but is primarily due to a decrease in the interference (carry-over) loads induced on the fuselage by the stabilator loads. This phenomenon has not been pursued to the point where a substantiated reason for the difference can be presented. However, it appears that the difference is primarily due to transient aerodynamic phenomena.

In the Mach number range where large differences in control effectiveness are shown, moderate stabilator deflections are required to obtain meaningful flight-test data. These deflections produce large pitch accelerations which result in high angle-of-attack rates. Furthermore, it is well known that a small but finite time is required for the steady-state pressure distributions (particularly in the after-body region) to be established after a control deflection is achieved. Therefore, it is difficult if not impossible for a high-agility aircraft to achieve the static aerodynamic load distributions in flight which are representative of the corresponding low-angle-of-attack static-wind-tunnel test conditions. Thus, it is indicated that the loss in stabilator effectiveness shown is an "apparent" loss which is, in large part, due to this aerodynamic "lag." In the Mach number range where the differences in control effectiveness are small, wind-tunnel and flight-test data show that the carry-over loads are small; therefore, the effect of materially reduced carry-over loads due to transient flow phenomena would not be expected to affect the correlation of control effectiveness. In addition, the local flows are definitely supersonic and "lags" are significantly reduced.

CONTROL SURFACES



LONGITUDINAL CONTROL EFFECTIVENESS



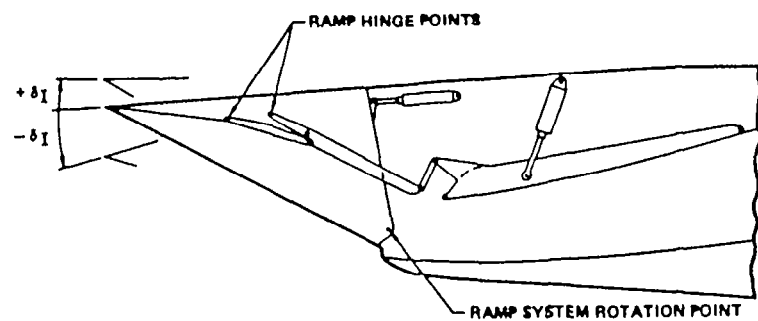
F-15 INLET-RAMP EFFECTIVENESS

A unique feature of the F-15 propulsion system is the movable first ramp of the inlet. Some of the details of this feature are indicated. The movable ramp is relatively large and is far enough forward of the center of gravity to have a significant effect on longitudinal stability and control characteristics and trim drag. Therefore, definition of inlet-ramp schedules required consideration of the impact on these areas as well as considerations of inlet pressure recovery and the flow distortion at the engine face. Since optimization of the ramp schedule depended on the longitudinal control effectiveness of the inlet ramp, it is of interest to address the correlation of wind-tunnel test data and flight-test data.

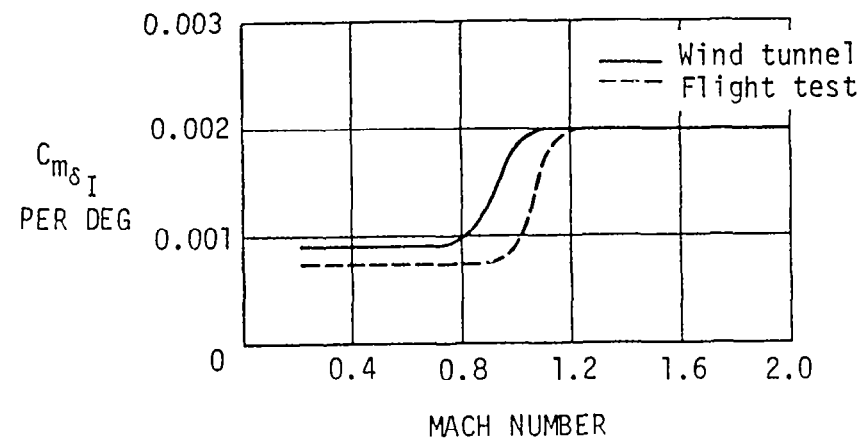
The inlet-ramp total travel is limited to 15° and varies with angle of attack to maintain a fixed relation relative to the free-stream velocity vector. The ramp angle at 0° angle of attack is scheduled with Mach number and free-stream total temperature to maximize excess thrust to the extent allowed by the other aforementioned considerations. For the deflections and angles of attack involved, no nonlinearities have been observed in either ground or flight tests. Thus, the longitudinal control effectiveness is adequately defined by the derivative $C_{m\delta_I}$.

It is seen that, except near $M = 1.0$, the flight-test and wind-tunnel values are in good agreement. The differences at transonic speeds may be due to the effects of cowl deflection on the wing-body shock locations on the upper surface of the aircraft. These shock locations are difficult to duplicate in model tests at transonic speeds. Similar effects are noted in differences observed in the tail angle to trim. The magnitude of the differences measured in these two parameters required revision of the ramp-angle schedule with Mach number.

INLET SYSTEM



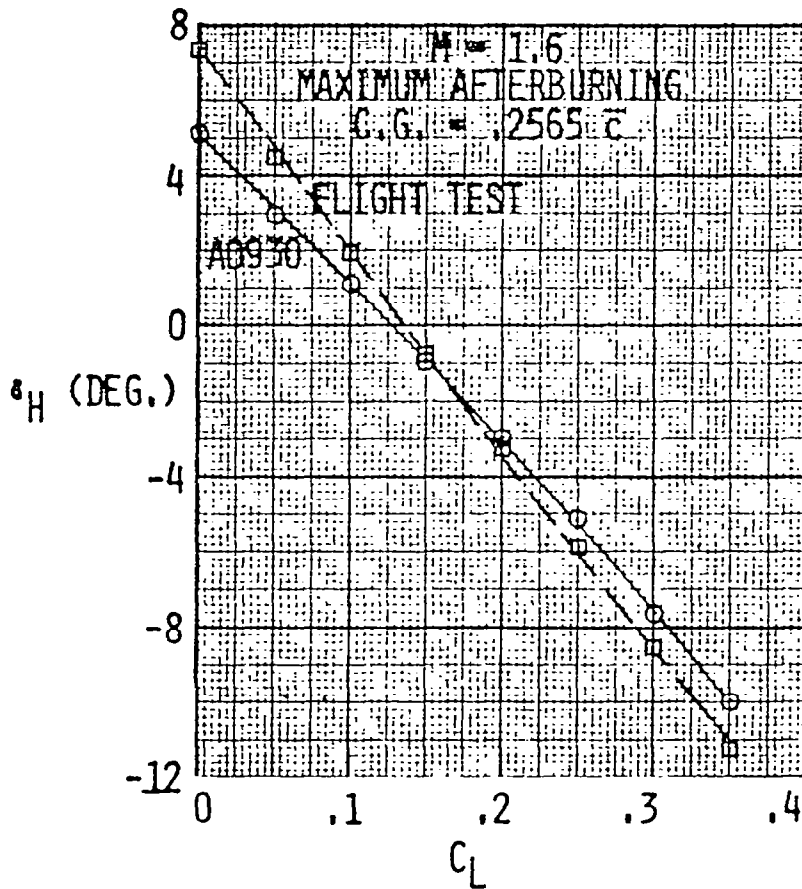
INLET LONGITUDINAL CONTROL EFFECTIVENESS



F-15 HORIZONTAL-TAIL SETTING FOR TRIM

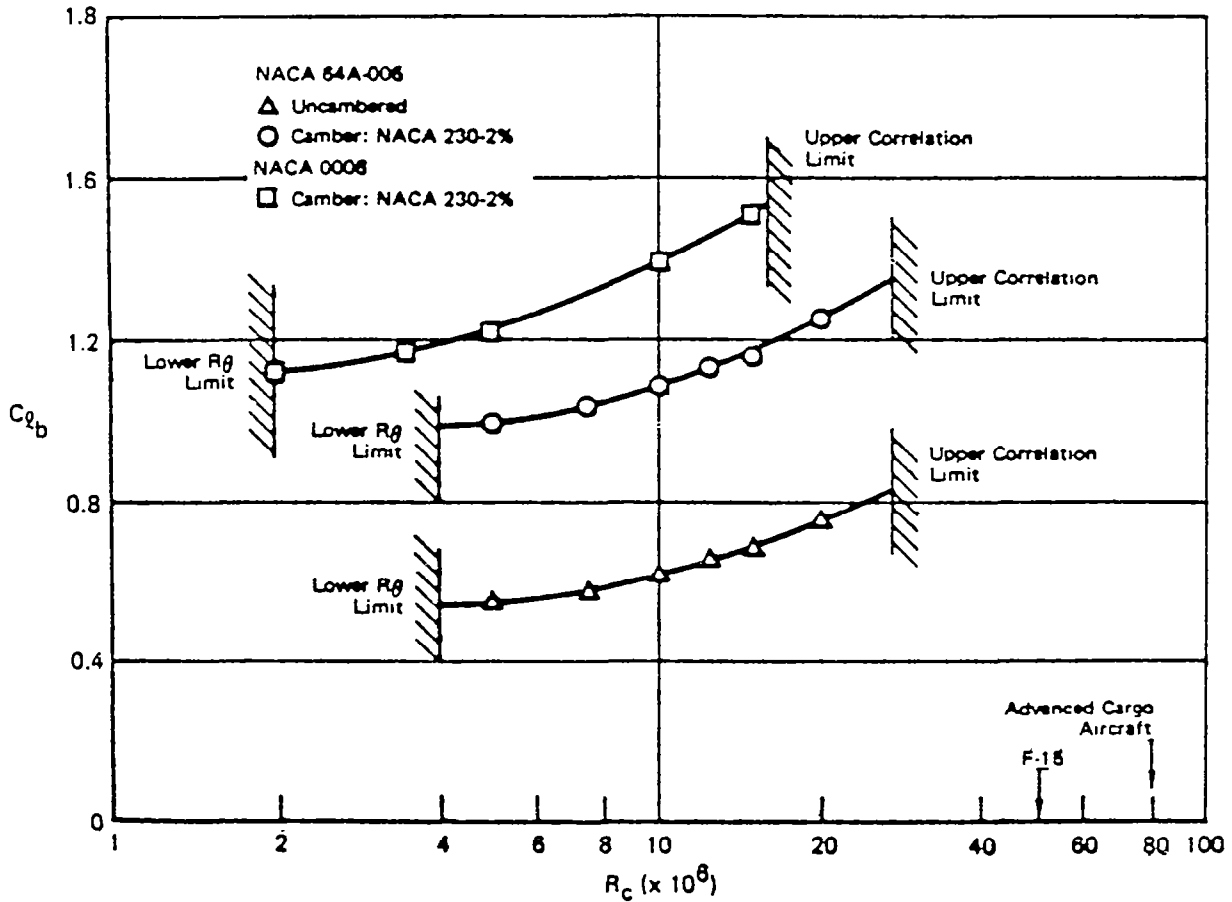
Correlations of F-15 horizontal-tail settings for trim are shown at a supersonic Mach number. The data are presented for the tail angle to trim as a function of lift coefficient. The existence of a more positive tail angle for trim at low lifts in flight suggests a more positive flight zero-lift pitching moment (C_{m_0}) relative to the wind-tunnel prediction. At transonic speeds the flight-test trim tail angles are less than 1° more negative than predicted in the wind tunnel suggesting a slightly more negative C_{m_0} . This C_{m_0} difference is believed to be due to model sting and distortion effects and/or model to flight Reynolds number.

The wind-tunnel data were obtained at Reynolds numbers of 6×10^6 based on mean aerodynamic chord.



REYNOLDS NUMBER EFFECT ON AIRFOIL LAMINAR BUBBLE BURST

Subsequent to the F-15 wing-development program, follow-on transonic-wing design studies were conducted to aid in the development of analytical wing-design methods. The studies eventually led to increased leading-edge camber designs which resulted in premature leading-edge stall when tested in the wind tunnel. This leading-edge stall was found to be a laminar short-bubble bursting phenomenon. Available airfoil data indicate that the lift coefficient for bubble burst (C_{l_b}) is strongly a function of Reynolds number. One means of compensating for low test Reynolds numbers is to increase the model leading-edge radius, as bubble burst is dependent on a momentum thickness at the separation-point based Reynolds number.



AERODYNAMIC COMPARISONS OF STS-1 SPACE SHUTTLE ENTRY VEHICLE

James C. Young
NASA Lyndon B. Johnson Space Center
Houston, Texas

Miniworkshop on Wind-Tunnel/Flight Correlation
November 19-20, 1981

SUMMARY

The flight-test program for the Space Shuttle Orbiter has required the aerodynamicist to take a new approach in determining flight characteristics. A conventional flight-test program, which slowly and cautiously approaches more severe flight conditions, was not possible with the Orbiter. On the first flight, the Orbiter entered the atmosphere at Mach 28 and decelerated through the Mach range. (The subsonic portion of flight had also been flown by another orbiter vehicle during the Approach and Landing Test Program.) Certification for the first flight was achieved by an extensive wind-tunnel test and analysis program and by restricting the flight maneuvers severely. The initial flights of the orbiter are heavily instrumented for the purpose of obtaining accurate aerodynamic data. Even without maneuvers to excite the system, the first flight provided comparisons between flight and wind-tunnel-derived predicted data in the areas of aerodynamic performance, longitudinal trim, and reaction-control jet interaction. Figures 1 to 14 present the aerodynamic performance comparisons.

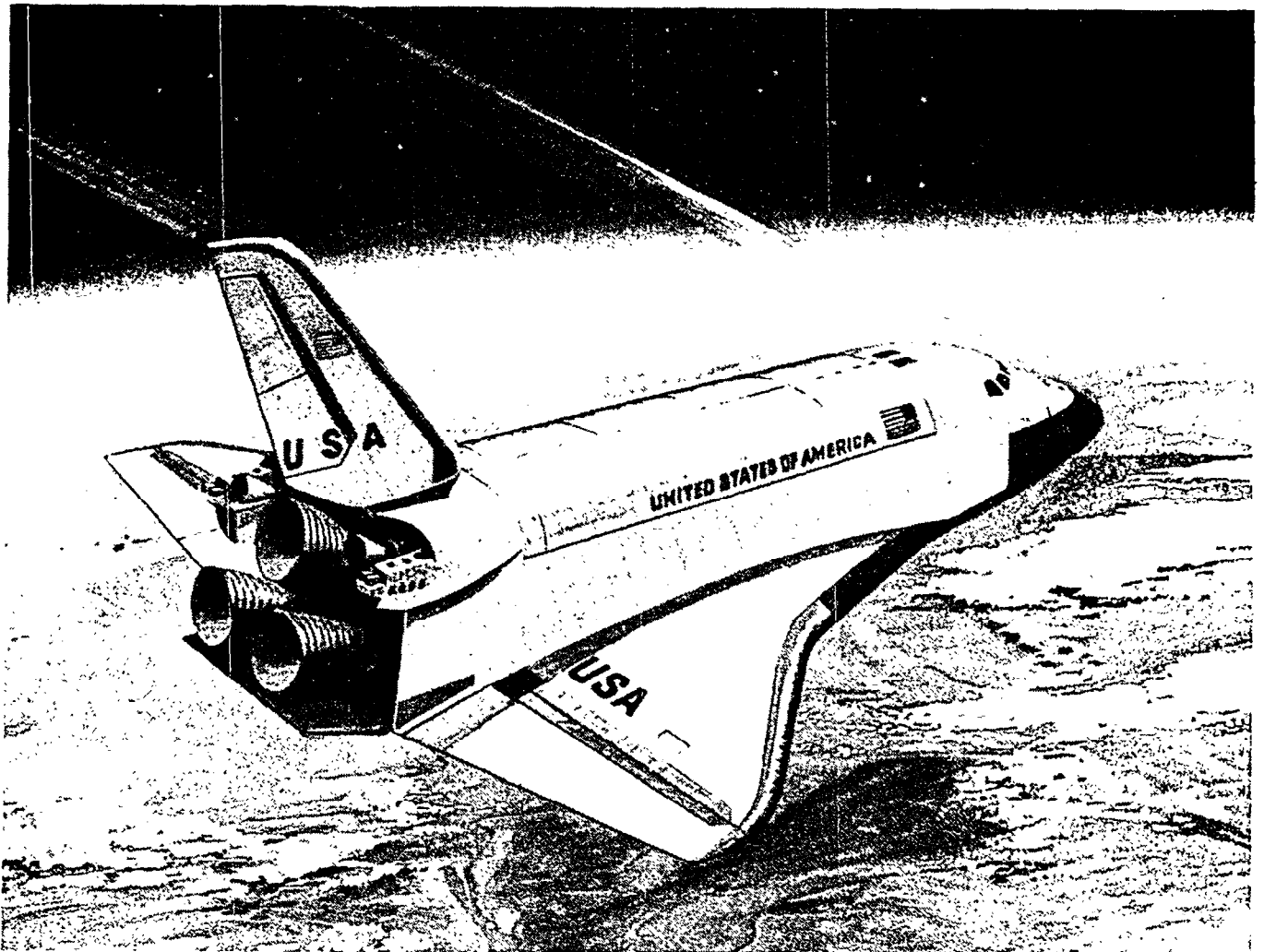
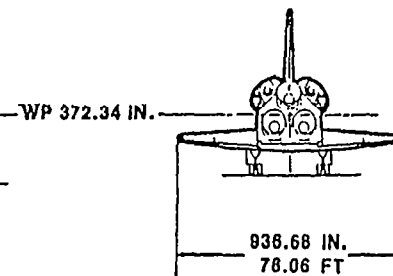
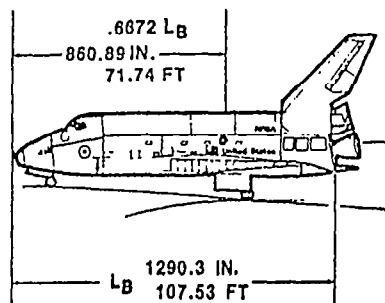
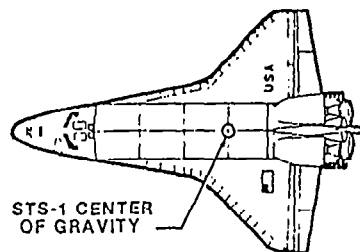


Figure 1.- Space Shuttle Orbiter during entry into the atmosphere.

PHYSICAL CHARACTERISTICS

- BODY FLAP
 - PRIMARY LONGITUDINAL TRIM DEVICE
- WING-MOUNTED ELEVONS/AILERONS
 - LONGITUDINAL STABILITY AUGMENTATION
 - LATERAL TRIM AND CONTROL
- VERTICALLY MOUNTED SPEEDBRAKE/RUDDER
 - APPROACH AND LANDING L/D MODULATION
 - SUPPLEMENTS SUPERSONIC YAW STABILITY
 - RUDDER
- AFT FIRING REACTION CONTROL JETS
 - SUPPLEMENT YAW STABILITY ABOVE SONIC SPEED



ORBITER REFERENCE DIMENSIONS

WING AREA	2690.0 FT ²
LONGITUDINAL REFERENCE LENGTH (MAC)	39.568 FT
LATERAL/DIRECTIONAL REFERENCE LENGTH (SPAN)	78.06 FT
ELEVON REFERENCE DIMENSIONS (HINGE MOMENTS)	
AREA (ONE SIDE)	210.0 FT ²
REFERENCE LENGTH	7.56 FT

Figure 2.- Design characteristics of Space Shuttle Orbiter.

- GLIDING ENTRY
- ENTRY TO 170,000 FT AT ANGLE OF ATTACK OF 40°
- PITCH DOWN STARTING AT MACH 14 AND TERMINATING AT 70,000 FT
- REMAINDER OF FLIGHT FROM MACH 2 FLOWN AT MORE CONVENTIONAL ANGLE OF ATTACK OF 3° TO 10°
- DOWNRANGE MODULATION ACCOMPLISHED BY PERIODIC BANK REVERSALS
- ANGLE OF SIDESLIP LESS THAN 1° ABOVE SONIC SPEEDS

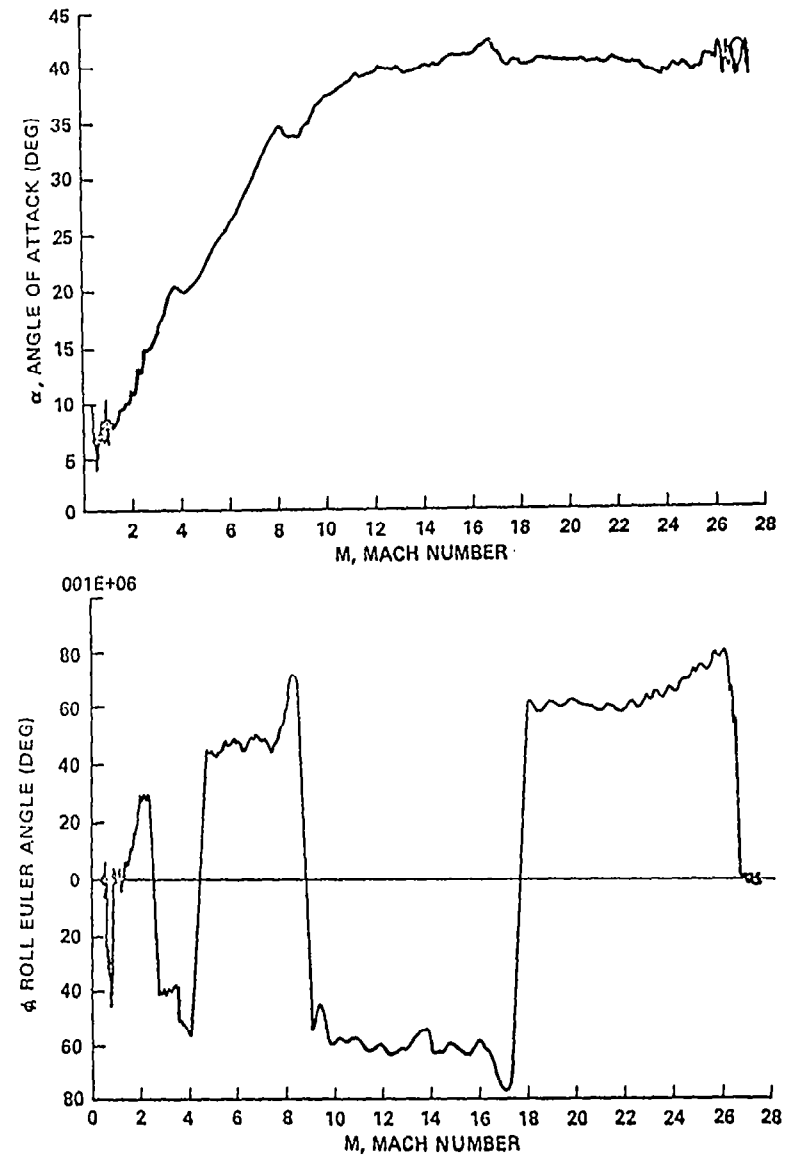


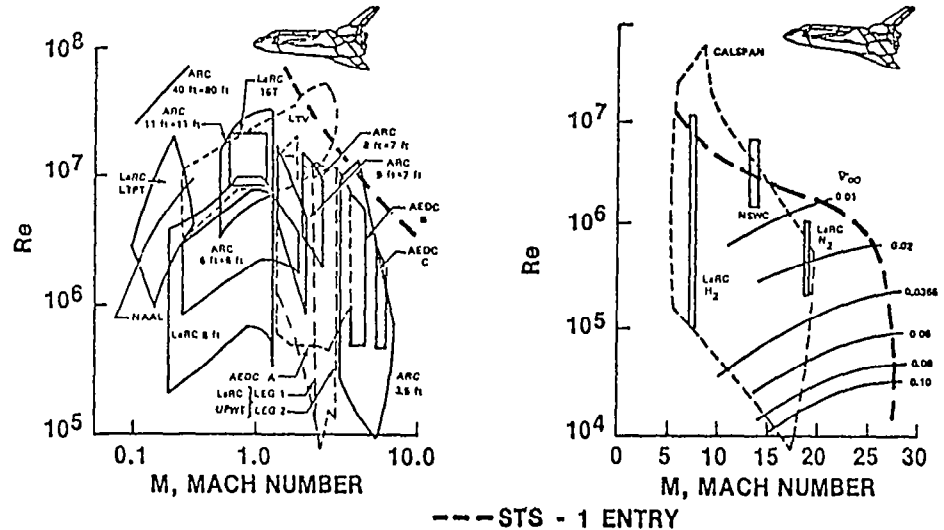
Figure 3.- STS-1 Space Shuttle entry.

AERODYNAMIC PREDICTIONS

- BASED ON 35,000 OCCUPANCY HOURS OF TESTING
 - SCALING PARAMETERS
 - REYNOLDS NUMBER (Re) BELOW MACH 10
 - VISCOUS-INTERACTION PARAMETER

$$\bar{V}_\infty = M_\infty \sqrt{\frac{\bar{c}'_\infty}{Re}}$$

- WIND-TUNNEL DATA BASE SELECTED BY COOPERATIVE EFFORT
- CORRECTIONS TO DATA BASE
 - SKIN-FRICTION DRAG
 - DRAG DUE TO THERMAL PROTECTION SYSTEM ROUGHNESS
 - AEROELASTIC EFFECTS



AERODYNAMIC UNCERTAINTIES (VARIATIONS)

- HISTORICAL ANALYSIS OF OTHER PROGRAMS
- SUPPLEMENTED BY WIND-TUNNEL REPEATABILITY

Figure 4.- Preflight predictions.

LONGITUDINAL CENTER OF PRESSURE
(LOCATION OF ZERO MOMENT)

- INDEPENDENT OF \bar{q} , MASS, AND ∞
- FLIGHT IS SAME AS CENTER OF GRAVITY WHEN TRIMMED
- PREDICTED ESTABLISHED FOR FLIGHT CONDITIONS

RESULTS

- BELOW MACH 2: WITHIN VARIATIONS
- MACH 2 TO 10: EXCELLENT AGREEMENT WHERE Re WAS MATCHED
- MACH > 10: FLIGHT AS MUCH AS NINE INCHES (1.9% \bar{c}) FORWARD
 - \bar{V}'_{∞} WRONG SIMULATION PARAMETER FOR PITCHING MOMENT?

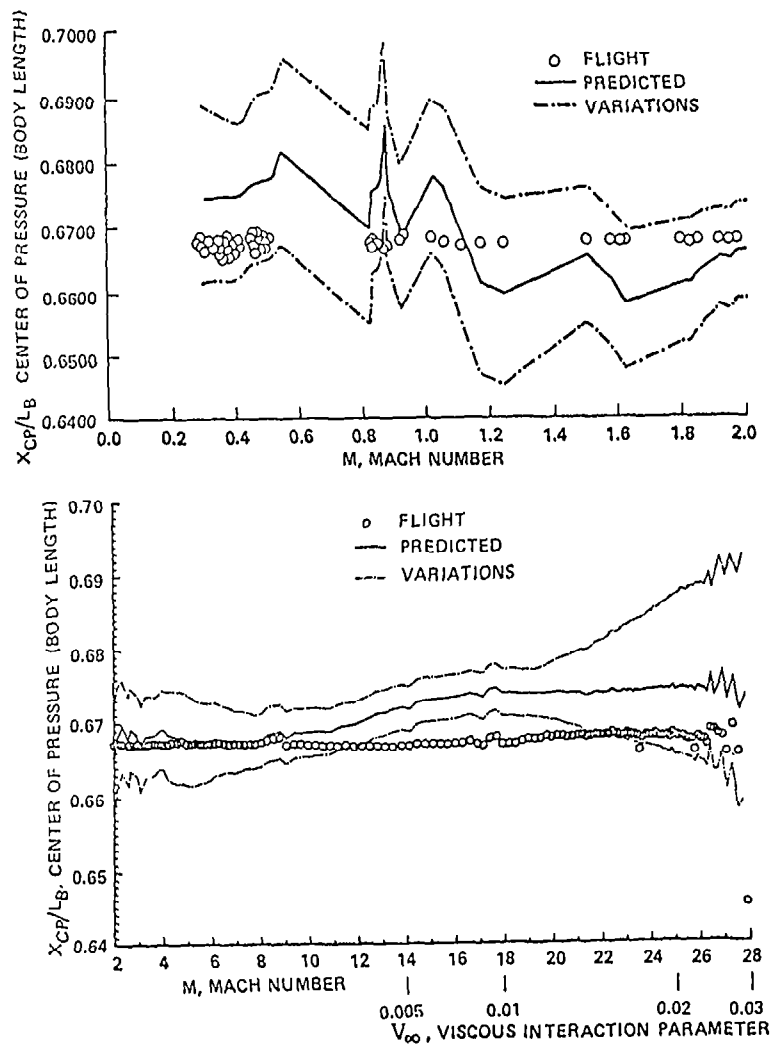


Figure 5.- Aerodynamic-trim comparison.

LIFT-TO-DRAG RATIO (L/D)

- INDEPENDENT OF \bar{q} AND MASS
- FLIGHT CALCULATED FROM FLIGHT α NORMAL AND AXIAL ACCELERATIONS
- PREDICTED VALUES DETERMINED FROM FLIGHT CONDITIONS

RESULTS

- MORE PERFORMANCE THAN PREDICTED BELOW MACH 1.4
- EXCELLENT AGREEMENT ELSEWHERE
 - \bar{V}'_{∞} CORRECT SCALING PARAMETER HYPERSONICALLY

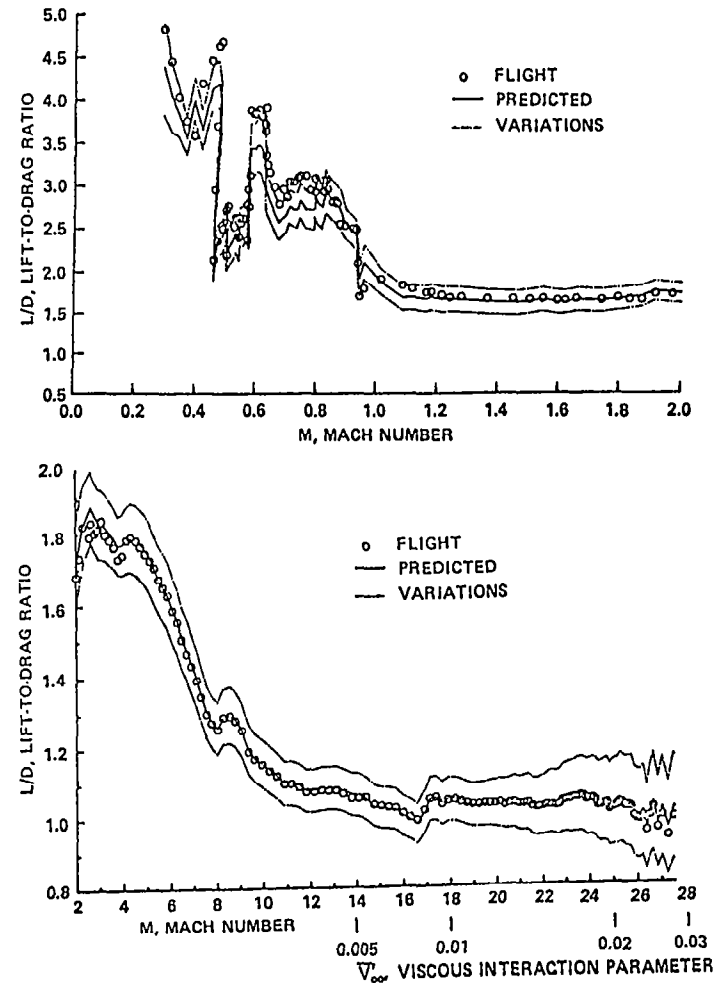


Figure 6.- Aerodynamic-performance comparisons.

- L/D HIGHER THAN PREDICTED
- NORMAL FORCE AS PREDICTED
- AXIAL FORCE OVERPREDICTED

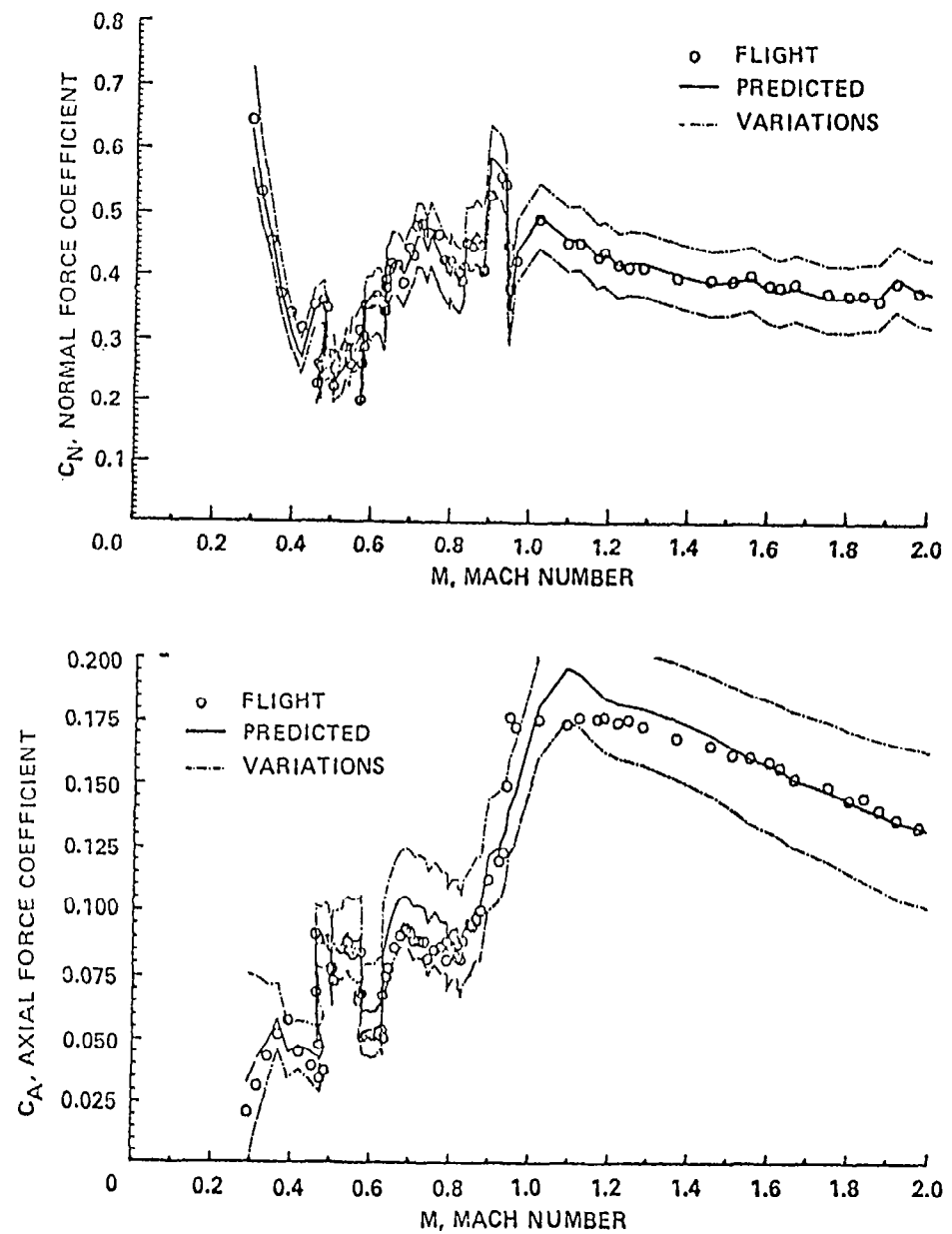


Figure 7.- Aerodynamic-performance analysis.

● STS-1 ALT 4 AND ALT 5 USED IN ANALYSIS

● ALL THREE FLIGHTS SHOW BIAS OF 0.0040

● BIAS CAN BE EQUATED TO PROFILE DRAG

● REDUCING PREDICTED PROFILE DRAG BY 40 COUNTS IMPROVES COMPARISONS FOR ALL THREE FLIGHTS

● CONCLUSION

● EFFECTS OF TPS SURFACE ROUGHNESS ON PROFILE DRAG OVERPREDICTED BY 40 COUNTS

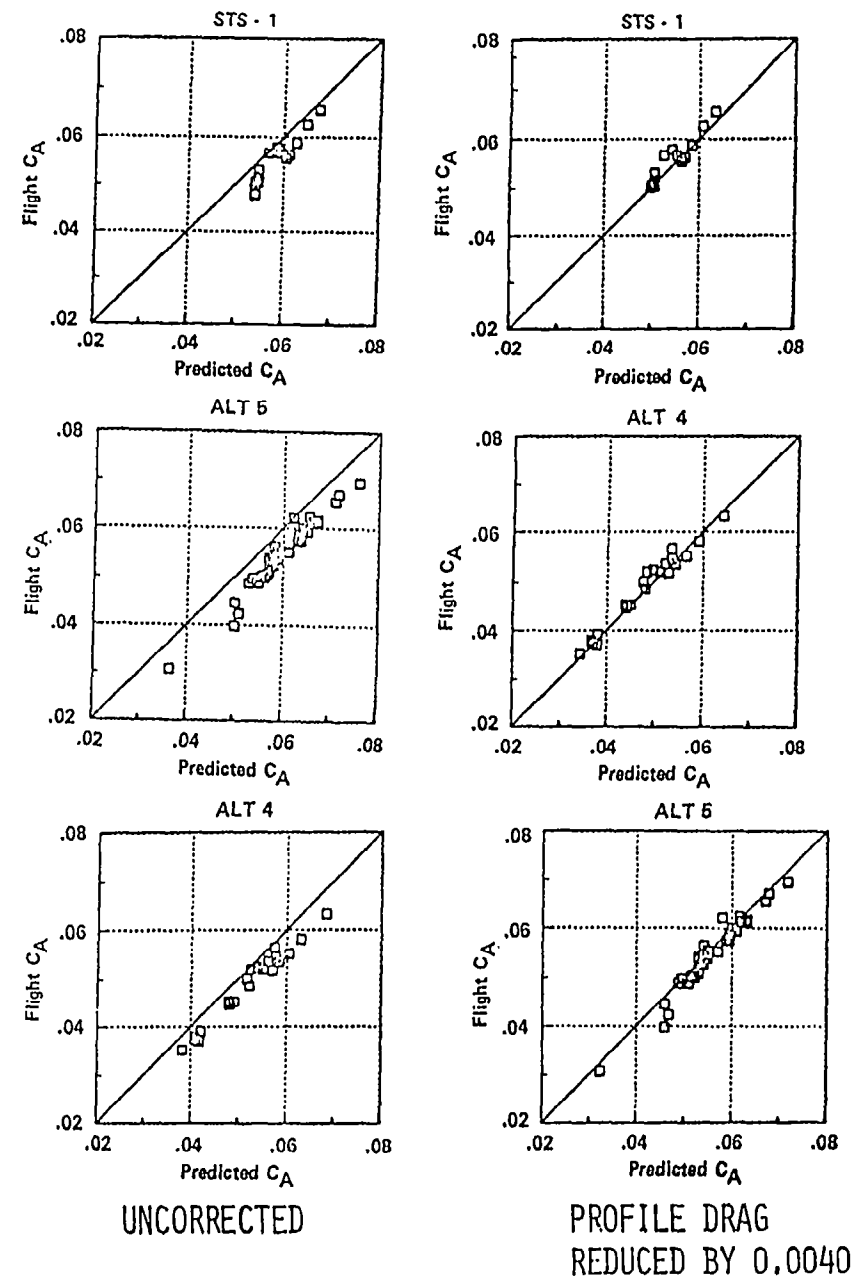


Figure 8.- Approach and landing-performance analysis of profile drag.

- NORMAL FORCE DUE TO SPEEDBRAKE AS PREDICTED
- C_A AT HIGHER SPEEDBRAKE, STS-1 SHOWS HIGHER EFFECTIVENESS
- C_A FOR STS-1 INCONSISTENT WITH ALT 4 AND ALT 5 RESULTS
- CONCLUSION
 - C_A RESULTS INCONCLUSIVE

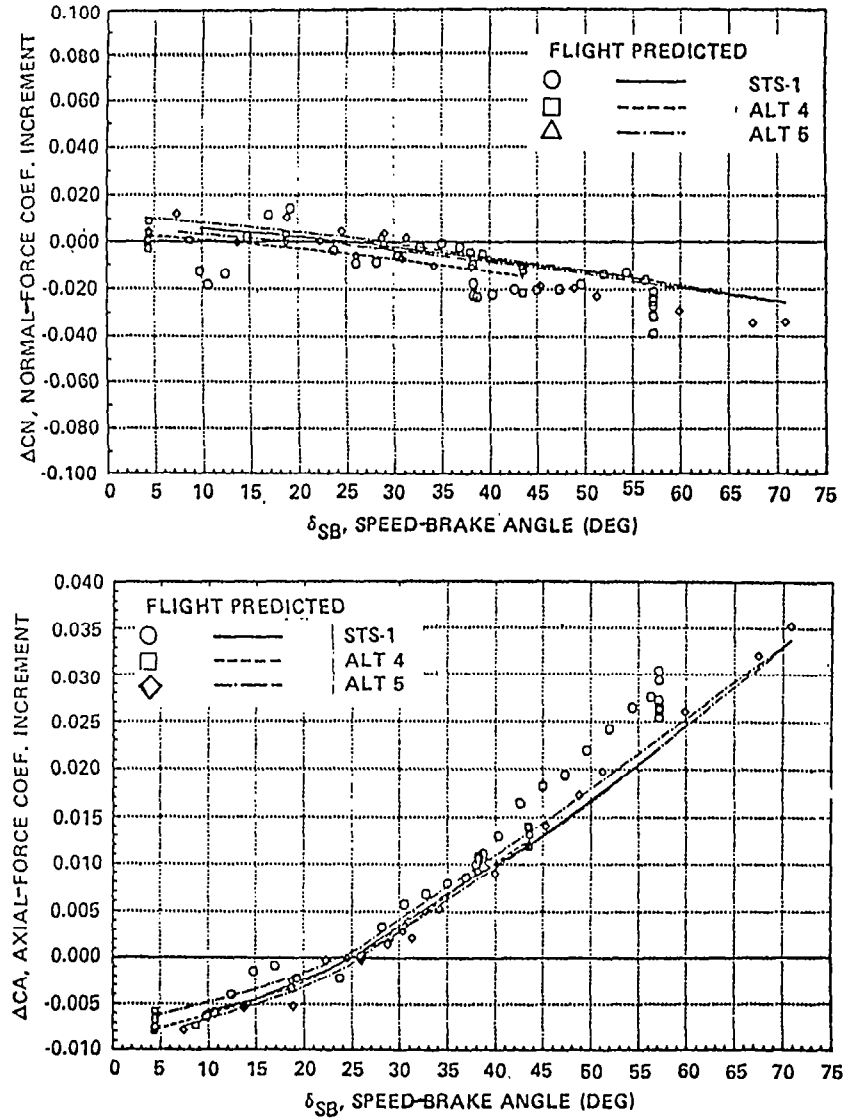


Figure 9.- Approach and landing-performance analysis of speedbrake effectiveness.

USES

- ORBITER CONTROL DURING SEPARATION FROM EXTERNAL TANK
- ON-ORBIT MANEUVERING
- INITIAL-ENTRY PITCH AND YAW CONTROL
- SUPPLEMENT YAW CONTROL AND STABILITY ABOVE SONIC SPEEDS

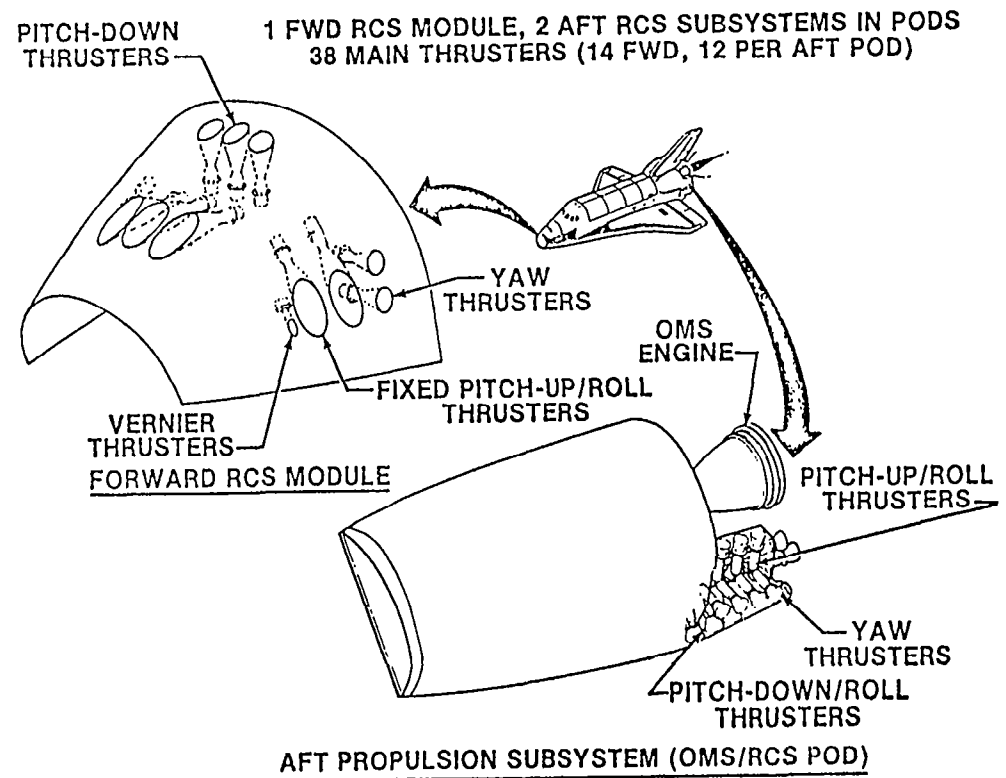
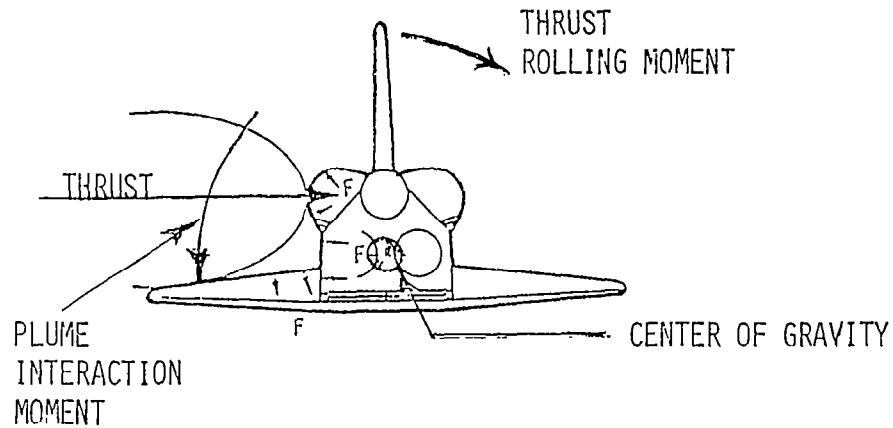


Figure 10.- Orbiter reaction control system (RCS).

PHYSICAL CONSIDERATIONS

- PLUME INTERACTING WITH FLOW OVER WING OF MAJOR CONCERN
- INTERACTION TENDS TO COUNTERACT JET THRUST ROLLING MOMENT
- PROBLEM - QUEST FOR SIMULATION PARAMETER THAT WILL PROPERLY SCALE PLUME/UPPER WING-FLOW INTERACTION OVER LARGE ANGLE-OF-ATTACK RANGE

WIND-TUNNEL SIMULATION

- COLD GAS
- MACH 2 TO 10
- SCALING PARAMETER SELECTED
 - JET TO FREE-STREAM MASS-FLOW RATIO

$$\text{MASS FLOW} \left(\frac{P_j^2 \gamma_j M_j^2 (RT)_j A_j^2}{P_\infty^2 \gamma_\infty M_\infty^2 (RT)_\infty A_\infty^2} \right)^{1/2}$$

Figure 11.- Yaw-RCS scaling considerations.

- PREDICTED MOMENTS INCLUDING INTERACTION COMPARED WITH FLIGHT

- YAWING MOMENT PREDICTED WELL

- ROLLING MOMENT

- SATISFACTORILY PREDICTED AT LOWER MACH AND ANGLE OF ATTACK

- AT HIGHER MACH NUMBERS INTERACTION OVERPREDICTED

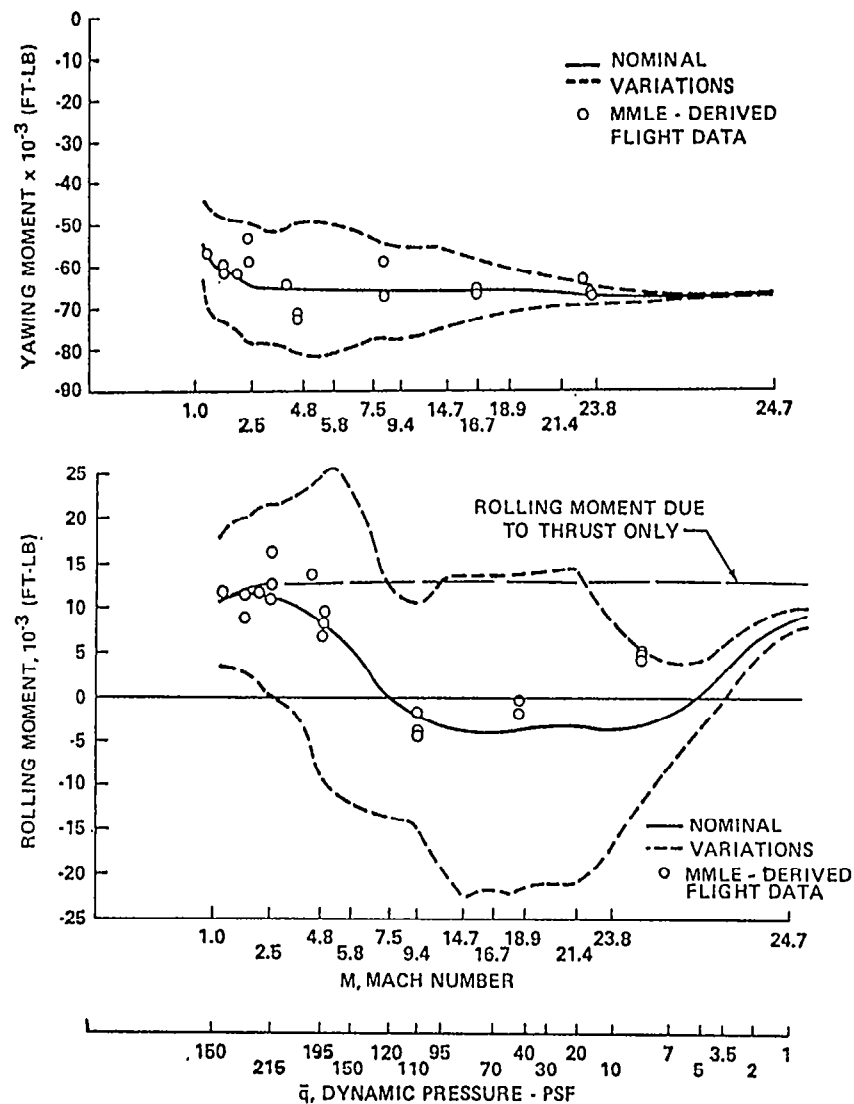


Figure 12.- Performance comparisons of RCS in roll and yaw.

- WHERE TEST MACH NUMBER AND MASS FLOW RATIO WERE SIMULATED AGREEMENT WAS EXCELLENT
- APPARENTLY AT THE HIGHER MACH NUMBERS EITHER THE WRONG SCALING PARAMETER WAS CHOSEN OR THERE WAS AN UNEXPECTED MACH EFFECT
- JET ACTUALLY EXHAUSTS INTO COMPLEX TRISONIC UPPER WING FLOWFIELD
 - MASS FLOW BASED ON LOCAL CONDITIONS?
 - SCALING PARAMETER THAT CHANGES WITH α ?
 - MACH/REYNOLDS EFFECT?

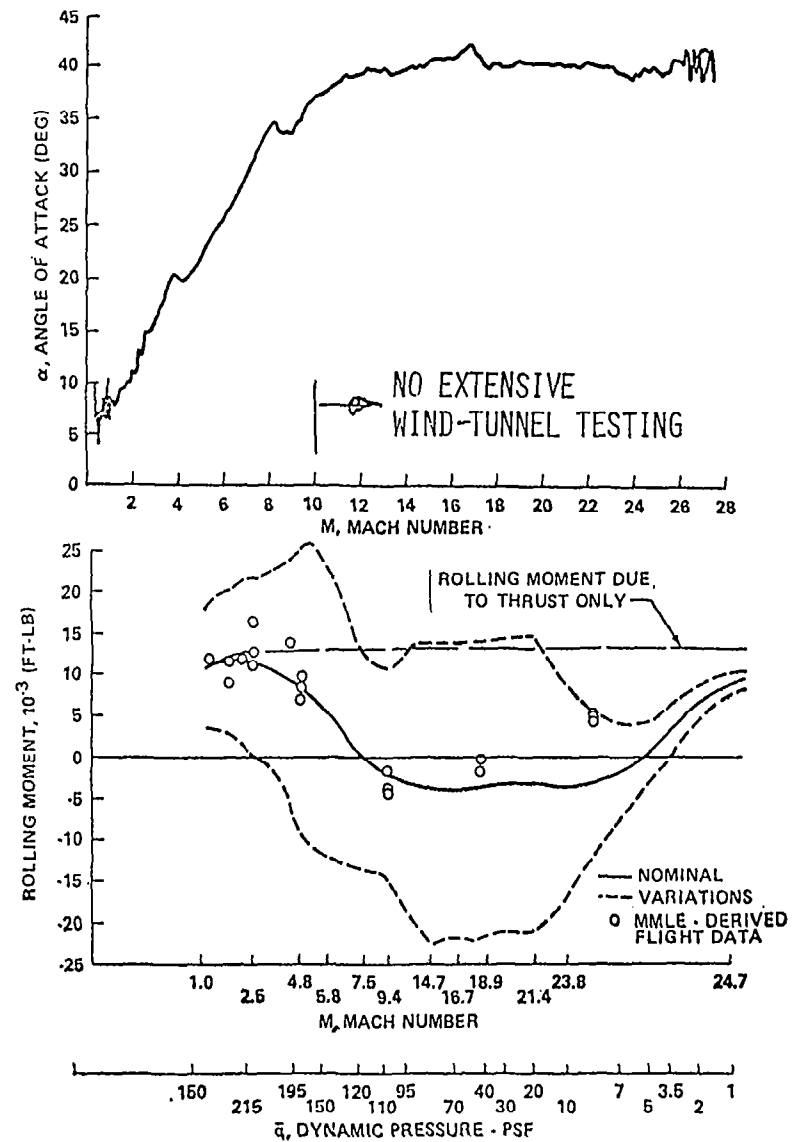


Figure 13.- Yaw-RCS difference analysis.

CONCLUSIONS

- AERODYNAMIC PERFORMANCE UNDERPREDICTED BELOW MACH 2
 - EXCELLENT AGREEMENT ELSEWHERE
- EXCELLENT TRIM AGREEMENT MACH 2 THROUGH 10 DESPITE HIGH ANGLES OF ATTACK
- TRANSONIC AND SUBSONIC SHOW TRADITIONAL TRIM PREDICTION PROBLEMS
- HYPERSONIC TRIM AND RCS INADEQUATELY PREDICTED

REMARKS

- DESPITE USE OF STATE-OF-THE-ART FACILITIES AND TECHNOLOGY HYPERSONIC/RAREFIED GAS AERODYNAMICS ARE NOT ADEQUATELY PREDICTED
- USING THE ORBITER AS AN AERODYNAMIC TEST BED COULD BRING UNDERSTANDING OF THIS SPEED REGION

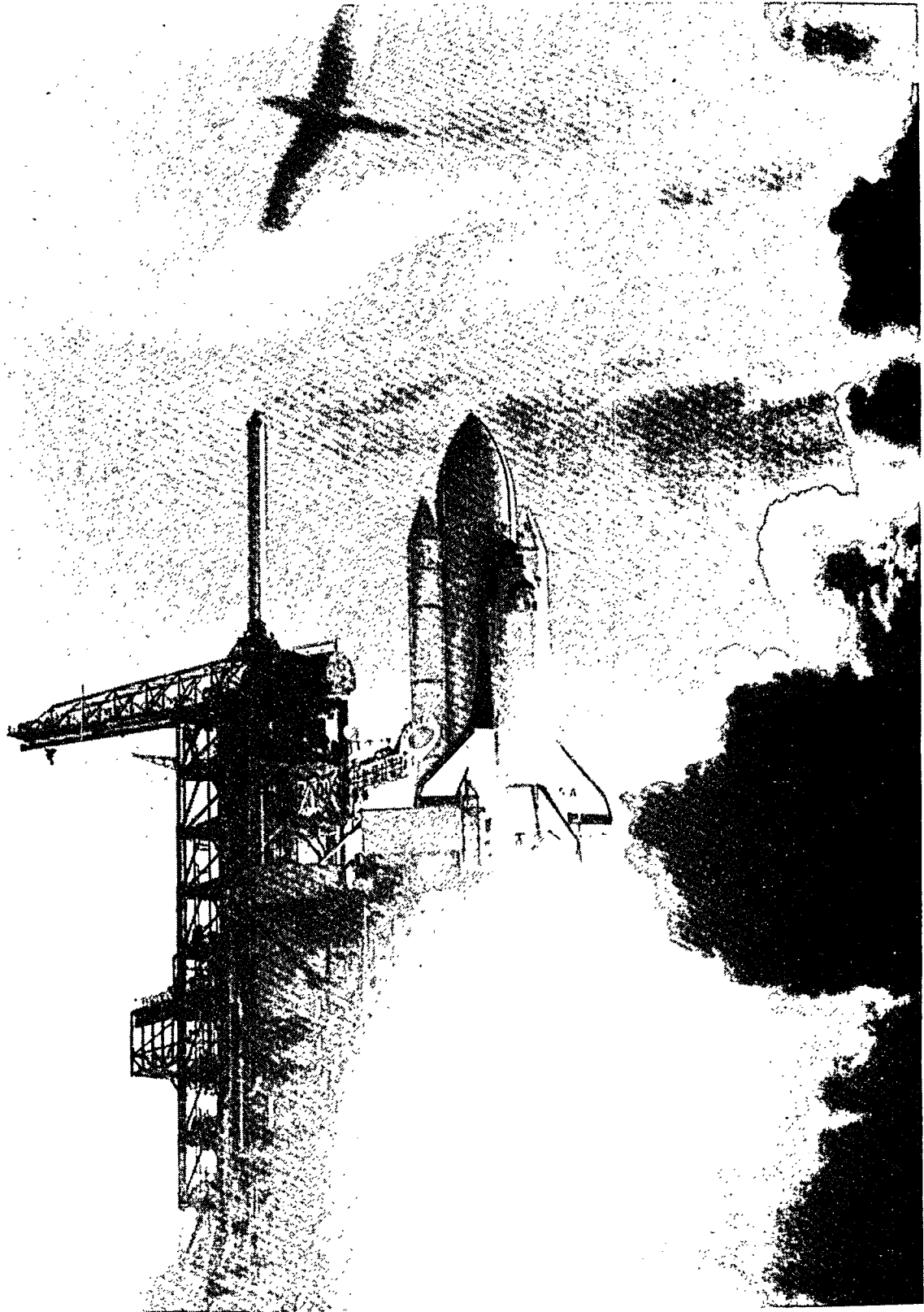
Figure 14.- Concluding remarks.

AERODYNAMIC COMPARISONS OF SPACE SHUTTLE ASCENT:
STS-1 FLIGHT VERSUS WIND-TUNNEL PREDICTIONS

Rodney O. Wallace
NASA Lyndon B. Johnson Space Center
Houston, Texas

Miniworkshop on Wind-Tunnel/Flight Correlation
November 19-20, 1981

STS-1 SPACE SHUTTLE AT LAUNCH



STS-1 LAUNCH VEHICLE

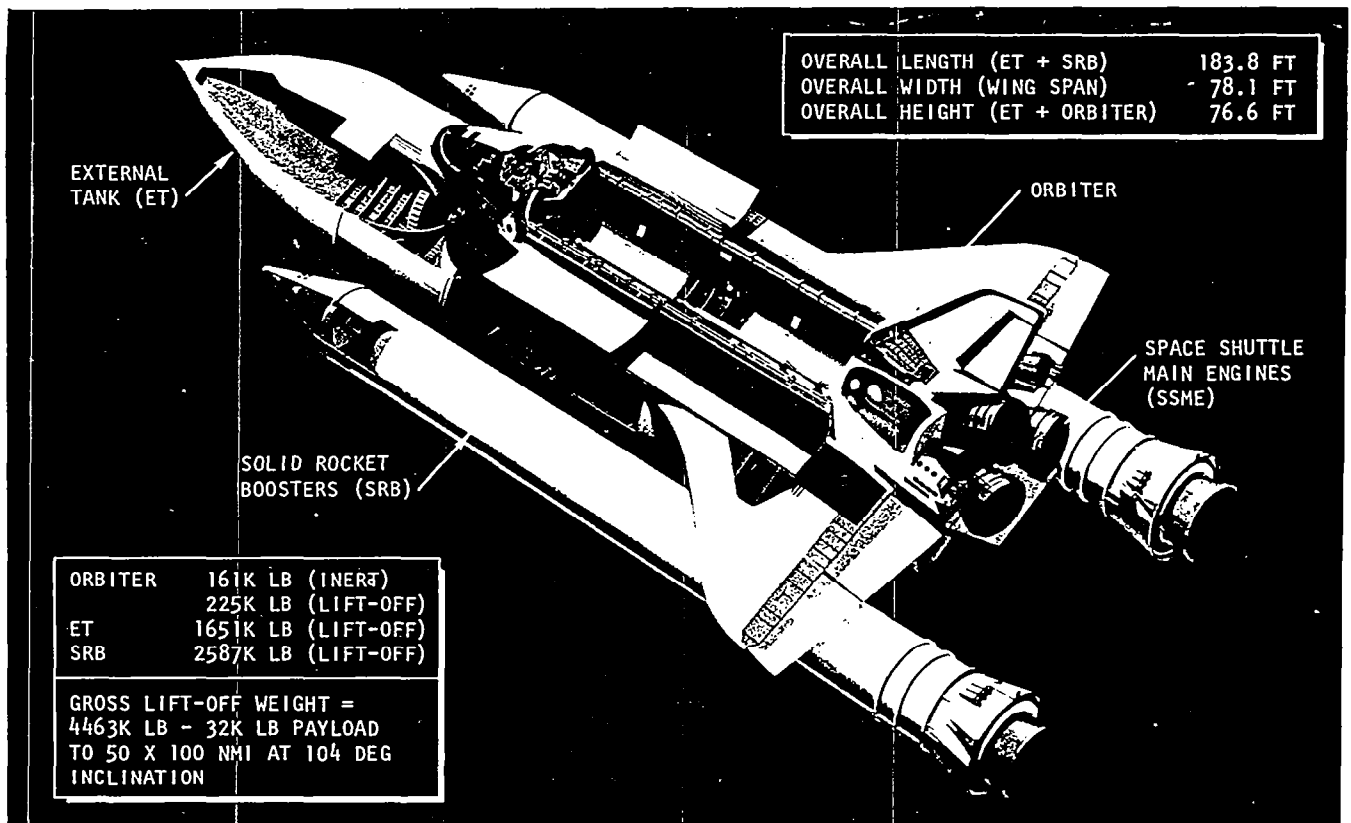
Launch-Vehicle Control

- Space Shuttle launch vehicle is composed of four elements: orbiter, external tank, and two solid-rocket boosters (SRB).
- Space Shuttle has a thrust-vector control system:
 - Space Shuttle main engines (SSME) thrust $\approx 470,000$ lb per SSME
 - SRB $\approx 1,500,000$ lb per SRB
- No aerodynamic control

Space Shuttle Trajectory

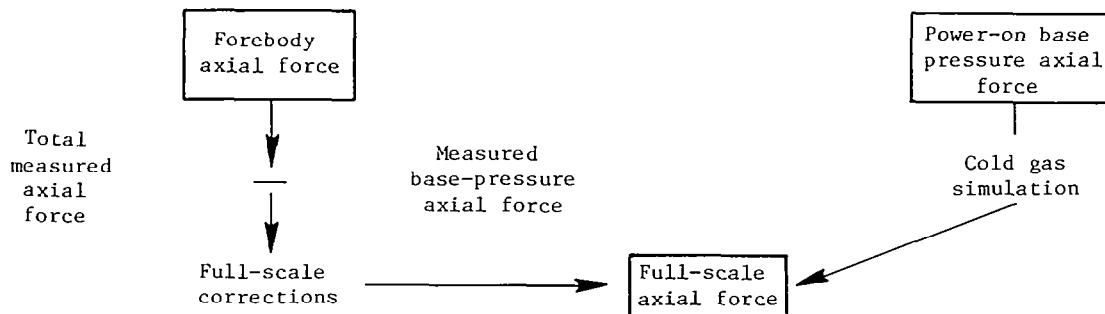
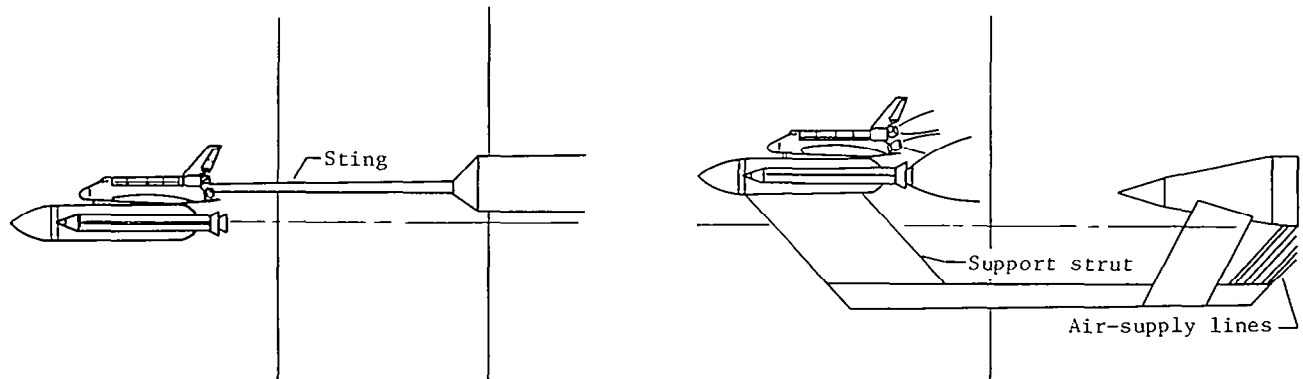
- First-stage flight is the most aerodynamically significant portion of the ascent trajectory.
- First-stage flight ends with SRB separation approximately 130 sec after lift-off.
- Approximately 176,000 ft of altitude is attained.
- Mach number changed from 0 to 3.75.
- Dynamic pressure maximized at 609 psf.
- An angle-of-attack time history covered a range from $\approx -5^\circ$ to $\approx 5^\circ$.
 - STS-1 trajectory was shaped to fly a predetermined dynamic pressure and angle-of-attack profile
 - $Q\alpha$ profile determined from structural loads assessment
- Angle-of-sideslip time history covered a range from -1° to 1° .

LAUNCH-VEHICLE GEOMETRY



WIND-TUNNEL DETERMINATION OF LAUNCH-VEHICLE AXIAL FORCE

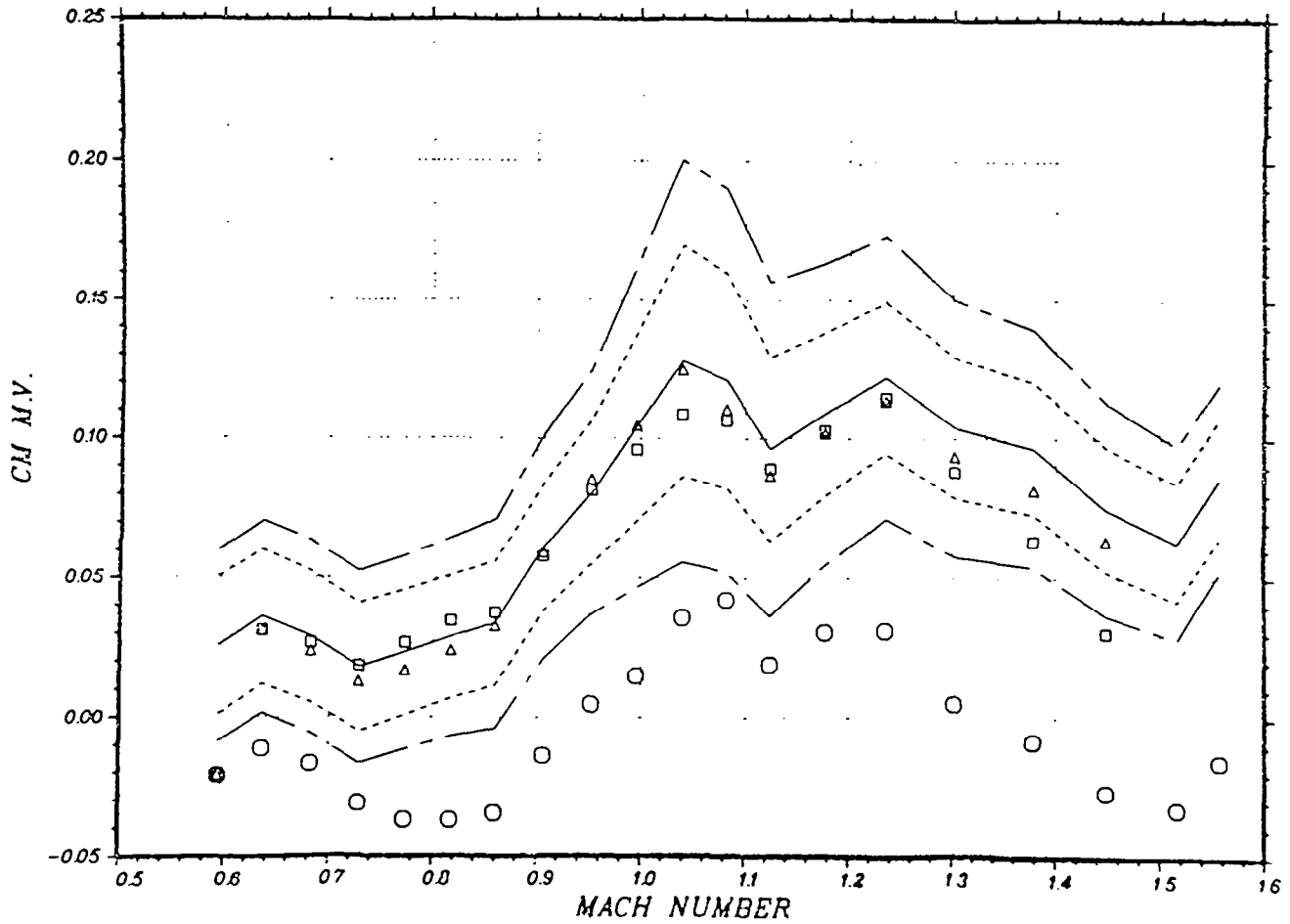
- Definition of launch-vehicle aerodynamics for powered flight requires multitest approach because of model limitations.
- Force and moment testing of sting-mounted models (power-off)
 - Total aerodynamics measured by model balances
 - Base pressures measured
 - Forebody coefficients calculated by subtracting calculated base coefficients from measured total coefficients
 - No Reynolds number corrections were made because of random trends seen in limited Reynolds number testing
- Pressure testing of strut-mounted plume-simulation model (power-on)
 - Plume simulated by exhausting high-pressure air
 - Plume-technology program determined a cold gas-simulation parameter: $f(\gamma, \delta, M_E)$
 - Data collected for plume-on and plume-off conditions
 - Base forces and moments determined from plume-on runs
 - Forebody plume effects determined by integrating delta-forebody external pressure measurements (plume-on minus plume-off)
- Forebody plume-effect calculations are added to the forebody power-off test data



LAUNCH-VEHICLE PITCHING-MOMENT COEFFICIENT C_m

- Comparison of launch vehicle C_m versus Mach number
 - Solid-line aero-design data-base prediction at STS-1 flight conditions
 - Dash-line aero tolerances (wind-tunnel data scatter)
 - Chain-dash-line aero variations (ratio times tolerances)
 - Ratio determined from historical data applied to free-stream orbiter
 - Circles STS-1 extracted aero
 - Squares multilinear interpolation of IA144 wind-tunnel test data
 - IA144 - 1-percent model tested in the ARC 11 foot
 - Triangles multilinear interpolation of IA156 wind-tunnel test data
 - IA156 - 2-percent model tested in the AEDC PWT 16T
- Prediction significantly different from extracted flight data
 - Difference is caused by a significant difference in C_N and probable difference in C_m at C_N
- Possible causes of observed difference
 - Flight base pressure was significantly higher than prediction
 - Increased forebody plume effects
 - Reynolds number effects on the flow between the orbiter and external tank
 - Error in extraction process

ASCADAP PLOT OF CM M.V. vs MACH NUMBER
 STS-1 FINAL CUT FLIGHT EXTRACTED - 8/05/81 FOREBODY DATA
 MRC Location in E.T. Stations : X = 976.0 Y = .00 Z = 400.0
 ○ FLT TEST □ IA44 △ IA156 ◇ IA105



CONCLUSIONS RELATIVE TO AERODYNAMIC COMPARISONS OF SPACE SHUTTLE ASCENT

Conclusions

- Large longitudinal aerodynamic difference exists between wind-tunnel predictions and flight measurements.
- Cold gas plume simulation underpredicted Shuttle base pressures.

Remarks

- Observed flight-prediction increments are probably caused by several factors such as input error, independent variable errors, plume effects, and Reynolds number effects.
- High Reynolds number testing could bring understanding to the Shuttle-launch-vehicle aerodynamics.

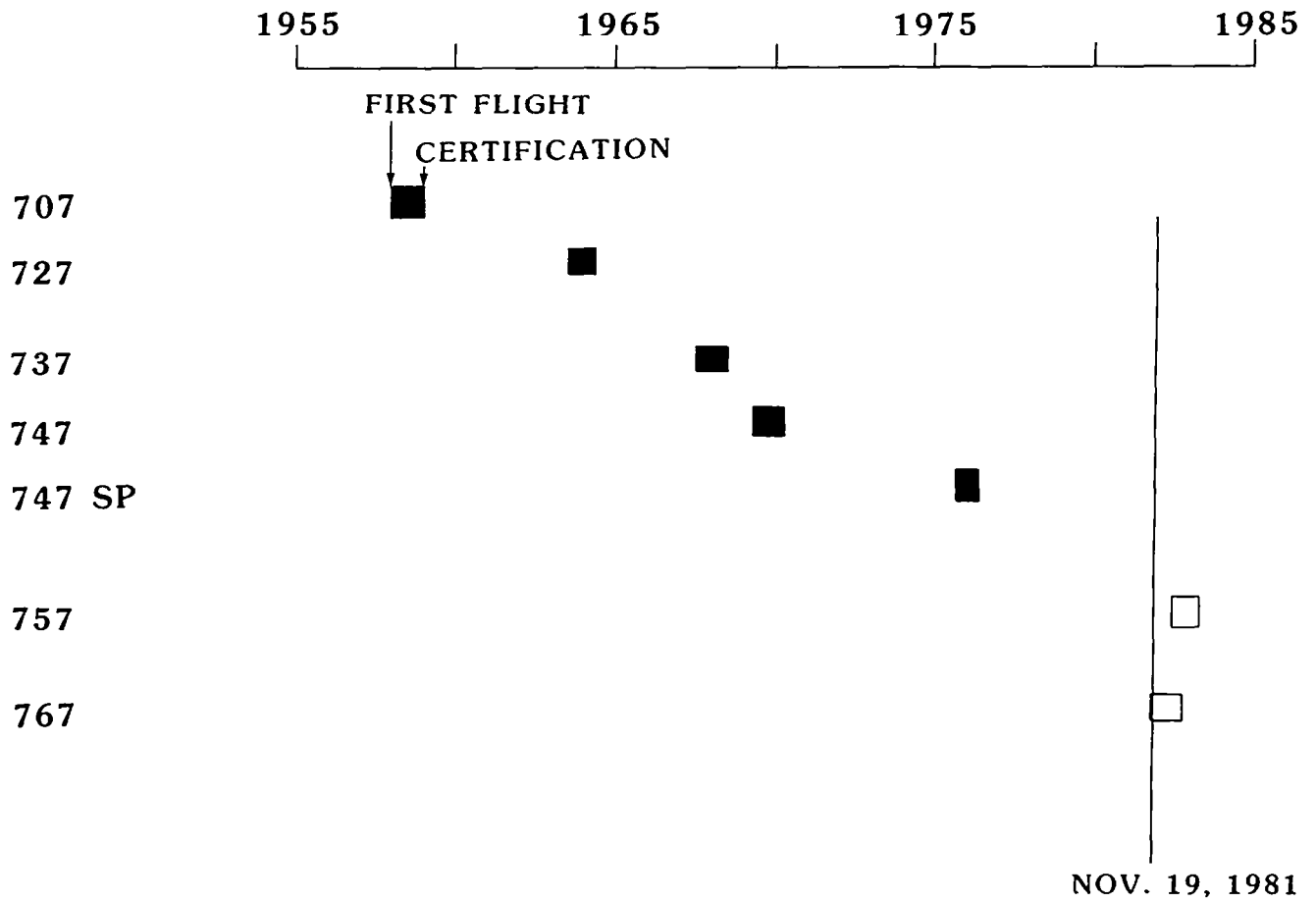
OPPORTUNITIES FOR WIND-TUNNEL/FLIGHT CORRELATION WITH NEW BOEING AIRPLANES

Adelbert L. Nagel
Boeing Commercial Airplane Company
Seattle, Washington

Miniworkshop on Wind-Tunnel/Flight Correlation
November 19-20, 1981

BOEING COMMERCIAL AIRPLANE CERTIFICATION PROGRAMS

This figure indicates the first flight and certification dates of the Boeing Commercial Airplane Company. The next few months will present the very unusual opportunity of having two new airplanes in their flight-test program.



NEW AIRPLANE FLIGHT-TEST REQUIREMENTS

Of course, the purpose of flight-test programs for new airplanes is not to obtain scientific data relating full-scale and wind-tunnel data. They are rather to qualify the airplane for safe operation and to verify that the performance guarantees have been met. As indicated in this figure, the initial flights are for the purpose of establishing airworthiness and determining such things as optimum low-speed flap settings and optimum flap rigging for high-speed cruise, as well as such possible additional items as vortex generators or other flow-control devices. When these have been achieved, the guarantee and certification demonstrations follow. The basic guarantee data are in nautical miles per pound and air speeds in cruise, take-off and landing-field lengths, and various air speeds from cruise to approach. Many individual qualities of the airplane, for example, lift-drag ratio, are usually not guaranteed but are measured or inferred in the process of determining performance.

AIRPLANE DEVELOPMENT

- INITIAL AIRWORTHINESS
- LOW-SPEED CONFIGURATION OPTIMIZATION
- HIGH-SPEED CONFIGURATION OPTIMIZATION

GUARANTEE COMPLIANCE

- FUEL CONSUMPTION
- AIRSPEEDS
- TAKEOFF AND LANDING PERFORMANCE

FAA CERTIFICATION DEMONSTRATIONS

- SAFETY AND FLUTTER
- CONTROL AND HANDLING QUALITIES
- SYSTEMS OPERATION
- HIGH AND LOW-SPEED CHARACTERISTICS

TYPES OF DATA AVAILABLE

The process of comparing wind-tunnel data and flight data is complicated by the fact that different kinds of data are obtained from the two types of testing. The usual wind-tunnel data consist of forces, moments, pressures, and, occasionally, flow-field surveys and various kinds of flow visualization. Flight-test data normally consist of engine parameters, control deflections, airplane weight, accelerations, etc. Pilot opinion and judgement are necessary to evaluate handling qualities and buffet. Occasionally, surface pressures and/or various kinds of flow surveys may be used when additional data are needed in order to understand the basic characteristics, or for special purposes.

FROM WIND-TUNNEL TEST

- FORCES AND MOMENTS
- PRESSURES
- FLOW VISUALIZATION
- FLOW SURVEYS

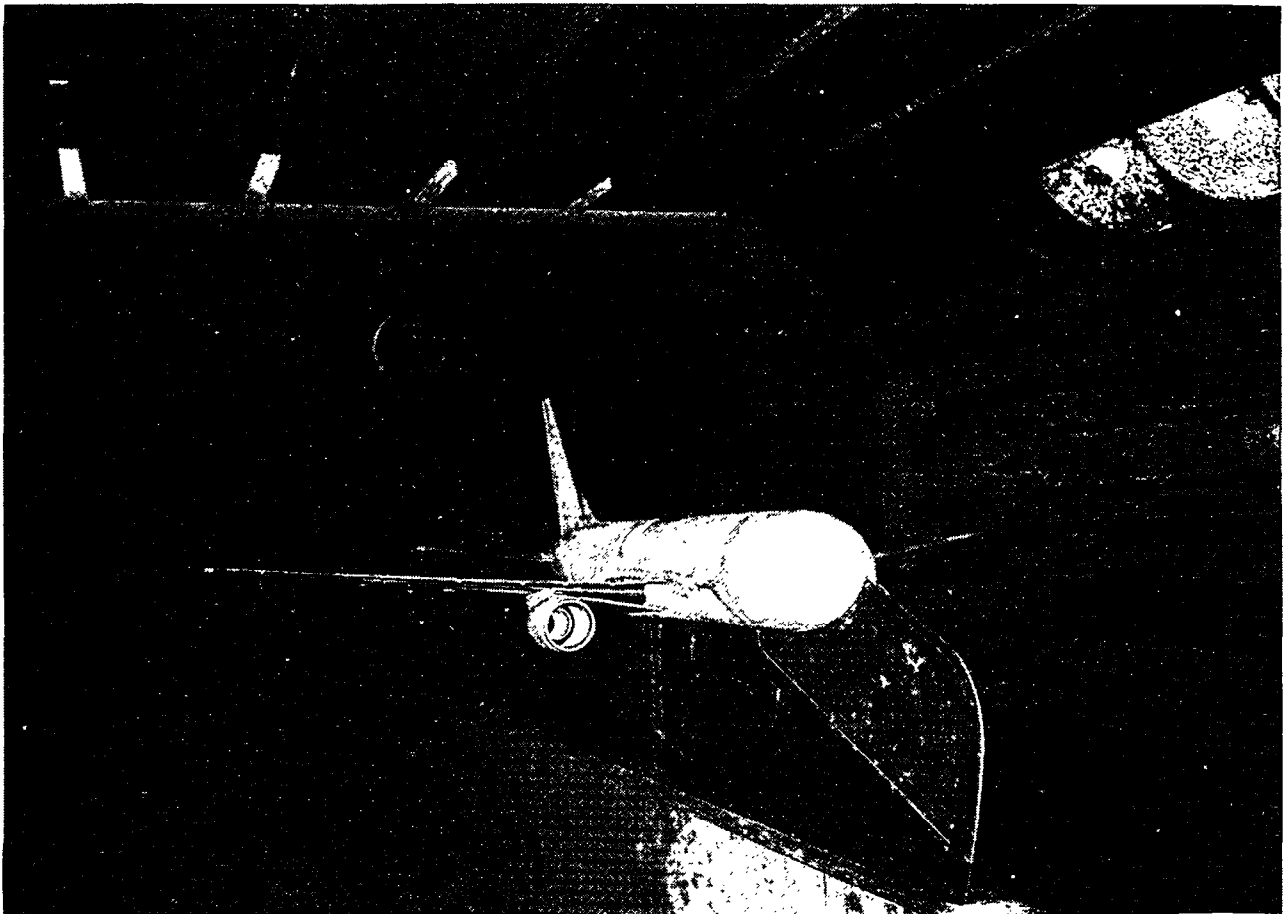
FROM FLIGHT TEST

- ENGINE PARAMETERS
(INCLUDING NET THRUST)
- CONTROL DEFLECTIONS
- AIRPLANE WEIGHTS
- ACCELERATIONS
- PILOT OPINION

-
- PRESSURES
 - FLOW SURVEYS
 - TUFTS AND DYE

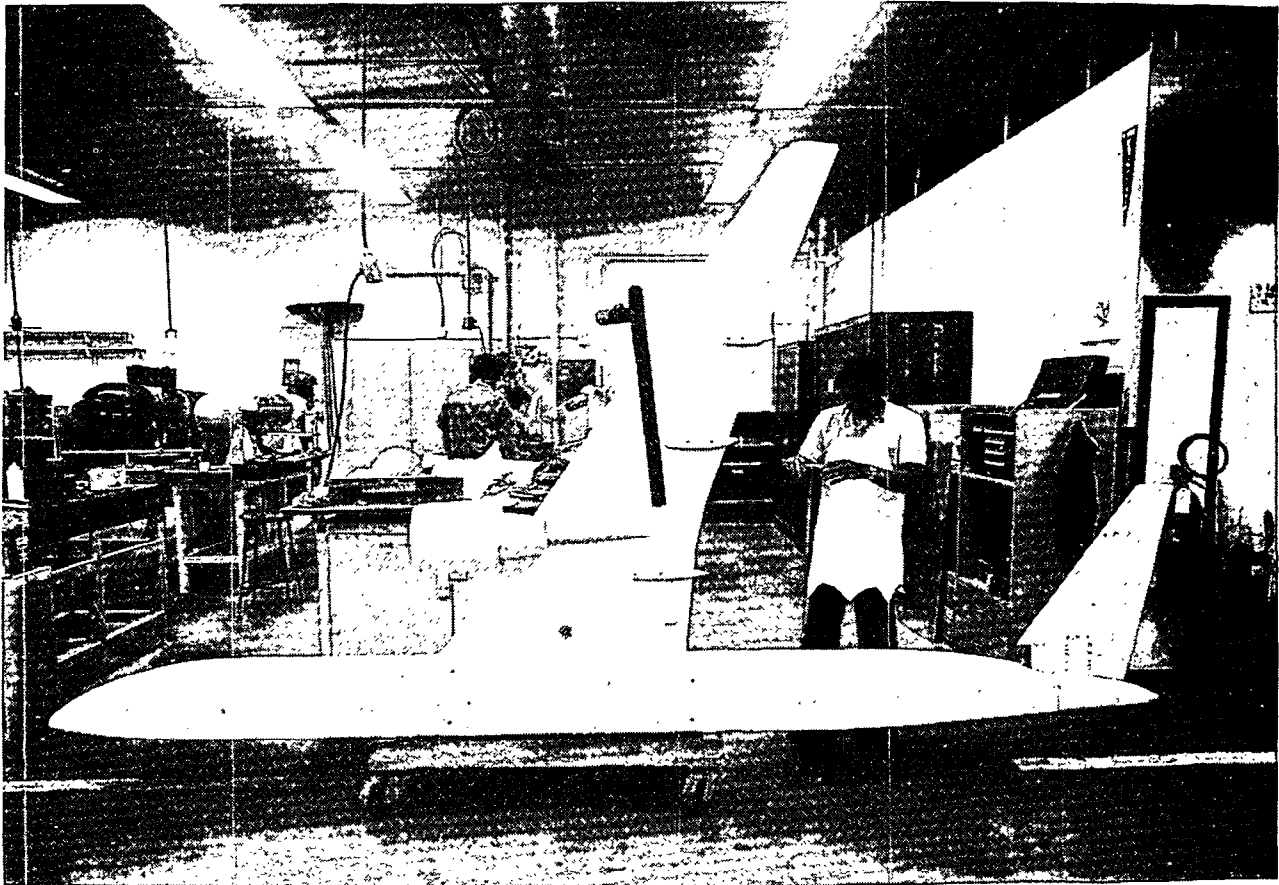
DEVELOPMENT TESTING OF THE 767 AIRPLANE IN THE BOEING TRANSONIC WIND TUNNEL

The next several figures illustrate some of the wind-tunnel test configurations that provide the backlog of data that will be compared to flight tests. The plate mount shown in this figure is one of several types used in development testing in the Boeing Transonic Wind Tunnel (BTWT).



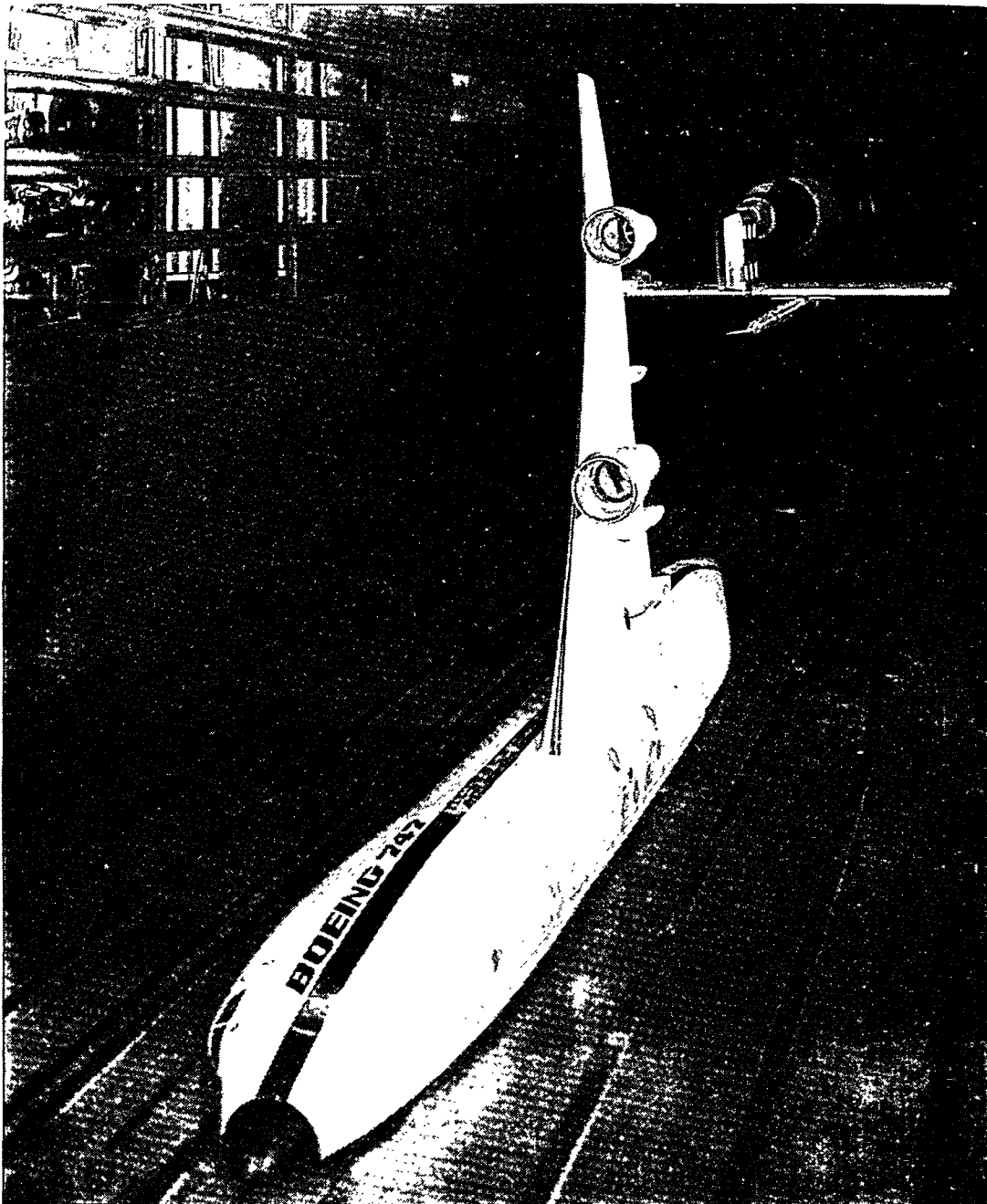
HIGH REYNOLDS NUMBER TEST MODEL OF THE 767 AIRPLANE

The model shown here was constructed for testing in the NASA Ames 11-foot Unitary Plan Wind Tunnel. In order to get the highest possible wing-chord Reynolds number a half-model configuration was chosen. The model was tested in late 1980.



HIGH REYNOLDS NUMBER TEST MODEL OF THE 747 AIRPLANE

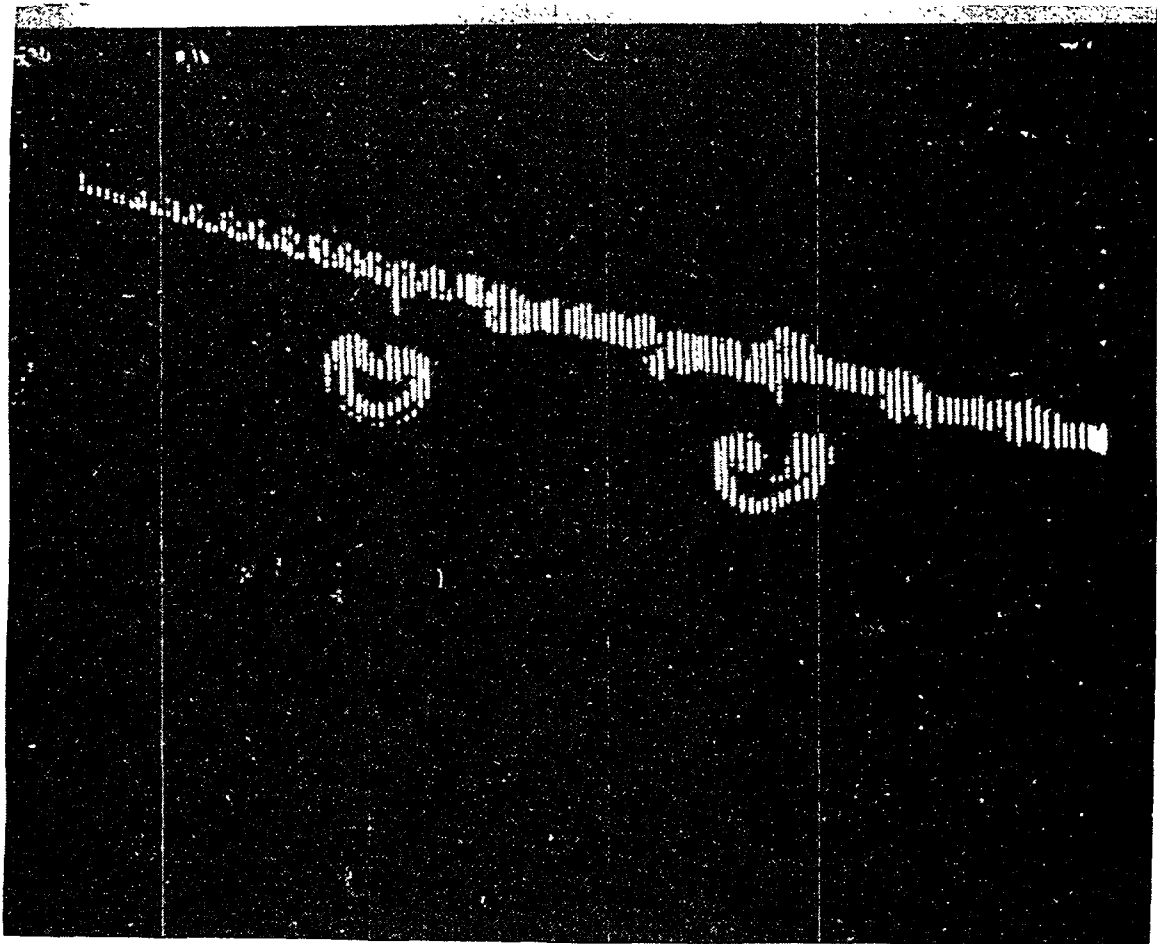
This model is similar in concept to that in the previous figure. Its purpose was to provide high Reynolds number data on an existing airplane to determine flight and wind-tunnel correlations. The facility is the NASA Ames 11-foot Unitary Plan Wind Tunnel. Note the traversing probe for the Wake Imaging System in the background.



WING-WAKE IMAGE OF THE 747 AIRPLANE

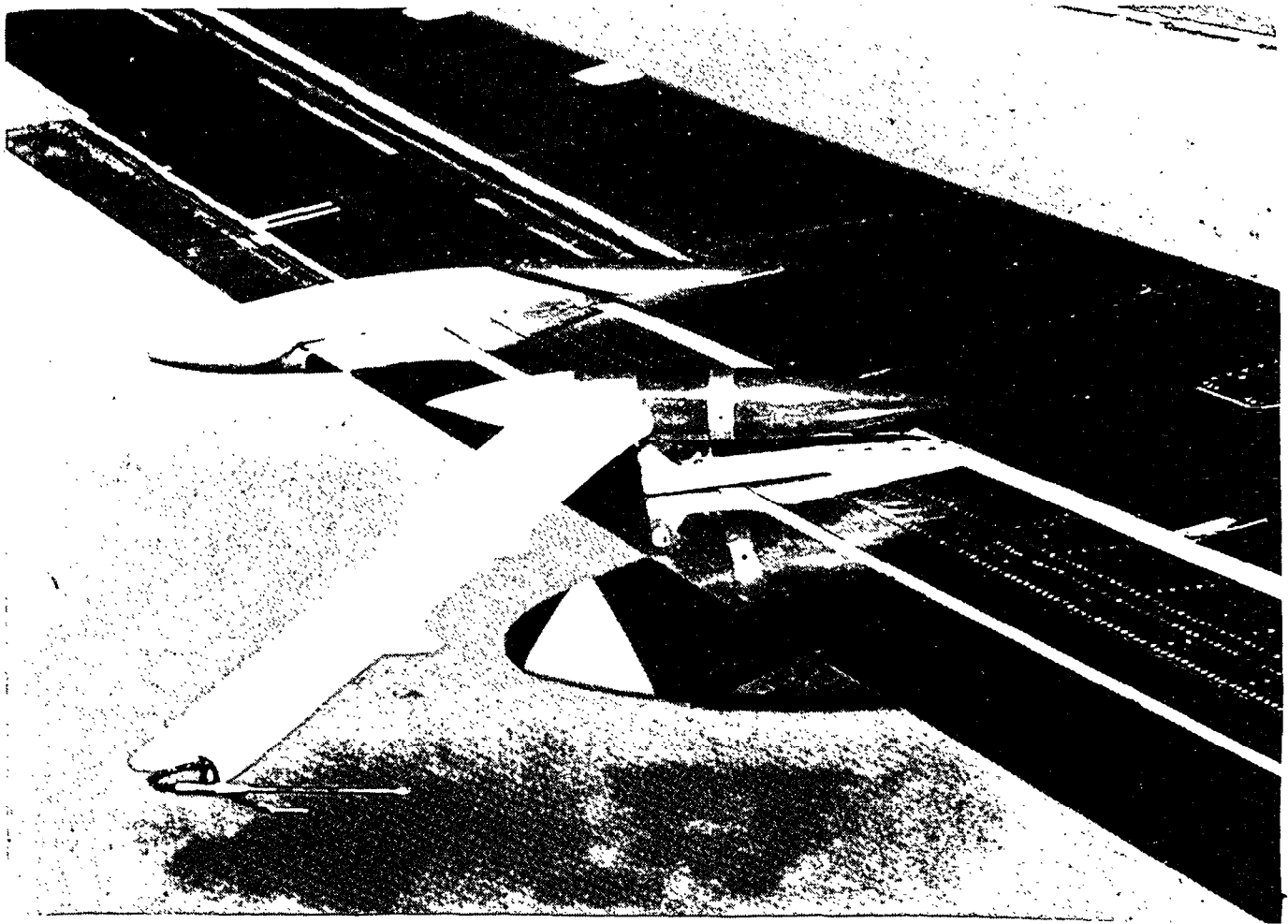
This figure shows an example of the output from the Wake Imaging System. The wing wake, from the side of body to the wing tip, is shown, with the wing tip being at the left of the figure and the upper part of the figure corresponding to the flow field of the upper surfaces.

The original of this figure is in color and shows much more detail than can be seen here. However, some detail in the nacelle wakes is easily seen, as well as disturbances from various features of the wing. The evenly spaced disturbances on the outboard upper surface are caused by vortex generators.



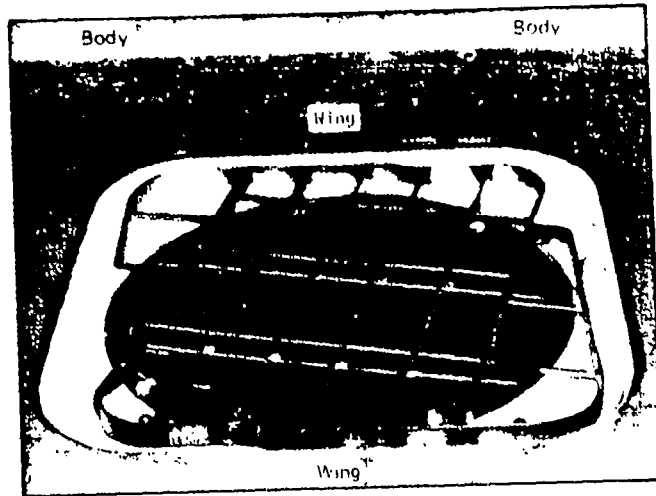
TRAVERSING-PROBE INSTALLATION ON THE 727 AIRPLANE

This figure illustrates a diagnostic device that has been used on several previous Boeing airplanes. It consists of a rotating-arm instrument carrier with a central drive mechanism and is designed to be relatively easily attached at most locations on an airplane. In this particular installation the device was used on the 727 airplane to obtain section-drag data for comparison to wind-tunnel data and analytic predictions.

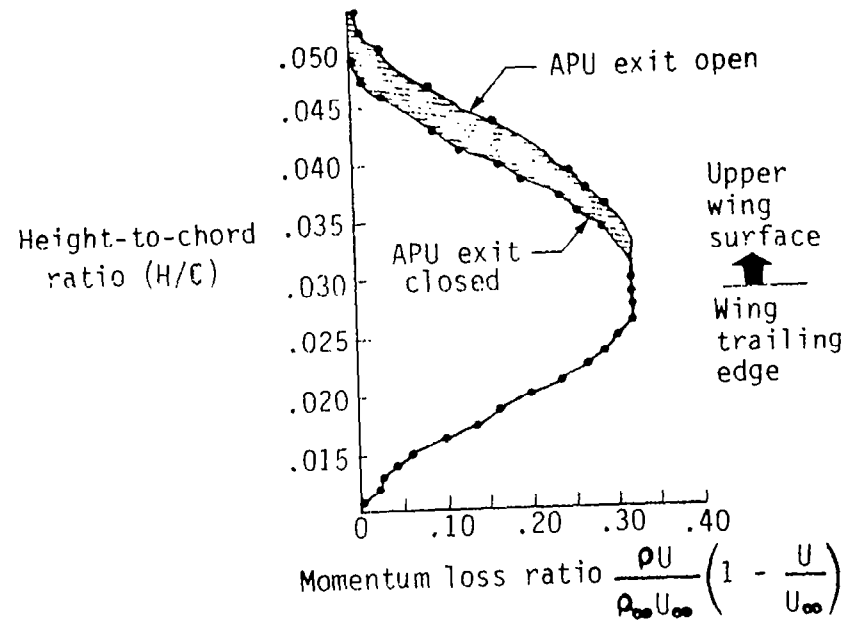


FLIGHT TEST OF AUXILIARY-POWER-UNIT (APU) EXIT DRAG

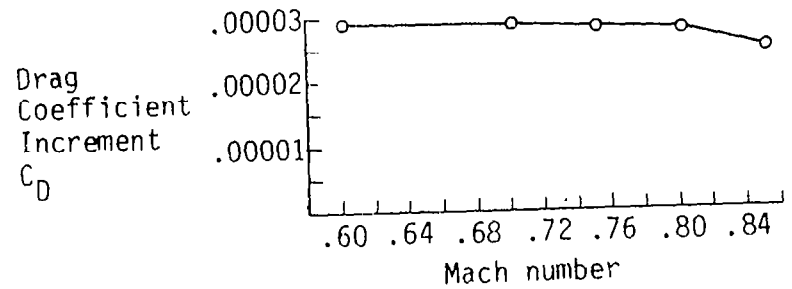
Of course, many kinds of excrescences are found on full-scale airplanes that affect the correlation of wind-tunnel and flight data. The example illustrated here is an auxiliary-power-unit exit on the upper wing of a 727 very near the fuselage. With the aid of the rotating wake probe illustrated in the previous figure, the wake-momentum defect with the auxiliary power unit closed and opened was measured. It was determined that there is approximately 3/10 of a count of drag resulting from this installation. Such a very small drag increment cannot be found in the usual flight-test procedure of equating airplane drag to thrust.



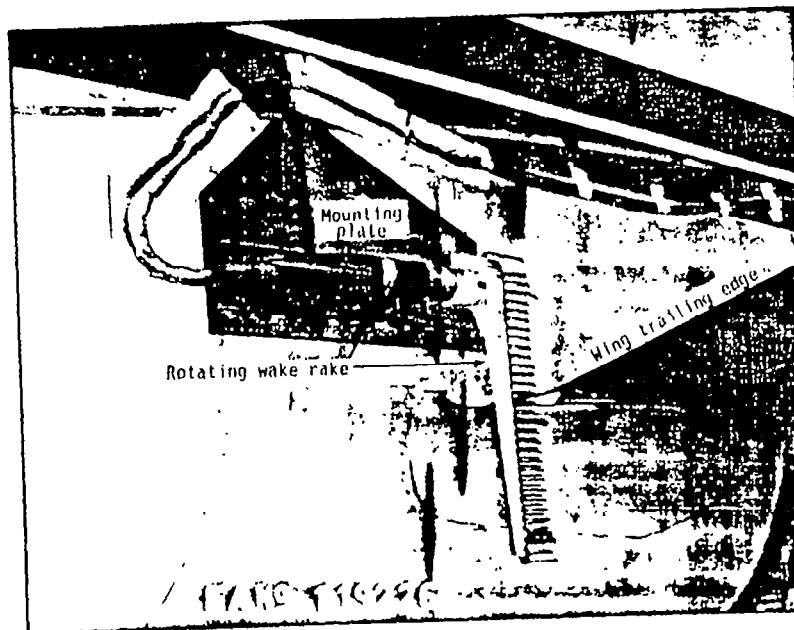
727-200 AUXILIARY-POWER-UNIT EXIT



MOMENTUM LOSS DISTRIBUTION
DOWNSTREAM OF APU EXIT



VARIATION OF APU EXIT DRAG
WITH MACH NUMBER

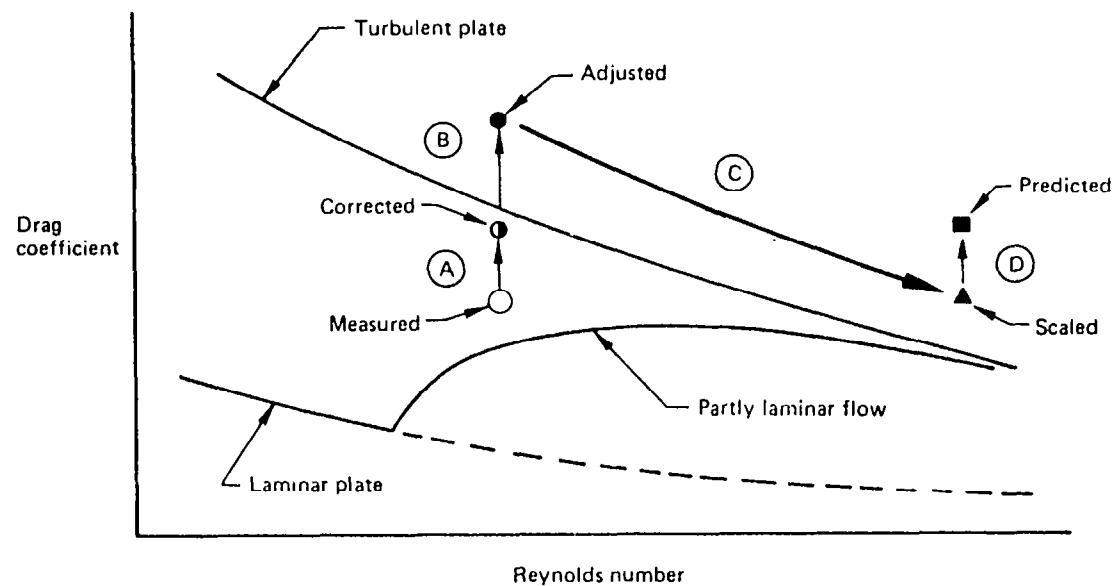


ROTATING WAKE RAKE INSTALLATION

WIND-TUNNEL/FLIGHT DATA ADJUSTMENTS

The relation of wind-tunnel and flight data involves several different corrections which are illustrated in this figure. Beginning with the basic wind-tunnel data, corrections for facility effects and mounting must first be made. These include wall effects, upflow, buoyancy, and various kinds of tare. Another class of corrections adjust the drag of the actual wind-tunnel model, as tested, to an idealized smooth sealed model. The primary adjustments required for most transport-airplane models are for the effects of boundary-layer trips and the internal drag of flow-through nacelles. Flow-nacelle internal drag is, of course, not representative of the full-scale airplane since the full-scale internal flow is accounted for in determining engine thrust.

Wind-tunnel data must be adjusted so that full-scale airplane performance can be predicted. For cruise drag predictions, the classic variation of skin friction with Reynolds number gives the basic trend. Some parts of the drag are presumed to scale with skin friction; other parts do not. The result of all of these corrections, however, is to arrive at the predicted drag of a full-size airplane that is still ideally smooth and sealed. Finally, several corrections are required for features not present on the wind-tunnel model. Every airplane has a certain amount of unavoidable drag due to nonsmooth surfaces or leakages, and these are corrected based on other kinds of tests or data from previous airplanes. In addition, aeroelastic deformations, trim, and various kinds of propulsion effects must be accounted for.



PHASE

Ⓐ WIND-TUNNEL CORRECTIONS

- WALL PLATE } INTERFERENCE
- UPFLOW
- BUOYANCY

Ⓑ ADJUSTMENTS TO MODEL DRAG

- TRIP-STRIP EFFECTS
- INTERNAL DRAG, ETC.

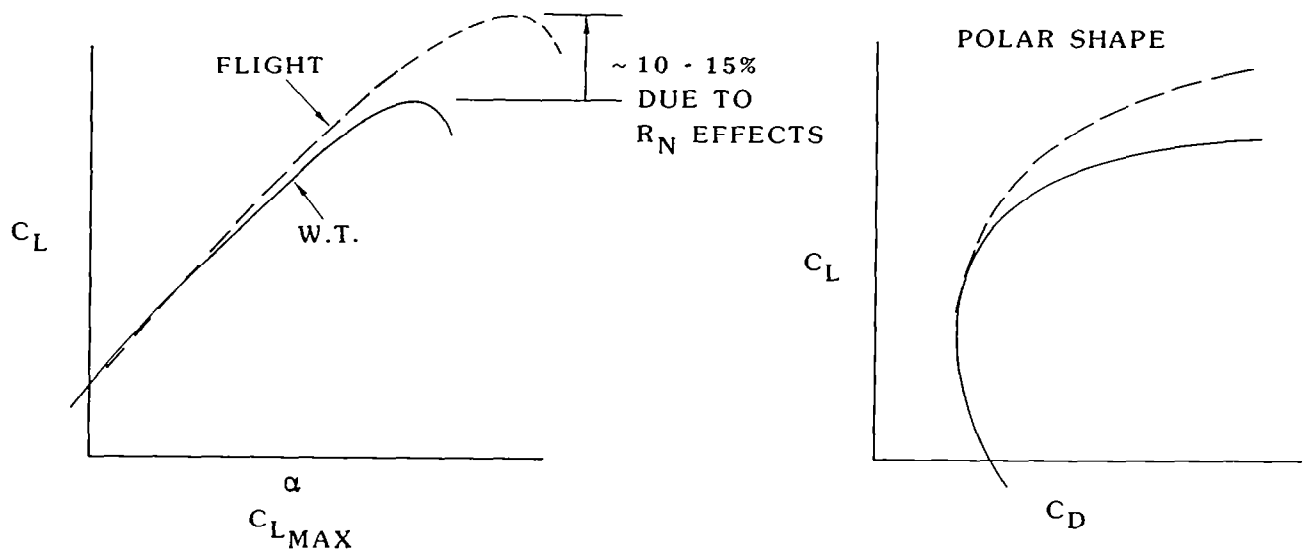
Ⓒ EXTRAPOLATION TO FLIGHT REYNOLDS NUMBERS

Ⓓ AIRPLANE CHARACTERISTICS

- ALLOWANCE FOR SURFACE ROUGHNESS AND EXCRESCENCES
- ELASTICITY AND TRIM
- INLET AND JET EFFECTS

LOW-SPEED DATA ADJUSTMENTS

Large corrections of low-speed wind-tunnel data are required to predict high-lift configuration performance in flight. Maximum lift at the higher flap settings and L/D at take-off settings are the two areas of low-speed performance that most affect the guarantees. Typically, high Reynolds number testing, analytical work, and previous wind-tunnel/flight results are employed to adjust low Reynolds number wind-tunnel data to flight conditions.

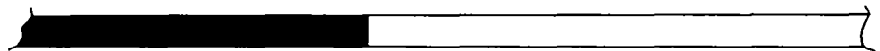


STATUS OF 767 HIGH-SPEED WIND-TUNNEL AND FLIGHT TESTING

In the case of the 767, there will be several years of wind-tunnel/flight correlation activities. There were many years of Boeing Transonic Wind Tunnel (BTWT) testing of potential new Boeing products which gradually crystalized into the 767 and 757 programs. Such testing can be expected to continue on through the entire useful life of the airplanes. High Reynolds number tests are done periodically (BTWT is an atmospheric tunnel), often in the Ames 11-foot Unitary Transonic Wind Tunnel (pressurized). The next major element in the 767 test program will be flight testing, which has already begun. The latest addition to the 767 test program is a test in the National Transonic Facility, wherein the full-scale Reynolds number is expected to be duplicated. The design and fabrication of the model has already begun. The test is anticipated to occur in early 1983.

1980	1981	1982	1983	1984
------	------	------	------	------

BTWT TESTING



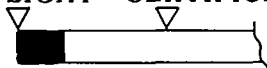
HIGH REYNOLDS NUMBER TESTS

TEST



1ST FLIGHT CERTIFICATION

FLIGHT TEST



NATIONAL TRANSONIC FACILITY

DESIGN AND FAB.

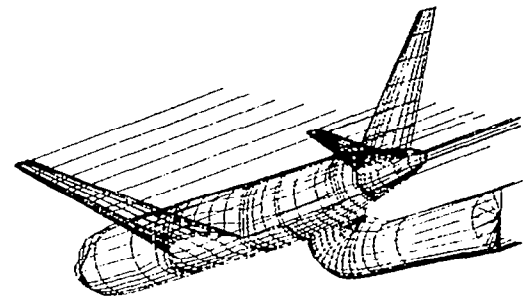
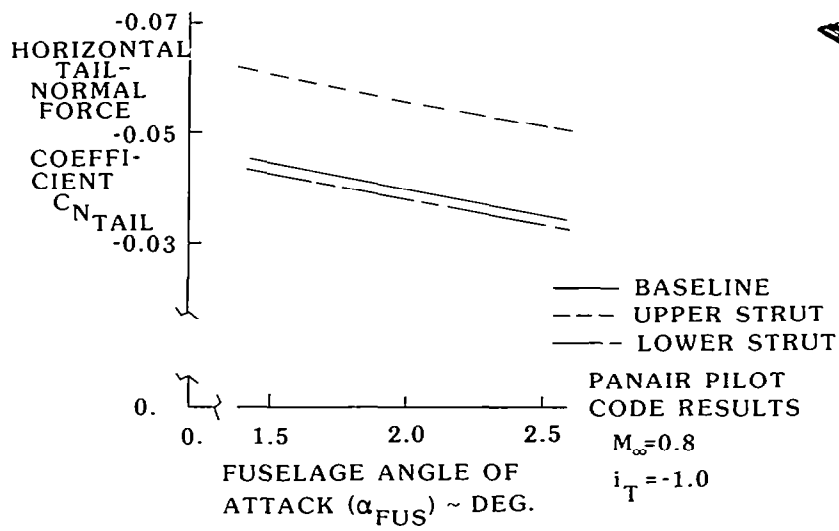


TEST

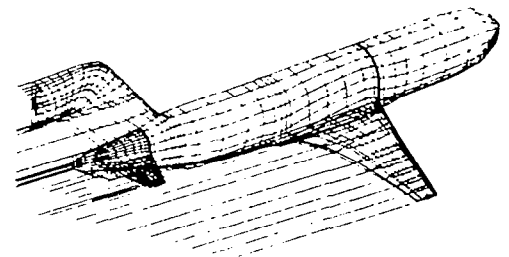


CALCULATION OF THE NTF 767 MODEL SUPPORT-STRUT EFFECT

This figure illustrates some of the analysis that is being done for the design of the 767 NTF model and support system. The inset graph shows one of the results from such calculations, showing the effects of the two support systems on the horizontal-tail force coefficient. These results illustrate the fact that adjustments and corrections will be required even in the NTF.



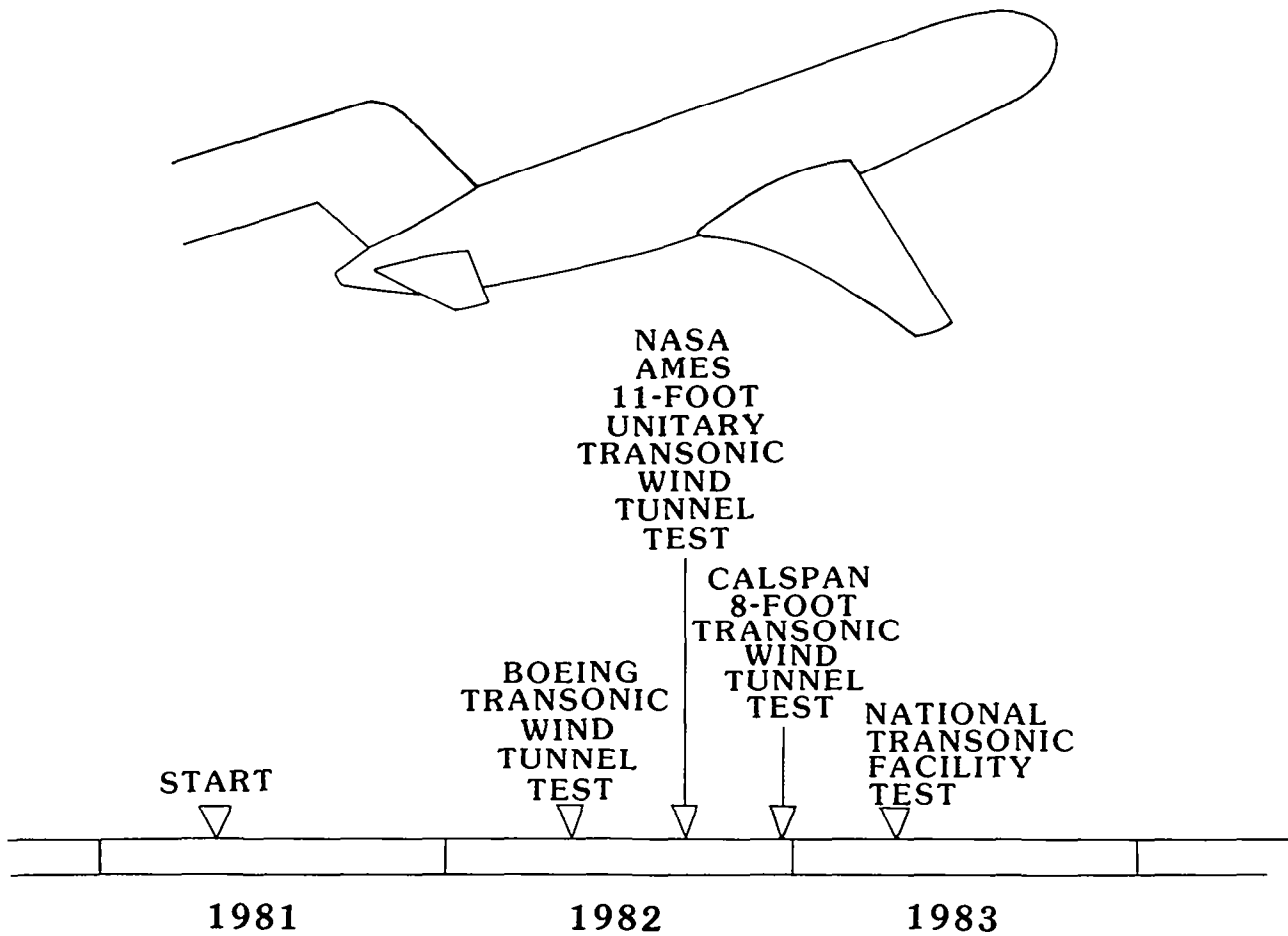
LOWER MOUNTING STRUT



UPPER MOUNTING STRUT

TUNNEL TESTING OF THE 767 CALIBRATION MODEL

The final figure shows in more detail the plan for testing the 767 NTF model. As indicated, the model will also be tested in several other facilities and so will provide a facility comparison as well as a flight/wind-tunnel correlation.



F-16E PROGRAM OVERVIEW AND WIND TUNNEL/FLIGHT CORRELATION

A. P. Madsen
General Dynamics
Fort Worth Division

Miniworkshop on Wind Tunnel/Flight Correlation
November 19-20, 1981

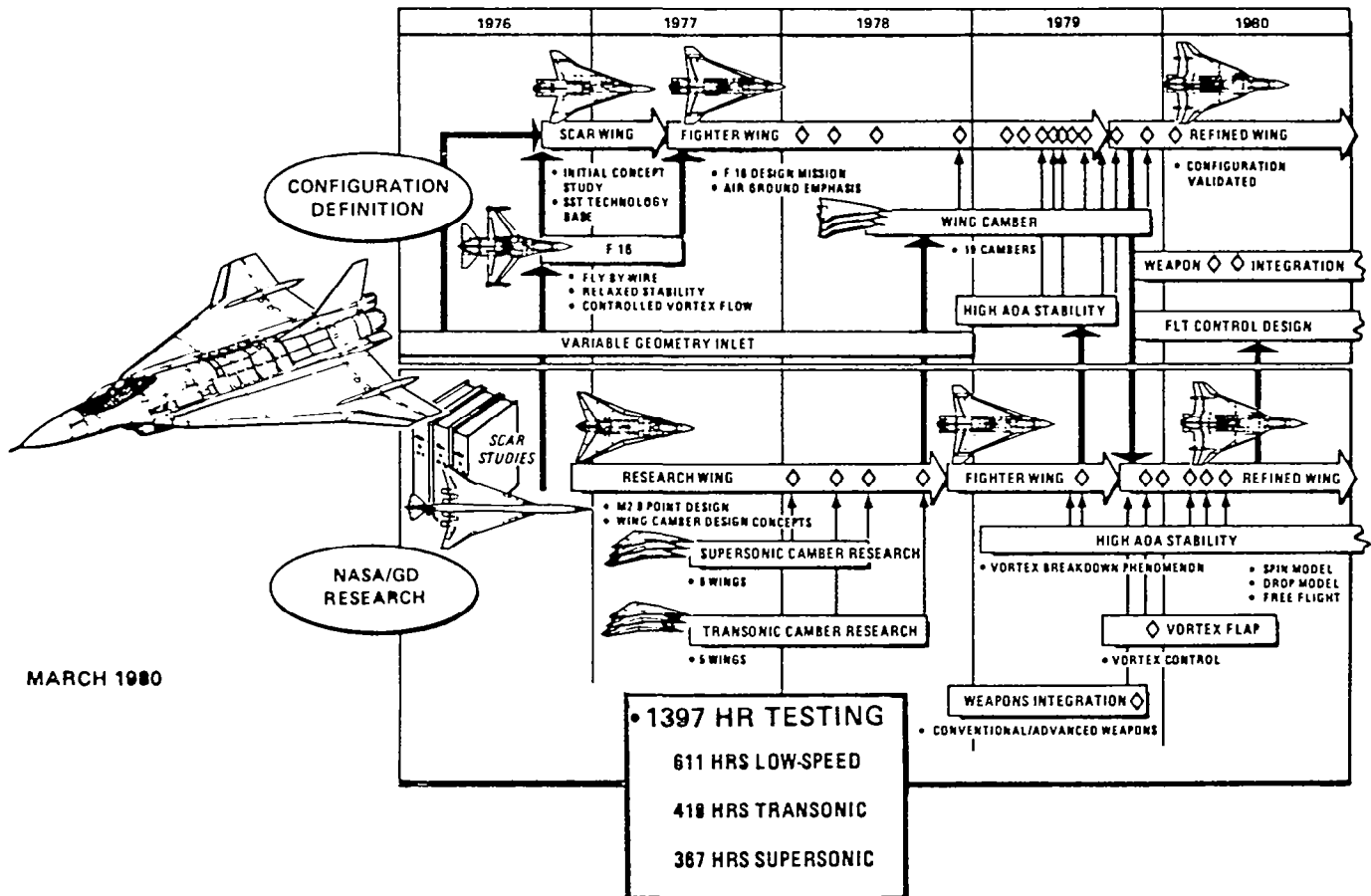
Introduction

- **In February 1980, General Dynamics Submitted an Unsolicited Proposal on the F-16E (Formerly Scamp and F-16XL) to USAF**
- **Since That Time, General Dynamics Has Continued Development of the F-16E Configuration and Program Planning:**
 - F-16E Team Maintained Intact
 - Configuration Refinement Studies Continued
 - Wind-Tunnel Testing Continued
 - General Dynamics Made a Corporate Commitment to Proceed With an F-16E Flight Demonstration Program
 - Development Planning Continued

F-16XL: DERIVED FROM EXTENSIVE COOPERATIVE EFFORT

The F-16E configuration is an outgrowth of studies that began in 1976. Building on the technology base developed during the SST and F-16 programs, a cooperative research effort by NASA Langley and General Dynamics was conducted to produce a refined fighter wing design. Several iterations were required to arrive at the combination of wing planform, camber, and twist which gives near optimum lift, drag, and high-angle-of-attack stability. Theoretical analyses were backed up by extensive experimental data to validate the design.

At the time of submittal of an unsolicited proposal to the Air Force, almost 1400 hours of wind tunnel testing had been accomplished by General Dynamics. In addition, high-angle-of-attack stability investigations had been conducted by NASA using spin, drop, and free-flight models.



Program Approach

- **Basic Task:**

- Establish Design for Flight Demonstrators and Production Configuration
- Modify F-16 A5 Into Single-Place F-16E
- Modify F-16 A3 Into Two-Place F-16E
- Provide Safety of Flight Certificates for Flight Demonstrators

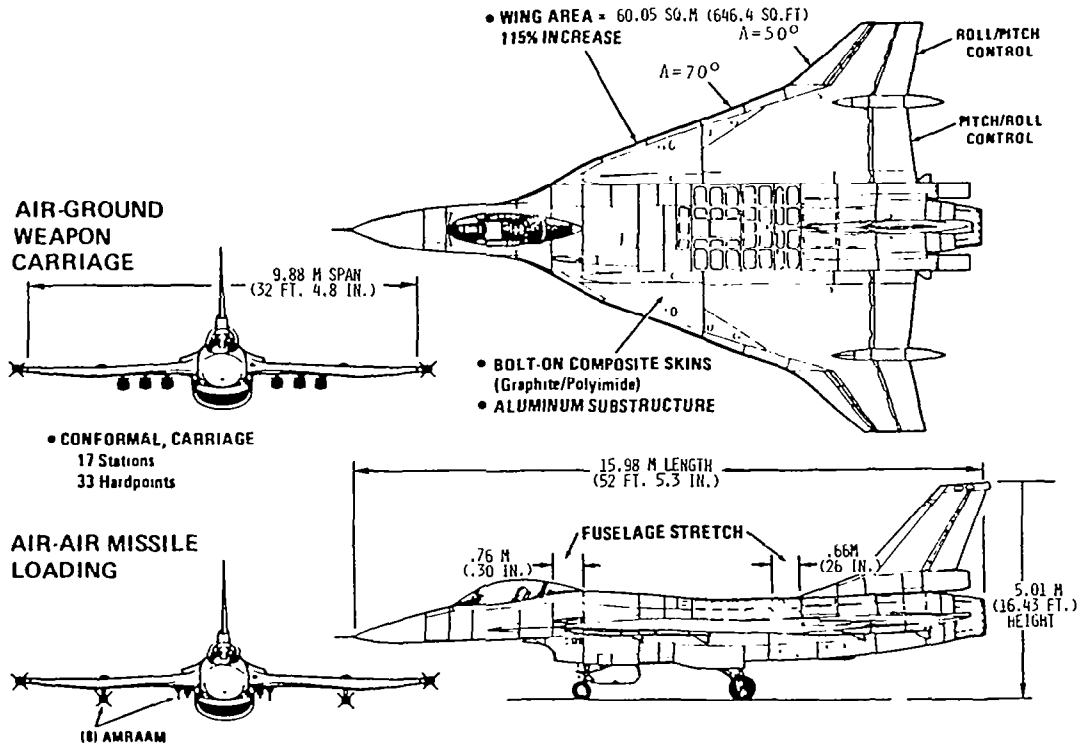
- **USAF Support Assumed:**

- Lease Aircraft and Equipment to Manufacture Flight Demonstrators
- Provide Supplemental Funding for Flight Test Program

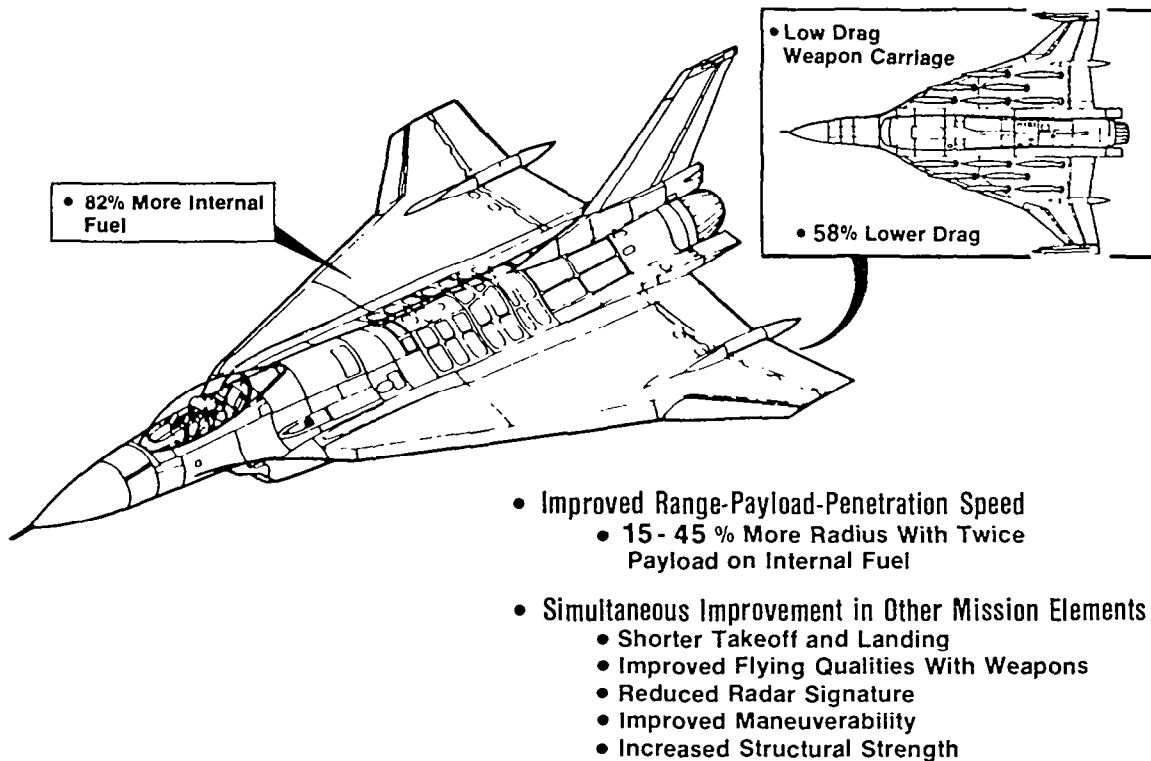
- **Management Approach:**

- Similar to the YF16 Prototype Program
 - Simplified WBS
 - Minimum Documentation
 - Co-location of Entire Team
 - Participation by Major Sub-contractors
- Early Air Force Participation
- Design and Test for Minimum Development Transition Into Production

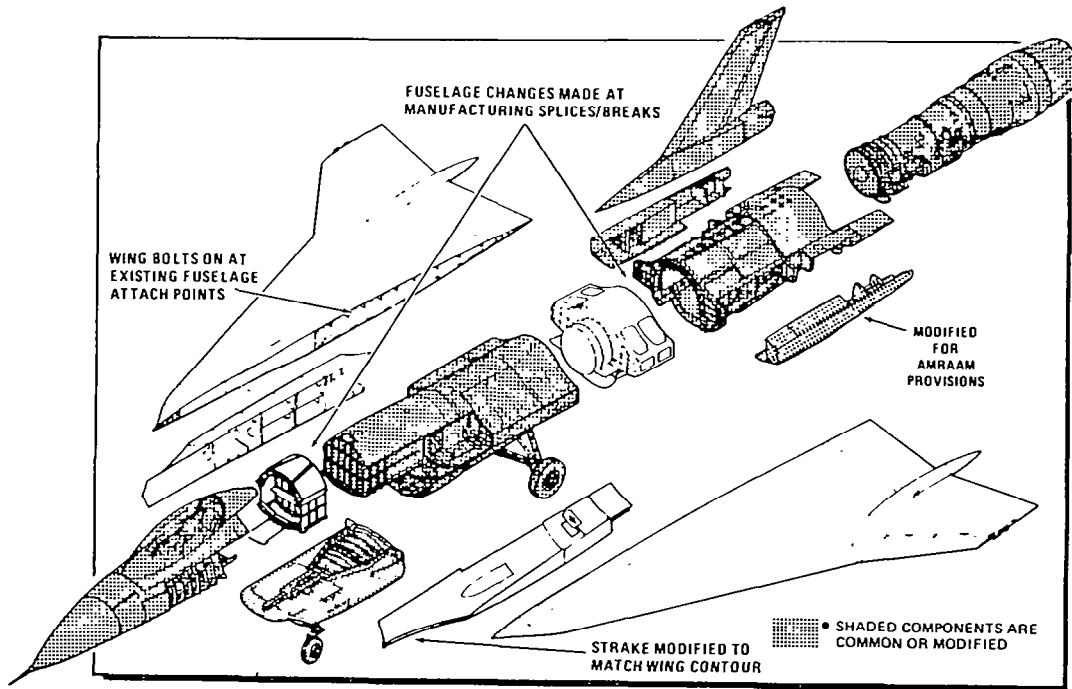
F-16E: A High Pay-Off Configuration



F-16E Operational Benefits



F-16E Modification of F-16



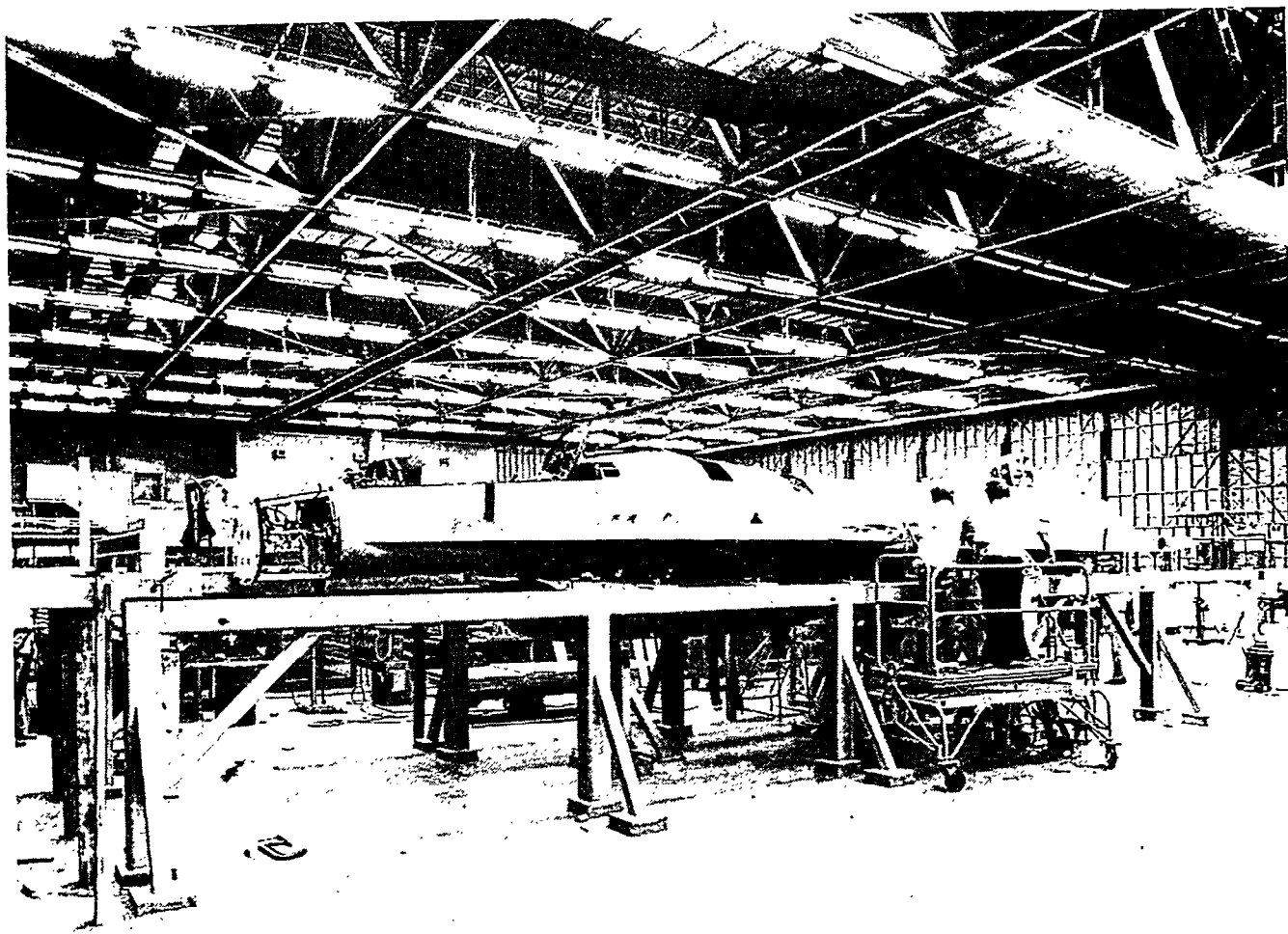
F-16E Status

- **The F-16E Program Is Moving at a Rapid Pace:**

- Go-Ahead 1 Dec 80
- First Engineering Release 18 Dec 80
- First Chips 21 Jan 81
- F-16A No. 3 Received 6 May 81
- F-16A No. 5 Received 26 June 81
- As of 1 August 81:
 - ✓ Configuration Frozen
 - ✓ Over 50% of Engineering Drawings Released
 - ✓ Over 2300 Hrs. of Wind-Tunnel Testing Completed
 - ✓ Over 512 Tools Completed
 - ✓ Over 536 Parts Fabricated
 - ✓ Over \$9.5M Worth of Materials Procurement in Work

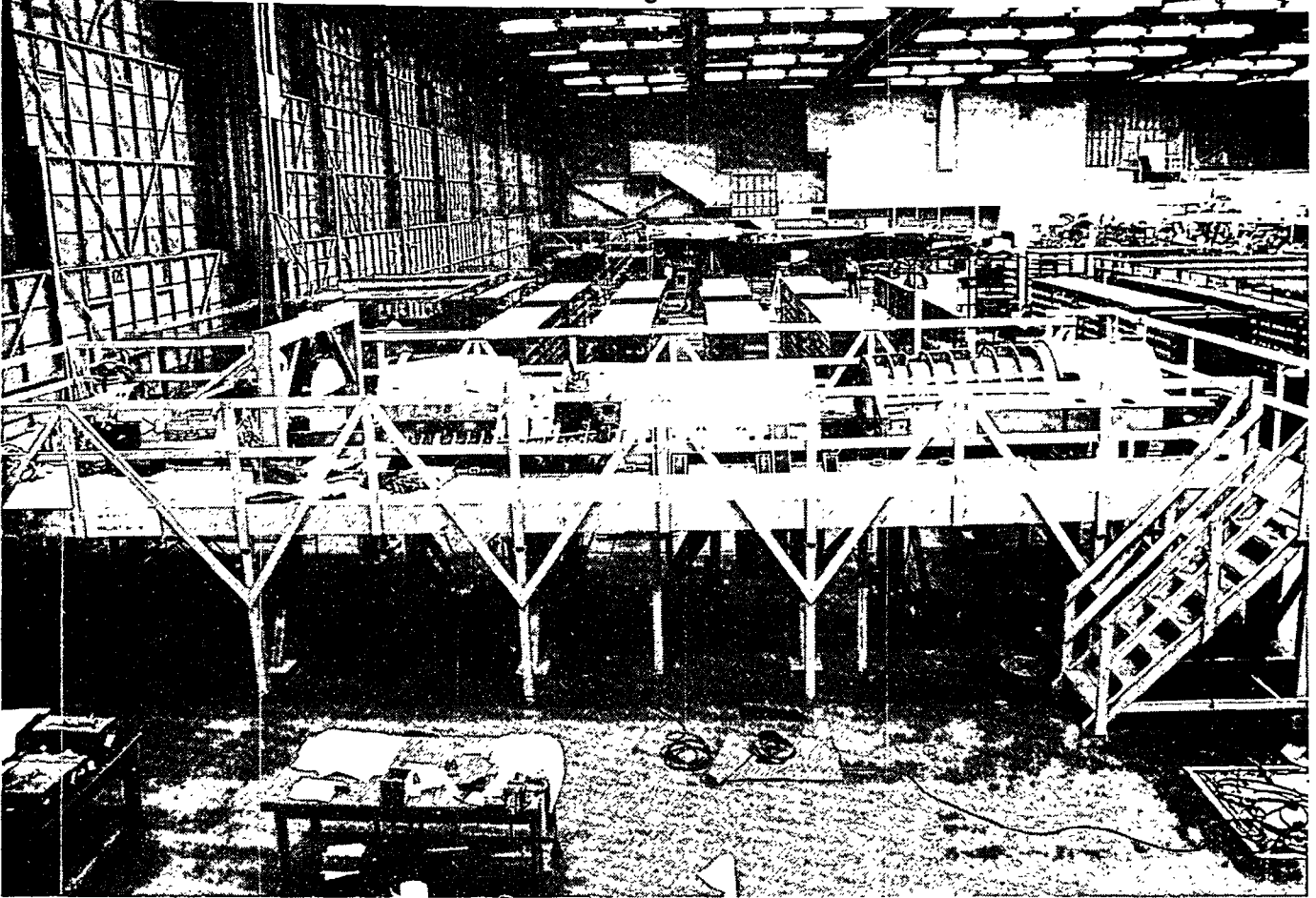
First Flight Will be July 1982

F-16A No. 5 Loaded In Tooling Fixture

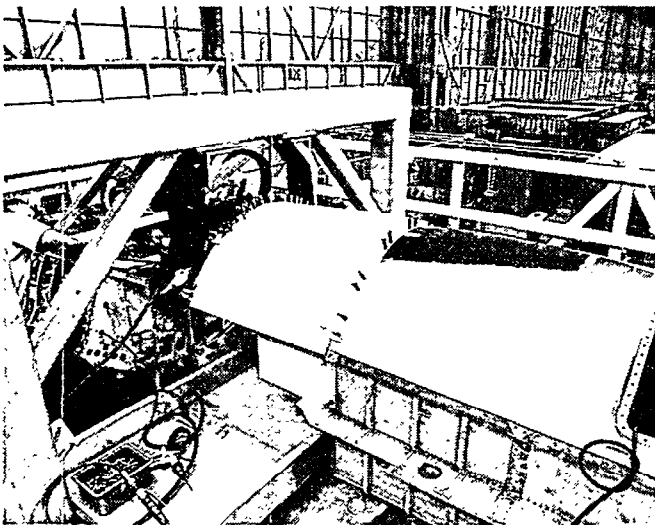


Fabrication and Assembly of F-16E Has Started

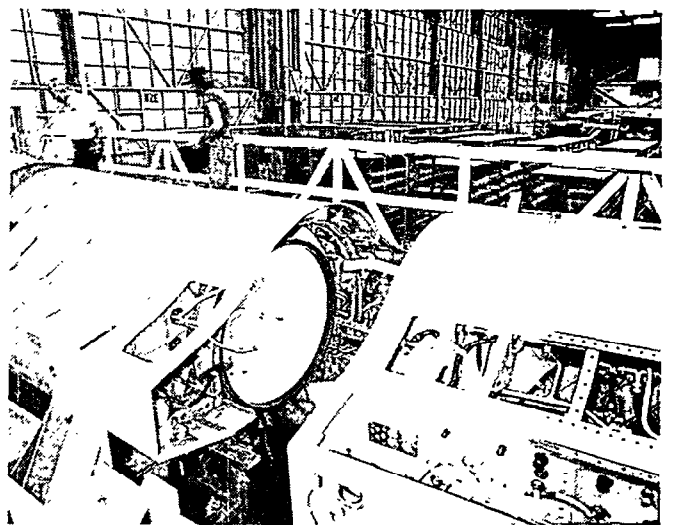
F-16A No. 5 Fuselage Demated for Stretch

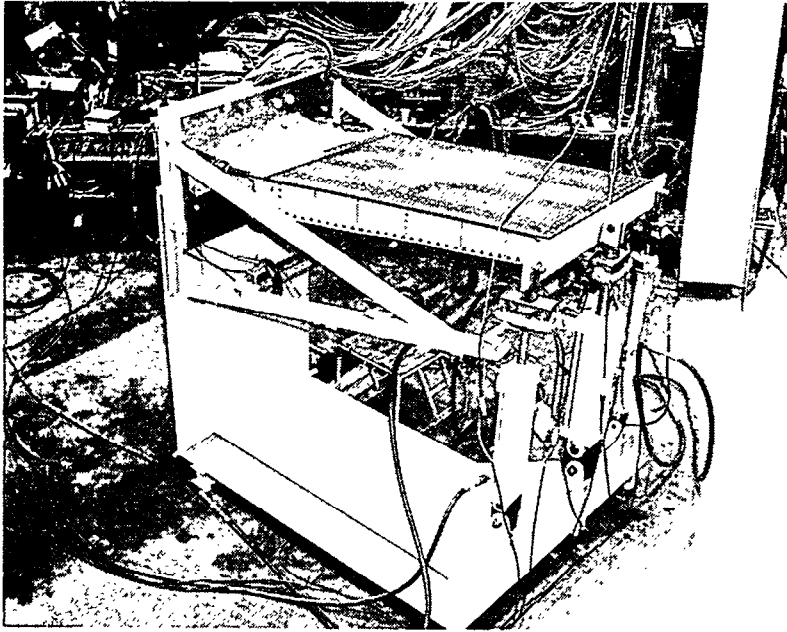


Forward Stretch



Aft Stretch

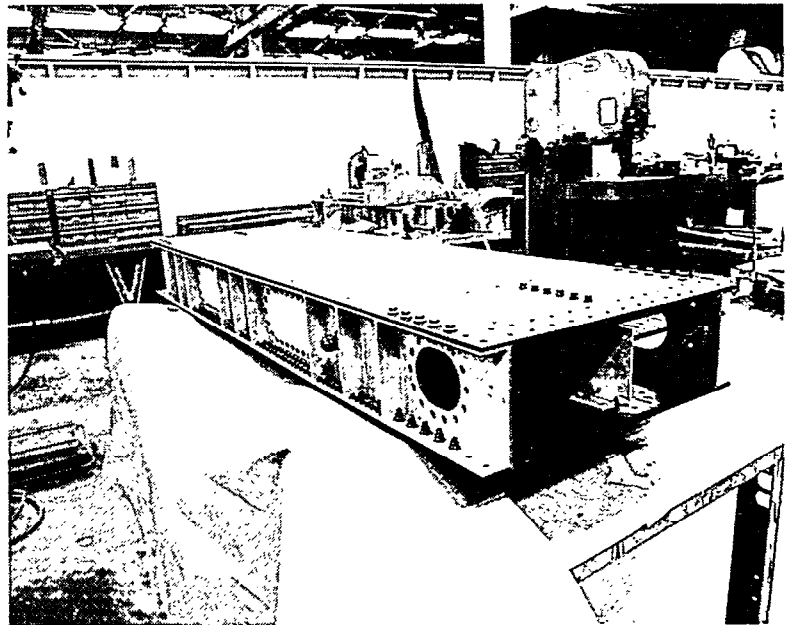




F-16E Parts are in Test

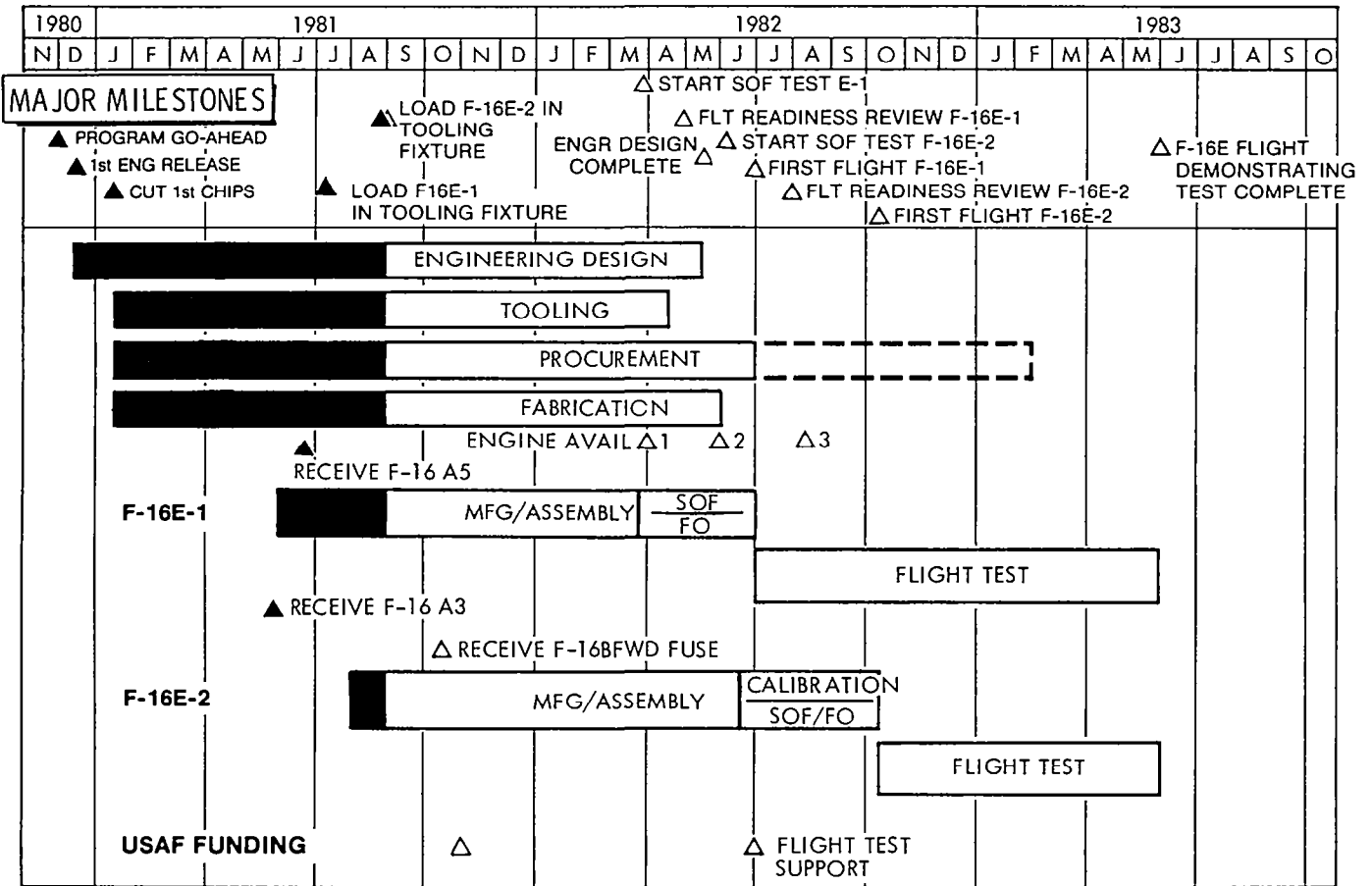
**Wing Root Attachment
Static Test**

**Fuel Sealant and
Fatigue Test**



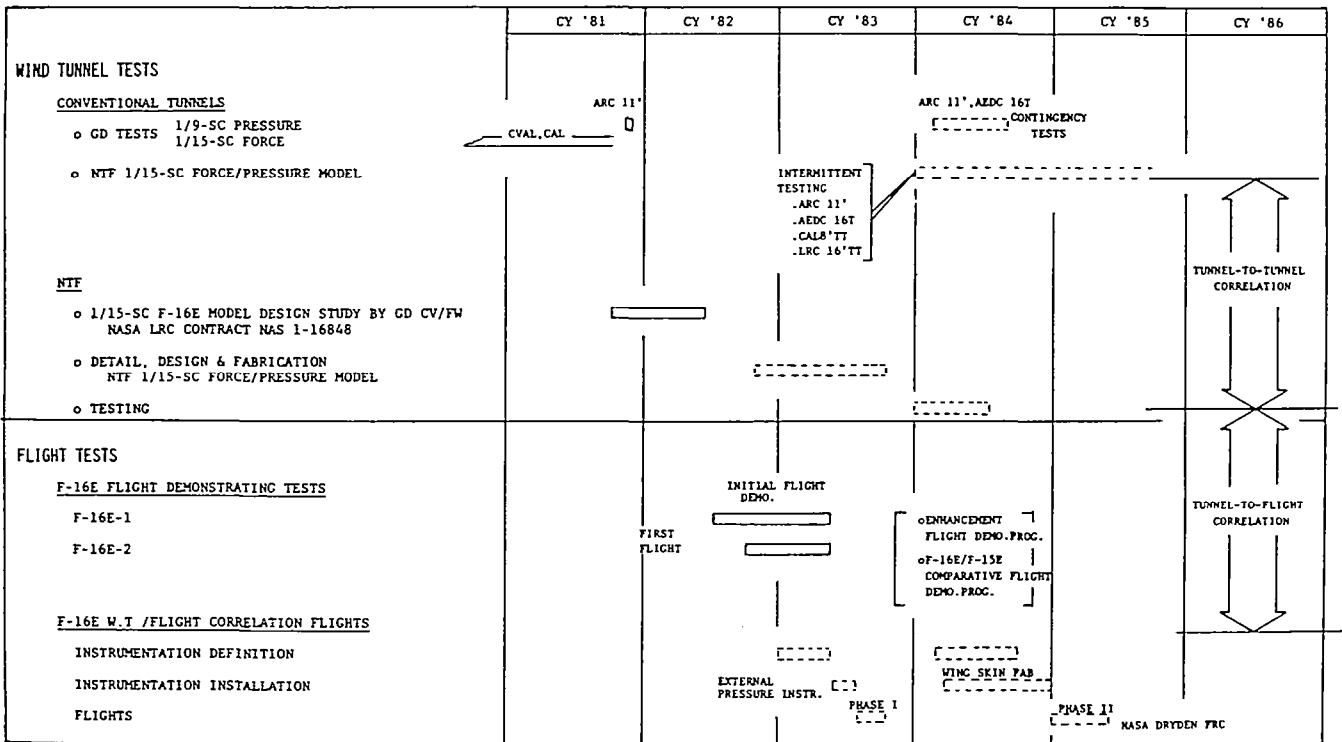
F-16E Flight Demonstrator Program Schedule

8-24-81



AX0012M

POSSIBLE F-16E WIND TUNNEL/FLIGHT CORRELATION PROGRAM



POSSIBLE F-16E WIND TUNNEL/FLIGHT CORRELATION PROGRAM

The F-16E program offers an excellent opportunity for wind tunnel to flight correlation on a configuration of advanced aerodynamic design which generates highly complex flow fields. The Reynolds number dependence of the flow phenomena involved is not fully understood in many cases and could impact the final design. Thus the NTF, which over its Mach number range of operation can simulate full-scale Reynolds numbers for the F-16E, could prove to be invaluable in helping to refine the design and solve problems should they arise in the flight test program.

As noted by T. G. Ayers (ref. 1), "correlation" can be defined in at least three different ways:

- (1) Comparisons of wind tunnel and/or theory with flight results
- (2) Detailed studies of total vehicle drag from wind tunnel and flight tests
- (3) Attempts to understand the fundamental mechanisms of fluid flows associated with aircraft components in specific areas of the flight environment

The last of these definitions is the one most applicable relative to the F-16E program and forms the basis for the discussion that follows.

Several factors deserve special consideration in attempting to define a possible wind tunnel/flight correlation program for the F-16E. These involve ongoing and planned wind tunnel and flight tests and model design studies. Further, a program of this type, involving the NTF, should also have as one of its basic objectives provisions for tunnel-to-tunnel data correlations.

As has already been noted, a large wind tunnel data base for the F-16E from conventional tunnels now exists, and additional detailed pressure distribution data will soon be available from tests in the NASA Ames 11-Foot Unitary Tunnel. Thus, data will be on hand for comparison with flight test data and NTF data as they become available. With allowance for contingencies, additional testing of the 1/9-scale pressure model could be performed if data of a specific nature were required for analyses.

A "Design Study of Test Models of Maneuvering Aircraft Configurations for the NTF" is being conducted by General Dynamics under contract to NASA. Go-ahead for this 9-month program was 1 October 1981 with the Convair (prime) and Fort Worth Divisions of General Dynamics working as a team. The F-16E is one of two aircraft configurations that will be studied. Successful completion of this program will develop designs in sufficient detail to insure that the models can be fabricated for testing in the NTF.

This will occur in mid-1982 and, provided that funding can be obtained to cover costs for detailed design and fabrication, it seems reasonable to assume that a 1/15-scale F-16E model could be ready for testing in the NTF in late 1983. Intermittent testing of this model in conventional tunnels of adequate size would provide data for direct tunnel-to-tunnel data correlation and help establish user confidence in the NTF.

Paralleling the wind tunnel effort, F-16E Flight Demonstrating Tests are scheduled to begin with the first flight of F-16E-1 in July 1982. First flight of F-16E-2 follows shortly thereafter in October 1982. The initial flight demonstration program will be completed by 1 June 1983 at which time the airplanes will be down for a short period before being readied for the second phase of testing in an Enhancement Flight Demonstration Program that is scheduled for FY 84.

This short downtime would provide the first opportunity for obtaining flight correlation data. This data however, would be limited to that obtainable with external pressure instrumentation such as tubing belts for obtaining wing and fuselage static pressures and boundary layer and wake survey rakes. The airplanes could also be tufted for surface flow visualization investigations in specific regions of the flow if desired. While this type of instrumentation leaves much to be desired, it would provide a limited but early set of data for analysis and evaluation. The period following the Enhancement Flight Demonstration Program is the one during which the type of correlation data desired could be obtained. Wing pressures are of primary importance for correlation purposes and these data will be the most costly to obtain. The modular design of the F-16E and the bolt-on composite wing skins, however, are conducive to keeping this cost as low as possible. Removal of an upper surface wing skin will be required for proper installation of pressure taps and leads. Since the composite skins serve to form the integral wing fuel tanks, it is not known for certain at this time if the upper skin can be reused and still be leakproof. In the worst case, fabrication of a new skin may be necessitated by the requirement for correlation data.

The projected timing of these tests of early 1985, though somewhat far off, would appear to come at a time when the NTF should be nearing maximum operational efficiency. This timing should also permit the application of real-time electro-optical scanning technology and/or real-time photogrammetric techniques to make accurate measurements of airplane shape in flight.

REFERENCE

1. Ayers, Theodore G.: Report of the Wind Tunnel/Flight Correlation Panel. High Reynolds Number Research - 1980, L. Wayne McKinney and Donald D. Baals, eds., NASA CP-2183, 1981, pp. 249-256.

SPACE-VEHICLE CORRELATION OF GROUND AND FLIGHT EXPERIMENTS

William I. Scallion
NASA Langley Research Center
Hampton, Virginia

Miniworkshop on Wind-Tunnel/Flight Correlation
November 19-20, 1981

A 2-PERCENT-SCALE MODEL OF THE SPACE SHUTTLE
ORBITER MOUNTED IN THE LANGLEY UNITARY PLAN WIND TUNNEL

The model shown on the left in figure 1 is a 2-percent-scale model of the Space Shuttle Orbiter. This model was used to verify the aerodynamics of the Shuttle Orbiter prior to flight through the test Mach number range from 1.5 to 4.65.



Figure 1

REMOTELY CONTROLLED MODEL OF THE SPACE SHUTTLE ORBITER
FOR SUBSONIC/TRANSONIC TESTS IN THE NTF

A 2-percent-scale model, identical to that of figure 1, is being designed to become one of the first models to be tested in the NTF. (See fig. 2.) This model will have remotely controlled elevons, body flap, and rudder to minimize tunnel entries associated with configuration changes in the NTF. The Shuttle Orbiter has a very large aerodynamic data base obtained in ground facilities. Since the vehicle flight-test program has already begun, there will be a large amount of flight data for analysis and correlation with the NTF results.

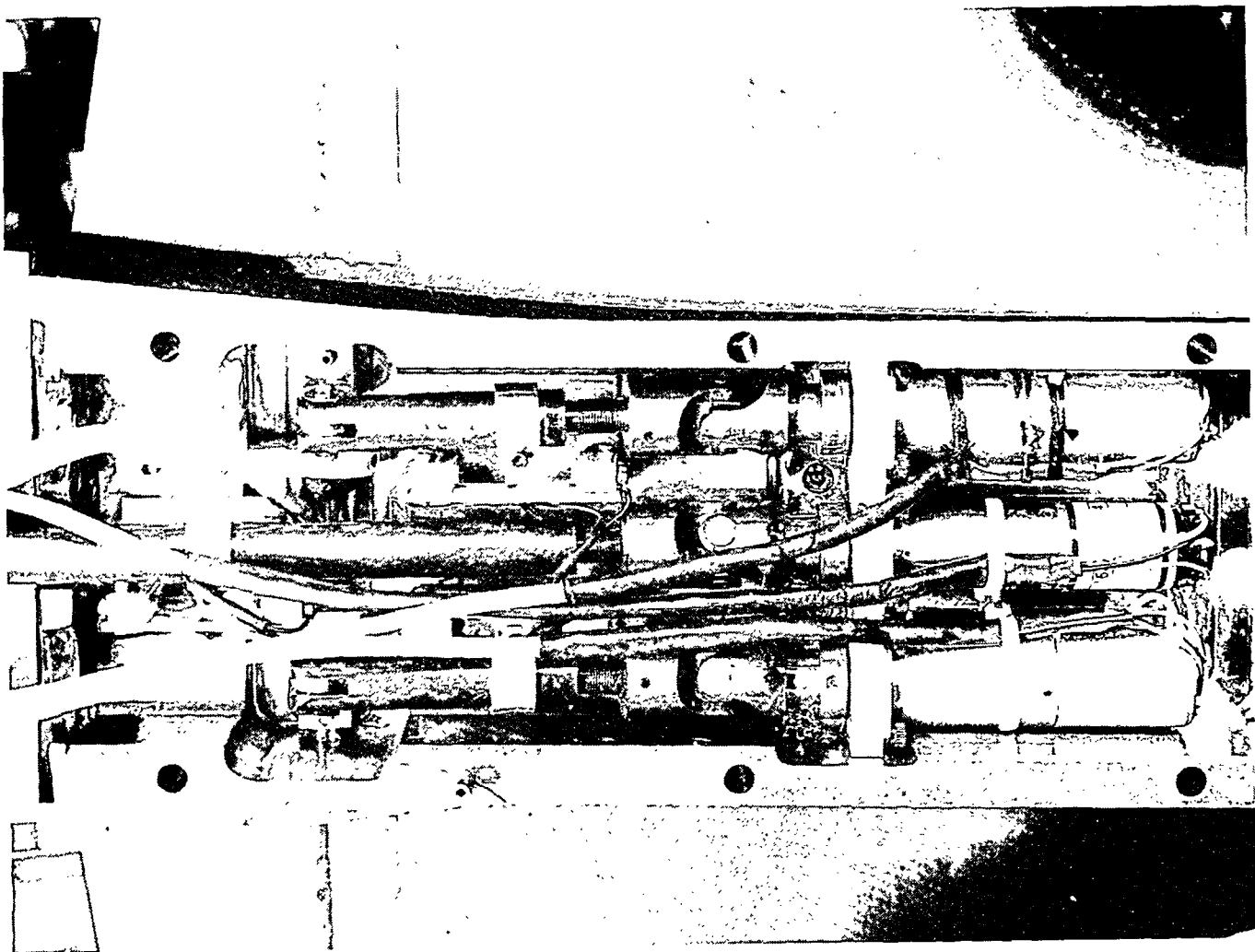


Figure 2

FUTURE LAUNCH-VEHICLE TECHNOLOGY ISSUES

The Langley Space Systems Division is engaged in an advanced, aerospace, vehicle system study aimed at identifying and developing the significant technologies that apply to future vehicles. (See fig. 3.) When development of such future vehicles begins, there will be a great need for transonic aerodynamic information at high Reynolds numbers which the NTF can provide. The Shuttle program required some 5,000 wind-tunnel hours at transonic speeds, and a few of those hours in the NTF would have greatly improved the preflight predictions at transonic speeds.

- MISSION ANALYSIS
 - STAGE OPTIMIZATION (1, 1½, OR 2 STAGES)
 - ABORT
 - RETURN PAYLOAD SIZE
 - ORBIT DEFINITION (OPTIMIZE WITH SOC)
 - CROSSRANGE
 - MISSION MODEL (NOT DEFINED BEYOND 2000)

- OPERATIONS/COST
 - VTO/HTO
 - PAYLOAD (WEIGHT AND DIMENSIONS)
 - EXPENDABLE/REUSABLE
 - AIR BREATHERS/ROCKET PROPULSION
 - FERRY/GROUND TRANSPORTATION
 - MANNED/UNMANNED (BOOSTER)
 - SITE SELECTION (FLYBACK BOOSTER/DOWN RANGE LANDING)

- PROPULSION
 - PROPELLANT SELECTION
 - PROPELLANT CROSS FEED (OPTIMUM BOOSTER SIZE)

- CONFIGURATION/STRUCTURES
 - TPS (RSI, METALLIC, ETC.)
 - HOT/COLD STRUCTURE (ORBITER)
 - HEAT SINK/TPS BOOSTER
 - INTEGRAL/NONINTEGRAL TANKAGE

Figure 3

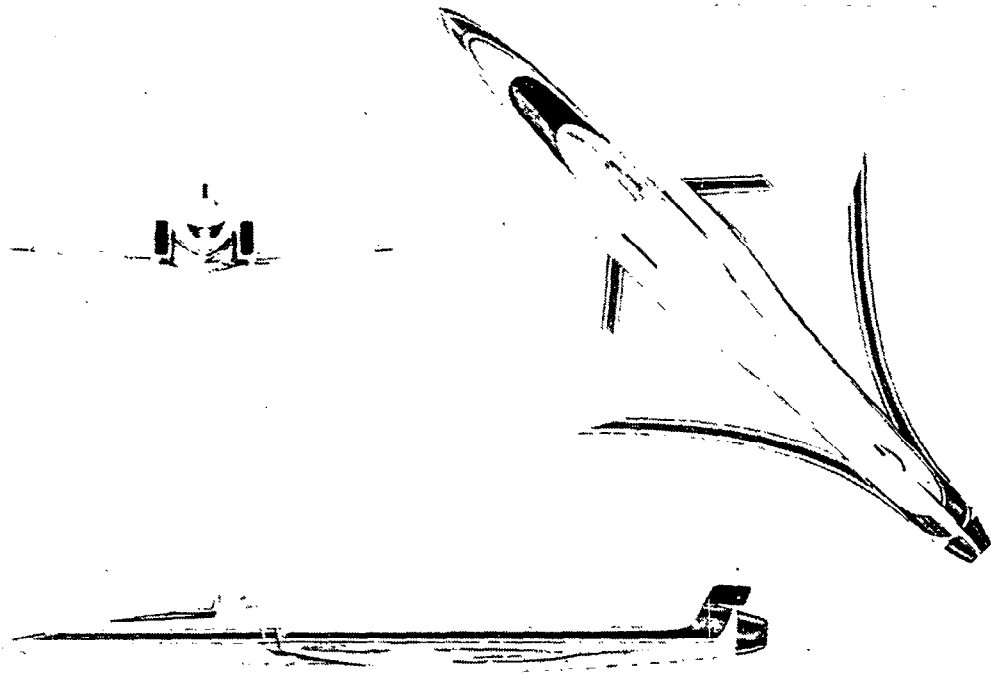
X-29A FORWARD-SWEPT-WING DEMONSTRATOR AIRPLANE

Douglas R. Frei
Grumman Aerospace Corporation
Bethpage, New York

Miniworkshop on Wind-Tunnel/Flight Correlation
November 19-20, 1981

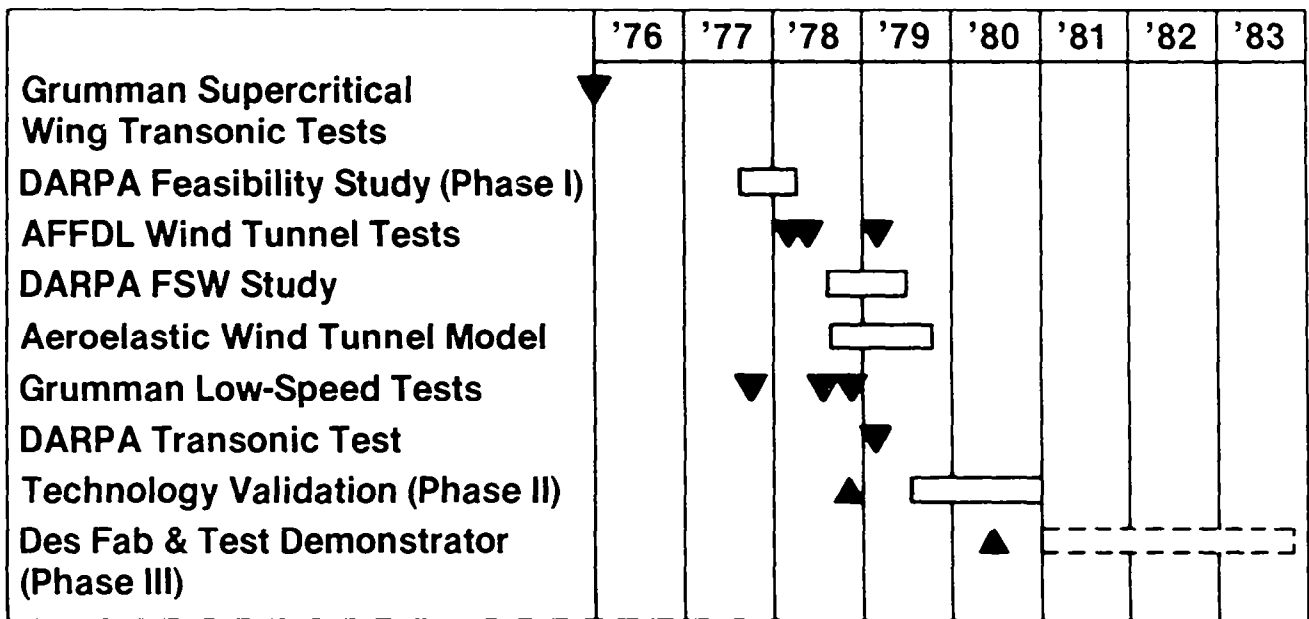
FORWARD-SWEPT-WING ADVANCED-TECHNOLOGY DEMONSTRATOR AIRPLANE

The Grumman Aerospace Corporation recently won the Defense Advanced Research Projects Agency (DARPA) sponsored competition to build a forward-swept-wing (FSW) technology demonstrator. The airplane has been designated the X-29A and is scheduled to fly in late 1983.



SUMMARY PROGRAM SCHEDULE

Grumman has been involved with the FSW concept since 1976. Grumman has conducted several feasibility studies and wind-tunnel tests that have developed confidence in the FSW design. Wind-tunnel tests have proven that conventional aft-swept-wing analytic tools are directly applicable to predict FSW characteristics.



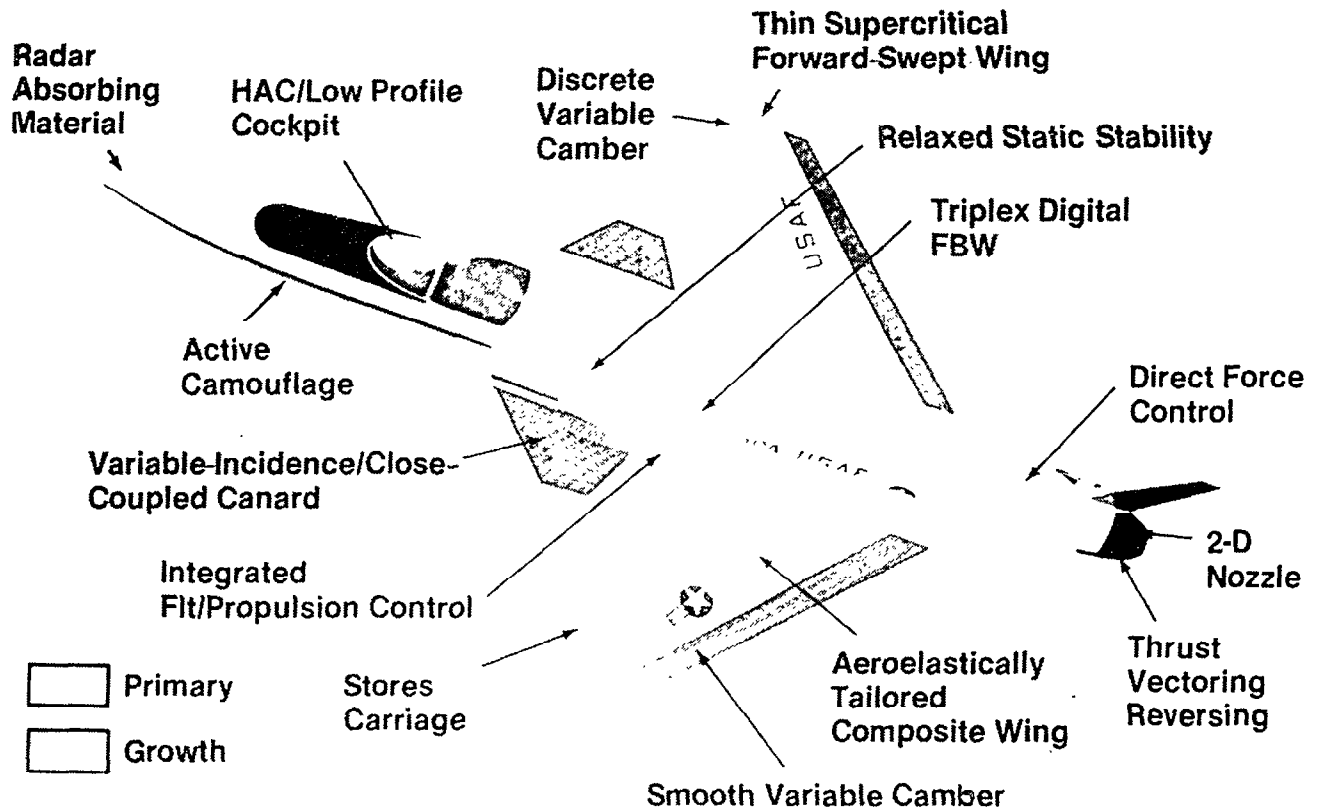
▲ Proposal

ADVANCED TECHNOLOGY DEMONSTRATOR

The X-29A is a technology demonstrator. The FSW is just one of the technologies. Others include the following:

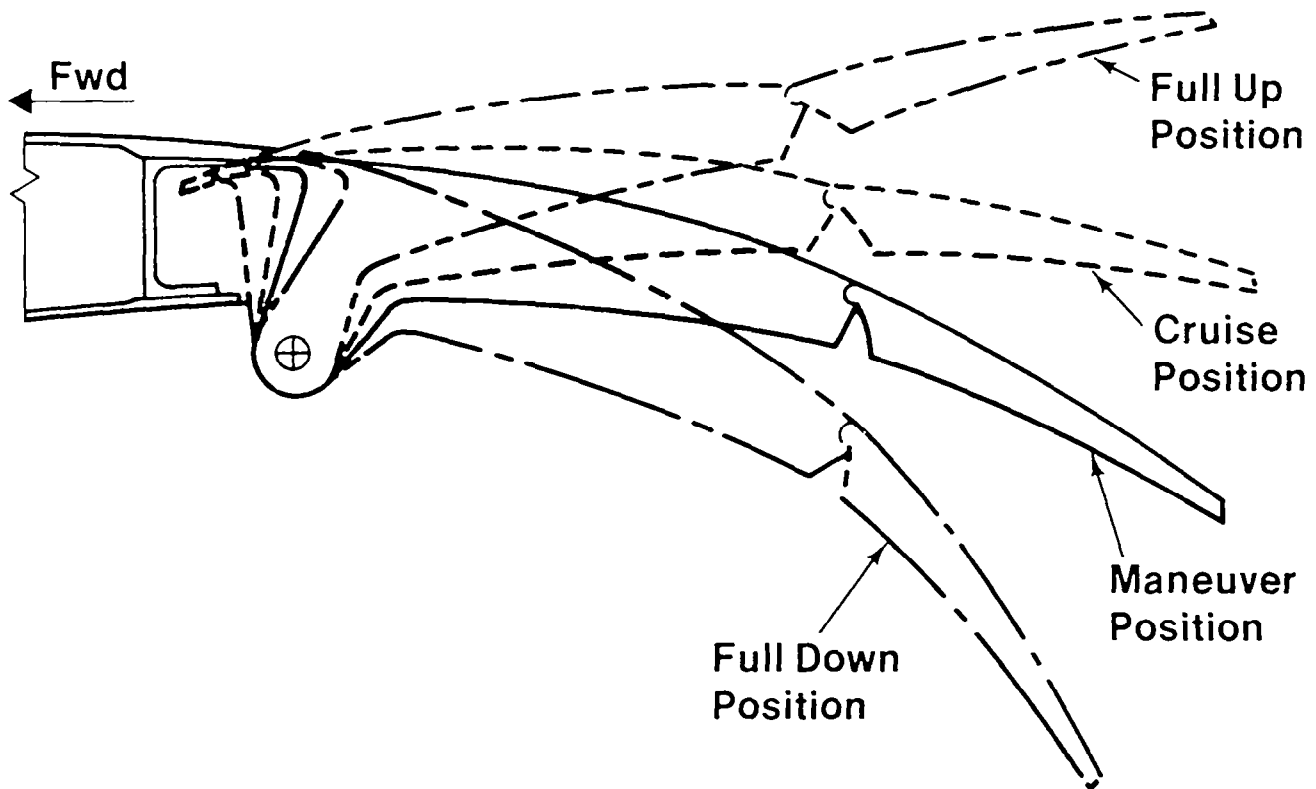
- o Discrete Variable Camber
- o Relaxed Static Stability
- o Triplex Digital Fly-By-Wire (FBW) Control System
- o Variable-Incidence/Close-Coupled Canard
- o Aeroelastically Tailored Composite Wing
- o Thin Supercritical Airfoil

The growth potential for additional technologies is also shown.



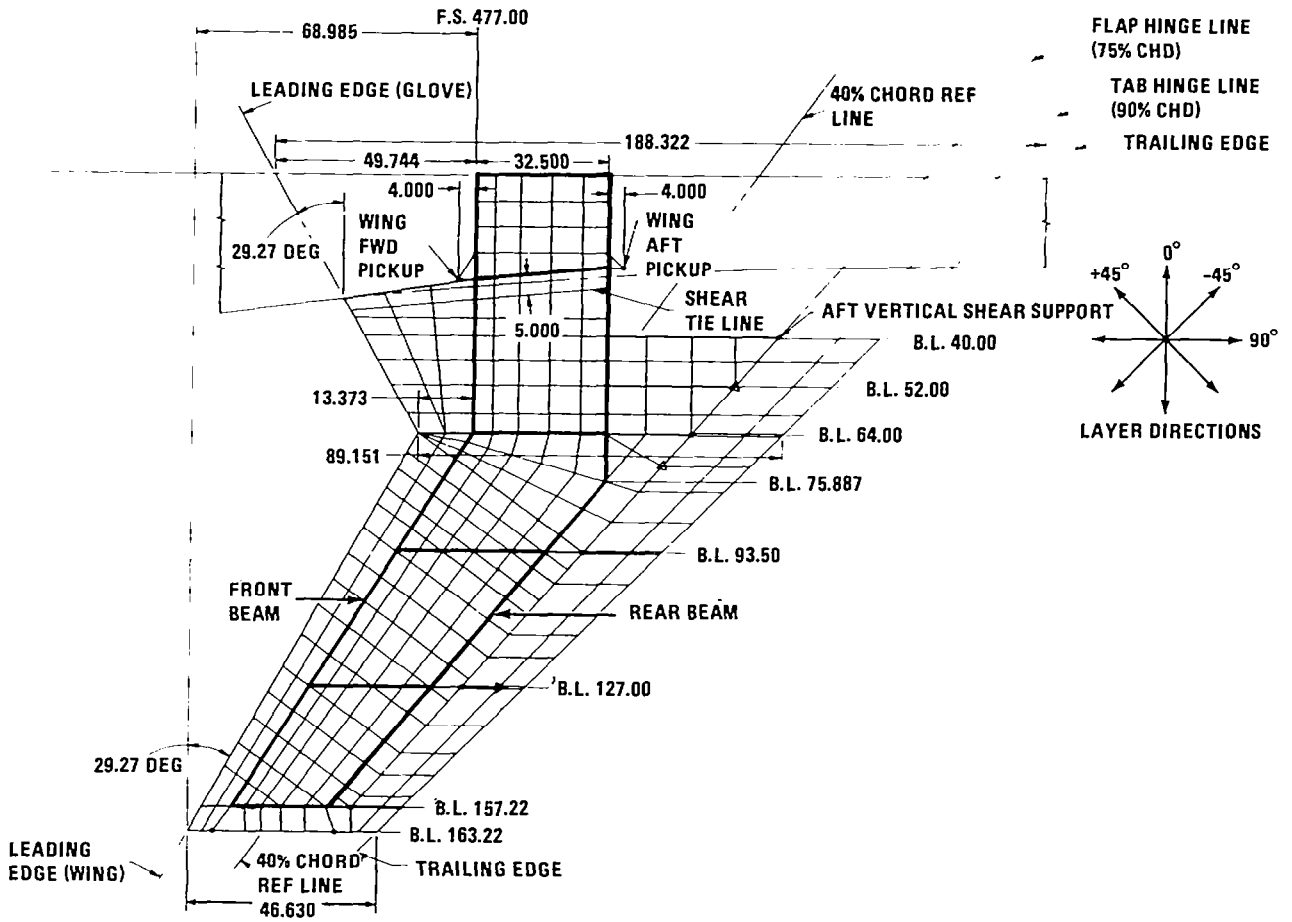
DISCRETE-VARIABLE-CAMBER SYSTEM

Discrete variable camber is obtained with a flap/lead-tab arrangement as shown. The smooth airfoil section, shown as the maneuver position, represents the designed airfoil section. At other flap positions the airfoil section does not remain smooth. Wind-tunnel tests have shown no subsonic drag penalties and low supersonic drag penalties for this type of system throughout the flap range.



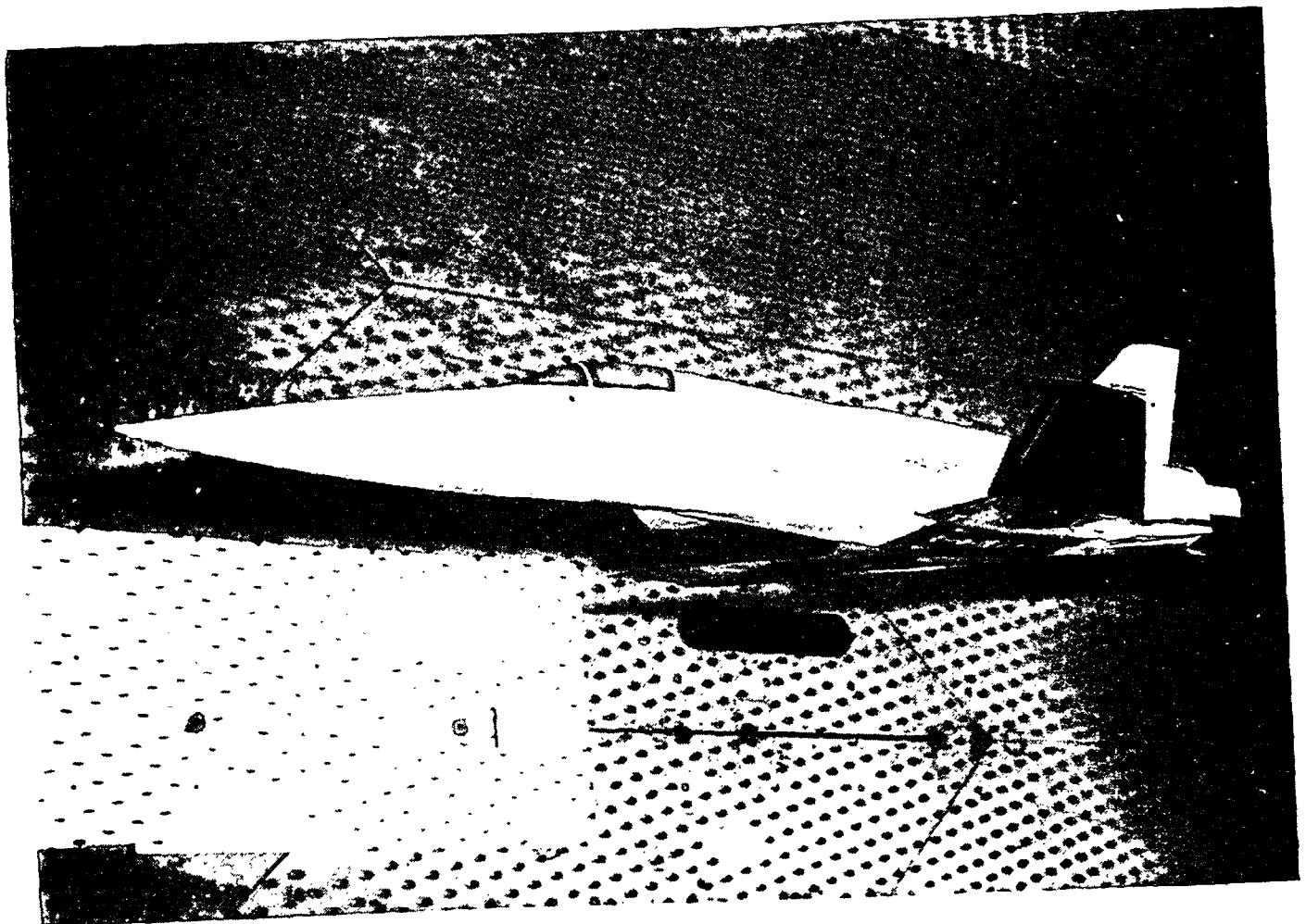
WING PLANFORM AND GEOMETRY OF STRUCTURAL GRID

The wing planform and wing substructure are shown. The front beam is at 0.15c, whereas the rear beam is at 0.62c. The wing covers are graphite-epoxy with 0°, ±45°, and 90° ply orientation.



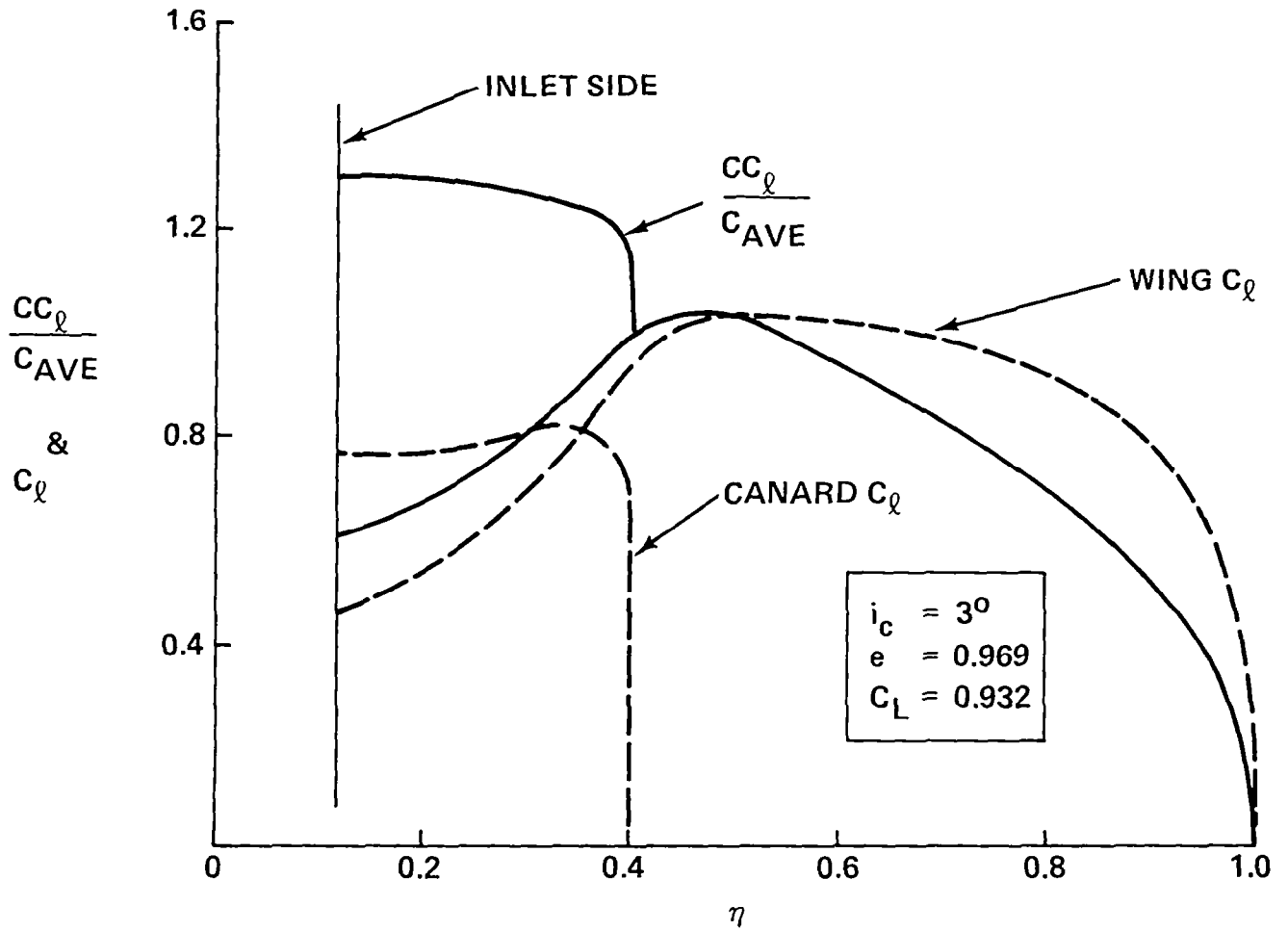
1/8-SCALE X-29A WIND-TUNNEL MODEL

The 1/8-scale aerodynamic wind-tunnel model is shown in AEDC 16 T. The total wind-tunnel test hours on the X-29A program will be 980.



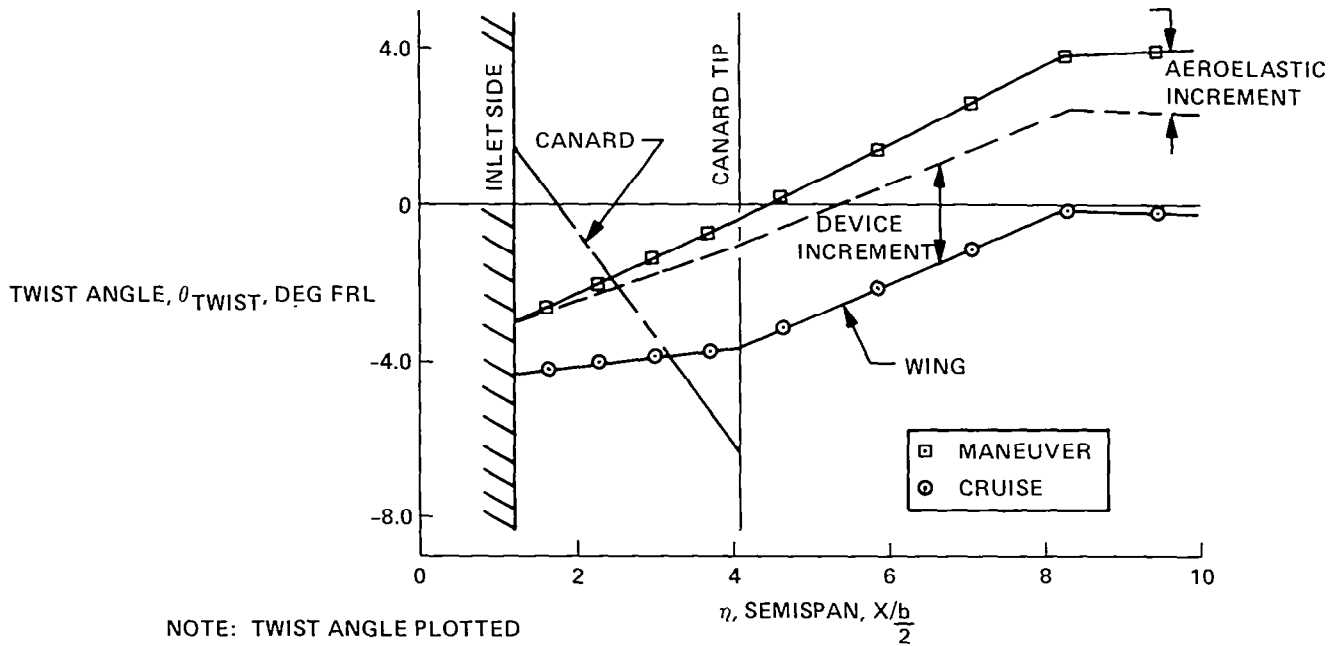
MANEUVER-DESIGN SPAN LOAD AT $M = 0.90$

The maneuver-design span load is achieved by designing for a close-coupled canard. The optimum span load is accomplished via wing-canard load sharing. The canard protects the wing root stall.

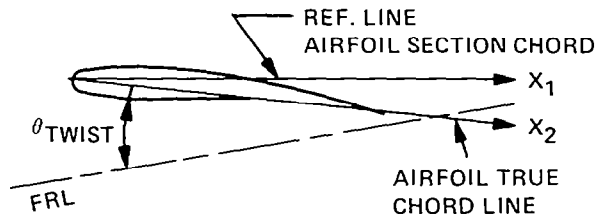


CANARD AND WING-TWIST DISTRIBUTION FOR THE 1/8-SCALE
FSW WIND-TUNNEL MODEL

The wing-twist change from cruise to maneuver is accomplished with variable camber (device increment) and aeroelastic tailoring. The FSW requires less twist for the maneuver design than for an equivalent aft-swept wing.

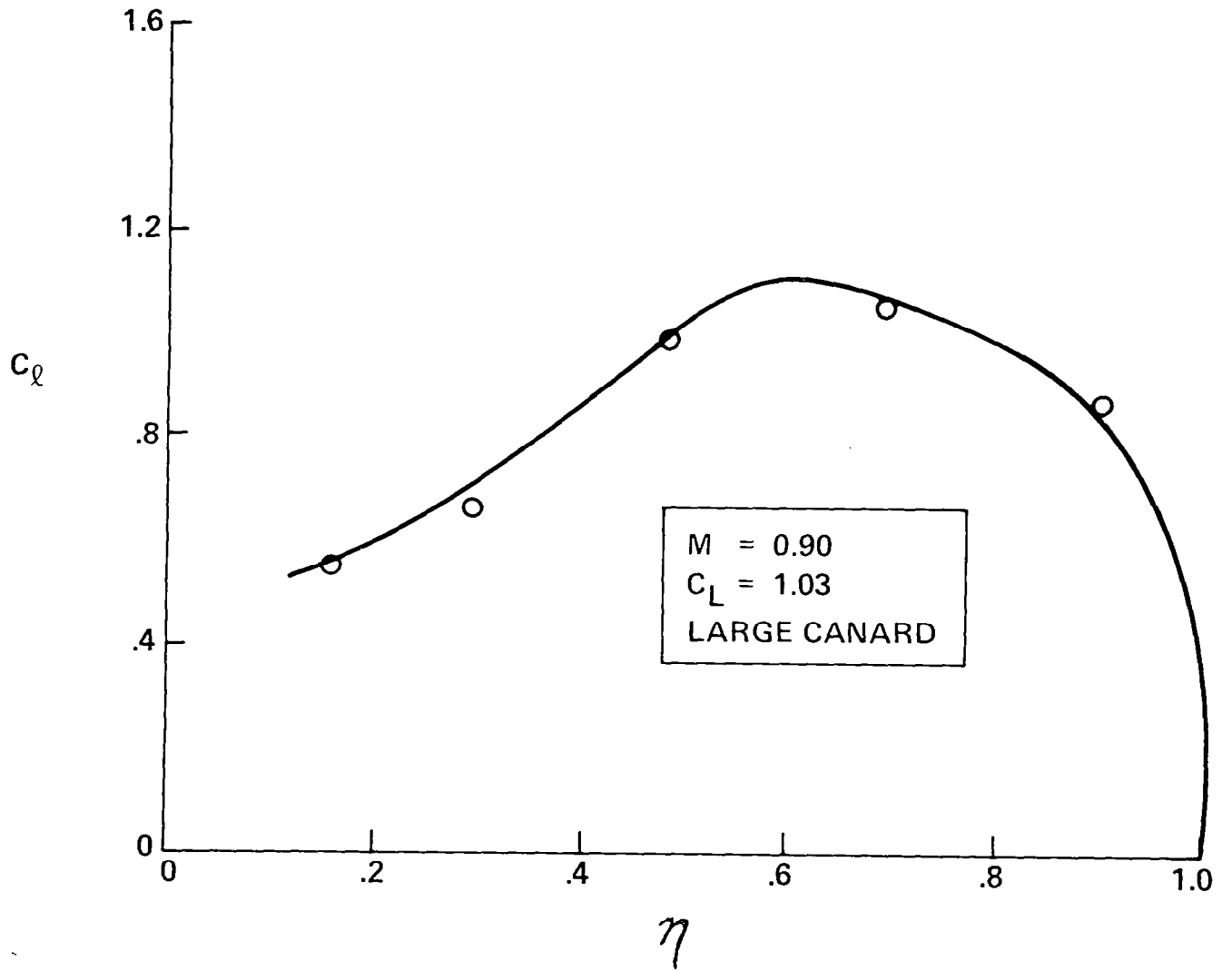


NOTE: TWIST ANGLE PLOTTED ABOVE REFERS TO ANGLE BETWEEN "AIRFOIL TRUE CHORDLINE" AND FUSELAGE REF. LINE AS SHOWN IN SKETCH AT RIGHT.



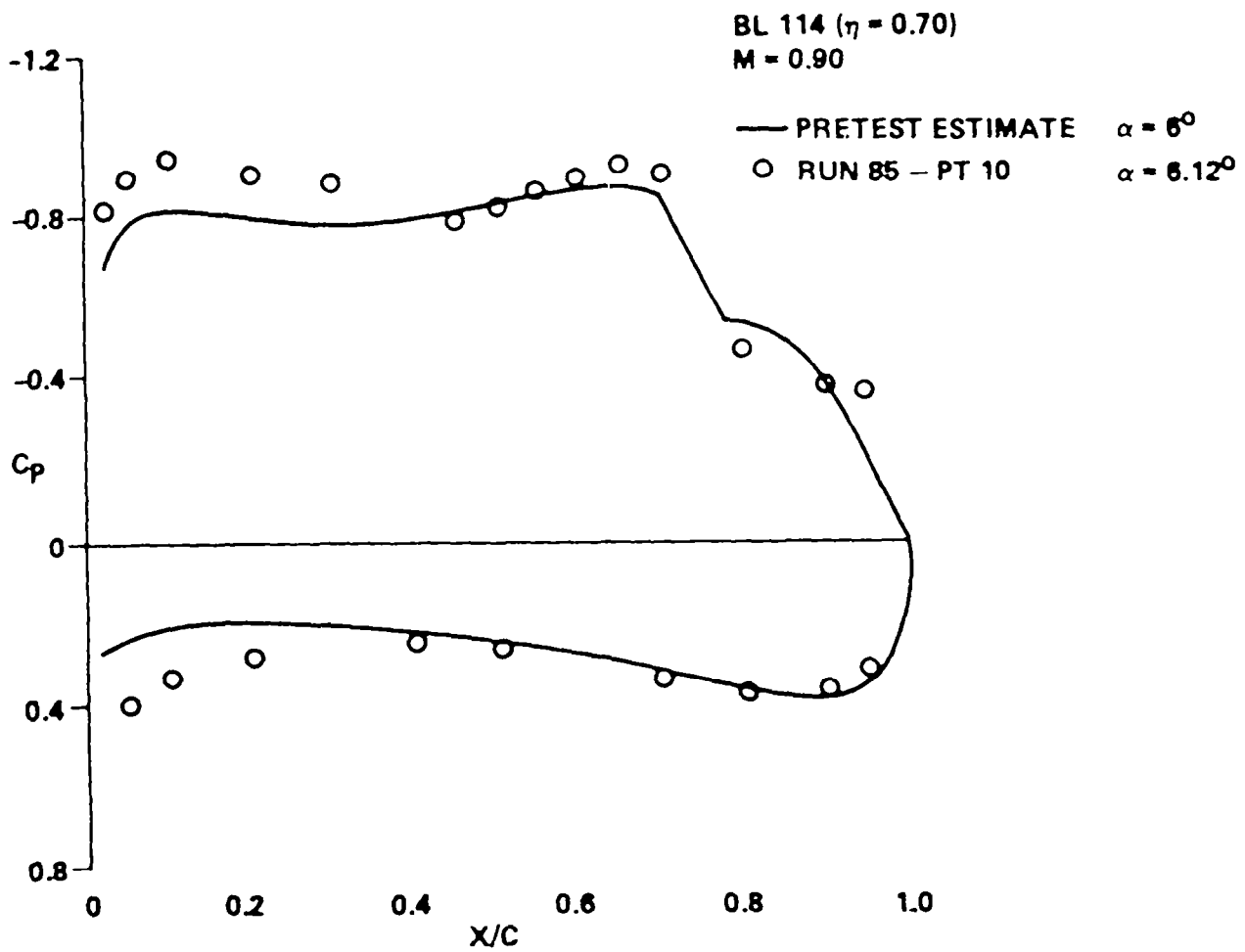
COMPARISON OF TEST DATA WITH ESTIMATE FOR MANEUVER WING

The design span load was achieved with the first wind-tunnel model entry. An estimate was made by using a subsonic lifting-surface code.



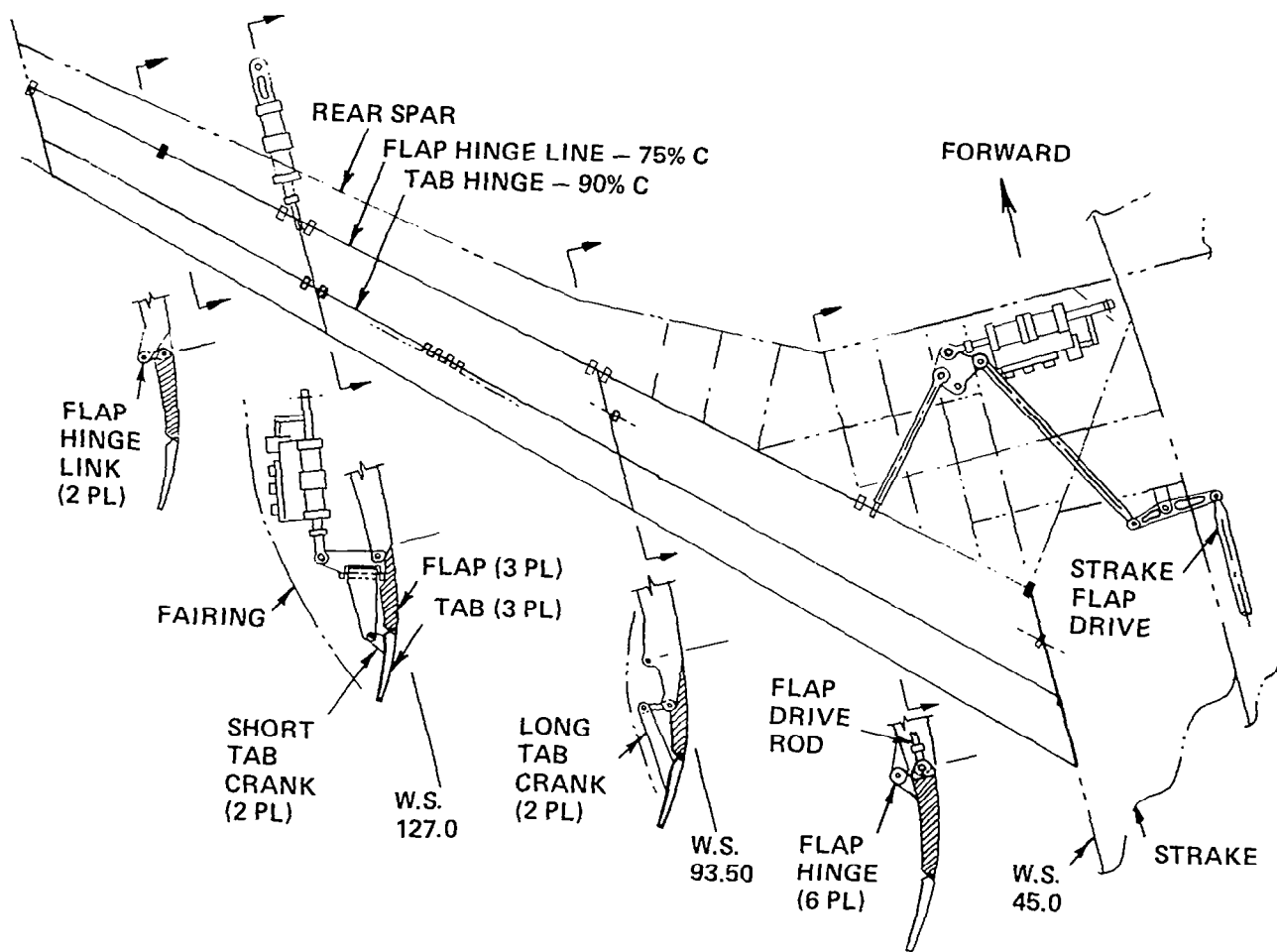
ESTIMATED AND MEASURED PRESSURE COEFFICIENTS

Excellent agreement with predicted and measured chordwise pressures was also obtained with the first wing design. Analytical tools work for FSW designs.



FLAPERON DRIVE CONFIGURATION

The discrete variable-camber flaperon drive system uses two F-16 rudder actuators. The outboard actuator is mounted externally because of composite cover requirements and wing-thickness constraints.



X-29A FOR NTF WIND-TUNNEL/FLIGHT CORRELATIONS

Gianky DaForno
Grumman Aerospace Corporation
Bethpage, New York

Miniworkshop on Wind-Tunnel/Flight Correlation
November 19-20, 1981

CONSIDERATIONS AND RECOMMENDATIONS
OF W.T./FLIGHT CORRELATION PANEL
(WORKSHOP DEC. 9-11, 1980)

- (1) BASIC TUNNEL CALIBRATION PRIOR TO R & D TESTS
- (2) ESTABLISH CONFIDENCE IN NTF/OTHER TUNNELS CORRELATION
- (3) AREAS OF CONCENTRATION
 - ⊙ WING CRUISE DRAG AND DRAG RISE
 - ⊙ WING SEPARATION AND STALL
 - ⊙ AFTERBODY AND BASE DRAG
 - ⊙ PROPULSION EFFECTS
 - ⊙ VORTEX FLOWS
 - ⊙ CAVITY FLOWS
 - ⊙ EXCRESCENCES
- (4) APPROACH TO VALIDATING SIMULATION OF FLIGHT ENVIRONMENT
 - ⊙ CORRELATION TEAM
 - ⊙ OPEN-ENDED, NON PROPRIETARY W.T./F.T. PROGRAM UTILIZING ADV. TECHNOLOGY (FIGHTER) CONFIGS.
 - ATTACHED - FLOW WINGS
 - 'VORTEX FLOW' WINGS
 - ⊙ DRAG CORRELATION ON WING PRESSURES AND WAKE PROFILES
 - ⊙ ACCOUNTABILITY

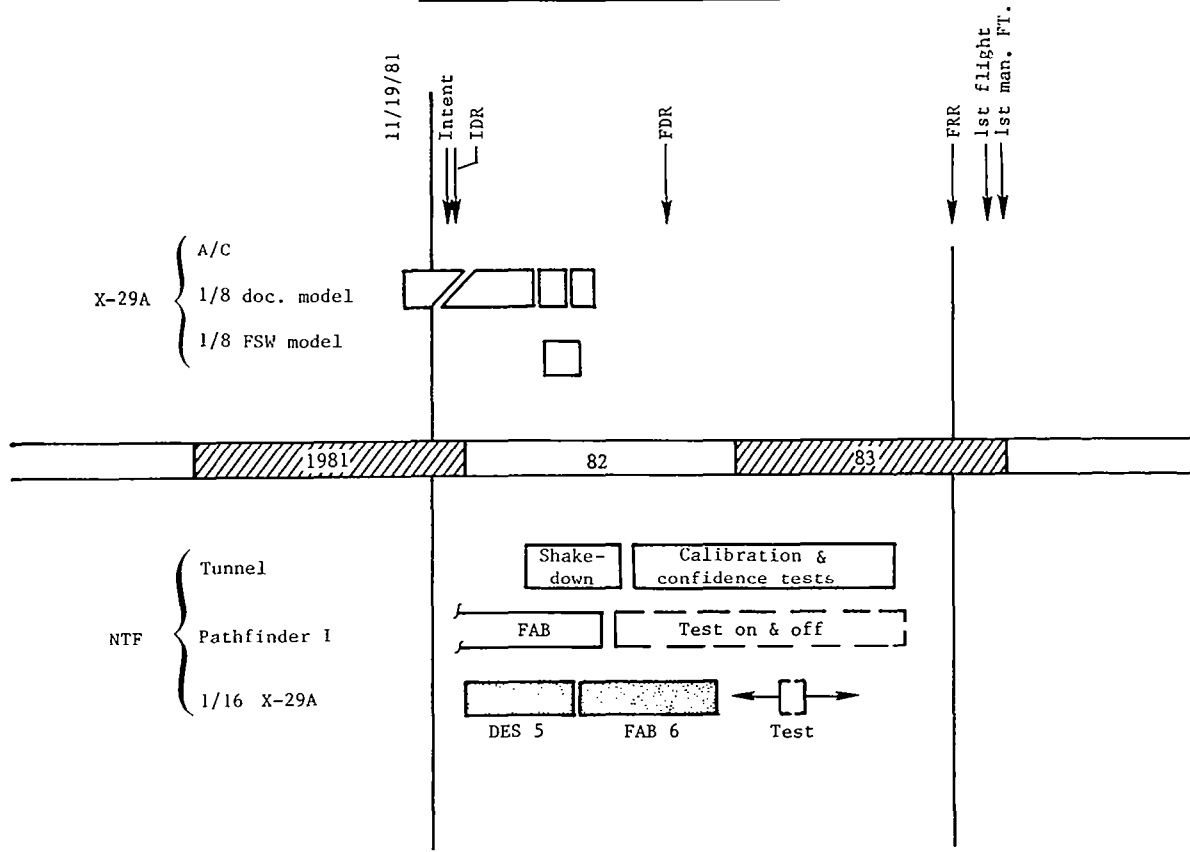
RECOMMENDATIONS OF 1976 CONFIG. AERODYNAMICS PANEL

- ⊙ PRECISE, CALIBRATED AIR DATA SYSTEM (M, q, P_{∞})
- ⊙ PRECISE α, β
- ⊙ STRUCTURAL DEFORMATION MEASUREMENTS (A/C, MODELS)

OTHER ISSUES

- ⊙ 4 ADDITIONAL AREAS OF COMPONENT CORRELATION THAT ARE SUSPECTED RE SENSITIVE
- ⊙ AIRPLANE SURFACE FINISH & LINE FIDELITY
- ⊙ STORES

WIND TUNNEL AND FLIGHT SCHEDULES



CONFIDENCE IN NTF/OTHER TUNNELS CORRELATION --
X29A W.T. MODELS AND DATA

(AS OF 11/17/81)

- o 1/8-SCALE DOCUMENTATION MODEL
 - MANEUVER, CRUISE, TOL CONFIGURATIONS
 - WING, CANARD, VTAIL ON SEPARATE BALANCES
 - 156 PRESSURE TAPS SAME LOCATIONS AS A/C
 - FLOW-THRU NACELLES

- o AMES 11' DOCUMENTATION TEST (1982)
 - 2800 RUNS, 320 TEST HOURS
 - M = 0.7 TO 1.2
 - BASELINE $Re = 4 \times 10^6 \text{ FT}^{-1}$, 250 RUNS AT $7 \times 10^6 \text{ FT}^{-1}$

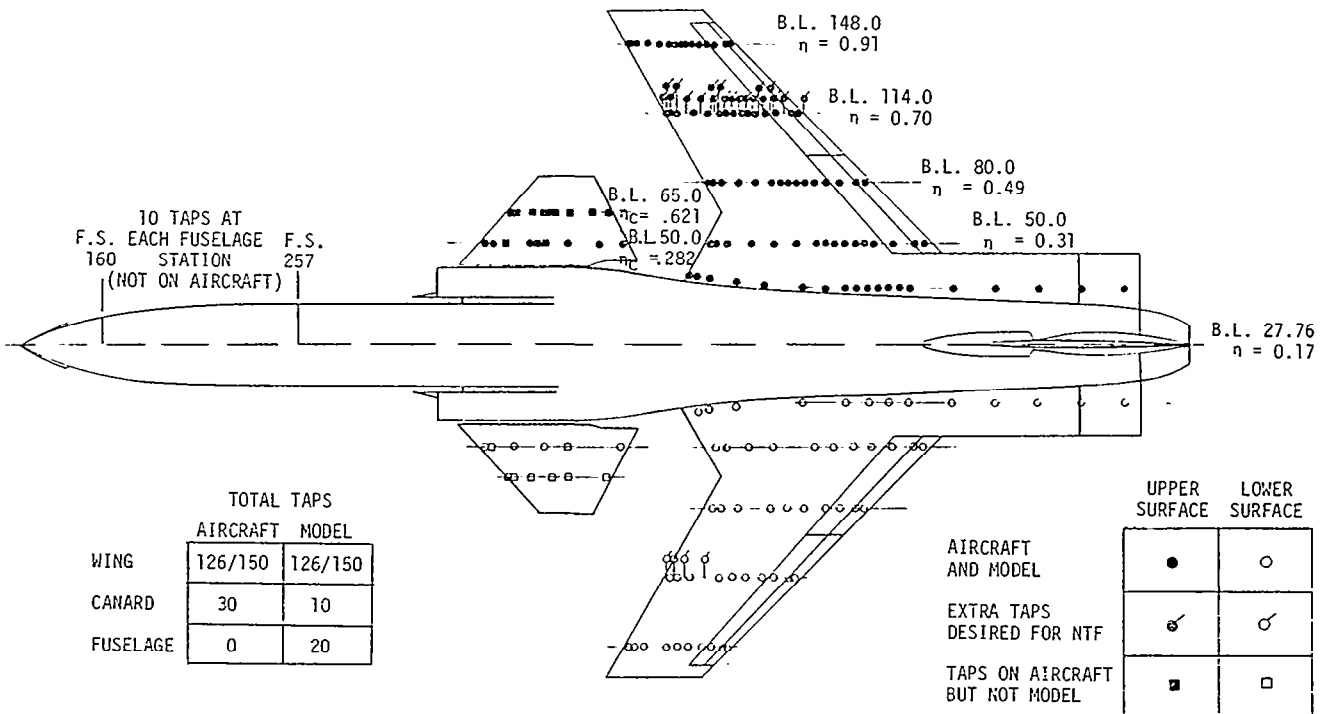
- o POTENTIAL FOR NTF AND AMES 12'

AREAS OF CONCENTRATION
 CLEARLY COVERED BY X-29A
 (11/17/81 MODELS AND INSTRUMENTATION)

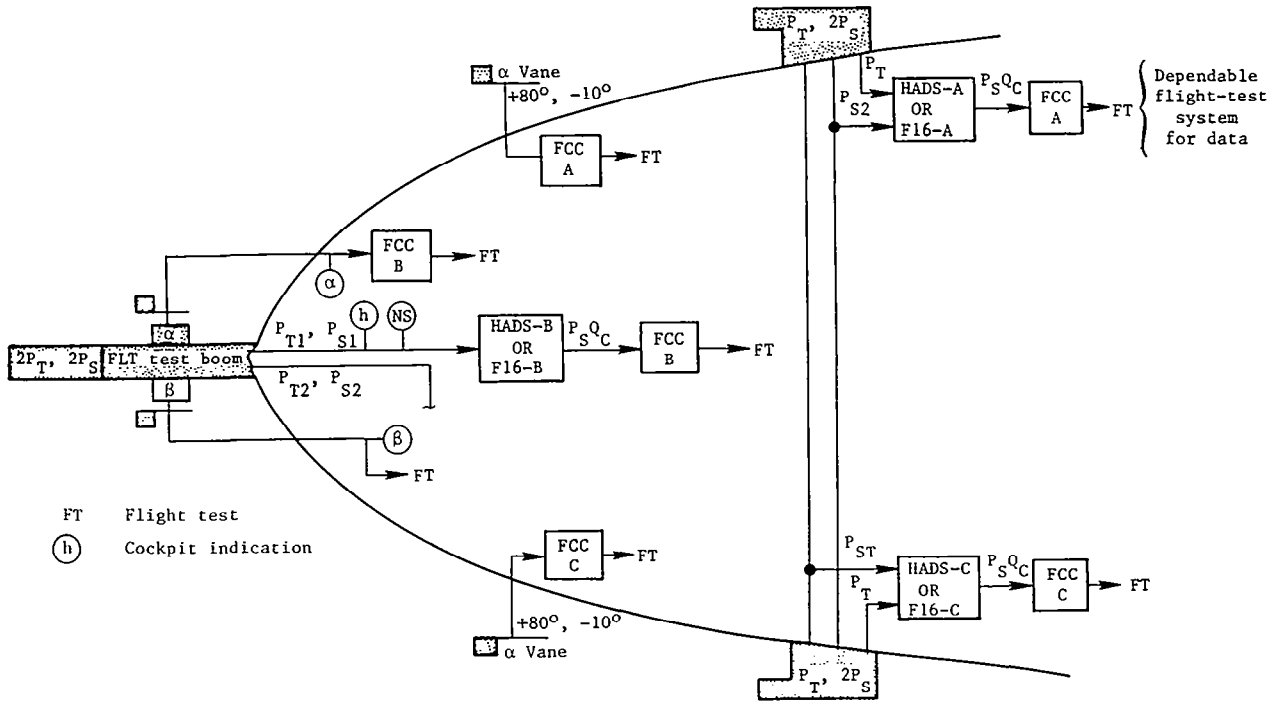
- WING CRUISE DRAG AND DRAG RISE YES
- WING SEPARATION AND STALL YES
- AFTERBODY AND BASE DRAG
- PROPULSION EFFECTS
- VORTEX FLOWS
 - FOREBODY VORTEX SHEDDING YES
 - L.E. VORTEX WINGS NO
 - STRUCTURAL LOADS YES
- CAVITY FLOWS
 - LANDING GEAR WELL
 - BAYS NO

AND MANEUVER WING!

PRESSURE TAP LOCATIONS ON X-29A AIRCRAFT
 AND/OR 1/8-SCALE WIND-TUNNEL MODEL
 (AS OF 11/17/81)



DELIVERY CONFIGURATION OF AIR DATA SYSTEM FOR FORWARD-SWEPT-WING AIRCRAFT



ACCURACY OF AIR DATA AND ATTITUDE DATA

QUANTITY	FCS REQ.	BOOM - ALONE
M_T	≈ 0.025	± 0.0025 (TYP 30K FT)
q	-	$\pm 0.9\%$
p_∞	-	$\pm 0.3\%$
α_T	$\pm 0.5^\circ$	(TARGET) $\pm 0.1^\circ$ ($\approx -10^\circ$ TO $+20^\circ$) TYPICAL $\pm 0.2^\circ$ ($\pm 90^\circ$)
β_T	-	(TARGET) $\pm 0.1^\circ$ ($\approx -25^\circ$ TO $+25^\circ$) TYPICAL $\pm 0.2^\circ$ ($\pm 90^\circ$)

X-29A STRUCTURAL DEFORMATION MEASUREMENTS

- o GRUMMAN FDMS
- o VALIDATED ON HiMAT AND (CURRENT) AFTI-111
- o ACCURACY $\pm 0.25\%$
- o UP TO 200 SAMPLES/SEC

REFERENCE: DeANGELIS, V.M. (NASA DRYDEN),
AIAA-81-2450 (NOV. 1981)

ADDITIONAL AREAS FOR COMPONENT CORRELATION THAT ARE SUSPECTED RE SENSITIVE

- DISCRETE VARIABLE CAMBER
- CANARD STALL AND ITS EFFECT ON THE WING
- FSW ROOT/AFT STRAKE/STRAKE-FLAP
 - ROOT PRESSURE DISTRIBUTION ($M \sim$ TRANSONIC)
 - C_M (LOW SPEED, HIGH α)
 - STRAKE-FLAP EFFECTIVENESS (LOW SPEED, ALL α)
- TAB

SURFACE FINISH AND LINE FIDELITY

X-29A COMPOSITE WING

SCALED TO
1/16 NTF MODEL

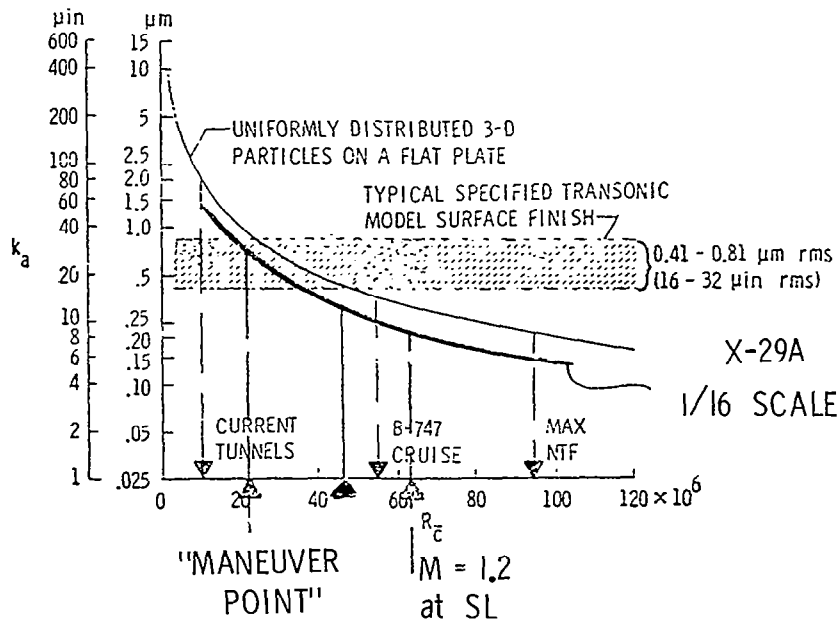
o TOOL SURFACE ON AIR-PASSAGE SIDE --
FINAL RMS $\pm 15-30 \mu\text{N}$. TYPE NUMBERS \rightarrow TYPICAL FINISH
FAIRLY GOOD
AT ALL $Re_{M.A.C.}$

o SURFACE CONTOUR (EXCLUDING LE):
POSSIBLY $\pm 0.030 - 0.090$ INCHES \rightarrow $\pm 2-6$ MILS

o LE: NO INFO

{ TYPICAL METAL: MAC ± 14 MILS, \perp TO LE } \rightarrow $\pm 0.3 \rightarrow 0.7$ MILS
TIP ± 6 MILS (\perp TO LE)

SURFACE FINISH FOR 1/16-SCALE MODEL



Admissable roughness (k_a) for typical NTF-size models.

$c = 0.2$ m (0.65 ft).

APPLICATIONS OF COMPUTATIONAL FLUID DYNAMICS (CFD)
IN TRANSONIC WIND-TUNNEL/FLIGHT-TEST CORRELATION

Earl M. Murman
Massachusetts Institute of Technology
Cambridge, Massachusetts

Miniworkshop on Wind-Tunnel/Flight Correlation
November 19-20, 1981

PURPOSE OF TALK

- To stimulate thinking and discussion on "how CFD can be used to help in wind-tunnel/flight-test correlation in the transonic regime."

OUTLINE OF TALK

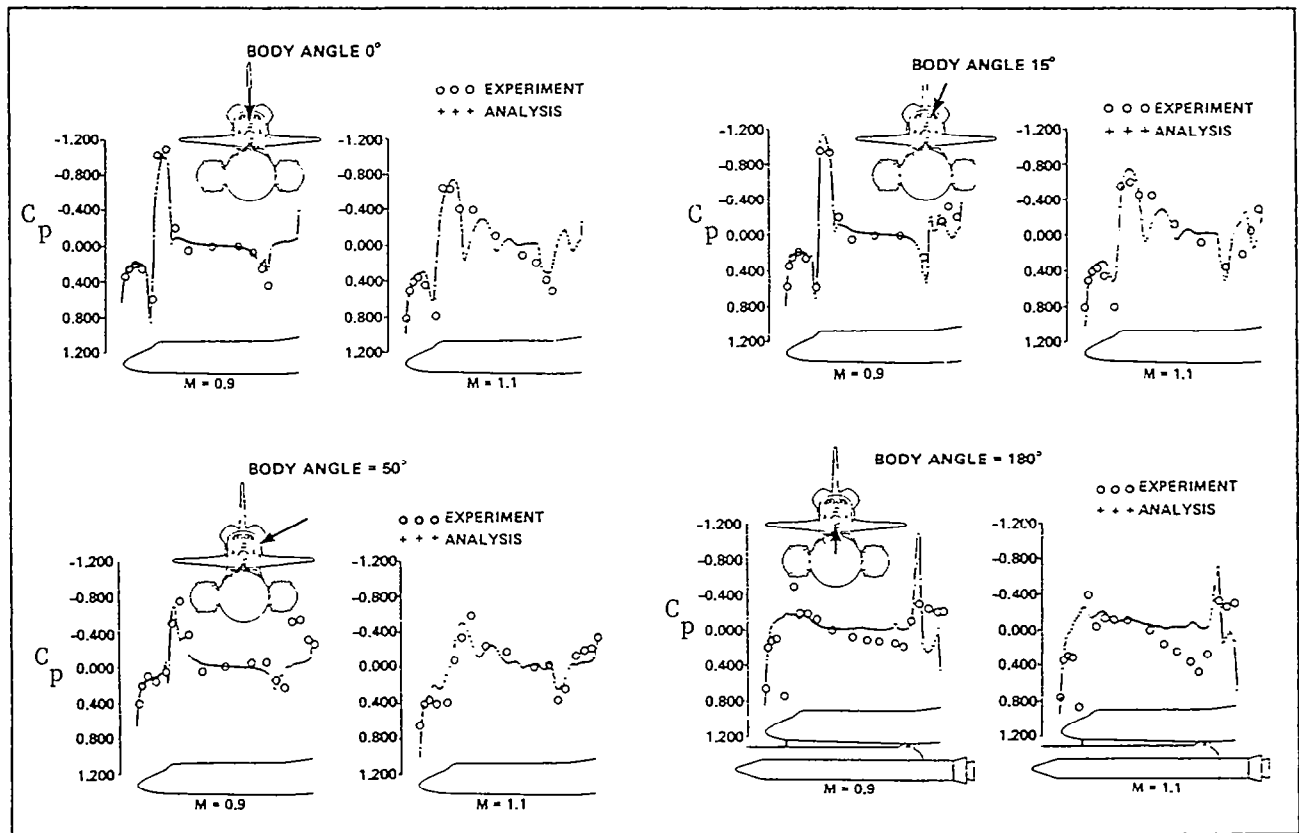
- Status of CFD codes for transonic aircraft in free air
- Status of methods for simulating transonic wind-tunnel effects
- Comments and suggestions

CFD CODES FOR TRANSONIC AIRCRAFT IN FREE AIR

	WING	WING/BODY	WING/BODY PYLON/NACELLE	WING/BODY PYLON/NACELLE PLUS OTHER
Transonic Small Perturbation (TSP)	1972 (1)	1975 (2)	1980 (3)	1980 (4)
Transonic Full Potential (TFP)	1974 (5)	1977 (6)	1981 (7)	
Euler	1981 (8)	1981 (8)		
TSP + 3D Viscous	1978 (9)	1978* (9)		
TFP + 3D Viscous	1979 (10)	1981* (11)		
TSP - Unsteady	1980 (12)			
Coupled TFP-Static Aeroelastic	1982 (13)			

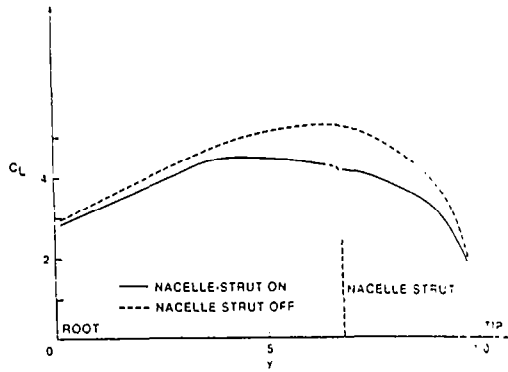
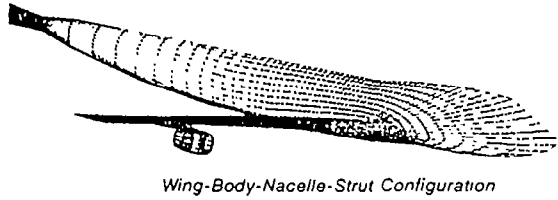
*Viscous calculation for wing only

Methods for computing 3D transonic flow for aircraft configurations have been under development for 10 years. Varying degrees of complexity may now be modeled. The following figures illustrate the most recent developments. Numbers in parentheses refer to references.

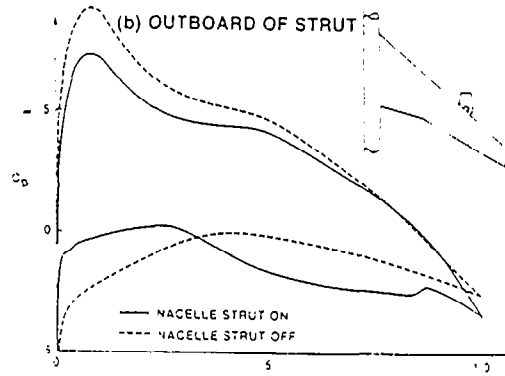
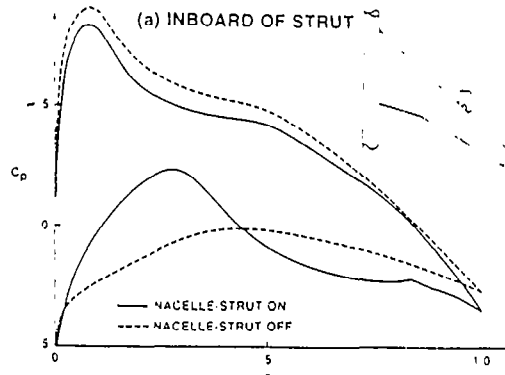


Space Shuttle Orbiter Pressure Distribution Correlation

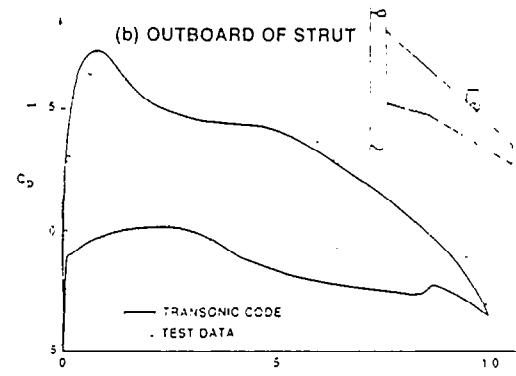
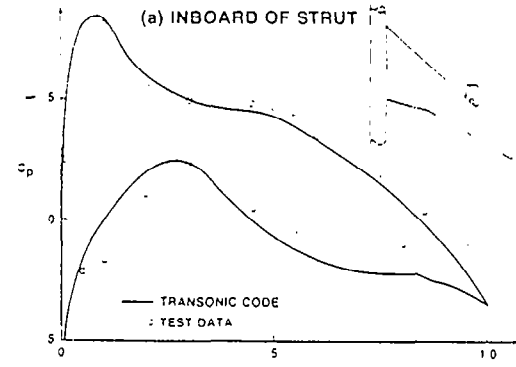
Very realistic geometries have been computed by Boppe and Aidala (4) using TSP methods with embedded meshes. This space shuttle launch configuration is the most complicated case. Comparisons with wind-tunnel data indicate that many of the complex inviscid-flow phenomena are being modeled.



Comparisons of Calculated Section Lift Coefficient, C_L , for a Transport configuration at $M_\infty = 0.80$, $\alpha = 2^\circ$.

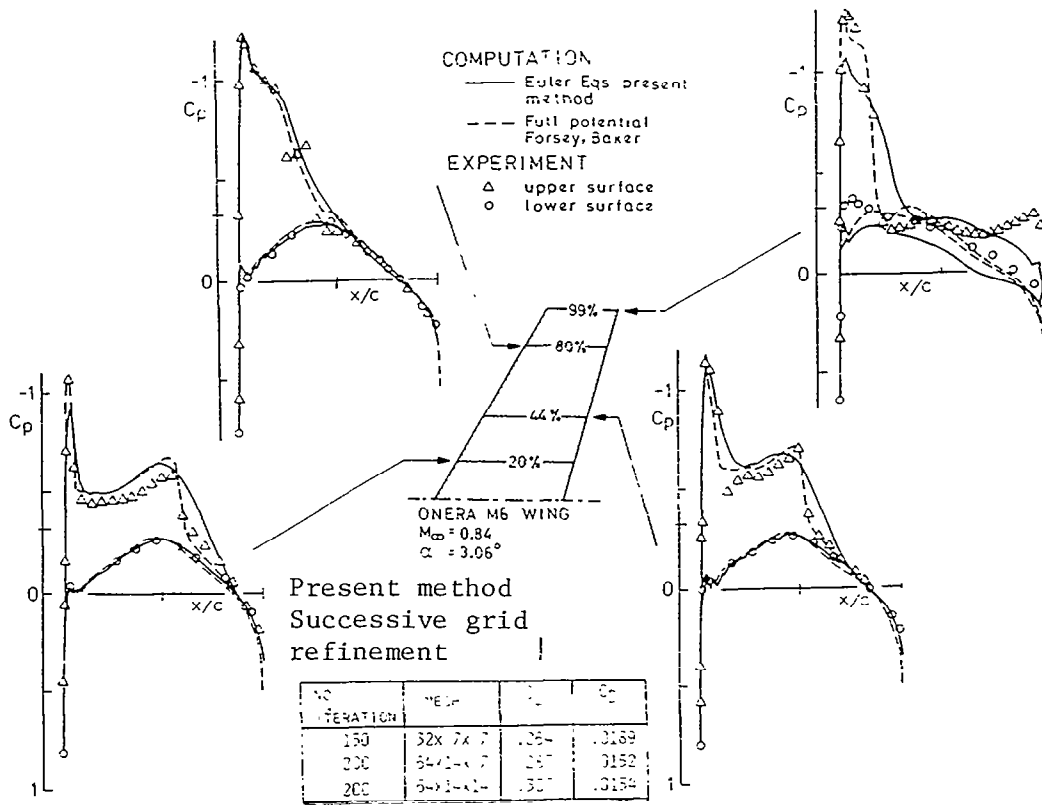


Comparisons of Calculated Wing Surface Pressures for a Transport Configuration at $M_\infty = 0.80$, $\alpha = 2^\circ$.



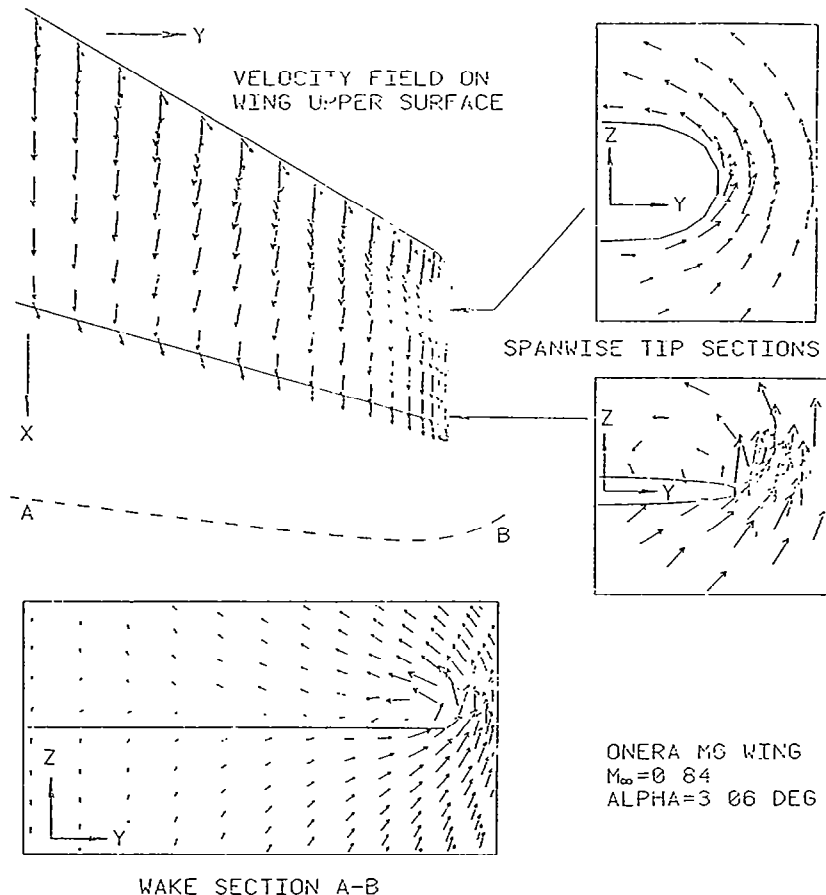
Test - Theory Comparisons of Wing Surface Pressures for a Transport configuration at $M_\infty = 0.80$, $\alpha = 2^\circ$.

The transonic full potential equation method has recently been extended by Yu (7) to model the effect of a pylon, nacelle and exhaust jet on the wing-body flow. Results shown for a transport configuration indicate the significant effects on the wing loading. Comparisons with wind-tunnel data are reasonably good.

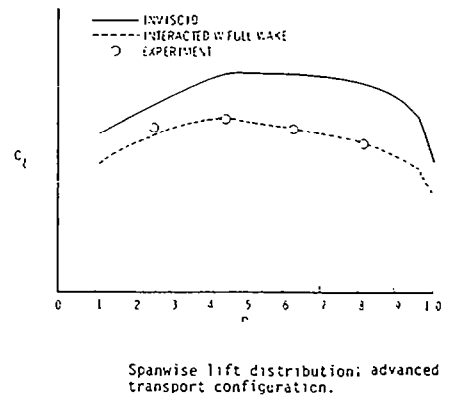
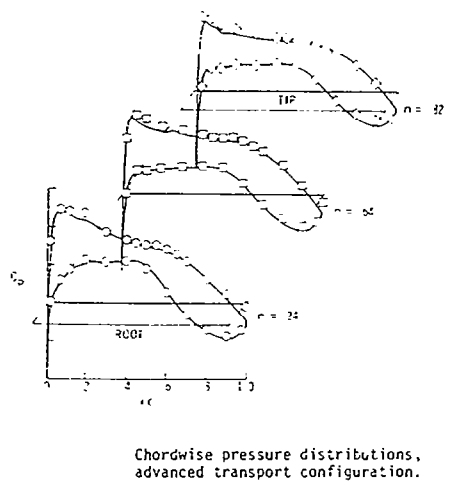
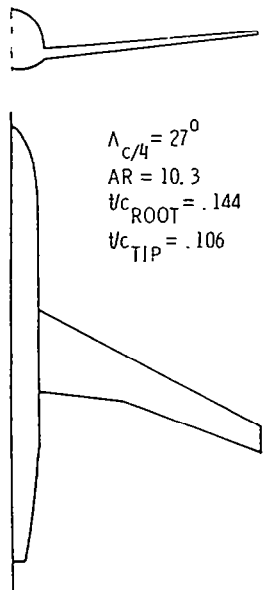


Comparison of computed and measured pressure coefficients c_p on ONERA M6 wing. $M_\infty = 0.84$ $\alpha = 3.06^\circ$.

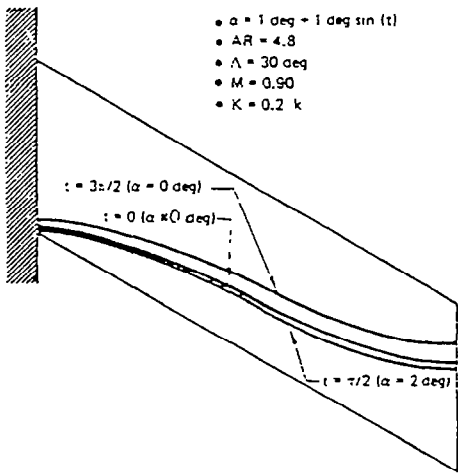
The solution of the Euler equations for wing and wing-body geometries has been presented by Rizzi and Ericksson (8). Practical computing times are achieved by using an efficient distribution of mesh points. Comparisons with potential calculations and tunnel data are favorable.



More refined calculations of the Euler equations reported subsequently by Eriksson and Rizzi (14) show the roll-up of the tip vortex. This non-linear flow phenomena cannot yet be modeled by the potential calculations.

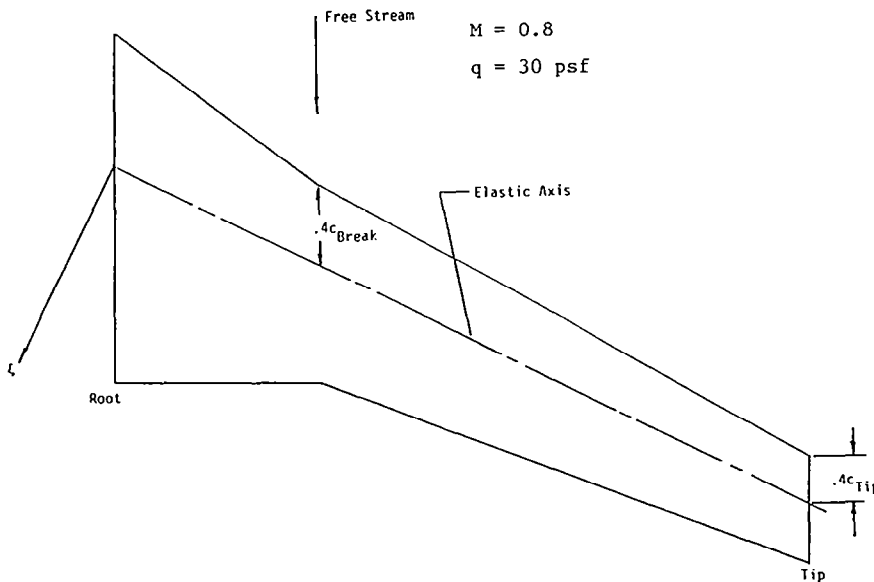


Three-dimensional integral boundary-layer calculations reported by Street (11) compare remarkably well with tunnel data. Note the large predicted change in lift distribution. The boundary layer on the fuselage is not treated. Additional calculations are reported for a flow with a shock wave but are not reproduced here.

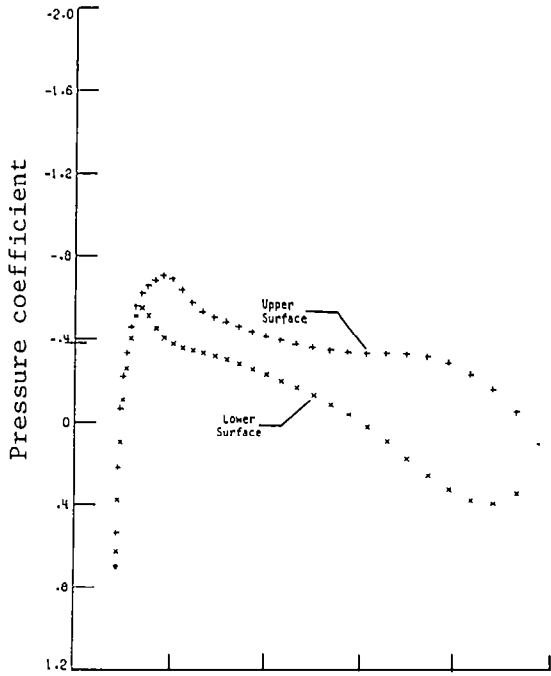


Three-dimensional unsteady transonic flow analysis using a TSP method has been reported by Borland, Rizzetta, and Yoshihara (12). Recent developments have included the coupling of the CFD code to structures model to predict flutter. Only simple wing planforms have been analyzed to date.

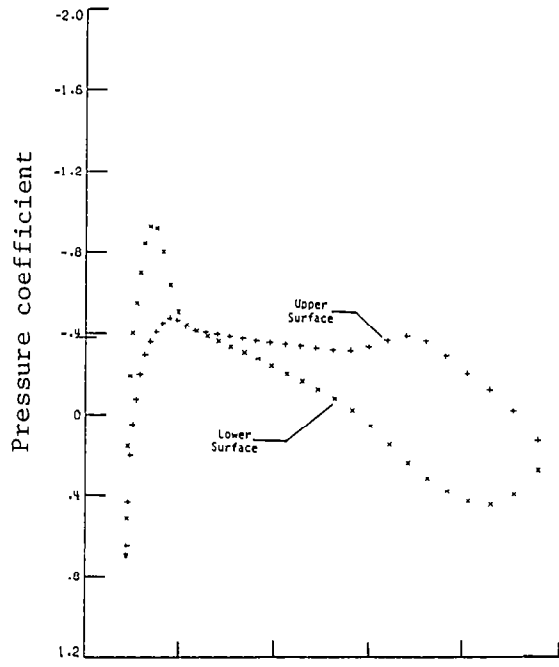
Predicted Shock Location for Unsteady Flow about a Swept Wing Oscillating in Pitch



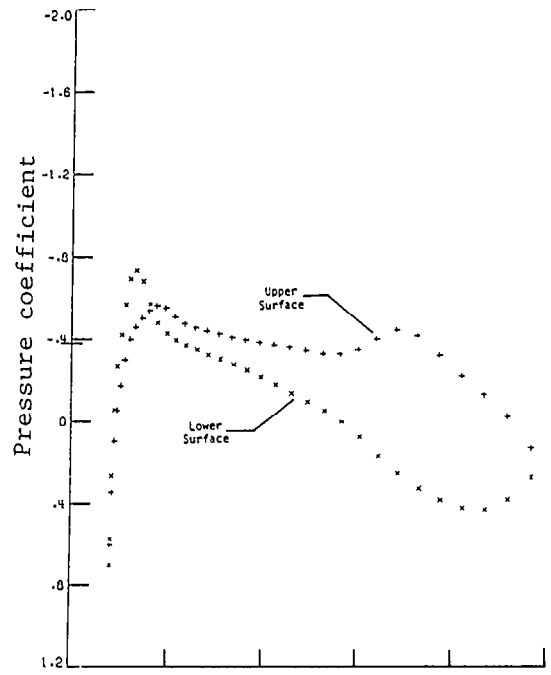
The coupled static aeroelastic and flow field effects have been modeled by Whitlow and Bennett (13). A TFP code is coupled to a finite element structures model. A swept wing configuration shown here has been studied. Results in the next figure show 3 cases. (1) rigid wing (no aeroelastic effects); (2) flexible wing with fixed root; and (3) flexible wing with angle of attack adjusted to match rigid wing lift. Note the effects of aeroelastic distortion on the tip section pressure and lift distributions.



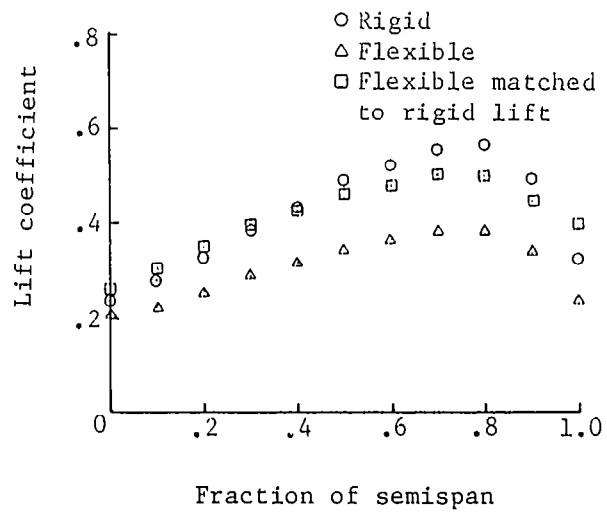
Pressure coefficient distribution at the tip of a rigid wing with a fixed root.

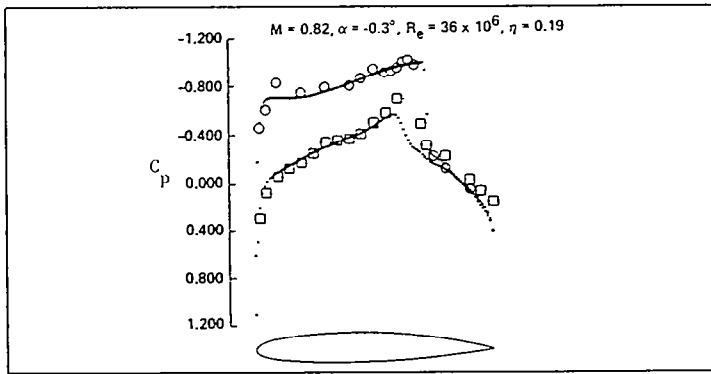


Pressure coefficient distribution at the tip of a flexible wing with a fixed root.



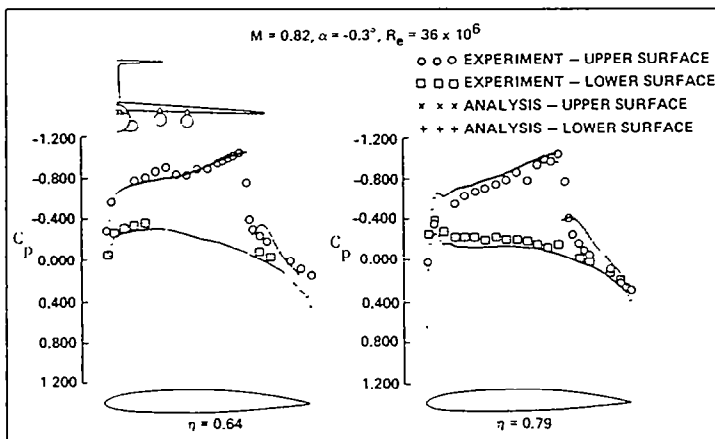
Pressure coefficient distribution at the tip of a flexible wing with total lift chosen to match the lift of a rigid wing with a fixed root.





C-141 Wing-Body Juncture Pressure Distribution Correlation

Only one published result comparing calculated results with flight-test data is available. Boppe and Aidala (4) present a TSP calculation for the C-141. Results are very encouraging and further comparisons are needed to determine the range of validity and the limitations of the CFD codes.

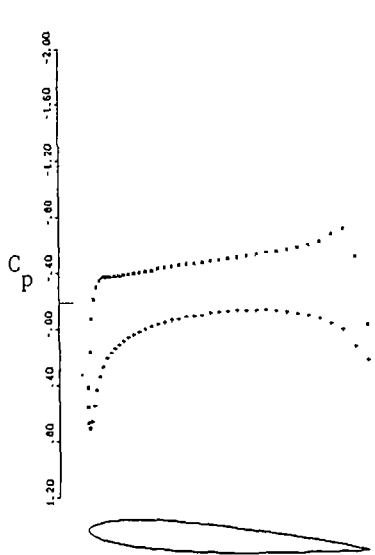


C-141 Wing Pressure Distribution Correlation

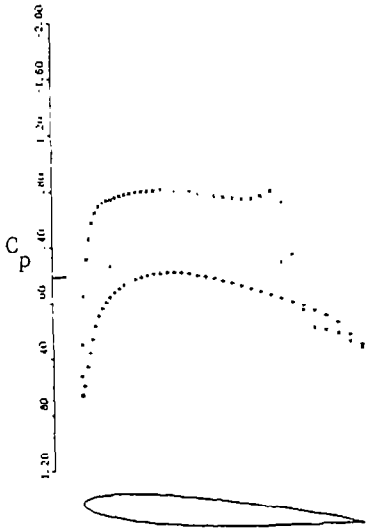
CFD CODES FOR SIMULATING TRANSONIC WIND-TUNNEL EFFECTS FOR THREE-DIMENSIONAL MODELS

- WALL EFFECTS - TSP - Rectangular wing - 1975 (15)
TFP - Swept wing - 1980 (16)
TFP - Wing/Body - 1981 (Jou)
- WALL CORRECTIONS - TSP/TFP - Wing - 1982 (17)
- FREE-STREAM
NONUNIFORMITIES - Euler - Tunnel empty - 1981 (18)
- STING EFFECTS - TSP - Body of revolution - 1972 (19)

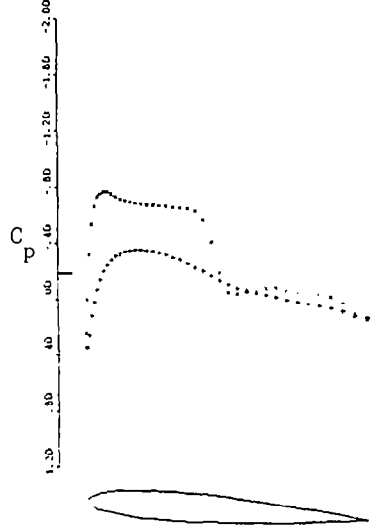
A variety of wind-tunnel effects can be simulated by using codes which have been developed recently or are under development. The following figures illustrate these capabilities.



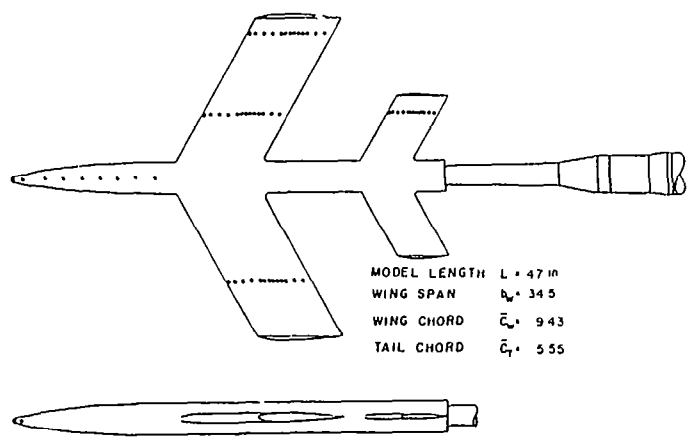
AEDC MODEL WING-BODY-TUN-70X60 FREE JET MACH = .9
MACH 0.900 ALPHA 4.000
Z 1.68 CL 0.4817 CO 0.1100



AEDC MODEL WING-BODY-TUN-70X60 FREE JET MACH = .9
MACH 0.900 ALPHA 4.000
Z 7.84 CL 0.4842 CO 0.0732

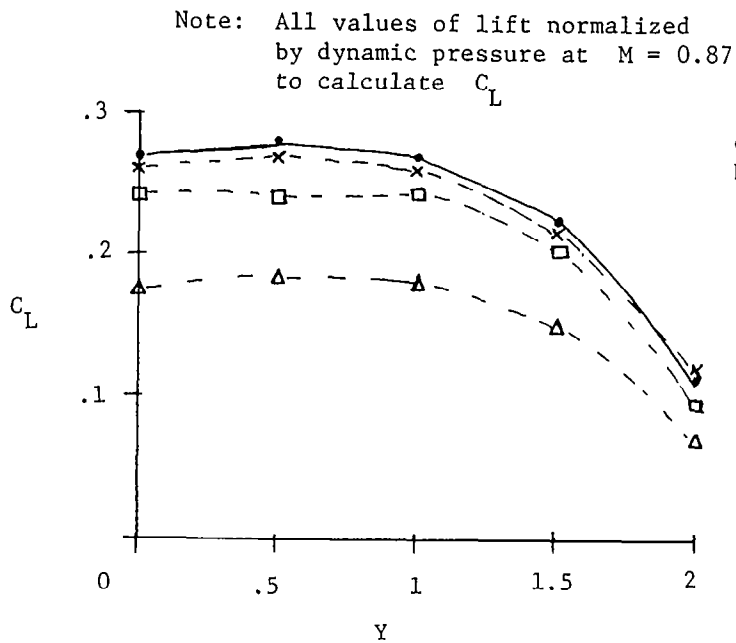


AEDC MODEL WING-BODY-TUN-70X60 FREE JET MACH = .9
MACH 0.900 ALPHA 4.000
Z 16.80 CL 0.2068 CO 0.0053

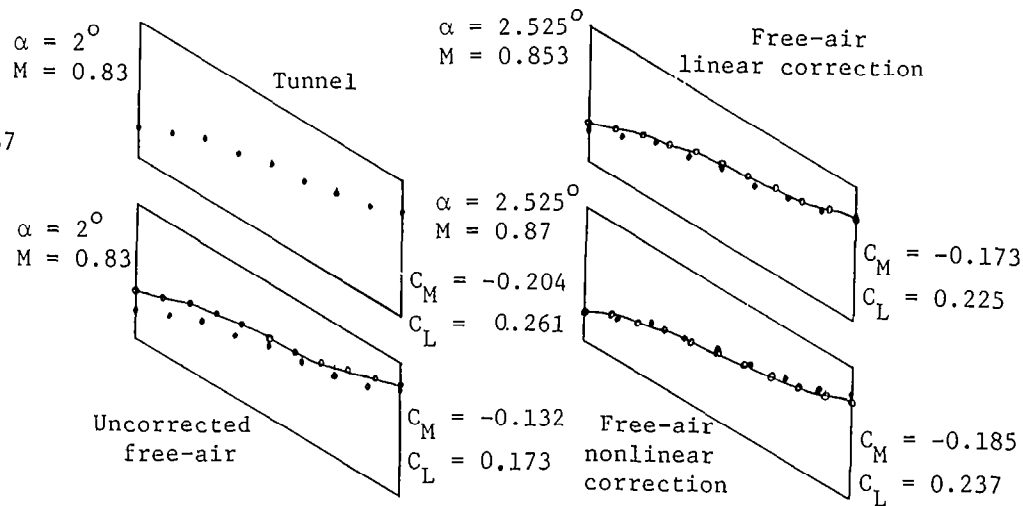


MODEL LENGTH $L = 47$ in
WING SPAN $b_w = 345$
WING CHORD $\bar{c}_w = 943$
TAIL CHORD $\bar{c}_t = 555$

A TFP code has been developed to compute the flow past a wing-body in a rectangular tunnel. Wall pressure or normal velocity must be prescribed. Results are shown for the AEDC calibration model in a free jet (Jou). The pressure distributions from left to right are near the root, midspan, and tip. The tail surface is not included in the calculations.



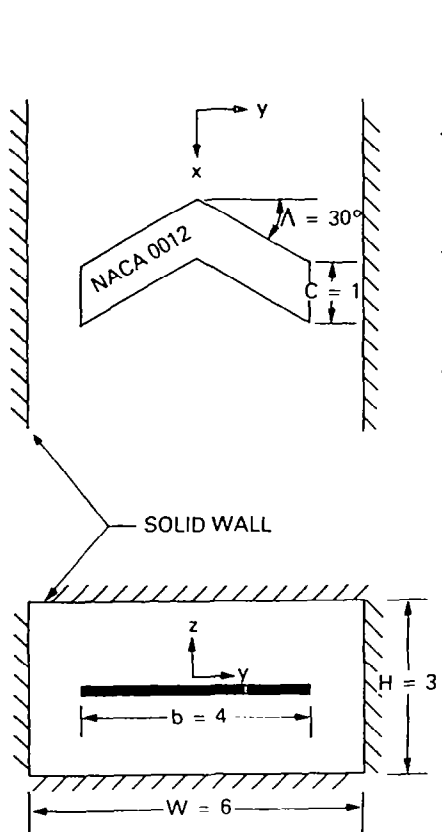
- Wind tunnel $M = 0.83$ $\alpha = 2^\circ$
- △-----△ Free air $M = 0.83$ $\alpha = 2^\circ$
- Free air $M = 0.853$ $\alpha = 2.525^\circ$
- ×-----× Free air $M = 0.87$ $\alpha = 2.525^\circ$



Location of shock wave in solid-wall tunnel, uncorrected free air, and corrected free-air conditions

A wind-tunnel wall-correction method has been developed by Rizk et al (17). The angle of attack and Mach number corrections are determined which match measured conditions to a free-air condition. An error estimate for the results is also determined. A preliminary calculation is shown here for the configuration given in the next figure. It is not expected that all wind-tunnel data will be correctable. This approach complements the adaptive wall studies.

PARAMETERS FOR TEST CASE



Model Frontal Area

Tunnel Cross-sectional Area

Test Case

0.0266

AGARD Criteria

<0.01

Model Span

Tunnel Width

0.667

<0.6

Model Wing Area

Tunnel Cross-sectional Area

0.222

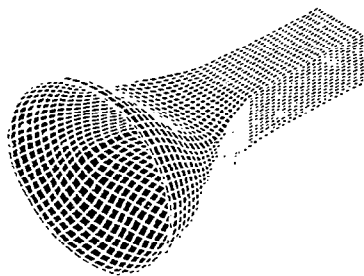
<0.05

Model Length

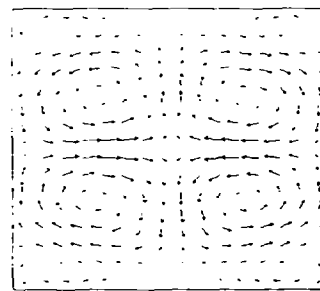
Tunnel Height

0.71

<1.0

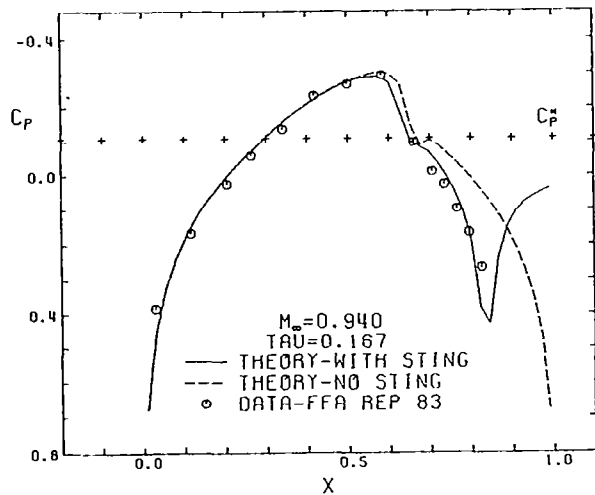


a. Duct geometry

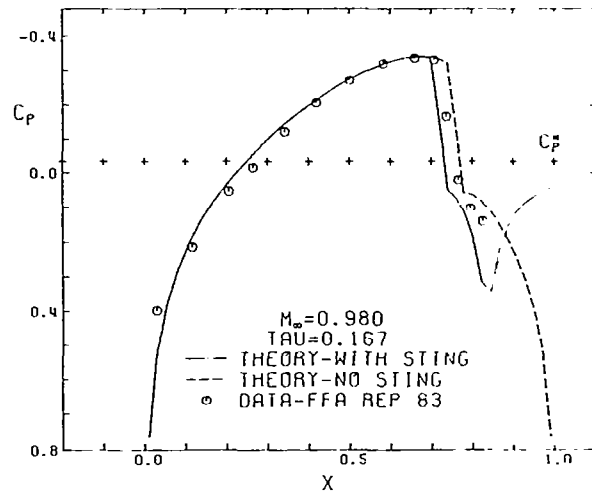


c. Exit-plane velocity vectors
Computation of flow within a wind-tunnel contraction.

The effects of free-stream nonuniformities due to a three-dimensional contraction have been modeled by Jacocks and Kneile (18) using the Euler equations. A maximum flow angularity of 0.1° is indicated. More complicated configurations have been analyzed (Jacocks).

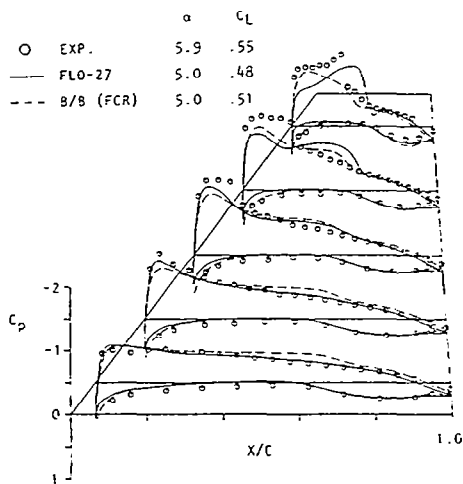


Parabolic arc of revolution.

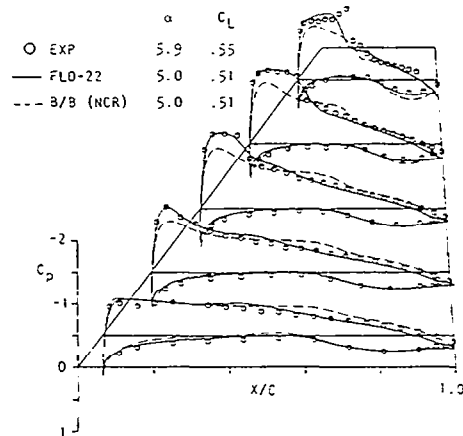


Parabolic arc of revolution.

The calculations of sting effects have not been reported for 3D aircraft configurations. Early results for a body of revolution (19) indicate this can be modeled. Since most grid systems for fuselages have an "open body," stings can be incorporated. The pitch sector may possibly be included also.



Comparison of conservative solutions with experiment for Wing C at $M = .85$.



Comparison of non-conservative solutions with experiment for Wing C at $M = .85$.

Predicted results are also influenced by the choice of the inviscid model equations and computational parameters. These calculations by Hinson and Burdges (20) show predictions using TFP (FLO) and TSP (B/B) models with two different finite difference treatments. The choice of mesh systems, iteration procedures, and implementation of boundary conditions can all influence the details of the resulting pressure distribution.

GENERAL COMMENTS

- An impressive capability for calculating transonic flows for realistic configurations and conditions is becoming available.
- Most calculations have been compared with wind-tunnel data but very limited comparisons with flight-test data are available.
- Various phenomena which have been modeled have the same order of magnitude on the influence of the predicted results. These include configuration effects, choice of governing inviscid equations, viscous effects, static aeroelastic effects, unsteady effects and tunnel-wall effects.
- Other phenomena which have not been quantified may also have significant effects on the predicted results. These include mesh system, convergence of the calculations, boundary conditions, model-support effects and free-stream nonuniformity.
- CFD should be able to make a significant contribution to the task of correlating wind-tunnel and flight-test data in the upcoming years.
 - Some effects of geometry differences and aeroelastic distortion may be predicted.
 - Tunnel-wall effects may be assessed and, perhaps, corrected for.
 - The effects of model-support systems and free-stream nonuniformities may be possible to model.
 - Some analysis of viscous effects can be modeled but our capability to analyze complicated 3D viscous flows is not yet well developed.
- There is a lack of coordination between the various investigations.
- Comparisons between calculations and data need to be done carefully to make sure that all numerical and experimental influences have been accounted for.

SUGGESTIONS

- An advocate, a program, and a team of investigators need to be identified to tackle this important application of CFD.
- A good wind-tunnel and flight-test data base is needed which contains the needed measurements and documentation.
- Instantaneous results cannot be expected. This is a complicated area and a careful study is needed. This should be viewed as a long-term effort rather than a two-year "hit and run" program.
- There can be a significant payoff in increased fidelity and understanding of the data and elimination of some tests.

REFERENCES

- (1) Ballhaus, W. F.; and Bailey, F. R.: Numerical Calculation of Transonic Flow About Swept Wings. AIAA-72-677, June 1972.
- (2) Bailey, F. R.; and Ballhaus, W. F.: Comparisons of Computed and Experimental Pressures for Transonic Flows About Isolated Wings and Wing-Fuselage Configurations. NASA SP-347, 1975.
- (3) Boppe, C. W.; and Stein, M. A.: Simulated Transonic Flows for Aircraft with Nacelles, Pylons, and Winglets. AIAA-80-130, Jan. 1980.
- (4) Boppe, C. W.; and Aidala, P. V.: Complex Configuration Analysis at Transonic Speeds. Paper 26 in Subsonic/Transonic Configuration Aerodynamics, AGARD CP-285, May 1980.
- (5) Jameson, A.: Iterative Solution of Transonic Flows Over Airfoils and Wings Including Flows at Mach 1. Comm. of Pure and Applied Math, Vol. 27, 1974, pp. 283-309.
- (6) Jameson, A.; and Caughey, D. A.: A Finite Volume Method for Transonic Potential Flow Calculations. AIAA-77-635, June 1977.
- (7) Yu, N. J.: Transonic Flow Simulations for Complex Configurations with Surface Fitted Grids. AIAA-81-1258, June 1981.
- (8) Rizzi, A.; and Eriksson, L. E.: Transfinite Mesh Generation and Damped Euler Equation Algorithm for Transonic Flow Around Wing-Body Configurations. AIAA-81-0999, June 1981.
- (9) Stock, H. W.: Three Dimensional Boundary Layers on Wings and Bodies of Revolution. US-German DEA meeting 1978, TR-AFFDL-TR-78-111, pp. 32-56, 1978.
- (10) McClean, J. D.; and Randall, J. L.: Computer Program to Calculate Three-Dimensional Boundary Layer Flows Over Wings With Wall Mass Transfer. NASA CR-3123, 1979.
- (11) Street, C. I.: Viscous-Inviscid Interaction for Transonic Wing-Body Configurations Including Wake Effects. AIAA-81-1266, June 1981.
- (12) Borland, C.; Rizzetta, D.; and Yoshihara, H.: Numerical Solution of Three Dimensional Unsteady Flow Over Swept Wings. AIAA-80-1369, 1980.
- (13) Whitlow, W., Jr.; and Bennett, R. M.: Application of a Transonic Potential Flow Code to the Static Aeroelastic Analysis of Three-Dimensional Wings. AIAA-82-0689, 1982.
- (14) Eriksson, L. E.; and Rizzi, A.: Computation of Vortex Flow Around Wings Using the Euler Equations. Proc. of IV GAMM Conference on Numerical Methods in Fluid Mechanics, Oct. 1981.
- (15) Newman, P. A.; and Klunker, E. B.: Numerical Modeling of Tunnel Wall and Body Shape Effects on Transonic Flows Over Finite Lifting Wings. NASA SP-347, 1975, pp. 1189-1212.

(16) Mercer, J. E.; Geller, E. W.; Johnson, M. L.; and Jameson, A.: A Computer Code to Model Swept Wings in an Adaptive Wall Transonic Wind Tunnel. AIAA-80-0156, Jan. 1980.

(17) Rizk, M. H.; Murman, E. M.; and Hafez, M. M.: Transonic Wind Tunnel Wall Interference Corrections for Three-Dimensional Models. AIAA-82-0588, 1982.

(18) Jacocks, J. L.; and Kneile, K. R.: Computation of Three-Dimensional Time-Dependent Flow Using the Euler Equations. AEDC TR 80-49, July 1981.

(19) Krupp, J. A.; and Murman, E. M.: Computation of Transonic Flows Past Lifting Airfoils and Slender Bodies. AIAA Jour., Vol. 10, No. 7, July 1972, pp. 880-886.

(20) Hinson, B. L.; and Burdges, K. P.: An Evaluation of Three-Dimensional Codes Using New Correlation-Tailored Test Data. AIAA-80-0003, Jan. 1980.

SOME IDEAS AND OPPORTUNITIES CONCERNING
THREE-DIMENSIONAL WIND-TUNNEL WALL CORRECTIONS

Paul E. Rubbert
Boeing Military Airplane Company
Seattle, Washington

Miniworkshop on Wind-Tunnel/Flight Correlation
November 19-20, 1981

INTRODUCTION

Opportunities for improving the accuracy and reliability of wall corrections in conventional ventilated test sections are presented. The approach encompasses state-of-the-art technology in transonic computational methods combined with the measurement of tunnel-wall pressures. The objective is to arrive at correction procedures of known, verifiable accuracy that are practical within a production testing environment. The following conclusions are presented:

1. Accurate and reliable correction procedures can be developed for cruise-type aerodynamic testing for any wall configuration.
2. Passive walls can be optimized for minimal interference for cruise-type aerodynamic testing (tailored slots, variable open area ratio, etc.).
3. Monitoring and assessment of noncorrectable interference (buoyancy and curvature in a transonic stream) can be an integral part of a correction procedure.
4. Reasonably good correction procedures can probably be developed for complex flows involving extensive separation and other unpredictable phenomena.

TERMINOLOGY

CORRECTABLE INTERFERENCE: WALL-INDUCED CHANGES
TO U AND W (M_∞ & α)

NONCORRECTABLE INTERFERENCE: WALL-INDUCED CHANGES
TO $\frac{\partial U}{\partial X}$, $\frac{\partial W}{\partial X}$, $\frac{\partial W}{\partial Y}$, ETC.
(BUOYANCY, CURVATURE, ETC.)

"AT THE WALL" MEANS AT SOME BOUNDARY ENVELOPING THE MODEL.
IT CAN BE INSET FROM THE WALL TO AVOID WALL VISCOUS EFFECTS
AND SLOT INHOMOGENEITIES.

$K \sim$ EMPIRICAL WALL PARAMETER(S) \sim RELATES PRESSURE AT WALL
TO TRANSPIRATION VELOCITY OR STREAMLINE CURVATURE.

ΔU , ΔV , ΔW , ETC. \sim INTERFERENCE VELOCITY COMPONENTS INDUCED
BY THE WALLS.

OBJECTIVES

1. TO PRESENT SOME UNIFYING CONCEPTS FOR WALL INTERFERENCE
2. TO PRESENT SOME IDEAS FOR MORE RELIABLE WALL CORRECTIONS
AND FOR IMPROVING THE DESIGN OF PASSIVE WALLS TO REDUCE
INTERFERENCE

UNIFYING WALL-INTERFERENCE CONCEPTS

I. ALL WALL CORRECTION METHODS DEAL (DIRECTLY OR INDIRECTLY) WITH KNOWLEDGE OF TWO INDEPENDENT QUANTITIES AT THE WALL.

COMMON QUANTITIES ARE:

- $U \sim$ AXIAL VELOCITY (RELATED TO C_p)
- $V_n \sim$ NORMAL VELOCITY COMPONENT
- $K \sim$ WALL PERMEABILITY PARAMETER(S)

II. THE VARIOUS CORRECTION METHODS DIFFER PRINCIPALLY IN THE ASSUMPTIONS USED TO ARRIVE AT TWO INDEPENDENT QUANTITIES AT THE WALL.

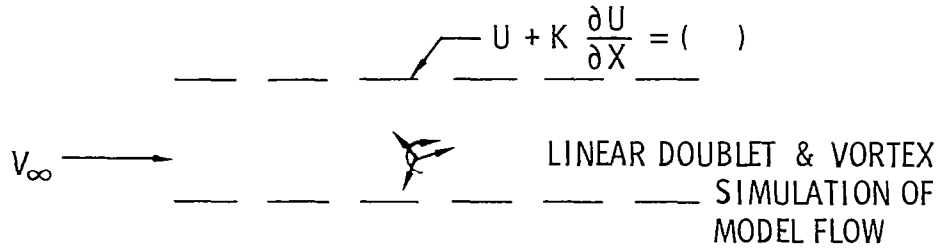
III. THE RELATIVE ACCURACY OR DEPENDABILITY OF WALL-CORRECTION METHODS CAN BE JUDGED ACCORDING TO THE ASSUMPTIONS OR MEASUREMENT ACCURACIES INHERENT IN PRODUCING TWO INDEPENDENT WALL QUANTITIES.

IV. WALL CORRECTIONS CAN BE CALCULATED DIRECTLY FROM KNOWLEDGE OF TWO INDEPENDENT WALL QUANTITIES, WITHOUT KNOWING ANYTHING ABOUT THE FLOW IN THE NEIGHBORHOOD OF THE MODEL.

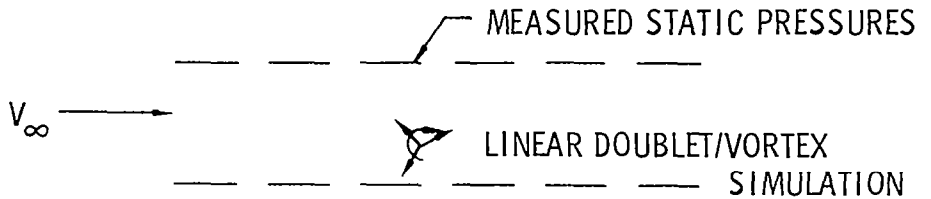
THE INDEPENDENT WALL QUANTITIES ASSOCIATED WITH KNOWN METHODS

CLASSICAL:

K AND CALCULATED WALL VELOCITY ARE INDEPENDENT



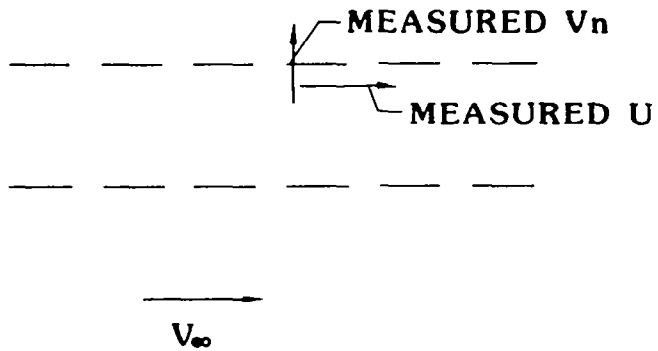
MOKRY, ET AL.:



KEMP:



ADAPTIVE WALL INVESTIGATORS:



CRITIQUE OF PRINCIPAL METHODS FOR PRODUCING INDEPENDENT WALL QUANTITIES

(i) ASSUMED K VALUES ~ IDEALIZED HOMOGENEOUS WALL MODELS ARE UNREALISTIC

(ii) LINEAR SIMULATIONS OF FLOW IN THE TUNNEL



• MISSES TRANSONIC BLOCKAGE TERM, I.E.

$$\phi \sim \underbrace{\int \sigma \left(\frac{1}{r}\right) dS + \int \mu \frac{\partial}{\partial n} \left(\frac{1}{r}\right) dS}_{\text{LINEAR}} + \underbrace{\iint U^2 \left(\frac{1}{r}\right) dV}_{\substack{\text{VOLUME} \\ \text{MISSING TERM} \\ \text{IMPORTANT IN} \\ \text{TRANSONIC FLOW}}}$$

• MISSES VISCOUS EFFECTS, WAKE BLOCKAGE, ETC.

• MODEL MAY BE TOO BIG FOR MULTIPOLE EXPANSION

(iii) TRANSONIC SIMULATIONS OF FLOW IN THE TUNNEL

• TOO EXPENSIVE FOR REGULAR USE

• WEAK ON VISCOUS-EFFECT SIMULATION

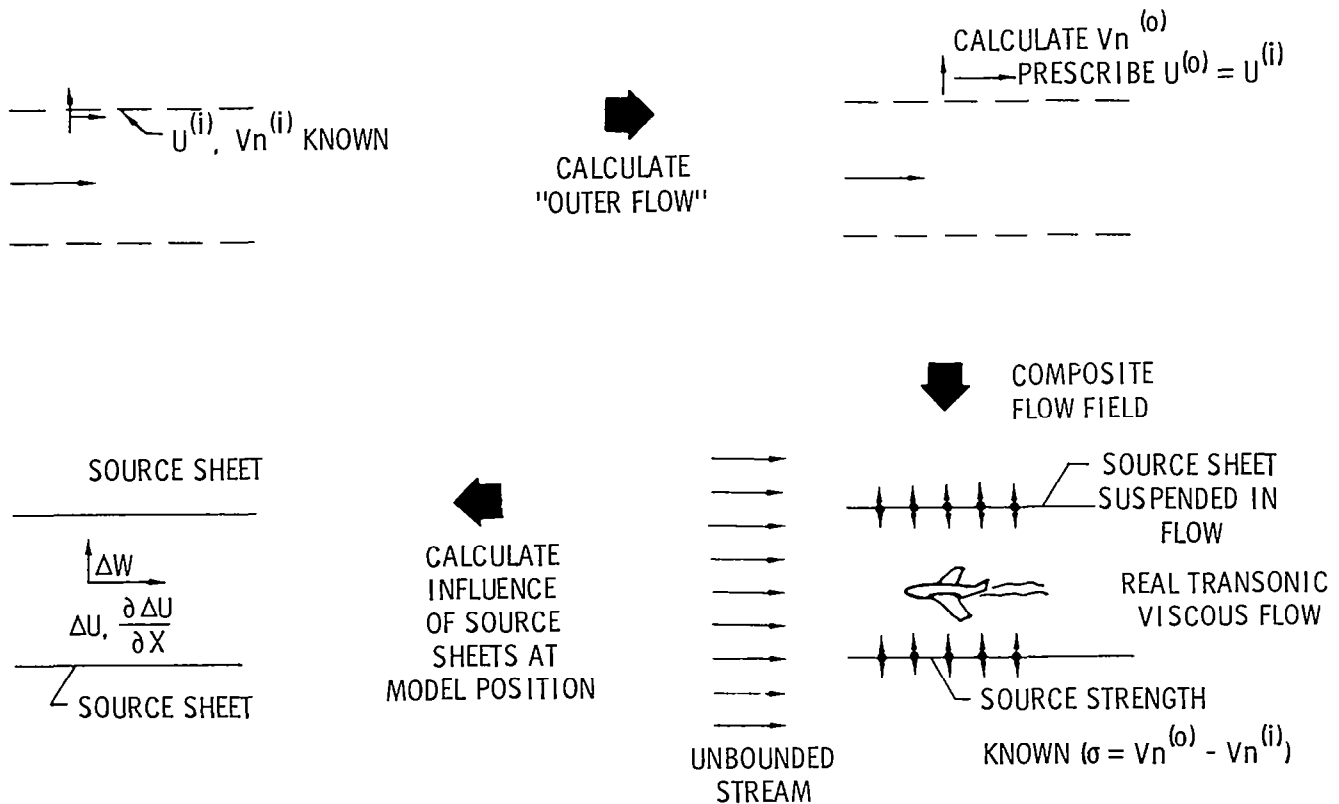
(iv) MEASURED STATIC PRESSURES

• PROBABLY PRETTY GOOD IF DONE CORRECTLY

(v) MEASURED NORMAL VELOCITY COMPONENT

• DIFFICULT TO DO WITH SUFFICIENT ACCURACY IN 3-D

OPPORTUNITIES: WALL-CORRECTION CALCULATIONS FROM WALL QUANTITIES



LIMITATIONS & GENERALIZATIONS OF INTERFERENCE CALCULATION

- FLOW MUST BE SUBCRITICAL AT THE WALLS
- CORRECTLY DEALS WITH LOCAL TRANSONIC FLOW NEAR THE MODEL, SEPARATION AND VISCOUS EFFECTS, WAKES, ETC.
- OUTER FLOW IS ARBITRARY. CAN BE TAKEN AS A UNIFORM STREAM FOR CONVENIENCE, ELIMINATING NEED FOR CALCULATING AN OUTER FLOW (SUSPENDED SHEET THEN INCLUDES VORTICITY ALSO~DOES NOT COMPLICATE ANYTHING)

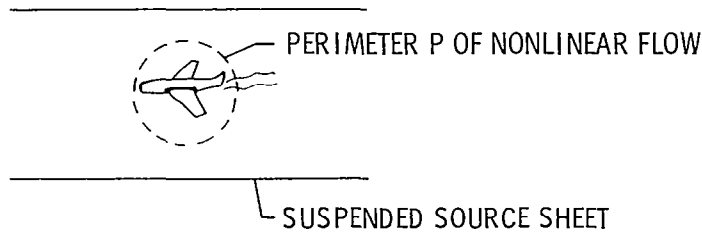
**THE KEY TO DOING A GOOD JOB WITH WALL CORRECTIONS
IS TO ACCURATELY KNOW TWO INDEPENDENT QUANTITIES
AT THE WALL**

OPPORTUNITIES

IF TWO INDEPENDENT QUANTITIES ARE KNOWN ACCURATELY AT THE WALL,
SEVERAL NICE OPPORTUNITIES EMERGE.

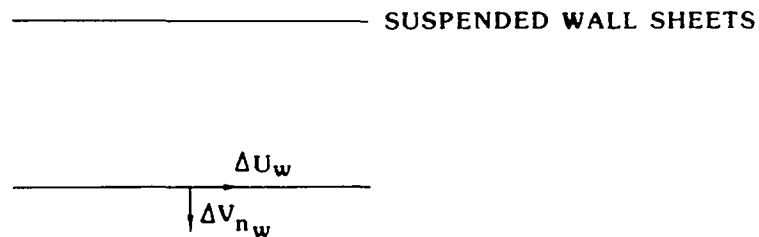
1. WALL CORRECTIONS CAN BE ACCURATELY CALCULATED,
INDEPENDENT OF THE TYPE OF FLOW NEAR THE MODEL
2. ACCURACY OF CORRECTIONS CAN BE ASSESSED (I.E.,
HOW BIG ARE THE NONCORRECTABLE EFFECTS)
3. OPTIMAL PASSIVE WALLS THAT MINIMIZE INTERFERENCE
CAN BE DEVELOPED
4. SIMPLE, TRADITIONAL METHODS OF WALL CORRECTION
CAN BE ADEQUATELY CALIBRATED.

**OPPORTUNITIES:
ASSESSMENT OF NONCORRECTABLE INTERFERENCE**



- CALCULATE ΔU , ΔW , ALONG P, INDUCED BY SUSPENDED SHEET
- IF ΔU , ΔW CONSTANT ALONG P, WALL CORRECTIONS WILL BE EXACT !
- VARIATION OF ΔU , ΔW ALONG P IS A MEASURE OF THE NONCORRECTABLE ERROR, AND CAN BE CORRELATED WITH OBSERVED (OR CALCULATED) CHANGES IN THE MODEL FLOW FIELD.
- A SIMPLE APPROXIMATION IS TO REPLACE THE ΔU VARIATION ON P BY $\frac{\partial \Delta U}{\partial X}$ AT MODEL CENTER, ETC. (I.E. MONITOR $\frac{\partial \Delta U}{\partial X}$, $\frac{\partial \Delta W}{\partial X}$, ETC.)

**OPPORTUNITIES:
CHANGING THE WALLS TO REDUCE OR MINIMIZE INTERFERENCE**



1. SUBTRACT INFLUENCE OF WALL SHEETS, CALCULATED AT THE WALLS, FROM VELOCITIES AT THE WALLS (I.E., CALCULATE ΔU_w , ΔV_{nw}). THIS YIELDS REQUIRED PRESSURE AND/OR SLOPE CHANGES.
2. CHANGE WALL CONFIGURATION ACCORDINGLY (CHANGE SLOT WIDTH, ETC.)

NOTE: IF PROCESS IS ITERATED TO DRIVE STRENGTH OF WALL SHEETS TO ZERO, THE FLOW WILL BE COMPLETELY FREE OF ALL INTERFERENCE. THIS IS THE "ADAPTIVE WALL" CONCEPT.

TOWARD MORE RELIABLE WALL CORRECTIONS

OBSERVATIONS: FOR CRUISE-TYPE AERODYNAMICS, ONE CAN ACCURATELY OBTAIN TWO INDEPENDENT QUANTITIES AT THE WALL

- MEASURED PRESSURES
- NORMAL VELOCITY COMPONENT, OBTAINED WITH A TRANSONIC CODE WITH BOUNDARY LAYER AND WAKE DISPLACEMENT MODEL, USING MEASURED WALL PRESSURES AS BOUNDARY CONDITIONS AT THE WALL, AND ADJUSTING α TO MATCH C_L WITH EXPERIMENT

STRATEGY: USE THIS CAPABILITY AS A MEANS FOR UNDERSTANDING AND IMPROVING TUNNEL WALL BEHAVIOR, AND TO FORMULATE AND VALIDATE CORRECTION PROCEDURES THAT ARE PRACTICAL FOR EVERYDAY USE.

ONE APPROACH

PHASE 1: PRELIMINARY STUDIES AND DEVELOPMENT

WALL PRESSURE MEASUREMENT

TRANSONIC VISCOUS CODE:

- WALL REPRESENTATION
- BOUNDARY LAYER AND WAKE MODEL
- INFLUENCE OF MODEL SUPPORT SYSTEM
- FIX FINITE-VOLUME FLUX BOX LEAKAGE
- CORRECT V_n FOR RESIDUALS (TINY FIELD SOURCES)
- GRID DENSITY STUDY NEAR WALL
- UPSTREAM AND DOWNSTREAM BOUNDARY CONDITION

PANEL CODE FOR INTERFERENCE CALCULATIONS

PHASE 2: VALIDATION AND ASSESSMENT

MODEL: SUBSONIC TRANSPORT, STING MOUNT

MACH NO: SUBSONIC THROUGH M_{DD}

ANGLES OF ATTACK: FOR ATTACHED FLOW

SPECIAL INSTRUMENTATION: WALL PRESSURES

CALCULATIONS: TRANSONIC VISCOUS CODE + PANEL CODE

TEST CONDITIONS:

- VARY VERTICAL POSITION OF MODEL
- OPEN AREA RATIO VARIATION
- SOLID WALLS (PROVIDE REDUNDANT INFORMATION ~ EXCELLENT FOR CONSISTENCY CHECK)

VALIDATION:

- DATA SHOULD COLLAPSE WHEN CORRECTIONS ARE APPLIED.
- CHECK CALCULATED v_n WITH SOLID WALLS
- INVERT METHOD FOR SOLID WALL CROSS-CHECK

ASSESSMENT:

- EXAMINE $\frac{\partial U}{\partial X}$, $\frac{\partial W}{\partial X}$, $\frac{\partial W}{\partial Y}$, ETC.

EVALUATION:

- ARE ΔU AND ΔW CORRECTIONS SIGNIFICANT?

PHASE 3: WALL-IMPROVEMENT PROGRAM

ASSUMPTION: PHASE 2 INDICATES A NEED TO DO BETTER

OBJECTIVES:

- MINIMIZE UNCORRECTABLE INTERFERENCE IN CRUISE REGIME.
- REDUCE CORRECTABLE INTERFERENCE TO INSIGNIFICANT LEVEL, OR TO WHERE SIMPLE AND PRACTICAL CORRECTION PROCEDURES ARE ADEQUATE.
- TOLERABLE INTERFERENCE LEVELS IN NONCRUISE REGIMES.

APPROACH:

- USE PHASE 2 RESULTS TO PREDICT DIRECTION OF WALL CHANGES (TAILORED SLOTS, HOLES, ETC.)
- CHANGE WALL AND EVALUATE (MORE THAN ONE CYCLE).
- EXPLORE SENSITIVITY TO MODEL CONFIGURATION.
- EXAMINE INTERFERENCE LEVELS OVER RANGE OF C_L , M_∞ , BLOCKAGE, ETC.

PHASE 4: EMPIRICAL CORRELATIONS TO DEFINE K

- PREVIOUS PHASES PROVIDE $U^{(i)}$ VS $V_n^{(i)}$ DATA BASE
- THEREFORE, K DISTRIBUTION AVAILABLE EVERYWHERE ON WALL FOR WIDE RANGE OF TEST CONDITIONS, EVEN WITH A NONHOMOGENEOUS OR TAILORED WALL

ATTEMPT TO CORRELATE K (OR SOME COMBINATION OF PARAMETERS) WITH OUTFLOW, INFLOW, PRESSURE, STREAMLINE CURVATURE, LENGTH OF RUN IN SLOTS, ETC.

PHASE 5: IDENTIFY STANDARD CORRECTION PROCEDURES FOR PRODUCTION USE

GROUND RULE:

- MUST BE PRACTICAL

APPROACH:

- SELECT FROM AMONG CANDIDATES.
- EVALUATE AGAINST THE MORE PRECISE METHODS PROPOSED IN THIS STUDY.

POTENTIAL CANDIDATES FOR STANDARD CORRECTION PROCEDURE

WALL C_{ps}	GOOD K CORREL.	CANDIDATES	COMMENTS
—	—	NO CORRECTIONS	MINIMAL INTERFERENCE WALL ACHIEVED
NO	NO	CORRELATE CORRECTIONS WITH MODEL SIZE, M_∞ , C_L , ETC.	GOOD ONLY WITHIN SCOPE OF DATA BASE
NO	YES	SECOND WALL CONDITION FROM COMPUTED FLOW ABOUT THE MODEL. <ul style="list-style-type: none"> • MULTIPOLE TYPE MODEL (HORSESHOE VORTEX, ETC.) • ABOVE METHOD INCLUDING TRANSONIC INTEGRAL TERM RELATED TO GLOBAL MODEL PARAMETERS • DETAILED MODEL FLOW CALC. 	<ul style="list-style-type: none"> • COMPARABLE TO CLASS- ICAL ~ ITERATIVE IF K IS NONLINEAR • BETTER THAN ABOVE, STILL PRACTICAL • IMPRACTICAL IN EVERY- DAY USE
YES	NO	SAME AS ABOVE	SAME AS ABOVE
YES	YES	SIMPLE DIRECT COMPUTATION OF INTERFERENCE	<ul style="list-style-type: none"> • ACCURATE • APPLICABLE TO ALL FLOWS • ASSESSMENT OF NON- CORRECTABLE INTERFERENCE

WHAT CAN PROBABLY BE ACHIEVED

- ACCURATE, VALIDATED CORRECTIONS WITH EXISTING WALLS, FOR CRUISE AERODYNAMICS.
- PASSIVE WALL CONFIGURATION OPTIMIZED FOR MINIMUM INTERFERENCE OF CRUISE AERODYNAMICS (TAILORED SLOTS, ETC.)
- PROCEDURES FOR ASSESSING NONCORRECTABLE INTERFERENCE OF CRUISE AERODYNAMIC FLOWS.
- REASONABLY GOOD CORRECTION PROCEDURES, WITH ANY WALL CONFIGURATION, FOR COMPLEX FLOWS INVOLVING EXTENSIVE SEPARATION, ETC.

LIST OF ATTENDEES

Non-Langley Attendees

AYERS, Theodore G.
NASA Dryden Flight Research Center
Code E-EA
Edwards, CA 93523

BYRNES, Andrew L., Jr.
Manager, Aerodynamics
Lockheed California Company
Burbank, CA 91520

CHILD, Richard D.
Rockwell International
North American Aircraft Division
MS 011-MB 03
P. O. Box 92098
Los Angeles, CA 90009

DaFORNO, Gianky
Grumman Aerospace Corporation
So. Oyster Bay Rd.
Bethpage, NY 11714

FREI, Douglas R.
Grumman Aerospace Corporation
So. Oyster Bay Rd.
Bethpage, NY 11714

HOWE, E. Dabney
Northrop Corporation
Mail Zone 3844/64
3901 W. Broadway
Hawthorne, CA 90250

KEEL, Lowell C., Major
AFWAL/FIMM
Wright Patterson AFB, OH 45433

KIRKPATRICK, Douglas
Naval Air Systems Command
AIR-320
Washington, DC 20361

KRAFT, Edward M.
AEDC/Calspan
Arnold AF Station, TN 37389

KUSHMAN, Keith
AEDC
Directorate of Technology
Mail Stop 900
Arnold AF Station
Tullahoma, TN 37389

LYNCH, Frank
Douglas Aircraft Company
Dept. C1-253 MS 3681
3855 Lakewood Boulevard
Long Beach, CA 90846

MADSEN, A. P.
General Dynamics
Fort Worth Division
Mail Zone 2866
Fort Worth, TX 76101

MITCHELL, James G.
US Air Force
AEDC/CCX
Arnold AF Station
Tullahoma, TN 37389

NAGEL, Adelbert L.
The Boeing Company
P. O. Box 3707
MS 3N-19
Seattle, WA 98124

NIEDLING, Larry G.
McDonnell Douglas Corporation
Dept. 341
P. O. Box 516
St. Louis, MO 63166

PATERSON, John H.
Lockheed-Georgia Company
96 S. Cobb Drive
Marietta, GA 30063

RUBBERT, Paul E.
Boeing Military Airplane Company
P. O. Box 3707
MS 3N-19
Seattle, WA 98124

SCHOENHEIT, Albert E.
Rockwell International
P. O. Box 92098
Los Angeles, CA 90009

VRETAKIS, Nicholas G.
AFSCLO
Mail Stop 221
Hampton, VA 23665

STEINLE, Frank W., Jr.
NASA Ames Research Center
Mail Code 277-5
Moffett Field, CA 94035

WALLACE, Rodney O.
NASA Johnson Space Center
Mail Code EX4
Houston, TX 77058

TOSCANO, Eugene J.
Grumman Aerospace Corporation
So. Oyster Bay Rd.
Bethpage, NY 11714

NASA-Langley Attendees

BARNWELL, Richard W.
BARTLETT, Dennis W.
BOBBITT, Percy J.
BOWER, Robert E.
CAMPBELL, James F.
CHAMBERS, Joseph R.
GILBERT, William P.
GLOSS, Blair B.
HALLISSY, James B.
HENDERSON, William P.
HOLMES, Bruce J.
IGOE, William B.
JOHNSON, Joseph L.
KILGORE, Robert A.

KIRKHAM, Frank S.
MARGASON, Richard J.
McKINNEY, L. Wayne
NEWMAN, Perry A.
PATTERSON, James C., Jr.
PETERSEN, Richard H.
PETERSON, John B., Jr.
REUBUSH, David E.
SCALLION, William I.
SMITH, Ronald H.
SOUTH, Jerry C.
STICKLE, Joseph W.
SWAIN, Robert L.
YOUNG, Clarence P.

BAALS, Donald D. Consultant
KEMP, William B. George Washington University

1. Report No. NASA CP-2225	2. Government Accession No.	3. Recipient's Catalog No.	
4. Title and Subtitle WIND-TUNNEL/FLIGHT CORRELATION - 1981		5. Report Date June 1982	6. Performing Organization Code 505-31-63-01
		8. Performing Organization Report No. L-15368	10. Work Unit No.
7. Author(s) L. Wayne McKinney and Donald D. Baals, editors		11. Contract or Grant No.	
9. Performing Organization Name and Address NASA Langley Research Center Hampton, VA 23665		13. Type of Report and Period Covered Conference Publication	
		14. Sponsoring Agency Code	
12. Sponsoring Agency Name and Address National Aeronautics and Space Administration Washington, DC 20546		15. Supplementary Notes L. Wayne McKinney: Langley Research Center Donald D. Baals: Consultant	
16. Abstract This report is a compilation of annotated illustrations presented at the Miniworkshop on Wind-Tunnel/Flight Correlation held November 19-20, 1981, at the Langley Research Center. This meeting had as its nucleus the members of the Wind-Tunnel/Flight-Correlation Panel of the 1980 workshop on High Reynolds Number Research (NASA CP-2183) supplemented by invited specialists. The miniworkshop was structured to review pertinent activities in the area of wind-tunnel/flight correlation to assure maximum effectiveness of the early experimental programs of the National Transonic Facility (NTF). Topics included a status report of the NTF, the role of tunnel-to-tunnel correlation, a review of past flight-correlation research and the resulting data base, the correlation potential of future flight vehicles, and an assessment of the role of computational fluid dynamics (CFD).			
17. Key Words (Suggested by Author(s)) Research facility Transonic High Reynolds number Wind-tunnel/flight correlation Cryogenic National Transonic Facility		18. Distribution Statement Unclassified - Unlimited Subject category 02	
19. Security Classif. (of this report) Unclassified	20. Security Classif. (of this page) Unclassified	21. No. of Pages 238	22. Price All

National Aeronautics and
Space Administration

SPECIAL FOURTH CLASS MAIL
BOOK

Postage and Fees Paid
National Aeronautics and
Space Administration
NASA-451



Washington, D.C.
20546

Official Business
Penalty for Private Use, \$300

050082 5100305
DEPT OF THE AIR FORCE
AF WEAPONS LABORATORY
ATTN: TECHNICAL LIBRARY (SOL)
CIRTLAND AFB TX 79117

NASA

POSTMASTER: If Undeliverable (Section 158
Postal Manual) Do Not Return